

# **The DNA Replication Initiation Machinery as a Target for Cancer Diagnosis and Therapy**

Alex Wollenschlaeger

The studies presented in this thesis were performed at the Wolfson Institute for Biomedical Research and the Department of Pathology, University College London, London, UK. The research described in this thesis was financially supported by grants C428/A3441 and C428/A6263 from Cancer Research UK.

Cover: Alex Wollenschlaeger

Layout: Alex Wollenschlaeger and L<sup>A</sup>T<sub>E</sub>X 2<sub>ε</sub>

# The DNA Replication Initiation Machinery as a Target for Cancer Diagnosis and Therapy

Het DNA replicatie initiatie mechanisme als doelwit  
voor kankerdiagnose en behandeling

Thesis

to obtain the degree of Doctor from the  
Erasmus University Rotterdam  
by command of the  
rector magnificus

Prof.dr. H.G. Schmidt

and in accordance with the decision of the Doctorate Board

The public defence shall be held on  
Wednesday 29 June 2011 at 0930 hours

by

Alex Wollenschlaeger  
born in Bloemfontein, South Africa



## **Doctoral Committee**

### **Promotor:**

Prof.dr. F.G. Grosveld

### **Other members:**

Prof.dr. J.N.J. Philipsen

Prof.dr.ir. D.N. Meijer

Dr.ir. G.W. Jenster

### **Copromotor:**

Dr. K. Stoeber

# Table of Contents

<b>1</b>	<b>Introduction</b>	<b>1</b>
1.1	Biomarkers for cancer detection . . . . .	2
1.2	Biomarkers for the diagnosis of bladder cancer . . . . .	3
1.2.1	Nuclear matrix protein 22 . . . . .	4
1.2.2	Bladder tumour associated antigen . . . . .	5
1.2.3	UroVysion . . . . .	6
1.2.4	ImmunoCyt/uCyt+ . . . . .	6
1.2.5	BLCA-4 . . . . .	7
1.3	Biomarkers for the diagnosis of prostate cancer . . . . .	8
1.3.1	Prostate specific antigen . . . . .	9
1.3.2	Prostate cancer antigen 3 . . . . .	10
1.3.3	TMPRSS2-ERG . . . . .	10
1.4	Biomarkers for the diagnosis of pancreaticobiliary tract cancer . . . . .	11
1.4.1	Biochemical biomarkers of pancreaticobiliary tract cancer . . . . .	13
1.4.2	Genetic biomarkers of pancreaticobiliary tract cancer . . . . .	13
1.5	The DNA replication initiation machinery as a promising target for biomarker development . . . . .	14
1.5.1	MCM loading licenses origins for replication . . . . .	15
1.5.2	MCMs detect aberrant growth and are potential diagnostic biomarkers . . . . .	18
1.5.3	Replication initiation proteins are potential prognostic and predictive biomarkers . . . . .	20
1.6	The DNA replication initiation machinery is a potential therapeutic target . . . . .	23
1.7	Scope of the thesis . . . . .	24
1.8	References . . . . .	27
<b>2</b>	<b>Bladder cancer diagnosis by combined detection of Mcm5 protein and nuclear matrix protein 22</b>	
	<i>Manuscript in preparation.</i>	<b>37</b>
<b>3</b>	<b>Diagnosis of prostate cancer by detection of minichromosome maintenance</b>	<b>5</b>

protein in urine sediments	
<i>British Journal of Cancer 2010 103 (5): 701-707.</i>	61
4 Diagnosis of pancreaticobiliary malignancy by detection of minichromosome maintenance protein 5 in bile aspirates	
<i>British Journal of Cancer 2008 98 (9): 1548-1554.</i>	69
5 DNA replication licensing factors and aneuploidy are linked to tumor cell cycle state and clinical outcome in penile carcinoma	
<i>Clinical Cancer Research 2009 15 (23): 7335-7344.</i>	77
6 Molecular architecture of the DNA replication origin activation checkpoint	
<i>EMBO Journal 2010 29 (19): 3381-3394.</i>	89
7 Targeting DNA replication before it starts: Cdc7 as a therapeutic target in p53-mutant breast cancers	
<i>American Journal of Pathology 2010 177 (4): 2034-2045.</i>	105
8 Discussion	119
Summary	131
Nederlandse Samenvatting	135
Acknowledgements	139
Curriculum vitae	140
PhD portfolio	142

# Chapter 1

## Introduction

As normal cells transform into cancer cells they undergo a large number of increasingly better understood changes. Among the most essential of these changes are an increased ability to passage unhindered through the cell cycle and a decreased sensitivity to the mechanisms that normally constrain aberrant growth (1, 2). This places the initiation of DNA replication at a key decision point important in tumourigenesis (3). Precise regulation of DNA replication initiation is a critical step in growth control in metazoan cells. DNA replication initiation lies at the convergence point of oncogenic and transduction signalling pathways that trigger proliferation. Unlike these pathways, which have an inherent redundancy, there appears to be only a single mechanism of DNA replication initiation that is conserved across eukaryotes (4). This makes the DNA replication initiation machinery a potentially attractive target for both diagnostic and therapeutic interventions.

The core of the DNA replication initiation machinery is the pre-replicative complex (pre-RC), a macromolecular complex of proteins known as replication licensing factors that couple growth regulatory and DNA damage response pathways to chromosomal replication (5). In the work described in this thesis I examine the use of replication licensing factors as biomarkers able to accurately diagnose cancer, to provide prognostic information about disease progression and to predict response to therapeutic intervention. The ability of replication licensing factors to detect cancer is demonstrated in the first prospective large-scale multicentre clinical study into the use of the DNA replicative helicase protein Mcm5 as a diagnostic biomarker for bladder cancer, a malignancy where there still exists an urgent need for simple non-invasive tools to detect clinically relevant disease. In addition, I present the results from two proof-of-principle studies of Mcm5 as a diagnostic biomarker for prostate and pancreaticobiliary tract cancers. Mcm5 is part of the Mcm2-7 replicative helicase complex that unwinds DNA during replication and is a key substrate for the cell cycle regulated kinase Cdc7 (6). Previous work has demonstrated that depletion of Cdc7 elicits a checkpoint that halts the cell cycle at or before the onset of DNA synthesis. This checkpoint is lost in cancer cells, resulting in cancer cell specific killing

following Cdc7 depletion (7). Here I describe for the first time the molecular architecture of this checkpoint and demonstrate that it is reversible in normal cells, thereby opening new avenues to cancer treatment. Finally I show that replication licensing factors are able to identify unique cancer cell cycle phenotypes and demonstrate how these may be used to predict the response to emerging pharmacological inhibitors of Cdc7 and existing cell cycle phase specific chemotherapeutic agents.

## 1.1 Biomarkers for cancer detection

Research in the post-genomic era into novel biomarkers for cancer has seen a concerted move towards high-throughput systemic approaches (8-11). Using tools that analyse the DNA, RNA and protein complements of normal cells and tumours, researchers are able to examine large-scale alterations brought about during tumourigenesis in unprecedented detail, allowing dissection of the complex network of interactions in signalling pathways that are perturbed during tumour development (12, 13). Such analyses not only deliver insight into the biological mechanisms of cancer but also simultaneously aid the development of biomarkers of dysregulated growth that may provide important diagnostic and prognostic information (11, 14, 15).

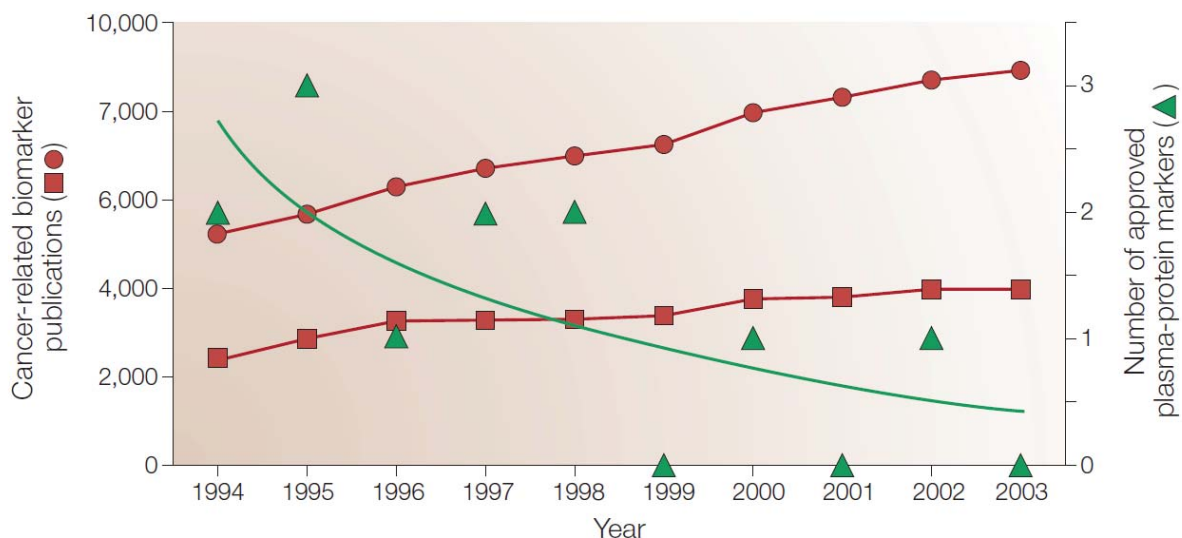


Figure 1.1: The biomarker paradox. The number of publications identified on MEDLINE using the search term “biomarker” (red triangles) or under the Medical Subject Heading “biomarker” (red squares), compared with the number of biomarkers receiving approval from the US Food and Drug Administration (green triangles). Reprinted by permission from Macmillan Publishers Ltd: Nature Reviews Cancer, (16).

Despite the rapid increase in the number of biomarkers studies, however, there has not been a concomitant rise in the number of regulator approved diagnostic biomarkers - what has been called the “biomarker paradox” (16) (Figure 1). An important limitation of genome-wide



approaches to the development of proliferation signatures in cancer is that these methods do not generally directly address tumour heterogeneity (3). Tumours exhibit both inter- and intra-tumoural heterogeneity that is thought to be a result of the different cancer initiating cells of origin (17). Together with the inherent heterogenous composition of contaminating normal tissue components, this heterogeneity can result in suboptimal proliferation signatures (3). Few of the new generation of biomarkers have been validated in multi-centre prospective clinical trials, and there remain issues related to the reliability and costs associated with these new tools and the feasibility of widely incorporating them into patient management (16). Consequently there is still an urgent need for new biomarkers with high sensitivity and specificity that are able to accurately diagnose cancer.

The maturity of the biomarker development process associated with any particular cancer depends in large part on the anatomical structures being investigated. Outlined below are profiles of diagnostic biomarker development in three cancers considered in later chapters of this thesis. Each cancer is in a different stage of the development pipeline and poses unique challenges. The first example is bladder cancer, which has seen extensive biomarker development, though most of these have had limited clinical impact. Prostate cancer, on the other hand, benefits from one mature marker that has seen extensive use over the past two decades but has of late seen its usefulness in certain treatment areas questioned, prompting further development of complementary or supplementary biomarkers. Meanwhile, pancreaticobiliary tract cancer is a relatively rare malignancy that is typically detected late and kills quickly and for which biomarker development is still largely in the experimental phase.

## **1.2 Biomarkers for the diagnosis of bladder cancer**

Bladder cancer is a leading cause of cancer death. The US National Cancer Institute predicted 70,530 new diagnoses and 52,760 deaths in the US in 2010 (18). The majority of urothelial transitional cell cancers do not invade deeply at presentation, but up to 80% of tumours recur within five years (19). The traditional route of diagnosis is direct visualization during flexible cystoscopy, the current gold standard, with confirmation of upper tract disease or carcinoma in situ normally provided by cytologic analysis. These techniques are expensive and rely on trained surgeons and pathologists. In addition they carry with them elements of subjectivity. Cystoscopy is also particularly uncomfortable for patients, resulting in both morbidity and frequently more serious side effects such as bleeding, perforation of the bladder wall and infection. Cytology has excellent specificity, typically approaching 100%, but suffers from reduced sensitivity due to low cellular yield, urinary tract infections and stones (20-22). Following surgical treatment, patients are typically followed up for several years also using a combination of cystoscopy and cytology.

Patients presenting with muscle invasive tumours (25-30% of tumours at diagnosis) have a significant risk of progression to metastasis (30-60%) and a significantly reduced 5-year survival rate despite aggressive local treatment (40%) (23-25). Therefore the early detection of bladder cancer through a non-invasive test would greatly affect disease management. A suitable biomarker should be highly specific, to prevent unnecessary cystoscopies, and highly sensitive for high grade transitional cell carcinomas. Sensitivity for the detection of low grade disease is of relatively lesser importance since there is only a 2% progression rate from low to high grade cancer, although this is significantly increased by the concomitant presence of carcinoma in situ (26, 27). In addition, survival rates are improved by early diagnosis, but subsequent surveillance results in high costs (20). Test specificity can be affected by infection, inflammation and haematuria, all of which are common in patients with bladder cancer and in patients treated with intravesical chemotherapy or immunotherapy. A simple, accurate, non-invasive test for detecting bladder cancer would improve the management of bladder cancer, decrease the morbidity associated with current surveillance methods and improve prognosis for patients with potentially invasive disease.

A particular advantage for tests for bladder cancer is the presence of a readily available substrate for analysis. Urine is exposed to few organs, as opposed to blood, which carries thousands of proteins in a very wide range of concentrations (21, 28). In addition, urine has a low pH that inactivates proteases and enriches it for those proteins produced by cells of the urothelium (21). Several biomarkers for bladder cancer are in development or have already been approved by the FDA for clinical use, though as of yet none has been recommended for routine clinical use (29). While some biomarkers have demonstrated high sensitivity, approaching 100%, compared with a sensitivity of 34% for cytology, they failed to surpass the specificity of 99% observed for cytology. (21). These new urinary biomarkers are also burdened by cost and in some cases the requirement of advanced equipment and training (21, 30, 31). Below I discuss some of the most promising investigational and regulator-approved bladder cancer biomarkers.

### **1.2.1 Nuclear matrix protein 22**

Nuclear matrix protein 22 (NMP22) is the name given by manufacturer Matritech (Newton, MA) to NuMA, the nuclear mitotic apparatus protein, which forms the key component of its FDA-approved qualitative and quantitative bladder cancer detection tests. NuMA is a 238 kDa nuclear protein with functions related to both assembly and maintenance of the mitotic spindle (32, 33). During mitosis, the protein is concentrated at the spindle pole bodies where it tethers microtubules to the poles. NuMA is also present throughout interphase, though there is little data on its precise role outside of mitosis. The structure and mitotic function of the protein led to the suggestion that it forms an integral part of the nuclear matrix (34).

The basis of the qualitative point-of-care NMP22 BladderChek and quantitative NMP22 Test

kits is the immunodetection of NuMA released into urine by dead and dying cells. The qualitative test employs a cut-off of 10 U/ml and leads to a binary result within one hour, while the quantitative test allows more accurate determination of protein levels in stabilized voided urine. In a multicentre study of 1331 patients at risk due to haematuria, a history of smoking or other factors, the point-of-care test detected 44 of 79 (56%) tumours compared to 12 of 76 (16%) by cytology (35). Although the sensitivity of the NMP22 test was higher than for cytology, specificity was lower (86% vs 99%). A similar improvement in sensitivity over cytology was observed in a study of 668 patients into the usefulness of NMP22 as a biomarker for recurrent bladder cancer in patients undergoing surveillance (36). In this setting, the NMP22 test correctly identified 50% of recurrent tumours compared with 12% for cytology. The test also detected 8 of 9 cancers initially missed by cystoscopy.

Follow-up studies by independent investigators using either alternative cut-points or the manufacturers recommended cut-point for the quantitative test demonstrated that NMP22 has variable performance (37, 38). While sensitivity of NMP22 is generally superior to that of cytology, the corresponding specificity varies widely. In their comprehensive review of published NMP22 studies, Mowatt and colleagues found that the NMP22 test had a sensitivity of 68% (95% CI 62-74%) and specificity of 79% (95% CI 74-84%) compared with a sensitivity of 44% (95% CI 38-51%) and specificity of 96% (95% CI 94-98%) for cytology (37). At least part of this reduced specificity relative to cytology is due to the susceptibility of the NMP22 tests to false-positives arising from benign conditions such as urinary tract infection, benign prostatic hyperplasia and urinary calculi (21, 35).

### 1.2.2 Bladder tumour associated antigen

Bladder tumour associated antigen (BTA) was identified in a commercial protein screen of urine samples from patients with confirmed bladder cancer (39). Partially purified urine protein preparations were used to immunize mice and generate a pool of 100 monoclonal antibodies. Two of the generated antibodies were then incorporated into a quantitative ELISA called BTA Test (Bard Diagnostics, Redmond, WA), which was later superseded by two new tests. Subsequent work with these antibodies identified the antigen recognized by these antibodies as a protein related to complement factor H (CFH) called complement factor H related protein (CFHrp) (39). CFHrp has similar structure and function to serum CFH. The protein has been shown to possess a binding site for C3b and accelerates degradation of this protein in the presence of CFI. More recent evidence suggests that upregulation of CFH is associated with tumour evasion of the immune system (40). Therefore, upregulation of CFHrp as seen in bladder cancer may aid tumour cell survival by providing a selective growth advantage (21, 39).

The quantitative BTA Trak test (Polymedco, Cortlandt Manor, NY) has a reported sensitivity

of 52-83% with a corresponding specificity of 50-90%. In comparison, the BTA Stat test (Polymedco) has much wider variability in sensitivity, ranging from 9-89% (21). The specificity of the point-of-care test is also particularly susceptible to influence by malign or benign genitourinary conditions other than bladder cancer (38, 41, 42). In one cohort study, the test had a specificity of 71% in patients without genitourinary disease compared with 46% for patients with malignant genitourinary disease other than bladder cancer (41). The poor specificity observed with the tests is explained in part by the ability of the antibodies employed to detect not only CFHrp but also CFH. Therefore the presence of blood in the urine due to benign conditions that result in release of CFH will also lead to false-positive results (38, 42, 43).

### 1.2.3 UroVysion

Bladder cancer is commonly associated with aneuploidy, specifically changes in the copy number of chromosomes 1, 3, 5, 7, 9, 11 and 17 (44). The UroVysion test (Abbott Molecular, Des Plaines, IL) for bladder cancer relies on exfoliated urothelial cells in urine for the detection of established chromosomal abnormalities by four-colour fluorescence in situ hybridization. The test uses three alpha-satellite repeat sequence probes that target pericentromeric regions of chromosomes 3, 7 and 13, thereby allowing enumeration to detect changes in chromosomal copy numbers. The test also includes a fourth probe that detects loss of the p16 tumour suppressor gene CDKN2A at chromosomal locus 9p21 (21). According to the manufacturers guidelines, cases are deemed positive for malignancy if there is: (i) gain of more than one chromosome in five or more cells, (ii) gain of one chromosome in 10 or more cells, or (iii) loss of both copies of the 9p21 locus in 10 or more cells (45, 46).

Studies into the efficacy of UroVysion demonstrate that the test has high sensitivity (69100%) and specificity (6596%) (44). The test has the advantage of relying on genetic alterations and as such is unaffected by benign conditions such as inflammation and benign prostatic enlargement while being able to detect occult tumours possibly missed by cystoscopy (21). The test has also been shown to detect disease at an early stage, before the appearance of neoplasia visible by cystoscopy (47). However, the test requires significant diagnostic expertise and specialised equipment, which together make it expensive to perform and thereby limit its potential clinical use.

### 1.2.4 ImmunoCyt/uCyt+

In contrast to the bladder cancer diagnostic tests discussed above, ImmunoCyt/uCyt+ (Diagnocure/Scimedex) is not an alternative to but rather serves as an adjunct to routine cytopathologic analysis. The test employs three fluorescently labelled antibodies to detect two surface mucin-like glycoproteins and a high molecular weight variant of carcinoembryonic antigen (CEA),

antigens associated with bladder transitional cell carcinomas (21, 48, 49). The test is deemed positive if any fluorescent signal is observed that is also confirmed by bright-field visualization and negative if no signal is observed in a slide with 500 or more epithelial cells.

The results reported for ImmunoCyt/uCyt+ have not borne out the potential for improving the sensitivity of cytology while retaining its high specificity. Reports show that, when combined with cytology, ImmunoCyt/uCyt+ has sensitivity of 63-85%, greater than for cytology alone. However, the specificity of the combination is in the range 62-78%, significantly lower than routine cytopathologic analysis (44). In addition, ImmunoCyt/uCyt+ is disadvantaged by the added technical requirements. The test requires specialist equipment and trained pathologists to examine material in conjunction with routine cytology, and the extended period required for analysis (up to 2 hours) means that it cannot be used intraoperatively (50). Moreover, studies have demonstrated that ImmunoCyt/uCyt+ generates false-positives results in the presence of benign conditions such as benign prostatic hyperplasia (38).

### 1.2.5 BLCA-4

BLCA-4 is a nuclear matrix protein identified in a screen of such proteins to distinguish between bladder cancer samples and normal samples (51). The protein is a member of the ETS family of transcription factors and is itself able to form complexes with other transcription factors, including AP-1 and NF-E1 (52). The protein is expressed in both tumour and adjacent normal areas in the urothelia of bladder cancer patients exclusively and it is not found in normal patients, including those with benign conditions such as benign prostatic hyperplasia and cystitis (21). Notably, BLCA-4 can be detected in primary tumours significantly before the development of visible tumours in a mouse model system (52).

In an early cohort study of 105 patients with or without confirmed bladder cancer, using an ELISA with monoclonal antibodies recognizing two different epitopes, BLCA-4 had 96% sensitivity and 100% specificity for bladder cancer detection (53). Interestingly, 20% of patients with spinal cord injuries also tested positive for the marker. A second cohort study of 140 patients confirmed these early positive results, showing that the test had 89% sensitivity and 95% specificity (54). While BLCA-4 appears to be a good marker for bladder cancer, these findings have not yet been confirmed in larger follow-up studies.

For non-muscle invasive bladder cancer the current European Association of Urology guidelines recommend cystoscopy and urine cytology, with histological examination and fluorescence cystoscopy of biopsy material recommended for cases of carcinoma in situ (19). For muscle invasive disease the guidelines recommend cystoscopy and biopsy (55). At present, none of the described biomarkers has been approved for diagnostic use by the EAU, for either non-muscle invasive or muscle invasive urothelial tumours, due to lower specificity relative to routine urine

cytology, although the guidelines do acknowledge the potentially higher positive predictive value offered by molecular biomarkers (see [www.uroweb.org](http://www.uroweb.org)). In the US, NMP22, UroVysion and ImmunoCyt/uCyt+ have all received FDA approval for screening or monitoring, though none has yet made a significant impact on clinical practise. A recent survey found that none of the current generation of urinary markers for bladder cancer was appropriate for clinical use, citing the need for larger validation studies (56). Thus there is still an urgent need for a simple, non-invasive biomarker for bladder cancer with high specificity and improved sensitivity over cytology that can complement cystoscopy (29).

### 1.3 Biomarkers for the diagnosis of prostate cancer

Prostate cancer is the second-most common cancer in men and a leading cause of cancer death with 217,730 new diagnoses and 32,050 deaths expected in the US in 2010. The median age at diagnosis is 64 or higher for 60% of cases, with a further 30% of diagnoses made in men with a median age of 55-64 (18). Management of the disease is complicated by its relatively late onset and the presence of indolent tumours, meaning that many men will die with prostate cancer but not from it. Clinical treatment of the disease was revolutionized by the introduction of testing for prostate-specific antigen (PSA) in serum, but limitations with the test in some contexts mean that there is still a need for new biomarkers to detect clinically relevant prostate cancer (57). Of particular importance is the decision of whether a biopsy is needed when PSA results are in the so-called “grey zone”, where patients present with elevated but still low PSA measurements of 2-10 ng/ml and negative digital rectal examinations.

There is growing consensus that prostate cancer is being overdiagnosed in the screening setting, leading to many men undergoing unnecessary surgical procedures (57-59). A recent large-scale European study of 182,000 men showed that the absolute risk difference between men in the screening group and men in the control group was 71 per 1000 men, meaning that in order to prevent one death from prostate cancer, an additional 48 men would need to be treated and 1410 men would need to be screened (60). The study showed that screening was associated with a drop of 20% in the rate of death. There is thus an urgent need for a biomarker than can complement the valuable clinical information provided by PSA by improving detection rates and providing information on the risk of progression.

A urine-based test would allow cells from multiple, possibly heterogenous, tumour foci to be assayed while avoiding the false-negative results associated with core-biopsies, which can only sample limited regions of the prostate (61, 62). Several approaches to prostate cancer detection have been taken over the past decade, including different measures of PSA and several novel biomarkers. Among the most promising of the new biomarkers are PCA3 and the chromosomal rearrangement TMPRSS2-ERG.



### 1.3.1 Prostate specific antigen

Prostate-specific antigen is a protein expressed exclusively in the prostate (63). However, PSA is not cancer specific, because the protein is elevated in the presence of benign conditions (64). In serum, PSA appears in two predominant forms: the small, inactive 36 kDa free PSA, which makes up 10-30% of total PSA, and a larger 96-100 kDa form complexed with protease inhibitor alpha-1-antichymotrypsin (ACT), which makes up the major fraction (65). Following work by numerous research groups around the world over several years, during which the protein was independently identified at least three times, PSA was confirmed to be a low-activity chymotrypsin-like protease that cleaves semenogelins during semen production (66). PSA is a member of the kallikrein family of proteins, of which human kallikrein 1 (hK1), hK2 and hK3 (PSA) are found principally in the prostate (63, 67). PSA shares up to 80% sequence homology with hK2 and several polyclonal PSA antibodies have been shown to cross-react with hK2, though the latter is present at significantly lower concentrations in the prostate and so is unlikely to influence interpretation in the majority of cases (63, 68).

As early as 1980, researchers were aware that PSA is elevated in benign conditions such as benign prostatic hyperplasia (69). The FDA approved PSA as a biomarker for prostate cancer detection in 1991, setting an upper limit of 3.9 ng/ml in the 50-54 year age group, following a study of 1653 men aged 50 and older (70). This cut-point has come under close scrutiny in recent years and there is also much controversy surrounding the appropriate cut-points to use, depending on the application (i.e. screening versus surveillance). One reason for the variable performance is that PSA levels increase naturally during life. Consequently one strategy has been to determine age group specific cut-points.

The specificity of PSA is also cause for concern. One study showed that only 40% of men with PSA levels of 4-10 ng/ml presented with a tumour at biopsy. In a study of 2950 men with PSA levels at or below 4 ng/ml, prostate cancer was diagnosed in 449 (15%) patients, including 68 men with high-grade cancer (71). In a separate study of 10,523 patients, 9211 with PSA values of 0-4 ng/ml, 478 men were diagnosed with prostate cancer. In addition, approximately half of the tumours not diagnosed using a PSA range of 0-4 ng/ml had aggressive characteristics (60). Other strategies using PSA have included determination of levels of PSA isoforms, specifically pro-PSA, an immature PSA precursor expressed predominately in tumours (as opposed to BPSA, which is largely confined to benign tumours), or determination of the so-called PSA velocity, which describes how PSA levels change over time. As yet, none of these alternative PSA measures has achieved universal acceptance.

### 1.3.2 Prostate cancer antigen 3

Rather than attempt to modify existing PSA tests, several research groups are working on new tools to augment or replace existing detection criteria. Among the tools being developed to complement PSA is detection of the prostate cancer marker PCA3 in urine. Prostate cancer antigen 3 (PCA3) is an evolutionarily conserved gene that is transcribed into a noncoding mRNA transcript with highly prostate-specific expression (72). The precise sequence of transcripts varies extensively due to the presence of five start sites and alternative splicing. There are also several stop codons, further suggesting that the resulting mRNA is noncoding. The biological role of PCA3 is still unclear. Some have suggested that the gene may be part of an RNA-mediated control mechanism, but so far no definitive evidence for such a role has been shown. The usefulness of PCA3 as a biomarker derives from the initial observation in a differential display study of 56 prostatectomy samples that it was exclusively present in prostate tissue (72). PCA3 is overexpressed 10-100 fold in prostatic tumours compared with adjacent normal tissue within the same patient and, unlike PSA, it is not influenced by the presence of benign conditions such as benign prostatic hyperplasia (72).

Initial development of a urine-based test for the detection of prostate cancer using PCA3 relied on the ratio of PCA3 mRNA, as determined by RT-PCR of RNA extracted from urine sediments, to PSA mRNA (73). Since PSA mRNA is present in healthy and diseased prostate cells and is only slightly overexpressed in tumour cells relative to normal cells, the ratio of mRNA levels allows for normalization of the number of prostate cells analysed (74). Early tests of PCA3 for prostate cancer detection yielded a sensitivity of 67% and specificity of 83% (73). In separate studies employing a nucleic acid sequence based amplification (NASBA) strategy, whereby RNA is amplified at constant temperature through double-stranded DNA intermediates, researchers found sensitivity of 66-82% and specificity 76-89% (74). Further development allowed use of whole urine instead of urine sediments and relied on transcription-mediated RNA amplification yielding sensitivity and specificity of 69% and 79% (75). The usefulness of PCA3 for the detection of high-grade prostatic intraepithelial neoplasia is currently unclear (76). Although the test relies on specialised sample handling and requires a reference laboratory for processing, a more important disadvantage of the PCA3 test is that it lacks sufficient sensitivity, despite significantly improved specificity, in comparison with PSA.

### 1.3.3 TMPRSS2-ERG

Prostate cancer is the result of a large number of genetic changes but one frequently occurring genetic alteration is the formation of the TMPRSS2:ERG fusion and subsequent overexpression of ETS-regulated gene, ERG. This mutation was identified by cancer outlier profile analysis (COPA), which uses nonparametric statistics to pick out outliers following compari-



son of tumour and normal material. In a meta-analysis of the Oncomine database comprising 132 genome expression data sets, Tomlins and colleagues identified the ETS family nuclear transcription factors ERG and ETV1 as being frequently involved in translocations with the androgen-dependent TMPRSS2 5' untranslated regulatory region, leading to overexpression of either ERG or ETV1 in prostate cancer epithelial tissue but not in adjacent precursor prostatic intraepithelial neoplasia or benign hyperplastic tissues (77).

ERG expression is common in prostate cancer, with one study reporting that 72% of cases showed elevated levels of the transcription factor (78). Despite the obvious importance of ERG expression in prostate cancer, there has so far been little success in employing ERG as a biomarker for prostate cancer detection. While follow-up studies showed that detection of ERG transcripts in urine following DRE is feasible, in a study of 237 patients, Rice and colleagues found that ERG score, a measure of ERG relative to PSA, had higher specificity (84%) but lower sensitivity (31%) than PSA at the 4 ng/ml cut-point (79). Biomarkers for the detection of genetic alterations such as TMPRSS2:ERG offer a promising new diagnostic approach with recent studies showing good specificity and sensitivity in cohort-based studies (80). Fusions other than TMPRSS2:ERG are also being explored, with early results identifying fusions involving CDKN1A (p21), CD9, and IKBKB (IKK-beta) (81).

At present PSA is the only biomarker approved by the FDA for prostate cancer detection in the screening setting. Several of the new molecular tools being developed have shown promising results, but these are not yet recommended in clinical guidelines, which instead rely on positive or suspicious digital rectal examination and/or elevated PSA levels observed in repeated tests (see [www.uroweb.org](http://www.uroweb.org)). Therefore there exists an urgent need for new biomarkers for prostate cancer detection.

## 1.4 Biomarkers for the diagnosis of pancreaticobiliary tract cancer

Pancreaticobiliary tract cancers are relatively infrequent and difficult to treat (82). Diagnostic tools are still required to confirm the presence of disease and to guide subsequent treatment (83, 84). Biliary strictures are commonly associated with pancreaticobiliary malignancy but the decision to proceed to treatment requires confirmation of the presence of disease. The ideal approach is to obtain material for analysis during endoscopic retrograde cholangiopancreatography (ERCP), so as to minimize invasive procedures and reduce the time to treatment. This is particularly important because pancreaticobiliary tract cancers are typically diagnosed late (83). Material should then be used in a simple, cost-effective test to provide an accurate diagnosis.

The current favoured approach is to collect cells by biliary brushing, which is then followed by cytological analysis based on morphological criteria to confirm malignancy. While brush cytology has excellent specificity, typically approaching 100%, sensitivity is variable, ranging from 30-57% in most studies (85, 86). The variation in part reflects the subjectivity inherent in pathological diagnosis, especially in the decision over how to treat cells in the so-called “cytological grey zone”, where strict morphological criteria for benign or malignant tumours are not met, but also reflects differences due to the primary site of the disease, reduced cellularity and pathologist experience (83, 84, 87). The need for accurate diagnosis of patients in the cytological grey zone is underlined by the progression model of cholangiocarcinoma, particularly for patients with biliary strictures resulting from primary sclerosing cholangiocarcinoma, which is a well-recognized risk factor for the development of malignancy (88). As yet there is no molecular biomarker in clinical use for surveillance of primary sclerosing cholangiocarcinoma, highlighting the urgent need for such a test.

While many cells are clearly malignant or benign, others present with a nonspecific atypical morphology (83). In several cases and under defined morphological criteria these atypia may be classified as malignant, thereby raising sensitivity albeit at the possible expense of lowering specificity. However this reclassification requires standard morphological criteria that researchers have yet to agree on (83). Cellular yield from biliary brushing is particularly problematic as it is affected by several parameters, including anatomic and tumour characteristics and the number of specimens collected per patient (83). Simple proposed solutions to increase the cellular yield such as increasing the number of brushings collected, processing the brush itself and using longer brushes have failed to significantly improve the number of cells available for analysis (83, 89, 90).

One alternative to the brush collection of cells is aspiration of bile directly from the biliary tree during ERCP. While the reported specificity using this technique is comparable to that of brush cytology, sensitivity is lower, ranging from 6-32% in a series of studies covering 351 patients (83). Although there is some evidence that this can be raised by taking multiple bile samples or dilating the stricture before sample collection, others report no such advantage and highlight the poor quality and low cellularity of bile samples (83, 91). Consequently there appears to be little benefit at present to direct analysis of bile. A second alternative is endoscopic ultrasound-guided fine needle aspiration. While initial studies suggested good sensitivity, subsequent reports indicated sensitivity comparable to brush cytology (83, 92).

In light of these concerns, researchers have in the last decade started looking at ways to expand existing protocols or define new markers for disease. The majority of this work is still experimental, though some has started to make inroads into clinical practise. Among the more promising avenues being explored are tests for soluble biomarkers such as CA 19-9 and CEA and genomic approaches that rely on the latest research into the genotypic characteristics uncovered in recent years.

### 1.4.1 Biochemical biomarkers of pancreaticobiliary tract cancer

The biochemical serum markers carbohydrate antigen 19-9 (CA19-9) and carcinoembryonic antigen (CEA) have been widely studied for the detection of pancreaticobiliary tract malignancy (93). CA19-9 is an antibody that detects the high molecular weight surface glycoprotein sialyl Lewis A, which has been implicated in cell-cell recognition and adhesion. It was originally identified as a circulating marker for colon cancer and was also found to be expressed in patients with gastric and pancreatic carcinomas (94).

A series of studies on the efficacy of CA19-9 for cholangiocarcinoma detection in patients with primary sclerosing cholangitis showed that CA19-9 had varying sensitivity and specificity, ranging from 38-89% and 50-98%, respectively (93). More recently, Morris-Stiff and colleagues showed that CA19-9 had good sensitivity and specificity (95). Using a cut-off of 70.5 U/ml, CA19-9 had 82% sensitivity and 86% specificity. These results were further improved by combining data from standard radiographic techniques. There have also been studies that demonstrate that pretreatment CA19-9 and CA19-9 kinetics may serve as a prognostic marker in advanced pancreatic cancer (96). One particular disadvantage for CA19-9 is that it is not normally expressed in approximately 7% of the general population, raising the chance of false-negative results (97). In addition, CA19-9 is nonspecific, being elevated in gastric, ovarian, hepatocellular and colorectal cancers and also in benign conditions such as obstructive jaundice (93, 94).

Another protein involved in cell adhesion is the glycoprotein carcinoembryonic antigen (CEA), which was initially discovered in colorectal carcinoma, where it has been extensively studied as a diagnostic marker (93, 98). CEA has similar diagnostic capacity as CA19-9, with a sensitivity of 33-68% and specificity of 79-100% found in a review of recent diagnostic assays using serum (93). A similar analysis for bile-based assays did not show any important differences (93). While the performance of CA19-9 and CEA alone for detection of malignancy has been disappointing, there is preliminary evidence that their combined efficiency is enhanced (99). Nevertheless, neither marker is currently recommended for the diagnosis of pancreaticobiliary malignancy.

### 1.4.2 Genetic biomarkers of pancreaticobiliary tract cancer

A different approach to the diagnosis of malignancy in biliary strictures is determination of loss of heterozygosity of tumour suppressor genes and mutation analysis, which potentially limits false-positives associated with benign inflammatory conditions. Khalid and colleagues isolated DNA from aggregated cell clusters obtained during ERCP and used PCR to amplify 12 microsatellite markers associated with tumour suppressor genes and also codon 12 of k-ras (100). In a study of 26 patients presenting with biliary strictures, LOH and mutation detection

had 100% sensitivity and specificity, however interpretation is complicated by the two methods used to obtain sufficient DNA for analysis.

Among the known genetic biomarkers for the detection of pancreaticobiliary malignancy are k-ras, which is abnormally expressed in 21-100% of cholangiocarcinomas, and TP53 (encoding p53), abnormally expressed in up to 37% (93). Studies suggest that k-ras activation is an early event in cholangiocarcinoma (101). However, these markers have as yet failed to outperform cytology, though there is evidence that combining k-ras evaluation with cytology improves the latter's sensitivity, albeit at the cost of reduced specificity (93, 102-104). Overall, however, the usefulness of TP53 and k-ras mutation analysis in the diagnosis of biliary strictures is questionable as studies on TP53 have shown conflicting results and k-ras codon 12 mutations have widely varying prevalence. In addition, both mutations are found in patients without evidence of carcinoma (87). There is thus a specific need for a test to aid in diagnosis of strictures in the cytological grey zone, which are usually classified as suspicious, atypical or dysplastic (84).

In a recent study, Morena Luna and colleagues examined the usefulness of aneuploidy, as determined by digital image analysis (DIA) or fluorescence in situ hybridization (FISH), for the diagnosis of pancreaticobiliary malignancy (105). In a cohort of 233 patients, cytology had a sensitivity of 4-20% compared with 35-60% for FISH using the UroVysion system (see section 3.3. above) for detection of changes in the copy numbers of chromosomes 3, 7 and 17 and locus 9p21. FISH had comparable specificity to cytology but lower sensitivity in patients with primary sclerosing cholangitis, suggesting that the test is susceptible to benign inflammatory conditions. DIA had intermediate sensitivity while specificity compared favourably with both cytology and FISH. A further disadvantage of this approach is that at present FISH is several times more expensive than cytology.

While recent research has resulted in promising leads, there are still no biomarker assays in routine clinical use that would allow detection of pancreaticobiliary tract disease. Thus there remains an urgent need for biomarkers that would allow the confirmation of suspicious biopsies obtained during ERCP by improving the poor sensitivity of biliary brush cytology and bile analysis while minimizing damage to the biliary tree in resectable cases.

## **1.5 The DNA replication initiation machinery as a promising target for biomarker development**

The search for biologically relevant biomarkers has led researchers to scrutinize the molecular networks that regulate cellular processes, from the mitogenic and oncogenic signalling pathways that control proliferation to such basic cellular functions as differentiation and apoptosis. Much

has been achieved in the past decade using the new tools of systems biology. Genome-wide analyses in particular increasingly yield new strategies for biomarker development. Although no genome wide assay has crossed into routine clinical use, the MicroArray Quality Control (MAQC) study, led by the US FDA, is examining the practicalities of standardizing assay performance across multiple institutions (106).

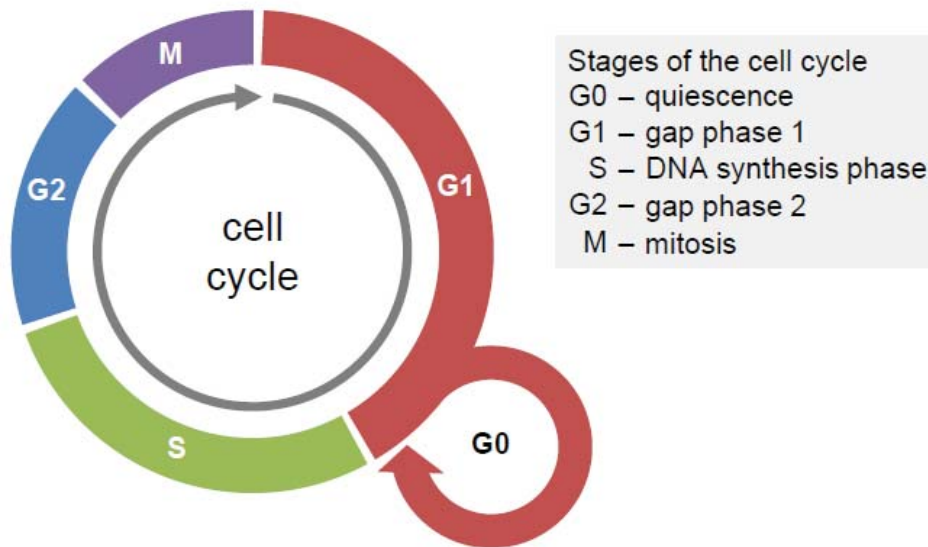


Figure 1.2: The cell cycle. The eukaryotic cell cycle consists of four distinct phases. In G1, undergo growth biosynthesis and are responsive to mitogens and other growth factors. In S phase, cells duplicate their DNA through semi-conservative DNA replication. In G2, cells undergo further growth and biosynthesis in preparation for mitosis. In M phase, cells undergo mitosis and cytokinesis. Cells are able to reversibly exit the cell cycle into the resting G0 state or exit irreversibly through differentiation and senescence.

Systems biology approaches to biomarker development focus on the complex and partially redundant signalling pathways that control cellular functioning. An alternative is to concentrate on the replication licensing proteins that license DNA for duplication and consequently serve as an integration point for the information transduced by upstream signalling pathways (3). Among the most promising targets are the minichromosome maintenance (Mcm) 2-7 proteins (collectively MCM), which participate in the assembly of pre-replicative complexes to establish competence for initiation of DNA synthesis in a process known as “licensing”.

### 1.5.1 MCM loading licenses origins for replication

In order to prevent aberrant replication and subsequent genomic instability, DNA replication requires precise duplication of the entire genome (107). The first step is the formation of the macromolecular pre-replication complex (pre-RC) at genomic sites of initiation called origins (Figure 3). Pre-RC assembly begins in late mitosis/early G1 phase with the binding of the heterohexameric origin recognition complex (ORC) comprising Orc1-6 proteins to approximately

30,000 origins of replication distributed across the genome (5, 108, 109). Evidence suggests more origins exist than are utilized during any genome duplication event and that this may be related to genomic stability (109, 110). The crucial event during DNA replication initiation is the loading of the Mcm2-7 heterohexameric complex that constitutes the core replicative helicase onto ORC at origins of replication (6). The Mcm2-7 proteins do not have inherent affinity for DNA and so must be actively brought to origins. This is achieved through the action of the proteins Cdc6 and Cdt1 and is critically dependent on their ability to utilize ATP (111, 112). Mcm2-7 are initially only loosely associated with DNA at the origin but ATP hydrolysis results in the complex being tightly bound, or “loaded”. Once the Mcm2-7 complex is loaded onto DNA the origin is “licensed” for replication (4).

DNA replication is initiated from licensed origins following the formation in S phase of the replisome containing Cdc45, GINS, replication protein A (RPA), DNA polymerase primase and DNA polymerase and the subsequent activation of replication forks (5, 113-115). The transition from licensed origins to active replication forks takes place during origin firing, which is crucially dependent on phosphorylation by cell cycle regulated kinases (5). The most important of these kinases regulating the initiation of replication are cyclin E and cyclin A-dependent kinases (CDKs) and the Dbf4- and Drf1-dependent kinase Cdc7 (also called DDK), all of which are essential for proper duplication of the genome (5, 6). A principle target of the phosphorylation activity during origin firing is the Mcm2-7 complex (116-120).

To ensure that origins are licensed once and only once during each passage through the cell cycle, cells employ a number of control mechanisms (4, 5). Cdt1, which chaperones Mcm2-7 to DNA, is an important regulatory target. After the onset of S phase, Cdt1 is targeted for proteolytic degradation by phosphorylation and ubiquitination (121-124). A second control mechanism involves the action of the novel regulator geminin (125). Geminin tightly binds Cdt1 and through steric hindrance is able to prevent binding of Cdt1 to MCM, thereby sequestering it away from the assembling pre-RC (126-128).

The Mcm2-7 proteins are present in all phases of the proliferative cell cycle but are absent in the quiescent, terminally differentiated and senescent out-of-cycle states (3). The majority of human cells are not actively engaged in the cell cycle but rather reside in out-of-cycle states, with only a minority of cells actively cycling (129, 130). Therefore the Mcm2-7 proteins appear to be attractive potential biomarkers of aberrant growth that are able to detect maturation arrested cells and malignancy. Evidence for this approach comes from a number of pilot studies which are discussed below demonstrating the clinical utility of replication initiation proteins as biomarkers.



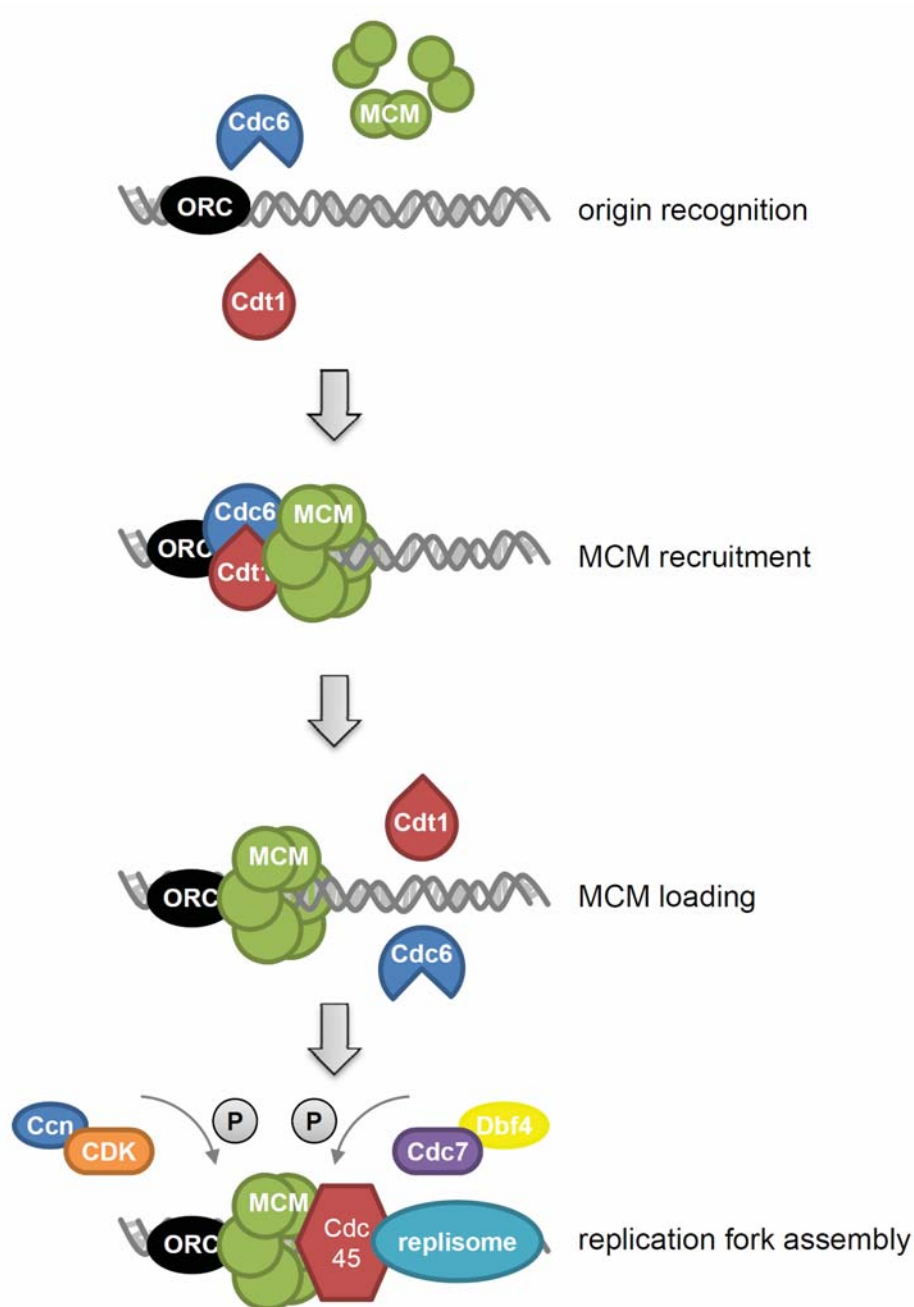


Figure 1.3: Initiation of DNA replication. Origins of DNA replication are recognized by the ORC complex, which serves as a platform for the assembly of the replication fork. Cdc6 and Cdt1 cooperate to recruit the Mcm2-7 heterohexameric replicative helicase complex to the origin. Initially, the Mcm2-7 proteins are loosely associated with DNA but the complex becomes stably associated, or loaded, in an ATP-dependent process. Mcm2-7 is subsequently phosphorylated by cyclin-CDK and Dbf4-Cdc7 complexes, followed by recruitment of the replisome, and assembly of the replication fork (4, 5).

### 1.5.2 MCMs detect aberrant growth and are potential diagnostic biomarkers

The loading of the Mcm2-7 replicative helicase on chromatin in G1 phase licenses origins for replication in the subsequent S phase and is the crucial event in the initiation of DNA replication. Early work using an *in vitro* cell-free tissue culture model system showed that the Mcm2-7 proteins are displaced from chromatin and Cdc6 is downregulated in mammalian cells following exit from the cell cycle into the G0 quiescent state (131). Nuclei isolated from quiescent 3T3 cells were unable to initiate replication in cytosolic extracts from S phase HeLa or 3T3 cells due to downregulation of Cdc6 and absence of chromatin-bound Mcm2-7, indicating that origins are not licensed in quiescent cells. Subsequent work demonstrated that downregulation of Cdc6 and MCM proteins is a characteristic of cells that have lost proliferative capacity during exit from the cell cycle into out-of-cycle states through reversible exit into G0 (quiescence), maturation during differentiation and irreversible exit during senescence (132). Interestingly, replication proteins have been shown to be directly important for mediating the loss of proliferative capacity that accompanies differentiation. In a study of the HL60 cell line differentiation model system, Cdc6 was found to be a rate-limiting factor that determined the loss of proliferative capacity that accompanies differentiation (133).

The finding that MCMs are downregulated in out-of-cycle states is supported by the expression profiles of MCM proteins observed in normal, dysplastic and malignant epithelial-lined self-renewing tissues (134, 135). In normal and reactive tissues of bladder, cervix, colon, lung and skin, MCMs were detectable by immunostaining in the basal proliferating compartment and were absent from mature, differentiated cells at the surface epithelial layer (134). MCM expression was similarly confined to the basal proliferative compartment in nondysplastic squamous epithelium and Barrett's oesophagus in oesophageal tissue (135). In contrast, dysplastic lesions of cervix, colon, oesophagus and skin and low grade non-muscle invasive bladder carcinoma showed aberrant MCM immunostaining in the layers above the basal proliferative compartment (134). MCM immunostaining was also detected suprabasally in dysplastic squamous epithelium and Barrett's mucosa (135). These findings demonstrate that MCMs are able to detect maturation arrest associated with expansion of the proliferative compartment in precancerous lesions (3). Aberrant MCM immunostaining was even more pronounced in neoplastic cells from these tissues (134, 135). In addition, the percentage of MCM positive cells detected in malignant cases had an inverse correlation with the degree of differentiation, with low grade (well differentiated) tumours showing lower labelling indices than high grade (poorly differentiated) tumours (134). Together these studies demonstrate that MCMs are markers of growth that are able to detect maturation arrested cells and are therefore of potential clinical importance for cancer detection (3).

In the first clinical test of the potential of MCMs to detect aberrant growth of maturation



arrested cells, Mcm5 was incorporated into an immunoenhanced Pap smear test and its performance was compared with that of the conventional test (136). The Pap smear test is a cytological test that is routinely used for the diagnosis of cervical cancer but it suffers from high false-negative rates (137). The immunoenhanced Pap smear test detected all positive dysplastic and neoplastic cases (28/58) identified by the conventional test. In addition, the Mcm5-incorporating test detected two high-grade squamous epithelial lesions that were missed by the conventional Pap smear test (136). This study suggested that Mcm5 is potentially a sensitive and specific cancer biomarker.

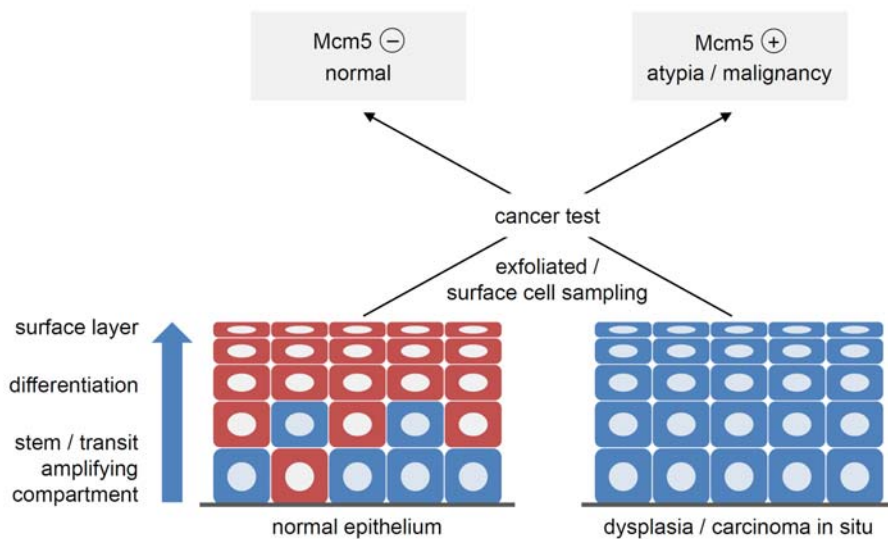


Figure 1.4: The MCM cancer detection test. In normal epithelium, MCMs are expressed solely in the basal stem/transit amplifying compartments and are absent from surface layers, where cells become fully differentiated. In premalignant/dysplastic epithelial lesions there is an expansion of the proliferative compartment coupled to arrested differentiation, resulting in cycling, MCM positive cells appearing in superficial layers. Superficial cells obtained either through exfoliation or by surface sampling should therefore be negative for MCMs. Detection of MCMs in these cells is therefore indicative of an underlying premalignant/dysplastic lesion or malignancy (3).

Expression analysis of Mcm5 in bladder urothelium showed that Mcm5 was detectable only in the basal stem-transit amplifying compartment in normal tissues (138). In contrast, Mcm5 immunostaining was present in basal, intermediate, and superficial epithelial cells in cases of both non-invasive and invasive bladder cancer, showing that maturation arrested cells were present throughout the urothelium, even in early stage disease (Figure 4). In a proof-of-principle study into the potential of Mcm5 as a diagnostic biomarker for bladder cancer, a novel two-site time-resolved immunofluorometric assay for the detection of Mcm5 in voided urine showed a significantly higher Mcm5 levels in bladder cancer cases compared with normal controls (138). In a separate study, application of this Mcm5 test to gastric aspirates from 40 patients demonstrated that Mcm5 had high sensitivity (85%) and specificity (85%) for identifying oesophageal cancer (139).

A second generation Mcm5 test employing europium-coupled monoclonal antibodies in a dissociation enhanced lanthanide fluorometric immunoassay (DELFI) showed that Mcm5 had high sensitivity and specificity for the detection of bladder cancer in urine sediments in a controlled clinical setting (140). The immunofluorometric Mcm5 assay had a high area under the receiver operator characteristic (ROC) curve (AUC=0.93). At the assay cut-point where specificity was equal to that of routine urine cytology, the test had enhanced sensitivity over cytology. Importantly, the Mcm5 immunoassay was not affected by benign conditions such as bacillus CalmetteGuerin (BCG)-induced granulomatous cystitis and benign prostatic hyperplasia (140). However, the test was susceptible to false-positives in the presence of bladder trauma such as stones, as a result of the surface exposure of normal cycling cells in underlying epithelial tissue layers to the bladder lumen. One intriguing observation from the same study was that the immunofluorometric assay also showed an ability to detect early stage organ-confined cases of prostate cancer (140).

Together, these findings suggest that Mcm5 holds promise as a biomarker for the diagnosis of bladder cancer and also has potential clinical utility for prostate cancer detection. These studies warrant further investigation in larger clinical studies to determine the efficiency of Mcm5 as a diagnostic biomarker for bladder and prostate cancer detection.

### **1.5.3 Replication initiation proteins are potential prognostic and predictive biomarkers**

MCMs are able to detect aberrant growth characteristic of maturation arrest. An important question is whether this is able to provide prognostic information about disease progression. In a retrospective study of 92 patients with prostate cancer and 5 normal controls, Mcm2 immunodetection was demonstrated to be an independent predictor of disease-free survival (141). Mcm2 expression was low in cells of the prostate gland basal epithelial layers, while tumours had higher Mcm2 labelling indices and the presence of Mcm2-positive cells at the luminal surface epithelial layers. An increased Mcm2 labelling index was associated with reduced disease-free survival and was independent of primary grade and the presence of neoadjuvant therapy on multivariate analysis. Additional evidence for the prognostic value of replication initiation proteins comes from a study of Mcm2, the Cdt1 inhibitor geminin (expressed in S, G2 and M phases), and the proliferation marker Ki67 in renal cell carcinoma (142). Labelling indices for all three markers increased significantly with increasing tumour grade, while Mcm2 and geminin indices also increased with tumour size. To identify cells that were licensed but not cycling, a novel Mcm2-minus-Ki67 index was calculated. This Mcm2Ki67 index also increased significantly with grade and tumour size. Increased indices for all four markers were associated with reduced disease-free survival. In addition, an Mcm2Ki67 index greater than 30% was a significant prognostic factor.

A further demonstration of the clinical utility of indices composed of combinations of DNA replication licensing factors comes from a study into the cell cycle kinetics of mammary neoplasia (143). Expression profiles of Ki67, Mcm2, geminin, estrogen receptor (ER), progesterone receptor (PR) and human epidermal growth factor receptor 2 (HER2) were used to determine the rate of cell cycle progression in normal breast and breast cancer tissues. Ki67 is detectable throughout the cell cycle, in contrast to Mcm2, which is present in cells progressing through the cell cycle and also in cells licensed for replication. Geminin, meanwhile, is expressed exclusively in S-G2-M. These cell cycle expression characteristics allow relative ratios of these proteins to provide insight into the dynamics of cell cycle progression. An increased ratio of Mcm2 to Ki67 (Mcm2/Ki67) is reflective of a relative increase in the number of cells that are licensing for replication but are not actively growing, while an increased ratio of geminin to Ki67 (geminin/Ki67) is associated with shortening of the G1 phase of the cell cycle (144, 145). Applying analysis of these markers to normal and neoplastic breast cancer tissue samples, Shetty and colleagues showed that ductal epithelial cells from normal, reduction mammary specimens reside predominantly in a primed state, with Mcm2 but not Ki67 or geminin staining (143). This intriguing state is perhaps an evolutionary holdover that allows normal breast cells to respond rapidly to pregnancy. In contrast to normal breast cancer cases, breast tumour specimens possessed cells in an actively cycling state, characterized by the presence of all three markers. A correlation was also observed between a higher geminin/Ki67 ratio, indicative of a shortening G1 phase, and increasing tumour grade. Replication initiation proteins therefore appear able to provide cell cycle kinetic information that is potentially of prognostic significance.

The findings of Shetty and colleagues are supported by a study of replication initiation proteins and markers associated with mitosis and genomic stability in the context of epithelial ovarian carcinoma (146). In a study of 143 women with epithelial ovarian carcinoma, Mcm2, geminin, Ki67 and the mitotic kinases Aurora A and Aurora B showed a significant association with tumour grade and also with the degree of divergence from the normal diploid chromosome complement (aneuploidy). Aurora A and its substrate, histone H3 phosphorylated on serine 10 (H3S10ph), were significantly associated with tumour stage. Aurora A and the aneuploidy status of the tumour were also found to be predictive of disease-free survival. The results suggest that replication initiation factors may contribute to a disease progression model for this common malignancy. In a separate study, Loddo and colleagues demonstrated that Mcm2, geminin, Ki67, Aurora A and B, phosphohistone H3 (H3S10ph) and the mitotic kinase Plk1 together identify three unique phenotypes in breast cancer: an out-of-cycle phenotype in which most cells do not express Mcm2; a G1-delayed/arrested phenotype in which cells show high levels of Mcm2 but low levels of the remaining markers; and an aggressive accelerated cell cycle progression phenotype in which cells show high levels of Mcm2 and the S-G2-M progression markers (Figure 5) (147).

Application of these markers to tumours from a cohort of 182 breast cancer patients showed that

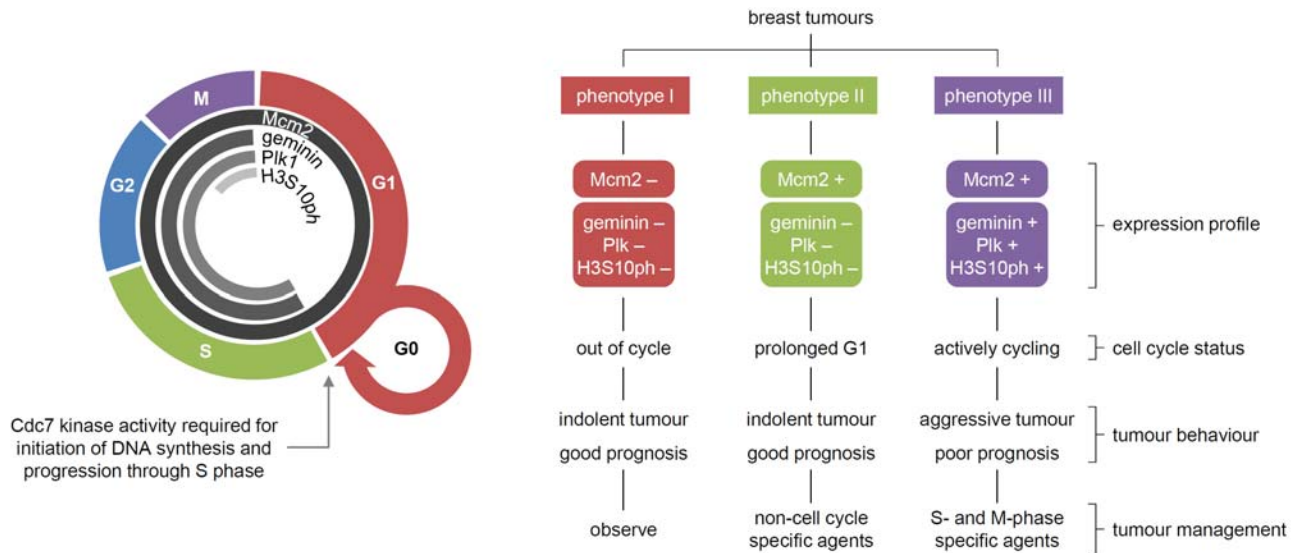


Figure 1.5: Identification of unique cell cycle phenotypes in breast cancer. Phase-specific distribution of cell cycle biomarkers in proliferating cells and out-of-cycle states. Three distinct cell-cycle phenotypes (I, II, and III) are characterized by the differential expression of the cell cycle markers Mcm2, geminin, Plk1, and histone H3 phosphorylated on serine-10 (H3S10ph) (147).

the accelerated cell cycle progression phenotype was significantly associated with HER2-positive and triple receptor negative phenotypes, breast cancer subtypes that have a significantly worse prognosis. In addition, the accelerated cell cycle progression phenotype was associated with a higher relapse rate than either the G1-delayed/arrested or out-of-cycle phenotypes. It appears that breast cancers with an accelerated cell cycle progression phenotype are actively engaged in the cell cycle and so are more likely to respond to targeted chemotherapies that act specifically in S- or M-phase of the cell cycle (147).

Therefore the profile of cell cycle markers provides a readout of upstream signalling pathways and delivers important prognostic and predictive information that has the potential to guide treatment decisions using cell cycle phase specific chemotherapeutic agents (3). The expression dynamics of replication initiation proteins are revealing new diagnostic and therapeutic targets. Elevated levels of Cdc7, a kinase essential for replication origin activation through its ability to phosphorylate the Mcm2-7 complex (see above), profoundly affect the malignant potential of tumours. A recent study of epithelial ovarian cancer showed that high Cdc7 levels were associated with arrested differentiation, advanced clinical stage, genomic instability and accelerated cell cycle progression (148). Cdc7 was also found to be an independent prognostic indicator of disease-free survival. Subsequent in vitro studies using the SKOV-3 and Caov-3 ovarian cancer tissue culture model systems demonstrated that Cdc7 downregulation induced apoptosis in transformed but not in untransformed cells, consistent with previous observations (7, 148). These findings demonstrate that the replication initiation factor Cdc7 is dysregulated during the development of ovarian cancer and serves as a potential anticancer target.

## 1.6 The DNA replication initiation machinery is a potential therapeutic target

The initiation of DNA replication is a crucial event in the cell cycle that is tightly regulated (149). Recent research suggests that disruption of the orderly events that initiate replication have a differential response on normal and cancer cells and can induce cancer cell specific killing. In an important early demonstration of this requirement for strict control of replication initiation, Shreeram and colleagues showed that U2OS and Saos-2 osteosarcoma cells expressing a nondegradable form of the origin licensing repressor geminin enter an abortive S phase followed by apoptotic cell death (150). In contrast, untransformed IMR90 primary fibroblast cells did not enter S phase or undergo cell death but rather arrested in G1 phase without the appearance of apoptosis. These results point to the existence of a previously unknown checkpoint that prevents normal cells from entering S phase if origin activation is impaired.

Further support for the existence of a putative origin activation checkpoint comes from a study into the effects of Cdc7 depletion on normal and cancer cells. Cdc7 is an important replication initiation protein that activates the Mcm2-7 complex during origin firing (151). In addition, Cdc7 has roles as both mediator and effector of the DNA damage response through its interaction with claspin and the DNA damage response pathway (151, 152). Abrogation of the DNA damage response allows cells to continue through the cell cycle, leading to mitotic catastrophe and cell death. Montagnoli and colleagues demonstrated that normal human diploid fibroblasts depleted of Cdc7 do not undergo cell death but rather accumulate with a DNA content characteristic of late G1 or early S phase (7). This cell cycle arrest is p53-dependent, as demonstrated by concomitant upregulation of p53 and p21 and phosphorylation of Rb at Ser807/811, and it does not lead to the phosphorylation events characteristic of the DNA damage response. However, co-depletion of p53 in normal cells prevented induction of p21 and led to phosphorylation of Rb at Ser807/811. Together these results demonstrate that in the presence of replication stress, normal cells induce a p53-dependent checkpoint following Cdc7 depletion (7). In contrast to the response in normal cells, depletion of Cdc7 in transformed cell lines results in cancer cell specific killing. Cancer cells depleted of Cdc7 proceed into S phase and do not engage the DNA damage checkpoint, instead undergoing mitotic catastrophe and apoptosis. The DNA damage checkpoint is mediated by the ATM/ATR kinase pathway, which induces phosphorylation of the DNA damage checkpoint kinases Chk1 and Chk2 and is further characterized by the degradation of Cdc25A phosphatase (153). Although depletion of Cdc7 in p53-mutant HeLa cells led to hypophosphorylation of Mcm2 it did not induce Chk1/Chk2 phosphorylation or Cdc25A downregulation, in contrast to the response observed following treatment with the DNA elongation inhibitor hydroxyurea (7, 154, 155). This result suggests that cancer cells do not arrest in G1 and are not able to engage the DNA damage checkpoint response following Cdc7 depletion (156). A similar pattern was observed in p53-wildtype HCT-116 colon carci-



noma cells, indicating that the cell death response following Cdc7 depletion is independent of p53 status (7).

These exciting results provided early support for the notion that Cdc7 could be useful as a therapeutic target to induce cancer cell specific killing in cycling p53-mutant cancer cells. Early work by Vanotti and colleagues identified the pyrrolopyridinone PHA-767491 as a potential inhibitor of Cdc7 (157). Subsequent studies using this molecule demonstrated in vitro cell death in cancer cell lines and reduction in tumour volume in nude mice carrying tumours induced by implantation of cells from the HL60 (acute myeloid leukaemia), A2780 (ovary carcinoma), Mx-1 (mammary adenocarcinoma) and HCT-116 (colon carcinoma) lines (158). However, the interpretation of these results is complicated by the ability of PHA-767491 to inhibit Cdk9, a component of Positive Transcription Elongation Factor b (P-TEFb), which is important for the elongation phase of transcription (159, 160). PHA-767491 was found to inhibit Cdk9 with a half-maximal inhibitory concentration (IC<sub>50</sub>) of similar magnitude (34 nM) to that of Cdc7 (10 nM), with further effects noted for Cdk1, Cdk2, Cdk5, Chk2, GSK3- and Plk1, albeit with 20- to 100-fold lower potency (158). A more recent study by the same group has identified a new compound with similar potency against Cdc7 (IC<sub>50</sub> 22 nM) and enhanced specificity (Cdk9 IC<sub>50</sub> 394 nM), though the compound has yet to be fully characterized in biological studies (161).

The past five years have seen a surge of interest in small molecule inhibitors that specifically target Cdc7 (151, 156, 157, 162-165). A crucial question that remains to be answered if Cdc7 is to be targeted for therapeutic intervention is whether the checkpoint induced by Cdc7 depletion is reversible in normal cells. Reversibility of the origin activation checkpoint would allow combination therapy with S- or M-phase directed agents and Cdc7 inhibitors. Under these conditions, cancer cells that have lost the checkpoint would undergo mitotic catastrophe and apoptosis while normal cells would be shielded from the deleterious effects of these agents. However, the checkpoint must be reversible if normal cells are to resume normal function once the cancer cell killing agents have been metabolised to avoid toxic effects on self-renewing tissues. Determination of the reversibility of the Cdc7-induced cell cycle arrest requires a more detailed molecular understanding of the nature of the checkpoint.

## 1.7 Scope of the thesis

The initiation of DNA replication is a key event in the cell cycle that acts as a convergence point for information transduced by the complex network of partially redundant upstream mitogenic and oncogenic signalling pathways. This identifies the components of the DNA replication initiation machinery as important targets for the development of novel biomarkers that are able to detect cancer, provide information about the progression of disease and predict the

response of targeted therapeutic agents directed against components of the cell cycle.

Bladder cancer is a common malignancy for which several biomarkers have received regulatory approval for use in screening and monitoring. However, these tests have had a limited effect on patient management and there still exists an urgent need for accurate noninvasive biomarkers. Previous pilot studies demonstrated that the replication licensing factor Mcm5 is a promising biomarker for bladder cancer detection, though these studies were conducted in small patient cohorts. In Chapter 2 I present the results from the first large-scale prospective double-blinded multicentre trial into the use of immunofluorometric detection of Mcm5 in urine sediments as a diagnostic biomarker for bladder cancer. In a patient cohort of 1677 patients, Mcm5 performance is compared with that of the FDA approved biomarker NMP22 and also with routine diagnostic tools, including cytology and ultrasound. In addition, the performance of Mcm5 is compared for gender related differences and the combination of Mcm5 and NMP22 is examined for possible additive effects in detecting clinically relevant disease.

Previous observations suggested that, in addition to bladder cancer, Mcm5 has clinical utility for the detection of prostate cancer. Diagnostic and treatment decisions in prostate cancer typically rely on detection of prostate specific antigen (PSA), a non-cancer specific marker of disease. The use of PSA has come under scrutiny and it is now recognized that there is a need for new biomarkers for this malignancy. In Chapter 3 I report the findings from a recent cohort study into the ability of detection of Mcm5 in urine sediments to diagnose prostate cancer. The study examined the efficacy of an immunofluorometric Mcm5 test to detect malignancy in a cohort of 88 men with clinically confirmed disease and two disease-free control groups, one group with low PSA values and a second group chosen irrespective of PSA status. In addition, the study tests the hypothesis that Mcm5 test performance can be increased by the use of prostate massage during digital rectal examination.

In Chapter 4 I present the findings of a recent clinical study of the ability of Mcm5 to detect pancreaticobiliary tract cancer. Currently diagnoses are made on the basis of biliary brush cytology, which is constrained by low sensitivity. In addition, clinical management is complicated because malignancy is usually detected late and at present there are no molecular biomarkers in routine use. Here I report the results from a proof-of-concept study of 102 patients with strictures of established or indeterminate aetiology to demonstrate the ability of the immunofluorometric Mcm5 test to detect malignancy in bile samples obtained during endoscopic retrograde cholangiopancreatography. The performance of the Mcm5 test is compared with that of biliary brush cytology and the test is analyzed for its sensitivity to benign conditions. In addition, normal and malignant strictures are examined immunohistochemically to determine the relationship between expression patterns of MCM proteins and neoplasia.

Replication licensing proteins have proven diagnostic utility for cancer detection. In addition these proteins have the potential to provide prognostic information about disease progression.

In Chapter 5 I present results from a clinical study examining the use of replication licensing factors and DNA ploidy status as prognostic markers in the setting of penile squamous cell carcinoma. PeSCC is a rare malignancy with poor outcome in men with advanced disease. Radical surgery is associated with improved survival but patient selection remains problematic. In addition, there are few prognostic markers currently available. This study of 141 patients with PeSCC explores the use of Mcm2, geminin, Ki67 and ploidy status to provide prognostic information in conjunction with conventional clinicopathological parameters and to stratify patients into low- and high-risk groups.

Previous studies demonstrated that perturbation of replication initiation leads to cell cycle arrest at or before the onset of DNA synthesis in normal cells. Depletion of the cell cycle kinase Cdc7, which activates the Mcm2-7 replicative helicase, has been shown to induce cell cycle arrest at the G1-S transition, suggesting the functioning of a putative origin activation checkpoint. In cancer cells, Cdc7 depletion leads to bypass of this checkpoint and induces cancer cell specific killing, an observation with important implications for targeted therapy. At present, the nature of this checkpoint is largely unknown. In Chapter 6 I present data outlining for the first time the molecular architecture of this novel checkpoint in normal human diploid fibroblasts and demonstrate that it requires key proto-oncogenic and tumour suppressor proteins frequently mutated in human cancers and which participate here in a non-redundant, tripartite response network to induce cell cycle arrest in G1. The checkpoint is further characterized using gene expression microarrays to identify key effector proteins involved in maintenance of the checkpoint response.

The differential response of normal and cancer cells to Cdc7 depletion makes Cdc7 an important target for therapeutic intervention. In Chapter 7 I present data from a detailed study of Cdc7 in breast cancer samples and in vitro cell culture model systems. Cdc7 is examined in luminal, HER2-overexpressing and triple receptor negative breast cancer subtypes to determine if overexpression is associated with aggressive disease. Breast cancer subtypes have been shown to correlate with cell cycle phenotypes derived from expression patterns of replication initiation and mitotic regulation markers. This study explores the potential of these phenotypes and their correlation with Cdc7 expression to predict the response to Cdc7 targeted therapies. In addition, Cdc7 depletion is examined in p53-mutant HER2-overexpressing and triple receptor negative breast cancer cell lines in which the checkpoint is inactive, and the study explores the reversibility of the origin activation checkpoint in human mammary epithelial cells. Reversibility of the checkpoint is essential to avoid toxicity in self-renewing tissues and has important implications for targeted therapy using Cdc7 small molecule inhibitors and cell cycle phase specific chemotherapeutic agents.

In Chapter 8 I summarize the results obtained in the work of this thesis, drawing together the separate studies to discuss the implications for diagnostic and prognostic biomarkers based on the replication initiation machinery. Moreover, I summarize the state of these biomarkers in



the transition from bench to bedside and address their potential impact on health care costs and patient care. In addition, I discuss the potential of replication initiation factors to provide predictive information and the implications this may have for disease treatment with available cell cycle phase specific chemotherapeutic agents and Cdc7 small molecule inhibitors currently in development.

## 1.8 References

1. Hanahan D, Weinberg RA. The hallmarks of cancer. *Cell* 2000;100:57-70.
2. Hanahan D, Weinberg RA. Hallmarks of cancer: the next generation. *Cell* 2011;144:646-74.
3. Williams GH, Stoeber K. Cell cycle markers in clinical oncology. *Curr Opin Cell Biol* 2007;19:672-9.
4. Sclafani RA, Holzen TM. Cell cycle regulation of DNA replication. *Annu Rev Genet* 2007;41:237-80.
5. Masai H, Matsumoto S, You Z, Yoshizawa-Sugata N, Oda M. Eukaryotic chromosome DNA replication: where, when, and how? *Annu Rev Biochem* 2010;79:89-130.
6. Labib K. How do Cdc7 and cyclin-dependent kinases trigger the initiation of chromosome replication in eukaryotic cells? *Genes Dev* 2010;24:1208-19.
7. Montagnoli A, Tenca P, Sola F, et al. Cdc7 inhibition reveals a p53-dependent replication checkpoint that is defective in cancer cells. *Cancer Res* 2004;64:7110-6.
8. Chin L, Gray JW. Translating insights from the cancer genome into clinical practice. *Nature* 2008;452:553-63.
9. Van't Veer LJ, Bernards R. Enabling personalized cancer medicine through analysis of gene-expression patterns. *Nature* 2008;452:564-70.
10. Hanash SM, Pitteri SJ, Faca VM. Mining the plasma proteome for cancer biomarkers. *Nature* 2008;452:571-9.
11. Swami M. Proteomics: A discovery strategy for novel cancer biomarkers. *Nat Rev Cancer* 2010;10:597.
12. Barabasi AL, Gulbahce N, Loscalzo J. Network medicine: a network-based approach to human disease. *Nat Rev Genet* 2011;12:56-68.
13. Sawyers CL. The cancer biomarker problem. *Nature* 2008;452:548-52.
14. Kulasingam V, Pavlou MP, Diamandis EP. Integrating high-throughput technologies in the quest for effective biomarkers for ovarian cancer. *Nat Rev Cancer* 2010;10:371-8.
15. Green ED, Guyer MS. Charting a course for genomic medicine from base pairs to bedside. *Nature* 2011;470:204-13.
16. Ludwig JA, Weinstein JN. Biomarkers in cancer staging, prognosis and treatment selection. *Nat Rev Cancer* 2005;5:845-56.
17. Visvader JE. Cells of origin in cancer. *Nature* 2011;469:314-22.

18. Altekruse SF, Kosary CL, Krapcho M, et al. SEER Cancer Statistics Review, 1975-2007. Bethesda, MD: National Cancer Institute; 2010.
19. Babjuk M, Oosterlinck W, Sylvester R, Kaasinen E, Bohle A, Palou-Redorta J. EAU guidelines on non-muscle-invasive urothelial carcinoma of the bladder. *Eur Urol* 2008;54:303-14.
20. Gaston KE, Grossman HB. Proteomic assays for the detection of urothelial cancer. *Methods Mol Biol* 2010;641:303-23.
21. Mitra AP, Cote RJ. Molecular pathogenesis and diagnostics of bladder cancer. *Annu Rev Pathol* 2009;4:251-85.
22. Lotan Y, Shariat SF. Impact of risk factors on the performance of the nuclear matrix protein 22 point-of-care test for bladder cancer detection. *BJU Int* 2008;101:1362-7.
23. Stein JP, Lieskovsky G, Cote R, et al. Radical cystectomy in the treatment of invasive bladder cancer: long-term results in 1,054 patients. *J Clin Oncol* 2001;19:666-75.
24. Landis SH, Murray T, Bolden S, Wingo PA. Cancer statistics, 1999. *CA Cancer J Clin* 1999;49:8-31, 1.
25. Fitzpatrick JM. The natural history of superficial bladder carcinoma. *Semin Urol* 1993;11:127-36.
26. Heney NM, Ahmed S, Flanagan MJ, et al. Superficial bladder cancer: progression and recurrence. *J Urol* 1983;130:1083-6.
27. Sylvester RJ, van der Meijden AP, Oosterlinck W, et al. Predicting recurrence and progression in individual patients with stage Ta T1 bladder cancer using EORTC risk tables: a combined analysis of 2596 patients from seven EORTC trials. *Eur Urol* 2006;49:466-5.
28. Rifai N, Gillette MA, Carr SA. Protein biomarker discovery and validation: the long and uncertain path to clinical utility. *Nat Biotechnol* 2006;24:971-83.
29. Lotan Y, Shariat SF, Schmitz-Drager BJ, et al. Considerations on implementing diagnostic markers into clinical decision making in bladder cancer. *Urol Oncol* 2010;28:441-8.
30. Proctor I, Stoeber K, Williams GH. Biomarkers in bladder cancer. *Histopathology* 2010;57:1-13.
31. Lotan Y, Roehrborn CG. Sensitivity and specificity of commonly available bladder tumor markers versus cytology: results of a comprehensive literature review and meta-analyses. *Urology* 2003;61:109-18.
32. Yang CH, Snyder M. The nuclear-mitotic apparatus protein is important in the establishment and maintenance of the bipolar mitotic spindle apparatus. *Mol Biol Cell* 1992;3:1259-67.
33. Tang TK, Tang CJ, Chao YJ, Wu CW. Nuclear mitotic apparatus protein (NuMA): spindle association, nuclear targeting and differential subcellular localization of various NuMA isoforms. *J Cell Sci* 1994;107 ( Pt 6):1389-402.
34. Radulescu AE, Cleveland DW. NuMA after 30 years: the matrix revisited. *Trends Cell Biol* 2010;20:214-22.
35. Grossman HB, Messing E, Soloway M, et al. Detection of bladder cancer using a point-of-care proteomic assay. *JAMA* 2005;293:810-6.

36. Grossman HB, Soloway M, Messing E, et al. Surveillance for recurrent bladder cancer using a point-of-care proteomic assay. *JAMA* 2006;295:299-305.
37. Mowatt G, Zhu S, Kilonzo M, et al. Systematic review of the clinical effectiveness and cost-effectiveness of photodynamic diagnosis and urine biomarkers (FISH, ImmunoCyt, NMP22) and cytology for the detection and follow-up of bladder cancer. *Health Technol Assess* 2010;14:1-iv.
38. Shariat SF, Karam JA, Lotan Y, Karakiewicz PI. Critical evaluation of urinary markers for bladder cancer detection and monitoring. *Rev Urol* 2008;10:120-35.
39. Kinders R, Jones T, Root R, et al. Complement factor H or a related protein is a marker for transitional cell cancer of the bladder. *Clin Cancer Res* 1998;4:2511-20.
40. Ferreira VP, Pangburn MK, Cortes C. Complement control protein factor H: the good, the bad, and the inadequate. *Mol Immunol* 2010;47:2187-97.
41. Leyh H, Marberger M, Conort P, et al. Comparison of the BTA stat test with voided urine cytology and bladder wash cytology in the diagnosis and monitoring of bladder cancer. *Eur Urol* 1999;35:52-6.
42. Sarosdy MF, Hudson MA, Ellis WJ, et al. Improved detection of recurrent bladder cancer using the Bard BTA stat Test. *Urology* 1997;50:349-53.
43. Thomas L, Leyh H, Marberger M, et al. Multicenter trial of the quantitative BTA TRAK assay in the detection of bladder cancer. *Clin Chem* 1999;45:472-7.
44. Budman LI, Kassouf W, Steinberg JR. Biomarkers for detection and surveillance of bladder cancer. *Can Urol Assoc J* 2008;2:212-21.
45. Sokolova IA, Halling KC, Jenkins RB, et al. The development of a multitarget, multicolor fluorescence in situ hybridization assay for the detection of urothelial carcinoma in urine. *J Mol Diagn* 2000;2:116-23.
46. Bubendorf L, Grilli B, Sauter G, Mihatsch MJ, Gasser TC, Dalquen P. Multiprobe FISH for enhanced detection of bladder cancer in voided urine specimens and bladder washings. *Am J Clin Pathol* 2001;116:79-86.
47. Yoder BJ, Skacel M, Hedgepeth R, et al. Reflex UroVysion testing of bladder cancer surveillance patients with equivocal or negative urine cytology: a prospective study with focus on the natural history of anticipatory positive findings. *Am J Clin Pathol* 2007;127:295-301.
48. Fradet Y, Lockhard C. Performance characteristics of a new monoclonal antibody test for bladder cancer: ImmunoCyt trade mark. *Can J Urol* 1997;4:400-5.
49. Mian C, Pycha A, Wiener H, Haitel A, Lodde M, Marberger M. Immunocyt: a new tool for detecting transitional cell cancer of the urinary tract. *J Urol* 1999;161:1486-9.
50. Lodde M, Mian C, Wiener H, Haitel A, Pycha A, Marberger M. Detection of upper urinary tract transitional cell carcinoma with ImmunoCyt: a preliminary report. *Urology* 2001;58:362-6.
51. Getzenberg RH, Konety BR, Oeler TA, et al. Bladder cancer-associated nuclear matrix proteins. *Cancer Res* 1996;56:1690-4.
52. Van Le TS, Myers J, Konety BR, Barder T, Getzenberg RH. Functional characterization

- of the bladder cancer marker, BLCA-4. *Clin Cancer Res* 2004;10:1384-91.
53. Konety BR, Nguyen TS, Dhir R, et al. Detection of bladder cancer using a novel nuclear matrix protein, BLCA-4. *Clin Cancer Res* 2000;6:2618-25.
54. Van Le TS, Miller R, Barder T, Babjuk M, Potter DM, Getzenberg RH. Highly specific urine-based marker of bladder cancer. *Urology* 2005;66:1256-60.
55. Stenzl A, Cowan NC, De SM, et al. The updated EAU guidelines on muscle-invasive and metastatic bladder cancer. *Eur Urol* 2009;55:815-25.
56. Vrooman OP, Witjes JA. Urinary markers in bladder cancer. *Eur Urol* 2008;53:909-16.
57. Strobe SA, Andriole GL. Prostate cancer screening: current status and future perspectives. *Nat Rev Urol* 2010;7:487-93.
58. Heijnsdijk EA, de Koning HJ, Wever EM, Draisma G, Roobol MJ, et al. Overdetection, overtreatment and costs in prostate-specific antigen screening for prostate cancer. *Br J Cancer* 2009; 101:1833-8.
59. Welch HG, Black WC. Overdiagnosis in cancer. *J Natl Cancer Inst* 2010;102:605-13.
60. Schroder FH, Hugosson J, Roobol MJ, et al. Screening and prostate-cancer mortality in a randomized European study. *N Engl J Med* 2009;360:1320-8.
61. Jamaspishvili T, Kral M, Khomeriki I, Student V, Kolar Z, Bouchal J. Urine markers in monitoring for prostate cancer. *Prostate Cancer Prostatic Dis* 2010;13:12-9.
62. Laxman B, Tomlins SA, Mehra R, et al. Noninvasive detection of TMPRSS2:ERG fusion transcripts in the urine of men with prostate cancer. *Neoplasia* 2006;8:885-8.
63. De AG, Rittenhouse HG, Mikolajczyk SD, Blair SL, Semjonow A. Twenty Years of PSA: From Prostate Antigen to Tumor Marker. *Rev Urol* 2007;9:113-23.
64. Ulmert D, O'Brien MF, Bjartell AS, Lilja H. Prostate kallikrein markers in diagnosis, risk stratification and prognosis. *Nat Rev Urol* 2009;6:384-91.
65. Lilja H, Christensson A, Dahlen U, et al. Prostate-specific antigen in serum occurs predominantly in complex with alpha 1-antichymotrypsin. *Clin Chem* 1991;37:1618-25.
66. Akiyama K, Nakamura T, Iwanaga S, Hara M. The chymotrypsin-like activity of human prostate-specific antigen, gamma-seminoprotein. *FEBS Lett* 1987;225:168-72.
67. Berg T, Bradshaw RA, Carretero OA, et al. A common nomenclature for members of the tissue (glandular) kallikrein gene families. *Agents Actions Suppl* 1992;38 ( Pt 1):19-25.
68. Finlay JA, Day JR, Rittenhouse HG. Polyclonal and monoclonal antibodies to prostate-specific antigen can cross-react with human kallikrein 2 and human kallikrein 1. *Urology* 1999;53:746-51.
69. Papsidero LD, Wang MC, Valenzuela LA, Murphy GP, Chu TM. A prostate antigen in sera of prostatic cancer patients. *Cancer Res* 1980;40:2428-32.
70. Catalona WJ, Smith DS, Ratliff TL, et al. Measurement of prostate-specific antigen in serum as a screening test for prostate cancer. *N Engl J Med* 1991;324:1156-61.
71. Thompson IM, Pauler DK, Goodman PJ, et al. Prevalence of prostate cancer among men with a prostate-specific antigen level  $\geq$  4.0 ng per milliliter. *N Engl J Med* 2004;350:2239-46.

72. Bussemakers MJ, van BA, Verhaegh GW, et al. DD3: a new prostate-specific gene, highly overexpressed in prostate cancer. *Cancer Res* 1999;59:5975-9.
73. Hessels D, Klein Gunnewiek JM, van O, I, et al. DD3(PCA3)-based molecular urine analysis for the diagnosis of prostate cancer. *Eur Urol* 2003;44:8-15.
74. Vlaeminck-Guillem V, Ruffion A, Andre J, Devonec M, Paparel P. Urinary prostate cancer 3 test: toward the age of reason? *Urology* 2010;75:447-53.
75. Groskopf J, Aubin SM, Deras IL, et al. APTIMA PCA3 molecular urine test: development of a method to aid in the diagnosis of prostate cancer. *Clin Chem* 2006;52:1089-95.
76. Ploussard G, de la Taille A. Urine biomarkers in prostate cancer. *Nat Rev Urol* 2010;7:101-9.
77. Tomlins SA, Rhodes DR, Perner S, et al. Recurrent fusion of TMPRSS2 and ETS transcription factor genes in prostate cancer. *Science* 2005;310:644-8.
78. Petrovics G, Liu A, Shaheduzzaman S, et al. Frequent overexpression of ETS-related gene-1 (ERG1) in prostate cancer transcriptome. *Oncogene* 2005;24:3847-52.
79. Rice KR, Chen Y, Ali A, et al. Evaluation of the ETS-related gene mRNA in urine for the detection of prostate cancer. *Clin Cancer Res* 2010;16:1572-6.
80. Nguyen PN, Violette P, Chan S, et al. A Panel of TMPRSS2:ERG Fusion Transcript Markers for Urine-Based Prostate Cancer Detection with High Specificity and Sensitivity. *Eur Urol* 2010.
81. Pflueger D, Terry S, Sboner A, et al. Discovery of non-ETS gene fusions in human prostate cancer using next-generation RNA sequencing. *Genome Res* 2011;21:56-67.
82. Henson DE, Albores-Saavedra J, Corle D. Carcinoma of the extrahepatic bile ducts. Histologic types, stage of disease, grade, and survival rates. *Cancer* 1992;70:1498-501.
83. de BM, Sherman S, Fogel EL, et al. Tissue sampling at ERCP in suspected malignant biliary strictures (Part 1). *Gastrointest Endosc* 2002;56:552-61.
84. Selvaggi SM. Biliary brushing cytology. *Cytopathology* 2004;15:74-9.
85. de BM, Sherman S, Fogel EL, et al. Tissue sampling at ERCP in suspected malignant biliary strictures (Part 2). *Gastrointest Endosc* 2002;56:720-30.
86. Lee JG. Brush cytology and the diagnosis of pancreaticobiliary malignancy during ERCP. *Gastrointest Endosc* 2006;63:78-80.
87. Gress TM. Molecular diagnosis of pancreatobiliary malignancies in brush cytologies of biliary strictures. *Gut* 2004;53:1727-9.
88. Holzinger F, Z'graggen K, Buchler MW. Mechanisms of biliary carcinogenesis: a pathogenetic multi-stage cascade towards cholangiocarcinoma. *Ann Oncol* 1999;10 Suppl 4:122-6.
89. Fogel EL, deBellis M, McHenry L, et al. Effectiveness of a new long cytology brush in the evaluation of malignant biliary obstruction: a prospective study. *Gastrointest Endosc* 2006;63:71-7.
90. Wight CO, Zaitoun AM, Boulton-Jones JR, Dunkley C, Beckingham IJ, Ryder SD. Improving diagnostic yield of biliary brushings cytology for pancreatic cancer and cholangiocarcinoma.

Cytopathology 2004;15:87-92.

91. Mohandas KM, Swaroop VS, Gullar SU, Dave UR, Jagannath P, DeSouza LJ. Diagnosis of malignant obstructive jaundice by bile cytology: results improved by dilating the bile duct strictures. *Gastrointest Endosc* 1994;40:150-4.

92. Jailwala J, Fogel EL, Sherman S, et al. Triple-tissue sampling at ERCP in malignant biliary obstruction. *Gastrointest Endosc* 2000;51:383-90.

93. Nehls O, Gregor M, Klump B. Serum and bile markers for cholangiocarcinoma. *Semin Liver Dis* 2004;24:139-54.

94. Koprowski H, Herlyn M, Stepkowski Z, Sears HF. Specific antigen in serum of patients with colon carcinoma. *Science* 1981;212:53-5.

95. Morris-Stiff G, Teli M, Jardine N, Puntis MC. CA19-9 antigen levels can distinguish between benign and malignant pancreaticobiliary disease. *Hepatobiliary Pancreat Dis Int* 2009;8:620-6.

96. Boeck S, Haas M, Laubender RP, et al. Application of a time-varying covariate model to the analysis of CA 19-9 as serum biomarker in patients with advanced pancreatic cancer. *Clin Cancer Res* 2010;16:986-94.

97. Steinberg W. The clinical utility of the CA 19-9 tumor-associated antigen. *Am J Gastroenterol* 1990;85:350-5.

98. Gold P, Freedman SO. Demonstration of tumor-specific antigens in human colonic carcinoma by immunological tolerance and absorption techniques. *J Exp Med* 1965;121:439-62.

99. Ramage JK, Donaghy A, Farrant JM, Iorns R, Williams R. Serum tumor markers for the diagnosis of cholangiocarcinoma in primary sclerosing cholangitis. *Gastroenterology* 1995;108:865-9.

100. Khalid A, Pal R, Sasatomi E, et al. Use of microsatellite marker loss of heterozygosity in accurate diagnosis of pancreaticobiliary malignancy from brush cytology samples. *Gut* 2004;53:1860-5.

101. Kubicka S, Kuhnel F, Flemming P, et al. K-ras mutations in the bile of patients with primary sclerosing cholangitis. *Gut* 2001;48:403-8.

102. Wang Y, Yamaguchi Y, Watanabe H, Ohtsubo K, Wakabayashi T, Sawabu N. Usefulness of p53 gene mutations in the supernatant of bile for diagnosis of biliary tract carcinoma: comparison with K-ras mutation. *J Gastroenterol* 2002;37:831-9.

103. Itoi T, Takei K, Shinohara Y, et al. K-ras codon 12 and p53 mutations in biopsy specimens and bile from biliary tract cancers. *Pathol Int* 1999;49:30-7.

104. Khan SA, Thomas HC, Davidson BR, Taylor-Robinson SD. Cholangiocarcinoma. *Lancet* 2005;366:1303-14.

105. Moreno Luna LE, Kipp B, Halling KC, et al. Advanced cytologic techniques for the detection of malignant pancreaticobiliary strictures. *Gastroenterology* 2006;131:1064-72.

106. Coyle VM, Johnston PG. Genomic markers for decision making: what is preventing us from using markers? *Nat Rev Clin Oncol* 2010;7:90-7.

107. Machida YJ, Hamlin JL, Dutta A. Right place, right time, and only once: replication



- initiation in metazoans. *Cell* 2005;123:13-24.
108. Cadoret JC, Meisch F, Hassan-Zadeh V, et al. Genome-wide studies highlight indirect links between human replication origins and gene regulation. *Proc Natl Acad Sci U S A* 2008;105:15837-42.
109. Mechali M. Eukaryotic DNA replication origins: many choices for appropriate answers. *Nat Rev Mol Cell Biol* 2010;11:728-38.
110. Tanaka S, Diffley JF. Deregulated G1-cyclin expression induces genomic instability by preventing efficient pre-RC formation. *Genes Dev* 2002;16:2639-49.
111. Randell JC, Bowers JL, Rodriguez HK, Bell SP. Sequential ATP hydrolysis by Cdc6 and ORC directs loading of the Mcm2-7 helicase. *Mol Cell* 2006;21:29-39.
112. Bowers JL, Randell JC, Chen S, Bell SP. ATP hydrolysis by ORC catalyzes reiterative Mcm2-7 assembly at a defined origin of replication. *Mol Cell* 2004;16:967-78.
113. Araki H. Cyclin-dependent kinase-dependent initiation of chromosomal DNA replication. *Curr Opin Cell Biol* 2010;22:766-71.
114. Moyer SE, Lewis PW, Botchan MR. Isolation of the Cdc45/Mcm2-7/GINS (CMG) complex, a candidate for the eukaryotic DNA replication fork helicase. *Proc Natl Acad Sci U S A* 2006;103:10236-41.
115. Im JS, Ki SH, Farina A, Jung DS, Hurwitz J, Lee JK. Assembly of the Cdc45-Mcm2-7-GINS complex in human cells requires the Ctf4/And-1, RecQL4, and Mcm10 proteins. *Proc Natl Acad Sci U S A* 2009;106:15628-32.
116. Sheu YJ, Stillman B. Cdc7-Dbf4 phosphorylates MCM proteins via a docking site-mediated mechanism to promote S phase progression. *Mol Cell* 2006;24:101-13.
117. Tsuji T, Ficarro SB, Jiang W. Essential role of phosphorylation of MCM2 by Cdc7/Dbf4 in the initiation of DNA replication in mammalian cells. *Mol Biol Cell* 2006;17:4459-72.
118. Montagnoli A, Valsasina B, Brotherton D, et al. Identification of Mcm2 phosphorylation sites by S-phase-regulating kinases. *J Biol Chem* 2006;281:10281-90.
119. Bruck I, Kaplan D. Dbf4-Cdc7 phosphorylation of Mcm2 is required for cell growth. *J Biol Chem* 2009;284:28823-31.
120. Sheu YJ, Stillman B. The Dbf4-Cdc7 kinase promotes S phase by alleviating an inhibitory activity in Mcm4. *Nature* 2010;463:113-7.
121. Blow JJ, Dutta A. Preventing re-replication of chromosomal DNA. *Nat Rev Mol Cell Biol* 2005;6:476-86.
122. Nishitani H, Sugimoto N, Roukos V, et al. Two E3 ubiquitin ligases, SCF-Skp2 and DDB1-Cul4, target human Cdt1 for proteolysis. *EMBO J* 2006;25:1126-36.
123. Li X, Zhao Q, Liao R, Sun P, Wu X. The SCF(Skp2) ubiquitin ligase complex interacts with the human replication licensing factor Cdt1 and regulates Cdt1 degradation. *J Biol Chem* 2003;278:30854-8.
124. Zhong W, Feng H, Santiago FE, Kipreos ET. CUL-4 ubiquitin ligase maintains genome stability by restraining DNA-replication licensing. *Nature* 2003;423:885-9.

125. McGarry TJ, Kirschner MW. Geminin, an inhibitor of DNA replication, is degraded during mitosis. *Cell* 1998;93:1043-53.
126. Lee C, Hong B, Choi JM, et al. Structural basis for inhibition of the replication licensing factor Cdt1 by geminin. *Nature* 2004;430:913-7.
127. Wohlschlegel JA, Kutok JL, Weng AP, Dutta A. Expression of geminin as a marker of cell proliferation in normal tissues and malignancies. *Am J Pathol* 2002;161:267-73.
128. Tada S, Li A, Maiorano D, Mechali M, Blow JJ. Repression of origin assembly in metaphase depends on inhibition of RLF-B/Cdt1 by geminin. *Nat Cell Biol* 2001;3:107-13.
129. Potten CS, Loeffler M. Stem cells: attributes, cycles, spirals, pitfalls and uncertainties. Lessons for and from the crypt. *Development* 1990;110:1001-20.
130. Hall PA, Watt FM. Stem cells: the generation and maintenance of cellular diversity. *Development* 1989;106:619-33.
131. Stoeber K, Mills AD, Kubota Y, et al. Cdc6 protein causes premature entry into S phase in a mammalian cell-free system. *EMBO J* 1998;17:7219-29.
132. Stoeber K, Tlsty TD, Happerfield L, et al. DNA replication licensing and human cell proliferation. *J Cell Sci* 2001;114:2027-41.
133. Barkley LR, Hong HK, Kingsbury SR, James M, Stoeber K, Williams GH. Cdc6 is a rate-limiting factor for proliferative capacity during HL60 cell differentiation. *Exp Cell Res* 2007;313:3789-99.
134. Freeman A, Morris LS, Mills AD, et al. Minichromosome maintenance proteins as biological markers of dysplasia and malignancy. *Clin Cancer Res* 1999;5:2121-32.
135. Going JJ, Keith WN, Neilson L, Stoeber K, Stuart RC, Williams GH. Aberrant expression of minichromosome maintenance proteins 2 and 5, and Ki-67 in dysplastic squamous oesophageal epithelium and Barrett's mucosa. *Gut* 2002;50:373-7.
136. Williams GH, Romanowski P, Morris L, et al. Improved cervical smear assessment using antibodies against proteins that regulate DNA replication. *Proc Natl Acad Sci U S A* 1998;95:14932-7.
137. Larsen NS. Invasive cervical cancer rising in young white females. *J Natl Cancer Inst* 1994;86:6-7.
138. Stoeber K, Halsall I, Freeman A, et al. Immunoassay for urothelial cancers that detects DNA replication protein Mcm5 in urine. *Lancet* 1999;354:1524-5.
139. Williams GH, Swinn R, Prevost AT, et al. Diagnosis of oesophageal cancer by detection of minichromosome maintenance 5 protein in gastric aspirates. *Br J Cancer* 2004;91:714-9.
140. Stoeber K, Swinn R, Prevost AT, et al. Diagnosis of genito-urinary tract cancer by detection of minichromosome maintenance 5 protein in urine sediments. *J Natl Cancer Inst* 2002;94:1071-9.
141. Meng MV, Grossfeld GD, Williams GH, et al. Minichromosome maintenance protein 2 expression in prostate: characterization and association with outcome after therapy for cancer. *Clin Cancer Res* 2001;7:2712-8.



142. Dudderidge TJ, Stoeber K, Loddo M, et al. Mcm2, Geminin, and KI67 define proliferative state and are prognostic markers in renal cell carcinoma. *Clin Cancer Res* 2005;11:2510-7.
143. Shetty A, Loddo M, Fanshawe T, et al. DNA replication licensing and cell cycle kinetics of normal and neoplastic breast. *Br J Cancer* 2005;93:1295-300.
144. Eward KL, Obermann EC, Shreeram S, et al. DNA replication licensing in somatic and germ cells. *J Cell Sci* 2004;117:5875-86.
145. Wharton SB, Hibberd S, Eward KL, et al. DNA replication licensing and cell cycle kinetics of oligodendroglial tumours. *Br J Cancer* 2004;91:262-9.
146. Kulkarni AA, Loddo M, Leo E, et al. DNA replication licensing factors and aurora kinases are linked to aneuploidy and clinical outcome in epithelial ovarian carcinoma. *Clin Cancer Res* 2007;13:6153-61.
147. Loddo M, Kingsbury SR, Rashid M, et al. Cell-cycle-phase progression analysis identifies unique phenotypes of major prognostic and predictive significance in breast cancer. *Br J Cancer* 2009;100:959-70.
148. Kulkarni AA, Kingsbury SR, Tudzarova S, et al. Cdc7 kinase is a predictor of survival and a novel therapeutic target in epithelial ovarian carcinoma. *Clin Cancer Res* 2009;15:2417-25.
149. Blow JJ, Gillespie PJ. Replication licensing and cancer—a fatal entanglement? *Nat Rev Cancer* 2008;8:799-806.
150. Shreeram S, Sparks A, Lane DP, Blow JJ. Cell type-specific responses of human cells to inhibition of replication licensing. *Oncogene* 2002;21:6624-32.
151. Swords R, Mahalingam D, O'Dwyer M, et al. Cdc7 kinase - a new target for drug development. *Eur J Cancer* 2010;46:33-40.
152. Chini CC, Chen J. Human claspin is required for replication checkpoint control. *J Biol Chem* 2003;278:30057-62.
153. Bartek J, Lukas C, Lukas J. Checking on DNA damage in S phase. *Nat Rev Mol Cell Biol* 2004;5:792-804.
154. Liu Q, Guntuku S, Cui XS, et al. Chk1 is an essential kinase that is regulated by Atr and required for the G(2)/M DNA damage checkpoint. *Genes Dev* 2000;14:1448-59.
155. Matsuoka S, Rotman G, Ogawa A, Shiloh Y, Tamai K, Elledge SJ. Ataxia telangiectasia-mutated phosphorylates Chk2 in vivo and in vitro. *Proc Natl Acad Sci U S A* 2000;97:10389-94.
156. Jackson PK. Stopping replication, at the beginning. *Nat Chem Biol* 2008;4:331-2.
157. Vanotti E, Amici R, Bargiotti A, et al. Cdc7 kinase inhibitors: pyrrolopyridinones as potential antitumor agents. 1. Synthesis and structure-activity relationships. *J Med Chem* 2008;51:487-501.
158. Montagnoli A, Valsasina B, Croci V, et al. A Cdc7 kinase inhibitor restricts initiation of DNA replication and has antitumor activity. *Nat Chem Biol* 2008;4:357-65.
159. Marshall NF, Price DH. Purification of P-TEFb, a transcription factor required for the transition into productive elongation. *J Biol Chem* 1995;270:12335-8.
160. Peng J, Marshall NF, Price DH. Identification of a cyclin subunit required for the function

of Drosophila P-TEFb. *J Biol Chem* 1998;273:13855-60.

161. Menichincheri M, Albanese C, Alli C, et al. Cdc7 kinase inhibitors: 5-heteroaryl-3-carboxamido-2-aryl pyrroles as potential antitumor agents. 1. Lead finding. *J Med Chem* 2010;53:7296-315.

162. Menichincheri M, Bargiotti A, Berthelsen J, et al. First Cdc7 Kinase Inhibitors: Pyrrolopyridinones as Potent and Orally Active Antitumor Agents. 2. Lead Discovery. *J Med Chem* 2009.

163. Ermoli A, Bargiotti A, Brasca MG, et al. Cell division cycle 7 kinase inhibitors: 1H-pyrrolo[2,3-b]pyridines, synthesis and structure-activity relationships. *J Med Chem* 2009;52:4380-90.

164. Sawa M, Masai H. Drug design with Cdc7 kinase: a potential novel cancer therapy target. *Drug Des Devel Ther* 2009;2:255-64.

165. Montagnoli A, Moll J, Colotta F. Targeting cell division cycle 7 kinase: a new approach for cancer therapy. *Clin Cancer Res* 2010;16:4503-8.

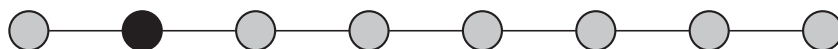
## Chapter 2

# Bladder cancer diagnosis by combined detection of Mcm5 protein and nuclear matrix protein 22

A Wollenschlaeger\*, JD Kelly\*, TJ Dudderidge\*, O Okoturo, K Burling, F Tulloch, I Halsall, T Prevost, AT Prevost, JC Vasconcelos, W Robson, HY Leung, N Vasdev, RS Pickard, GH Williams, K Stoeber

Manuscript in preparation

\* These authors contributed equally



## Bladder cancer diagnosis by combined detection of Mcm5 protein and nuclear matrix protein 22

Alex Wollenschlaeger<sup>1,\*</sup>, John D. Kelly<sup>2,\*</sup>, Tim J. Dudderidge<sup>2,\*</sup>, Odu Okoturo<sup>3</sup>, Keith Burling<sup>4</sup>, Fiona Tulloch<sup>4</sup>, Ian Halsall<sup>4</sup>, Teresa Prevost<sup>5</sup>, A. Toby Prevost<sup>6</sup>, Joana C. Vasconcelos<sup>5</sup>, Wendy Robson<sup>7</sup>, Hing Y. Leung<sup>8</sup>, Nikhil Vasdev<sup>7</sup>, Robert S. Pickard<sup>7</sup>, Gareth H. Williams<sup>1,2,†</sup>, Kai Stoeber<sup>1,2</sup>

<sup>1</sup> Wolfson Institute for Biomedical Research, University College London, Cruciform Building, Gower Street, London, WC1E 6BT, UK; <sup>2</sup> Department of Pathology and Cancer Institute, University College London, Rockefeller Building, 21 University Street, London, WC1E 6JJ, UK; <sup>3</sup> Department of Medicine, Imperial College London, Princes Gardens, London, SW7 1NA, UK; <sup>4</sup> Department of Clinical Biochemistry, Addenbrooke's Hospital, University of Cambridge, Hills Road, Cambridge, CB2 2QR, UK; <sup>5</sup> Department of Public Health and Primary Care, Centre for Applied Medical Statistics, University of Cambridge, Institute of Public Health, Forvie Site, Robinson Way, Cambridge CB2 0SR, UK; <sup>6</sup> Department of Primary Care and Public Health Sciences, King's College London, Capital House, 42 Weston Street, London, SE1 3QD, UK; <sup>7</sup> Department of Urology, Freeman Hospital, High Heaton, Newcastle upon Tyne, NE7 7DN, UK; <sup>8</sup> Beatson Institute for Cancer Research, University of Glasgow, Garscube Estate, Switchback Road, Bearsden, Glasgow, G61 1BD, UK

**Key words:** Mcm5, NMP22, bladder cancer, diagnosis

### Abstract

**Background:** Urinary biomarkers for bladder cancer detection are constrained by inadequate sensitivity or specificity. Here we evaluate the diagnostic accuracy of Mcm5, a novel cell cycle biomarker of aberrant growth, alone and in combination with NMP22.

**Methods:** 1677 consecutive patients under investigation for urinary tract malignancy were recruited to a prospective blinded observational study. All patients underwent ultrasound, intravenous urography, cystoscopy, urine culture and cytologic analysis. An immunofluorometric assay was used to measure Mcm5 levels in urine cell sediments. NMP22 urinary levels were determined with the Matritech NMP22 Test Kit.

**Results:** Genito-urinary tract cancers were identified in 144/1451 (9.9%) patients with an Mcm5 result and in 195/1396 (14%) patients with an NMP22 result. At the assay cut-point where sensitivity and specificity were equal, the Mcm5 test detected primary and recurrent bladder cancers with 65% sensitivity (95% CI=56–72%) and 94% NPV (95% CI=93–96%). The area under the ROC curve for Mcm5 was 0.71 (95% CI=0.66–0.77) and 0.72 (95% CI=0.67–0.77) for NMP22. Importantly, Mcm5 combined with NMP22 identified with high specificity (70%, 95% CI=67–73%) all muscle invasive tumors and 97% of grade 3 tumors including cases of carcinoma in situ.

**Conclusions:** The Mcm5 immunoassay is a simple, accurate, non-invasive standalone test for identifying patients with urothelial cancers. In combination with NMP22 the Mcm5 test identifies nearly all life-threatening disease. Multi-centre trials for the combined Mcm5 and NMP22 test as a cost-effective diagnostic and screening tool need to be urgently initiated to reduce the high morbidity and mortality associated with bladder cancer.

## Introduction

Transitional cell carcinoma (TCC) of the urinary bladder is the 4th most common cancer in the US, with an estimated 70980 new cases and 14330 deaths from bladder cancer in 2009 (1). Worldwide there are an estimated 356600 new cases diagnosed each year (2). Most bladder cancers do not invade deeply at presentation, but 80% of tumors recur within three years. Patients presenting with muscle invasive TCC (25–30% of tumors at diagnosis) have a significant risk of progression to metastasis (30–60%) and a significantly reduced 5-year survival rate (40%) despite aggressive local treatment (3–5). Cystoscopy is the standard method of bladder tumor detection, however it is an uncomfortable and invasive procedure which results in urinary infection in up to 5% of cases (6). Early detection of bladder cancer with a non-invasive tumor marker test would impact on management of the disease by decreasing the morbidity associated with current surveillance methods, improving the quality of life of patients and reducing the costs associated with frequent cystoscopies.

---

\*These authors contributed equally

†Correspondence: Gareth Williams, Department of Pathology, University College London, Rockefeller Building, 21 University Street, London, WC1E 6JJ, UK. Tel: +44 20 7679 6304, Fax: +44 20 8377 4408, E-mail: gareth.williams@ucl.ac.uk

Urinary biomarkers for the detection of bladder cancer hold great promise and up to six different markers have received US Food and Drug Administration approval for use as an aid to improve detection (7), yet none of these markers is in routine clinical use and of all, it is urinary cytology which is most widely utilized because of high specificity although poor sensitivity. Novel technologies and biomarkers, however, have the potential to improve diagnostic accuracy, with the most effective diagnostic and surveillance strategies to date utilizing photodynamic cystoscopy and biomarkers (7). Nuclear matrix protein 22 (NMP22), for example, is a nuclear mitotic apparatus protein that regulates chromatid and daughter cell separation (8,9) and has emerged as one of the promising urinary biomarkers for TCC. The FDA approved, laboratory-based quantitative NMP22 immunoassay (Matritech, Freiburg, Germany) and a qualitative point-of-care test, NMP22 Bladder Check (Matritech), are now available for clinical use. However, although urinary NMP22 levels are elevated in bladder cancer, dead and dying urothelial cells in many non-malignant and inflammatory conditions can also release NMP22, thus reducing specificity. Moreover, a wide marked range in test performance has been reported among different studies using NMP22, with sensitivity ranging from 33% to 100% and specificity from 40% to 93% (7). The constrained accuracy of available biomarkers, along with their expense, has therefore so far limited introduction of urinary biomarkers into routine clinical practice. Hence there is an urgent need to identify new biomarkers that might improve diagnostic accuracy, either when used in isolation or in combination with existing biomarker tests (10).

The DNA replication initiation machinery represents a final and critical step in growth control downstream of complex redundant oncogenic signaling pathways and is therefore a potentially attractive diagnostic and therapeutic target (11). Proteins of the minichromosome maintenance (Mcm) family (Mcm2-7, collectively referred to as MCM), assemble into hexameric complexes that have DNA helicase activity, which is essential for initiation of DNA synthesis (12,13). In epithelial-lined organ systems MCM proteins become dysregulated and overexpressed in hyperproliferative dysplastic (preinvasive) and malignant states, resulting in exfoliation of MCM-positive tumor cells (11,14-16). Mcm2-7 protein expression in normal epithelium is restricted to the basal stem/transit compartments and is absent from surface layers as cells adopt a fully differentiated phenotype. In premalignant/dysplastic epithelial lesions there is an expansion of the proliferative compartment coupled to arrested differentiation, resulting in the appearance of cycling MCM-positive cells in superficial layers. The detection of exfoliated MCM-positive cells in clinical samples therefore provides a potentially sensitive method for detecting preinvasive and invasive cancers (11,17,18). In a proof-of-principle study we previously showed that elevated Mcm5 levels in cells in urine sediments is predictive of the presence of bladder cancer (19). In addition to detection of urothelial cancers, this test has been applied successfully to the diagnosis of a wide range of other malignancies, including cervical, esophageal, pancreaticobiliary, lung, oral and anal cancers (11,14,20-22).

Here we describe a prospective blinded observational bladder cancer trial to critically evaluate the accuracy of the Mcm5 test for detection of urothelial bladder and upper urinary tract carcinoma. An immunofluorometric assay was used to quantitatively measure Mcm5 levels in the urine sediments of 1677 patients presenting with hematuria or lower urinary tract symptoms. In parallel we tested patients for NMP22, a comparator urinary biomarker, and compared all results to the clinical diagnosis based on standard clinical investigations.

## Materials and Methods

### Study subjects

Ethical and institutional approvals were obtained. Single voided urine specimens were obtained from 1677 patients who were investigated at the Freeman Hospital (Newcastle upon Tyne Hospitals NHS Foundation Trust, Newcastle upon Tyne UK), a regional urological cancer center, following a diagnosis of haematuria in order to exclude urinary tract malignancy. Patients were recruited between September 2003 and January 2006 after written consent was obtained. The database was completed in November 2006 with a minimum follow up period of 6 months from the time of initial investigations. Patients with a history of recent genitourinary instrumentation or surgery within the previous 2 weeks were excluded. Patients with a history of concomitant malignancy or other malignancy within 5 years prior to study were also excluded. With these exceptions all consecutive patients attending for investigation during the study period were approached for recruitment into the trial, excluding days when research staff were unavoidably absent.

Urine samples were split equally for: (i) urinalysis and microbiological culture, (ii) cytological analysis, (iii) Mcm5 measurement and (iv) NMP22 measurement. Patients underwent upper urinary tract imaging including ultrasound and intravenous urography. Patients also underwent cystoscopy after producing the urine samples. Patients with suspected tumors subsequently underwent a therapeutic resection providing a pathological diagnosis. Male patients were examined by digital rectal examination and ultrasound for the presence of prostatic disease. Prostate-specific antigen (PSA) testing was not mandated and PSA levels were checked in a proportion of cases in whom cancer was suspected or who requested the test. If PSA levels were elevated patients were offered trans-rectal ultrasound guided core biopsies of the prostate. Typically all hematuria tests were completed within 24 hours and within 2 weeks for all patients. Clinical data were entered into a database prospectively prior to Mcm5 and NMP22 analysis. The reference standard for this study was the clinical diagnosis based on conventional clinical investigations, supported by pathology in all cases of malignancy, performed under the supervision of a consultant urologist. This approach to the investigation of hematuria has been shown by our group to be an effective method of identifying urothelial carcinoma (23).

Urine samples were analyzed in a blinded fashion for Mcm5 detection, NMP22 testing, and cytologic analyses. On completion of the study, we decoded the patient data and compared immunofluorometric Mcm5 signals and NMP22 results with clinical diagnoses based on cystoscopy, biopsy histology, imaging and urine cytology. Staging and grading of malignant tumors was performed by a specialist uro-pathologist using the TNM (tumor-node-metastasis) classification system (24) and the 1973 World Health Organization (WHO) grading system respectively (25). Ethical approval was obtained from the Local Research Ethics Committees (LREC Numbers: Cambridge: 00/236; London: 04/Q0502/1; Newcastle: 2002/161).

### **Urine cytology**

Urine samples (50 mL) were centrifuged at 1500 g for 5 min. Cytospin preparations were prepared on poly-L-lysine coated slides using Shandon cytospin tubes and a cytocentrifuge according to the manufacturers instructions (Thermo Shandon, Runcorn, UK). Samples were fixed in industrial methylated spirits and stained using the Papanicolaou technique for smears (26). Specimens were evaluated by a consultant cytologist experienced in uro-pathology. Cytology was scored as positive if atypical or malignant cells were identified

### **NMP22 assay**

NMP22 was measured by enzyme-linked immunosorbent assay (ELISA) using a kit purchased from Matri-tech (Freiburg, Germany). The assay was adapted to run on a Dade Behring BEP 2000 automated ELISA processor (now Siemens Healthcare). All reagents, calibrators and controls were prepared as recommended by the manufacturer. All standards, quality controls and samples were analyzed in duplicate. Results were calculated using the data processing software supplied with the BEP 2000. The lower limit of detection of the assay was found to be 2 U/mL. Samples with concentrations greater than the top standard were repeated after dilution in assay buffer. The between-batch coefficient of variation was 13.3% at a concentration of 11.3 U/mL, 8.8% at 34 U/mL and 9.5% at 65 U/mL.

### **Immunofluorometric assay to measure Mcm5 levels in urine sediments**

Mcm5 was measured by two-site time-resolved fluorescence immunoassay on the AutoDELFIAnalyzer (Perkin Elmer). All standards, quality controls and urine samples were prepared and processed as described (19). Nunc Maxisorp microtiter plates (Perkin Elmer) were coated with 12A7 mouse anti-human Mcm5 monoclonal antibody (19) at a concentration of 8 mg/L by Dako UK Ltd (Ely, UK). A large batch (approximately 200) of plates were prepared by Dako and used throughout the study. Plates were received pre-blocked and ready for use. A second mouse anti-human Mcm5 monoclonal antibody (4B4) (19) was conjugated with europium by Dako. The europium-labeled antibody was at a concentration of 1.75 mg/mL. The assay was calibrated with processed HeLa cell standards at a concentration of 150000 cells/well. A series of standards spanning the concentration range 150000 to 15000 cells/well were prepared by diluting



the stock standard in phosphate buffered saline containing 0.04% SDS and 0.02% sodium azide. Quality control samples containing four different concentrations of HeLa cells were analyzed at the beginning and end of each batch. The protocol for the AutoDELFIA assay was as follows. 50 L standard, sample or quality control was added (in duplicate) to the antibody-coated microtiter plate along with 100 L DELFIA multibuffer (Perkin Elmer product code 1380-3614). The plate was incubated for 2.5 h with continuous shaking. The plate was then washed four times with DELFIA wash buffer (Perkin Elmer product code B117-100). Europium-labeled detection antibody 4B4 was diluted 1:1,800 in DELFIA multibuffer. 100 L of diluted antibody was added to each well and the plate incubated for a further 4 h with continuous shaking. The plate was then washed six times with DELFIA wash buffer and 200 L DELFIA enhancement solution (Perkin Elmer product code B118-100) was added to each well. The plate was incubated on a shaker for a further 10 min. The amount of europium in each well was measured on the AutoDELFIA plate reader. Data were automatically transferred to a MultiCalc software package (Perkin Elmer), which was used to generate a calibration curve and calculate the concentration of the unknowns. The lower limit of detection of the assay was found to be 1000 cells/well. Samples with concentrations greater than the top standard were repeated after dilution in the standard dilution buffer. The between-batch coefficient of variation was 11.5% at a concentration of 2648 cells/well and 11.0% at 26382 cells/well.

### Statistical analysis

Sensitivity and specificity characteristics of Mcm5 and NMP22 for the detection of TCC of the bladder are presented as receiver operating characteristics (ROC) curves. The area under the nonparametric ROC curve was used to assess the overall accuracy of each test. Three cut-points were used to demonstrate test performance under different circumstances for Mcm5 and NMP22 as follows: (i) at the lower detection limit of the assay (i.e. 1000 cells/well for Mcm5, 2 U/mL for NMP22), where sensitivity of the test was maximal, (ii) where sensitivity and specificity were equal (i.e. 1700 cells/well for Mcm5, 4.5 U/mL for NMP22), and (iii) where specificity was 99% (i.e. 17200 cells/well for Mcm5, 100 U/mL for NMP22). An exact 95% confidence interval (CI) for each proportion, including sensitivity, specificity and predictive values for Mcm5 and NMP22, was derived assuming a binomial distribution.

False positive rates (FPR) for the Mcm5 and NMP22 tests in patients with benign diagnosis were compared with clear normal patients using a Chi-squared test. The Mcm5 and NMP22 values were summarized using medians and interquartile ranges (IQR) and compared with the clear normal patients using the Mann-Whitney U-test. For each biomarker, the ROC analysis was repeated for males and females separately and the areas under the ROC curves were compared using a Chi-squared test with one degree of freedom. ROC analysis was also undertaken to examine the sensitivity of the main results to the exclusion of those with benign disease. The values of the urinary biomarkers for patients with different tumor grades and stages and normal patients were compared using Mann-Whitney U-tests between neighboring categories, and using the Jonckheere-Terpstra test for trend across grades and stages. The Chi-squared test for linear by linear association was used to assess the evidence for a trend in the false positive rates by increasing tumor grade and stage. The sensitivity determined for urinary cytology was compared with that of the immunofluorometric Mcm5 test using McNemar's test for paired proportions. All statistical tests were two-tailed, and a 5% level was used to indicate statistical significance.

A multi-ROC analysis (27) was performed to determine the additional performance resulting from using both biomarkers together. In this analysis, NMP22 was kept fixed at the recommended cut-point of 10 U/mL and Mcm5 was included with a varying cut-point. Raised values of either marker could predict positive for TCC. The additional performance of Mcm5 was assessed using the nonparametric area under the multi-ROC curve, using a Chi-squared test with one degree of freedom. In order to demonstrate test performance, Mcm5 was then fixed at the cut-point which provided equal sensitivity and specificity on the multi-ROC curve from using the combined markers. These were compared with the equal sensitivity and specificity that could be provided by use of NMP22 alone.



## Results

### Demographics and clinical investigation

The demographic characteristics, mode of presentation, final diagnosis, and tumor grade and stage for the 1677 patients included in this study are summarized in Table 1. Figure 1 shows a flow chart indicating the patient numbers in each of the patient groups (i.e. mode of presentation, clinical diagnosis, Mcm5 result at the 1700-cell cut-point (see Materials and Methods), and patients without Mcm5 result). The study population was predominantly male (62%) and had a mean age of 60.7 years (SD, 16.3 years). Of those with a recorded presentation, 55% had visible hematuria and 45% had non-visible hematuria. These patients were nearly all newly presenting cases, although four patients had a previous history of TCC. Conventional clinical investigation included multiple tests as described above. Not all patients underwent all investigations. Investigations were omitted when clinically not indicated, the diagnosis becoming apparent prior to the test being performed, or through patient choice. Tests omitted included ultrasound scan in 186 patients and intravenous urography in 223 patients. Urine cytology was unavailable for 109 patients due to insufficient sample collection or, alternatively, because the test was not undertaken. Cystoscopy was not performed in 20 patients. No imaging procedure was performed in 77 patients, including a 20-year-old male with a urethral stricture, who had neither imaging nor diagnostic cystoscopy. All patients had a clinical diagnosis attributed to them by their clinician. The Venn diagram in Supplementary Figure 1 shows the distribution of patients with incomplete investigations. Data were not formally collected on the adverse effects of standard clinical testing and no adverse effects of urinary testing for Mcm5 or NMP22 were recorded. Analysis of the performance of the Mcm5 and NMP22 tests was only performed for patients with biomarker results available, i.e. patients with no Mcm5 result available were excluded from Mcm5 sensitivity and specificity analyses and ROC curve calculations, but would have been included in NMP22 analyses if an NMP22 result was available.

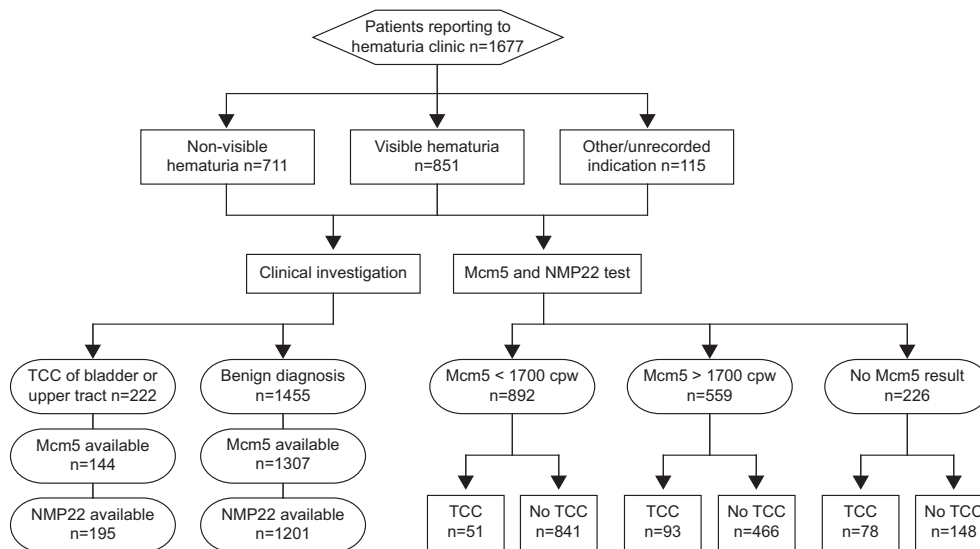


Figure 1: Study flow diagram showing the outcome of clinical investigation and the outcome of Mcm5 testing at the 1700 cells/well cut-point for all study participants.

Following clinical investigation, urinary tract tumors were identified in 222/1677 patients (13%). Nearly all tumors were TCCs, but, investigation also identified one case of adenocarcinoma and two cases of squamous cell carcinoma of the bladder. The TCCs were predominantly bladder tumors, with only seven patients with upper tract tumors. The upper tract TCCs are included alongside the bladder tumors for the analysis reported below. The patients were evenly distributed across tumor grades; 26 (12%) were grade 1, 129 (58%) were grade 2, and 66 (30%) were grade 3 (including cases of carcinoma in situ). The tumor stage in these patients was pTa in 122 (55%), pT1 in 50 (23%), pT2/3 in 41 (18%), pTis in eight (4%) and pTx in one. The diagnoses in the remaining patients included other malignancies, previous urothelial carcinoma,

Table 1: Patient demographics and clinicopathological data

	No. (%) or mean (SD)
Patients recruited	1677
Age, y	60.7 (16.3)
Gender	
Male	1040 (62)
Female	637 (38)
Bladder/upper tract tumour, No. (%)	
Positive	222 (13)
Negative	1455 (87)
Grade <sup>a</sup>	
1	26 (12)
2	129 (58)
3 (including CIS)	66 (30)
Stage <sup>b</sup>	
T0	1455
Tx	1
Tis	8 (4)
Ta	122 (55)
T1	50 (23)
T2/3/3a	41 (18)
Initial referral <sup>c</sup>	
Non-visible hematuria	711 (45)
Visible hematuria	851 (55)
Unrecorded	115

Abbreviations: SD, standard deviation

<sup>a</sup> n=221

<sup>b</sup> Percentage of patients excluding those at stage T0 or Tx

<sup>c</sup> Percentage of recorded cases only

benign lesions or cysts of the kidney, benign inflammatory and congenital conditions, urolithiasis, benign prostatic hyperplasia and nephrological diseases. The diagnoses are listed in Supplementary Table 1.

### Mcm5, NMP22 and cytology test performance

A result for the immunofluorometric Mcm5 test was available in 1451 patients including 144 patients (10%) with a urothelial tumor. Individual Mcm5 data grouped by diagnosis are shown in Supplementary Figure 2A. The sensitivity, specificity, and positive and negative predictive values (PPV and NPV) for Mcm5 are shown in Table 2. The performance of the Mcm5 immunoassay is shown as an ROC curve (Figure 2A). The Mcm5 test discriminated, with high specificity and sensitivity, between patients with and without bladder cancer, as demonstrated by the large AUC (0.71 [95% CI = 0.66–0.77]), statistically significantly larger than the area assumed by the null hypothesis (0.5;  $P < 0.001$ ). The cut-points, 1000 cells/well (lower detection limit of the assay), 1700 cells/well (approximately equal sensitivity and specificity), and 17200 cells/well (specificity of 99% for all patients tested), demonstrated a wide range of test performance levels (Table 2). At the 1000-cell cut-point, the test had 74% (95% CI = 66–81%) sensitivity and 14% (95% CI = 12–17%) PPV. At the 1700-cell cut-point, the test had 65% (95% CI = 56–72%) sensitivity and 17% (95% CI = 14–20%) PPV. At the 17200-cell cut-point, the test had 29% (95% CI = 22–37%) sensitivity and 76% (95% CI = 63–87%) PPV. Importantly, at the cut-point where the specificity of the Mcm5 test was equal to that of cytology (97%), the immunofluorometric test was statistically significantly more sensitive than cytologic analysis of urine (37% [95% CI = 29–46%] vs 7% [95% CI = 3–12%],  $P < 0.001$ ).

A result for the NMP22 test was available in 1396 patients, including 195 patients (14%) with a urothelial tumor. Individual NMP22 data are shown in Supplementary Figure 2B. The sensitivity, specificity, and positive and negative predictive values for NMP22 are shown in Table 2. The NMP22 test discriminated

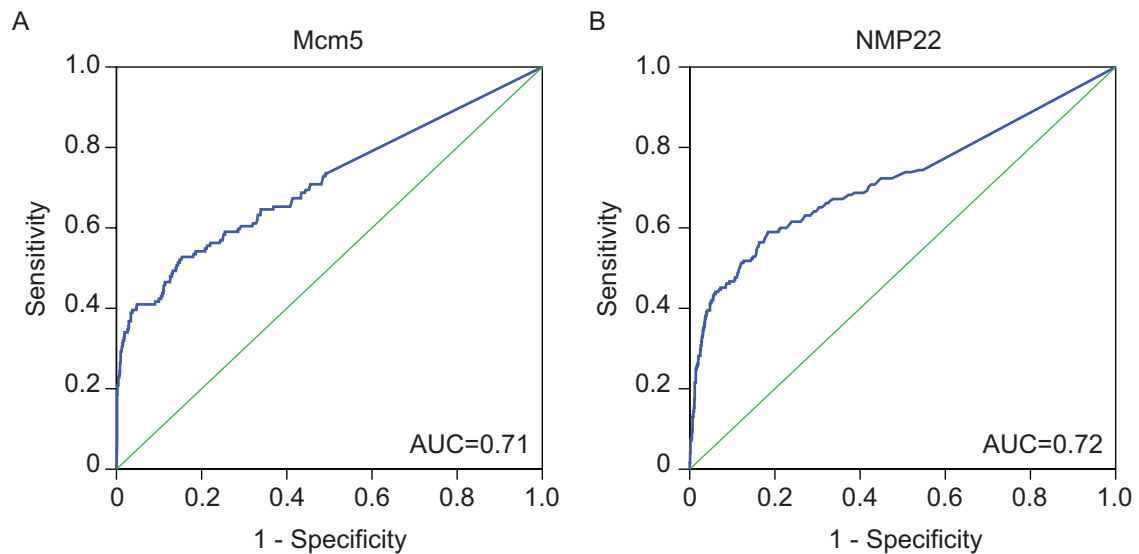


Figure 2: ROC curves for (A) Mcm5 and (B) NMP22 tests for the detection of bladder cancer in all studied patients with valid test results.

with high specificity and sensitivity as demonstrated by the large AUC (0.72 [95% CI = 0.67–0.77]; null hypothesis [0.5;  $P < 0.001$ ]) (Figure 2B). Our analysis was performed using cut-points that correspond to NMP22 values of 2 U/mL (to obtain maximum sensitivity), 4.5 U/mL (the point where sensitivity and specificity were equivalent), and 100 U/mL (providing 99% specificity; Table 2). At the NMP22 2 U/mL cut-point, the test had 74% (95% CI = 68–80%) sensitivity and 18% (95% CI = 15–21%) PPV. At the NMP22 4.5 U/mL cut-point, the test had 67% (95% CI = 60–74%) sensitivity and 24% (95% CI = 21–28%) PPV. At the NMP22 100 U/mL cut-point, the test had 14% (95% CI = 10–20%) sensitivity and 70% (95% CI = 53–83%) PPV. Where the specificity of the NMP22 test was equal to that of cytology (NMP22 specificity at 32 U/mL cut-point = cytology specificity = 97%), the NMP22 test was statistically significantly more sensitive than cytologic analysis of urine (35% [95% CI = 28–42%] versus 9% [95% CI = 5–14%],  $P = 0.002$ ).

The ROC analyses were repeated excluding those normal patients with a benign diagnosis (Supplementary Figure 3). Based on 144 TCC patients and 640 clear normal patients with Mcm5 values, the AUC for Mcm5 was 0.72 (95% CI = 0.66–0.77). For 195 TCC patients and 589 clear normal patients with NMP22 values, the AUC for NMP22 was 0.74 (95% CI = 0.69–0.79). For both Mcm5 and NMP22, the AUC values were statistically significant ( $P < 0.001$ ). These AUC values were only marginally higher than the AUC values including all patients (Mcm5: 0.71 vs 0.72, NMP22 0.72 vs 0.74), indicating that the presence of patients with benign disease did not influence the performance of the two tests overall.

The test performance characteristics of urine cytology and ultrasound examination of the urinary tract were also calculated (Table 2). Cytology had a sensitivity of 9% (95% CI = 5–14%; including atypical cytology) with specificity of 88% (95% CI = 86–89%) and PPV of 10% (95% CI = 7–15%). The sensitivity of ultrasound was 54% (95% CI = 46–62%), with a PPV of 32% (95% CI = 27–37%).

### Biomarker false positive analysis

False positives were found in 446/1258 (35%) of clear normal and benign diagnosis patients with the Mcm5 test at the 1700 cell cut-point. There was a significantly higher rate of false positive results in female patients, 45% (223/499) compared to 29% (223/759) in males ( $P = 0.002$ ). Urinary Mcm5 levels were also significantly higher in normal/benign females compared to males (median 1480 cells/well [IQR = <1000–3240 cells/well] vs median <1000 cells/well [IQR = <1000–2147 cells/well],  $P < 0.001$ ). Furthermore, compared to other benign groups, urinary calculi were associated with a significantly higher false posi-

Table 2: Sensitivity, specificity and positive and negative predictive values of Mcm5, NMP22, cytology and ultrasound for all patients with test results available

	No.	Sensitivity % (95% CI)	Specificity % (95% CI)	PPV % (95% CI)	NPV % (95% CI)
Mcm5 test cut-point, cells/well					
1000	1451	74 (66–81)	51 (48–53)	14 (12–17)	95 (93–96)
1700		65 (56–72)	64 (62–67)	17 (14–20)	94 (93–96)
17200		29 (22–37)	99 (98–99)	76 (63–87)	93 (91–94)
NMP22 test cut-point, U/mL					
2	1396	74 (68–80)	45 (42–48)	18 (15–21)	92 (89–94)
4.5		67 (60–74)	66 (64–69)	24 (21–28)	93 (91–94)
100		14 (10–20)	99 (98–99)	70 (53–83)	88 (86–89)
Cytology (positive and atypical)	1568	9 (5–14)	88 (86–89)	10 (7–15)	87 (85–88)
Cytology (positive)	1568	2 (1–5)	97 (95–97)	8 (2–19)	87 (85–89)
Ultrasound scan	1479	54 (46–62)	84 (82–86)	32 (27–37)	93 (92–95)

Abbreviations: CI, confidence interval; PPV, positive predictive value, NPV, negative predictive value

tive rate (50% [52/104] vs 34% [173/514],  $P=0.004$ ) and higher urinary levels of Mcm5 protein (median 1690 cells/well [ $<1000$ –3940 cells/well] vs  $<1000$  cells/well [ $<1000$ –2510 cells/well],  $P<0.001$ ; Table 3). There was no evidence of an association between the false positive rate and any of the other benign groups including inflammatory conditions and benign prostatic hyperplasia. In the clear normal and benign patient groups there were no significant differences ( $P=0.99$ ) in NMP22 levels between males and females. A raised NMP22 signal and increased false positive rate was observed for those patients with urinary tract infections (FPR: 41% [91/222] vs 29% [168/589],  $P=0.003$ ; median NMP22 result: 3.35 U/mL vs 2.2 U/mL,  $P<0.001$ ) and urinary calculi (FPR: 43% [41/96] vs 29% [168/589],  $P=0.008$ ; NMP22: 2.55 U/mL vs 2.2 U/mL,  $P=0.05$ ) (Table 3).

The ROC analysis for Mcm5 and NMP22 was repeated observing the results in all males and females and in males and females excluding patients with stones (Supplementary Table 2 Supplementary Figures 4 and 5). For males, the AUC values were 0.73 (95% CI = 0.67–0.79) for Mcm5 and 0.69 (95% CI = 0.64–0.75) for NMP22, and for females 0.70 (95% CI = 0.60–0.80) for Mcm5 and 0.80 (95% CI = 0.72–0.88) for NMP22. There were no significant differences in AUC values for Mcm5 between males and females, but there was a significant difference ( $P=0.024$ ) in the NMP22 AUC value between males and females, apparently related to the greater NMP22 sensitivity in females. Interestingly, while the Mcm5 false positive rate was higher in women, this did not impact on the Mcm5 AUC value, presumably due to the slightly greater sensitivity of Mcm5 in females compared to males (e.g. 69% vs 63% at the 1700-cell cut-point, data not shown). Excluding patients with stones from the analysis made no significant difference to test performance (Supplementary Table 2).

### Biomarker false negative analysis

Table 4 and Supplementary Table 3 show the false negative rates of urinary Mcm5 and NMP22 grouped by tumor grade and stage. There was evidence of a decreasing trend in the false-negative rate with increasing tumor grade and stage for both urinary biomarkers. For grades 1, 2 and 3 respectively, the false negative rates for urinary Mcm5 at the 1700-cell cut-point were 62% (95% CI = 32–86%), 40% (95% CI = 29–51%) and 17% (95% CI = 6–33%; trend  $P=0.002$ ). For NMP22 at the 4.5 U/mL cut-point, the corresponding false negative rates were 72% (95% CI = 51–88%), 32% (95% CI = 24–42%) and 14% (95% CI = 6–26%;  $P<0.001$ ). Similar trends were observed for tumor stage. The false negative rate for Mcm5 was 51% (95% CI = 39–92%), 11% (95% CI = 2–28%) and 18% (95% CI = 6–37%) for pTa, pT1 and pT2/3/3a tumors

Table 3: Comparison of values and false positive rates for Mcm5 and NMP22 tests across benign conditions

Benign condition	No.	Test value <sup>a</sup> , cells/well	P <sup>b</sup>	FPR, % <sup>c</sup>	P <sup>d</sup>
<b>Mcm5 test</b>					
Normal	640	<1000 (<1000–2435)		35	
Benign prostatic hyperplasia	128	<1000 (<1000–2367)	0.08	30	0.32
Calculi	104	1690 (<1000–3940)	<0.001	50	0.004
Nephrological	38	<1000 (<1000–2122)	0.23	29	0.5
Prostatitis	14	<1000 (<1000–3432)	0.4	29	0.67
Urethral stricture	21	1100 (<1000–2620)	0.84	38	0.76
Urinary tract infection	236	<1000 (<1000–2670)	0.95	37	0.54
Other	77	<1000 (<1000–2285)	0.83	32	0.73
Test value <sup>a</sup> , U/ml					
<b>NMP22 test</b>					
Normal	589	2.20 (<2–5.30)		29	
Benign prostatic hyperplasia	110	<2 (<2–5.60)	0.96	29	0.32
Calculi	96	2.55 (<2–9.47)	0.05	43	0.008
Nephrological	38	2.04 (<2–6.42)	0.92	34	0.5
Prostatitis	13	<2 (<2–3.50)	0.14	15	0.67
Urethral stricture	18	2.85 (<2–6.82)	0.36	39	0.76
Urinary tract infection	222	3.35 (<2–8.62)	<0.001	41	0.003
Other	68	2.80 (<2–8.02)	0.018	40	0.73

Abbreviations: CI, confidence interval; FPR, false-positive rate; IQR, interquartile range; med, median

<sup>a</sup> median (interquartile range)

<sup>b</sup> Mann-Whitney test, comparison of test value with normals

<sup>c</sup> Determined using 1700-cell cut-point for Mcm5 test, 4.5 U/mL cut-point for NMP22 test

<sup>d</sup> Chi-squared test, comparison of false-positive rate with normals

respectively (P<0.001). For NMP22 the false negative rates were 45% (95% CI = 35–55%), 20% (95% CI = 10–35%) and 9% (95% CI = 2–24%) for pTa, pT1 and pT2/3/3a tumors respectively (P<0.001). A significant decrease in the amplitude of the Mcm5 and NMP22 signal with lower tumor grade and stage was observed, in keeping with the increasing false negative rates observed for these groups (Table 4 and Supplementary Table 3).

### Combined biomarker Multi-ROC analysis

There were 117 bladder TCCs and 1053 normal patients with assay data available for both urinary markers. The sensitivity and specificity of NMP22 were both equal to each other at the cut-point of 4.15 U/mL, being 65% (76/117) and 65% (686/1053), respectively. Mcm5 at the cut-point 1620 cells/well also had a sensitivity (76/117) equal to specificity (686/1053) at 65%.

At the recommended (Matritech) cut-point of 10 U/mL for NMP22, sensitivity is 49% (57/117) with specificity 85% (894/1053). On the basis of Multi-ROC analysis, the immunofluorometric Mcm5 test, in combination with NMP22 at the recommended 10 U/mL cut-point, offers a statistically significant increase in performance (P=0.002) compared with NMP22 alone at the recommended cut-point (area under multi-ROC curve = 0.62, 95% CI = 0.54–0.69). If in combination with NMP22 at 10 U/mL, the immunofluorometric Mcm5 test is applied using a cut-point of 3470 cells/well, this provides sensitivity (82/117) and specificity (738/1053) both equal to 70%, which is an improvement over use of NMP22 alone where sensitivity (76/117) and specificity (686/1053) both equal 65%.

The sensitivity of the Mcm5 test in combination with NMP22 was analyzed according to grade and stage. The combined test identified 53% (36/68) of pTa tumors, 91% (21/23) of pT1 tumors, 100% (21/21) of pT2 or more advanced tumors and 80% (4/5) of patients with carcinoma in situ. Grade 1 disease was identified

Table 4: Comparison of Mcm5 and NMP22 test performance across grade and stage

	No.	Test value <sup>c</sup> cells/well	P (normal) <sup>d</sup>	P (adjacent) <sup>e</sup>	P (trend) <sup>f</sup>	FNR % (95% CI)	P (normal)	P (adjacent)	P (trend)
<b>Mcm5 test<sup>a</sup></b>									
Normal	1307	<1000 (<1000–2650)				64 (62–67)			
Grade									
1	13	1030 (<1000–7445)	0.52	0.52	<0.001	62 (32–86)	0.94	0.94	0.002
2	88	2615 (<1000–12800)	<0.001	0.2	<0.001	40 (29–51)	0.002	0.15	0.002
3	36	19850 (3910–94500)	<0.001	<0.001	<0.001	17 (6–33)	0.002	0.021	
Stage									
pTa	81	1610 (<1000–5870)	0.001	0.001	<0.001	51 (39–92)	0.015	0.015	<0.001
pT1	28	29050 (5100–136250)	<0.001	<0.001	<0.001	11 (2–28)	0.002	0.002	
pT2/3/3a	28	17700 (3505–70800)	<0.001	0.45		18 (6–37)	0.002	0.69	
<b>NMP22 test<sup>b</sup></b>									
Normal	1201	2.40 (<2–6.30)				66 (64–69)			
Grade									
1	25	<2 (<2–8.45)	0.31	0.31	<0.001	72 (51–88)	0.57	0.57	<0.001
2	112	10.20 (2.67–39.82)	<0.001	<0.001	<0.001	32 (24–42)	0.002	0.002	
3	51	62.50 (9.90–145.50)	<0.001	<0.001	<0.001	14 (6–26)	0.002	0.026	
Stage									
pTa	109	6.00 (<2–24.50)	<0.001	<0.001	<0.001	45 (35–55)	0.002	0.002	<0.001
pT1	45	31.30 (5.70–125.90)	<0.001	<0.001	<0.001	20 (10–35)	0.002	0.007	<0.001
pT2/3/3a	34	70.65 (22.67–258.50)	<0.001	0.099		9 (<2–24)	0.002	0.31	

Abbreviations: CI, confidence interval; FNR, false-negative rate; IQR, interquartile range; med, median

<sup>a</sup> Data analysis using 1700-cell cut-point for Mcm5 test<sup>b</sup> Data analysis using 4.5 U/mL cut-point for NMP22 test<sup>c</sup> median (interquartile range)<sup>d</sup> Mann-Whitney test, comparison with normals<sup>e</sup> Mann-Whitney test, comparison with adjacent grade, i.e. grade 1 vs normal, grade 2 vs grade 1, grade 3 vs grade 2<sup>f</sup> Jonckheere-Terpstra test for trend across grades or stages, excluding normals



in 42% (5/12), grade 2 disease in 62% (44/71) and grade 3 disease (including 5 cases of CIS) in 97% (33/34) of cases. Notably the Mcm5 test in combination with NMP22 identifies nearly all cases of life threatening disease, i.e. high grade muscle invasive tumors with high specificity (70%, 95% CI = 67–73%).

### Renal cell carcinoma and prostate cancer detection

Of the 1677 patients investigated with hematuria, 34 men were diagnosed with prostate cancer (and an additional five with prostate cancer previously successfully treated with radiotherapy) and 14 patients had a renal cell carcinoma. The 34 men with prostate cancer in the cohort included 31 men with an Mcm5 result and 29 men with an NMP22 result available. The prostate cancer patients had a median Mcm5 level of 1150 cells/well (IQR = <1000–3160 cells/well) and an NMP22 level of 2.8 U/mL (IQR = 1.99–6.58 U/mL). The diagnostic sensitivity for Mcm5 at the 1700 cell cut-point was 39% (12/31) and for NMP22 at the standard 10 U/mL cut-point was 10% (3/29). Renal cell carcinomas had a median Mcm5 level of 1455 cells/well (IQR = <1000–5145 cells/well) and an NMP22 level of 15.2 U/mL (IQR = 2.45–57.3 U/mL). There were 14 men with renal cell carcinoma and an Mcm5 result available. Of these 14 men, 11 also had an NMP22 result available. The diagnostic sensitivity for Mcm5 at the 1700 cell cut-point was 43% (6/14) and for NMP22 at the standard 10 U/mL cut-point was 64% (7/11).

### Discussion

In an earlier proof-of-concept study we showed that elevated Mcm5 levels in urine cell sediments are highly predictive of bladder cancer (19). The prospective blinded observational trial reported here, involving a large patient cohort, confirms our initial observations that Mcm5 is a sensitive and specific biomarker for detection of TCC. Importantly, through multi-ROC analysis, we show here that the Mcm5 test, in combination with NMP22 at the established cut-point 10 U/mL, enhances diagnostic accuracy over NMP22 in isolation and identifies nearly all life threatening disease. Moreover, both tests had much higher sensitivity when compared to conventional cytological analysis.

Despite numerous studies over the last decade, the reported accuracy of the NMP22 test is highly variable. Many of the earlier studies recruited small to moderate numbers of subjects and reported high sensitivities and specificities, above 80% (28-31). However, a wide range in test performance has been observed in more recent studies with sensitivity ranging from 33-100% and specificity from 40% to 93% (7). A pooled analysis including more recent trials suggests a sensitivity of around 68% and a specificity of 79% (7). A recent large multi-institutional international trial revealed a marked variability in the performance of the NMP22 test across participating institutions with sensitivity and specificity ranging from 36% to 86% and 50% to 94% respectively (32). Variability has been attributed to many confounding factors including biological, analytical and epidemiological variables and methodological bias. Our study represents the largest prospective observational trial ever undertaken using the NMP22 urinary biomarker. Notably, the performance at the 10 U/mL cut-point, with a sensitivity of 49% and specificity of 85%, is somewhat below that reported in the pooled analysis, but almost identical to the diagnostic performance reported in the Matritech supported large patient cohort trials using the NMP22 point-of-care proteomic assay (7,33).

The analysis of false positive Mcm5 results in this study revealed an unexpected difference between the male and female groups. The overall false positive rate in females was 45% compared to 29% in males. Rather than being related to benign pathology, the difference was most marked in the clear normal group. This had a minor impact on AUC values with a higher value for males (0.73 vs 0.69, Supplementary Figure 5). This difference requires further investigation. Possible causes could be fungal contamination by vaginal flora (e.g. *Candida* species) or mixing of menstrual endometrial contaminants in samples, both sources of extraneous MCM expressing cells. Patients with urinary calculi had the highest incidence of false positive Mcm5 results in both males (42%) and females (63%). As previously reported, higher false positive rates are expected in patients with urinary calculi due to the associated mucosal injury, which exposes the underlying MCM expressing transit amplifying compartment of the transitional epithelium to the urinary tract (11,19,22). However, exclusion of patients with calculi from the ROC analysis did not make a significant improvement to the overall performance, presumably because they were a relatively small group. Notably, other benign conditions such as urinary tract infection or benign prostatic hyperplasia were not associated



with false positive Mcm5 results, in keeping with our proof-of-concept study (19). In contrast to the Mcm5 test, false positive NMP22 results were linked to urinary tract infection. This biological difference as cause for false positives in the NMP22 and Mcm5 tests may contribute to the improved performance observed when combining the two urinary biomarkers.

Decreasing urinary Mcm5 and NMP22 signals were observed with lower stage and grade of TCC, and this was associated with an increasing false negative rate for both tests. This trend most likely relates to the fact that well differentiated small TCCs are less prone to spontaneous shedding of tumor cells due to stronger cell-cell and cell-matrix attachments. Similarly, increasing cytology and ultrasound false negative rates were associated with early stage and well differentiated TCCs. Commercial development of the Mcm5 test is currently underway to improve sensitivity and thereby reduce false negative rates associated with early stage, well differentiated tumors. As is the case for the NMP22 test, the Mcm5 test can also detect genito-urinary tract malignancies other than transitional cell carcinomas including prostate cancer and renal cell carcinomas. When considering use of the Mcm5 immunoassay in routine clinical testing, the fact that Mcm5 is a marker of epithelial dysplasia and malignancy and not an organ specific marker will need to be understood by clinicians. Clinical pathways to appropriately investigate patients with positive findings will therefore be required.

Current routine initial investigations for hematuria or other symptoms suggestive of bladder cancer include flexible cystoscopy and rigid white light cystoscopy. However an estimated 10-40% of tumors can be missed due to poor visualization as a result of inflammatory conditions or bleeding and flat urothelial lesions such as severe dysplasia and carcinoma in situ (34-36). Photodynamic diagnosis is a technique that can enhance tumor detection but its increased sensitivity is associated with higher false positive rates leading to additional unnecessary investigations, biopsies and thus increased cost (37). Urinary biomarkers also have potential to enhance tumor detection and identify tumors not visualized during initial endoscopy. A systematic review of the clinical effectiveness and cost-effectiveness of photodynamic diagnosis, cytology and urine biomarkers, including FISH, ImmunoCyt and NMP22, for detection and surveillance of bladder cancer has recently been undertaken using UK National Health Service data sources (7). Notably, of eight strategies included in a probabilistic sensitivity analysis using combinations of photodynamic diagnosis, flexible cystoscopy, white light cystoscopy, cytology and urinary biomarkers, four were associated with around a 20% chance of being considered cost-effective. Three of these four strategies involved the use of either a biomarker or photodynamic diagnosis. Importantly, we demonstrate here that the Mcm5 test identifies aggressive tumors with high sensitivity.

In conclusion, we have demonstrated that immunofluorometric detection of Mcm5 in urine sediments is a sensitive and specific diagnostic test for bladder cancer. The test detects bladder cancers of all stages and grades and is more accurate than urinary cytology. Importantly, Mcm5 in combination with the FDA-approved Matritech NMP22 Test Kit identifies nearly all life threatening disease.

### Acknowledgements

The authors thank Diane Walia for data entry and spreadsheet management. Mcm5 and NMP22 assays were performed by the National Institute for Health Research Cambridge Biomedical Research Centre, Core Biochemical Assay Laboratory. W.R. was supported by the Newcastle upon Tyne Experimental Cancer Medicine Centre, funded by the UK Department of Health and Cancer Research UK. This work was supported by Cancer Research UK (grant number C428/A3441 to K.S. and G.H.W).

### References

1. American Cancer Society. Cancer Facts & Figures 2009. 2010. Atlanta, American Cancer Society.
2. Cancer Research UK. CancerStats Key Facts Bladder Cancer. 2009. Cancer Research UK.
3. Stein JP, Lieskovsky G, Cote R, et al. Radical cystectomy in the treatment of invasive bladder cancer: long-term results in 1,054 patients. *J Clin Oncol*. 2001;19(3):666-675.
4. Landis SH, Murray T, Bolden S, Wingo PA. Cancer statistics, 1999. *CA Cancer J Clin*. 1999;49(1):8-31, 1.
5. Fitzpatrick JM. The natural history of superficial bladder carcinoma. *Semin Urol*. 1993;11(3):127-136.

6. Almallah YZ, Rennie CD, Stone J, Lancashire MJ. Urinary tract infection and patient satisfaction after flexible cystoscopy and urodynamic evaluation. *Urology*. 2000;56(1):37-39.
7. Mowatt G, Zhu S, Kilonzo M, et al. Systematic review of the clinical effectiveness and cost-effectiveness of photodynamic diagnosis and urine biomarkers (FISH, ImmunoCyt, NMP22) and cytology for the detection and follow-up of bladder cancer. *Health Technol Assess*. 2010;14(4):1-iv.
8. Compton DA, Cleveland DW. NuMA is required for the proper completion of mitosis. *J Cell Biol*. 1993;120(4):947-957.
9. Shelfo SW, Soloway MS. The role of nuclear matrix protein 22 in the detection of persistent or recurrent transitional-cell cancer of the bladder. *World J Urol*. 1997;15(2):107-111.
10. Gaston KE, Grossman HB. Proteomic assays for the detection of urothelial cancer. *Methods Mol Biol*. 2010;641:303-323.
11. Williams GH, Stoeber K. Cell cycle markers in clinical oncology. *Curr Opin Cell Biol*. 2007;19(6):672-679.
12. Machida YJ, Hamlin JL, Dutta A. Right place, right time, and only once: replication initiation in metazoans. *Cell*. 2005;123(1):13-24.
13. Remus D, Diffley JF. Eukaryotic DNA replication control: lock and load, then fire. *Curr Opin Cell Biol*. 2009;21(6):771-777.
14. Williams GH, Romanowski P, Morris L, et al. Improved cervical smear assessment using antibodies against proteins that regulate DNA replication. *Proc Natl Acad Sci U S A*. 1998;95(25):14932-14937.
15. Going JJ, Keith WN, Neilson L, Stoeber K, Stuart RC, Williams GH. Aberrant expression of minichromosome maintenance proteins 2 and 5, and Ki-67 in dysplastic squamous oesophageal epithelium and Barrett's mucosa. *Gut*. 2002;50(3):373-377.
16. Blow JJ, Gillespie PJ. Replication licensing and cancer—a fatal entanglement? *Nat Rev Cancer*. 2008;8(10):799-806.
17. Eward KL, Obermann EC, Shreeram S, et al. DNA replication licensing in somatic and germ cells. *J Cell Sci*. 2004;117(Pt 24):5875-5886.
18. Barkley LR, Hong HK, Kingsbury SR, James M, Stoeber K, Williams GH. Cdc6 is a rate-limiting factor for proliferative capacity during HL60 cell differentiation. *Exp Cell Res*. 2007;313(17):3789-3799.
19. Stoeber K, Swinn R, Prevost AT, et al. Diagnosis of genito-urinary tract cancer by detection of minichromosome maintenance 5 protein in urine sediments. *J Natl Cancer Inst*. 2002;94(14):1071-1079.
20. Freeman A, Morris LS, Mills AD, et al. Minichromosome maintenance proteins as biological markers of dysplasia and malignancy. *Clin Cancer Res*. 1999;5(8):2121-2132.
21. Williams GH, Swinn R, Prevost AT, et al. Diagnosis of oesophageal cancer by detection of minichromosome maintenance 5 protein in gastric aspirates. *Br J Cancer*. 2004;91(4):714-719.
22. Ayaru L, Stoeber K, Webster GJ, et al. Diagnosis of pancreaticobiliary malignancy by detection of minichromosome maintenance protein 5 in bile aspirates. *Br J Cancer*. 2008;98(9):1548-1554.
23. Khadra MH, Pickard RS, Charlton M, Powell PH, Neal DE. A prospective analysis of 1,930 patients with hematuria to evaluate current diagnostic practice. *J Urol*. 2000;163(2):524-527.
24. UICC International Union Against Cancer. TNM Classification of Malignant Tumours Seventh Edition. Indianapolis: Wiley-Blackwell; 2009.
25. Mostofi FK, Sobin LH, Torloni H. Histological typing of urinary bladder tumours. Geneva: World Health Organization; 1973.
26. Papanicolaou GN. A new procedure for staining vaginal smears. *Science*. 1942;95(2469):438-439.
27. Shultz EK. Multivariate receiver-operating characteristic curve analysis: prostate cancer screening as an example. *Clin Chem*. 1995;41(8 Pt 2):1248-1255.
28. Saad A, Hanbury DC, McNicholas TA, Boustead GB, Morgan S, Woodman AC. A study comparing various noninvasive methods of detecting bladder cancer in urine. *BJU Int*. 2002;89(4):369-373.
29. Sanchez-Carbayo M, Herrero E, Megias J, Mira A, Soria F. Evaluation of nuclear matrix protein 22 as a tumour marker in the detection of transitional cell carcinoma of the bladder. *BJU Int*. 1999;84(6):706-713.
30. Zippe C, Pandrangi L, Agarwal A. NMP22 is a sensitive, cost-effective test in patients at risk for bladder cancer. *J Urol*. 1999;161(1):62-65.
31. Ponsky LE, Sharma S, Pandrangi L, et al. Screening and monitoring for bladder cancer: refining the use of NMP22. *J Urol*. 2001;166(1):75-78.
32. Shariat SF, Marberger MJ, Lotan Y, et al. Variability in the performance of nuclear matrix protein 22 for the detection of bladder cancer. *J Urol*. 2006;176(3):919-926.
33. Grossman HB, Soloway M, Messing E, et al. Surveillance for recurrent bladder cancer using a point-

of-care proteomic assay. *JAMA*. 2006;295(3):299-305.

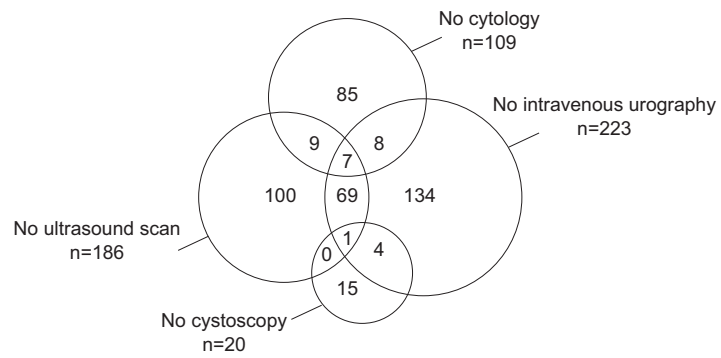
34. Zaak D, Kriegmair M, Stepp H, et al. Endoscopic detection of transitional cell carcinoma with 5-aminolevulinic acid: results of 1012 fluorescence endoscopies. *Urology*. 2001;57(4):690-694.

35. Schneeweiss S, Kriegmair M, Stepp H. Is everything all right if nothing seems wrong? A simple method of assessing the diagnostic value of endoscopic procedures when a gold standard is absent. *J Urol*. 1999;161(4):1116-1119.

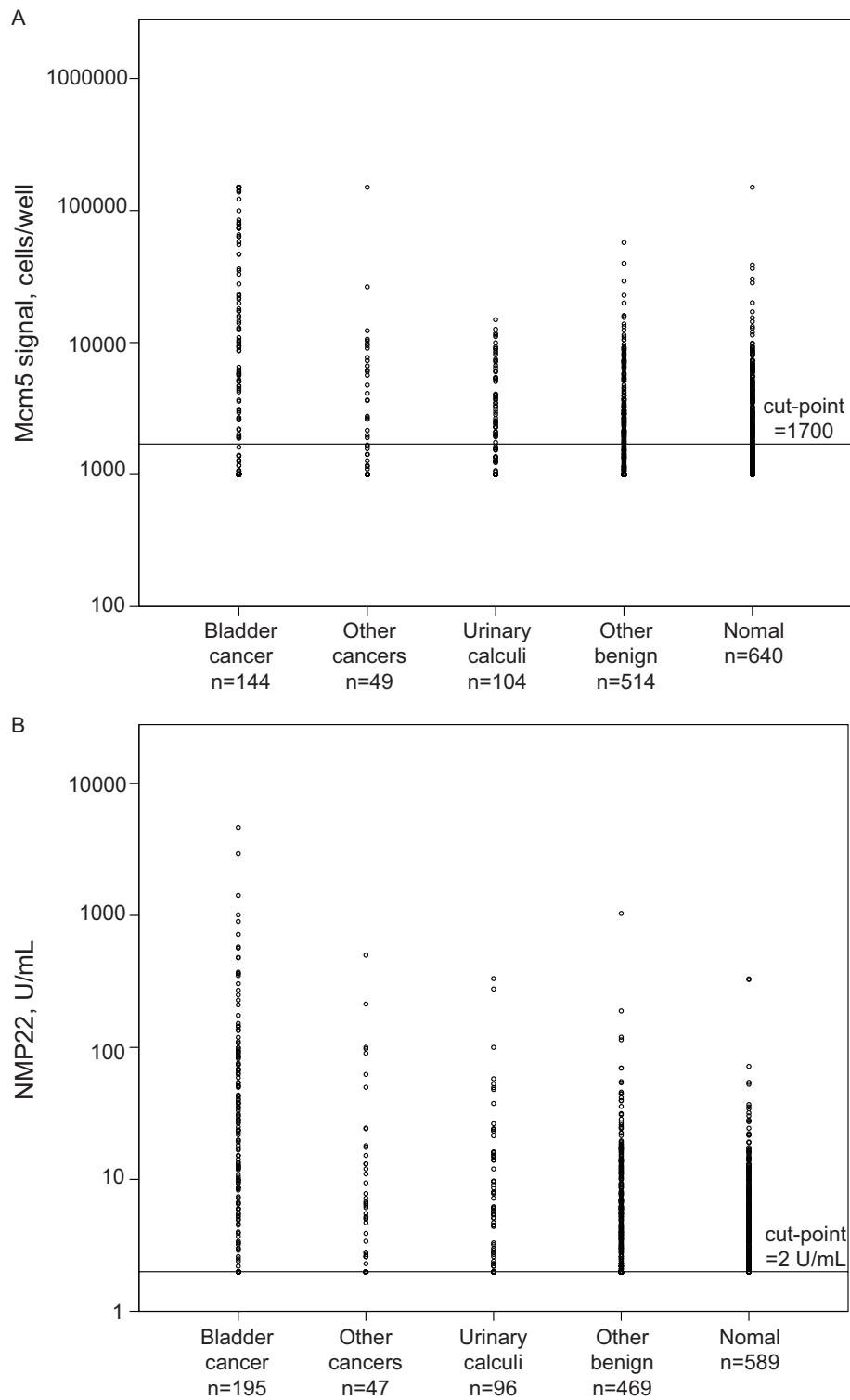
36. Kriegmair M, Baumgartner R, Knuchel R, Stepp H, Hofstadter F, Hofstetter A. Detection of early bladder cancer by 5-aminolevulinic acid induced porphyrin fluorescence. *J Urol*. 1996;155(1):105-109.

37. Gakis G, Kruck S, Stenzl A. Can the burden of follow-up in low-grade noninvasive bladder cancer be reduced by photodynamic diagnosis, perioperative instillations, imaging, and urine markers? *Curr Opin Urol*. 2010;20(5):388-392.

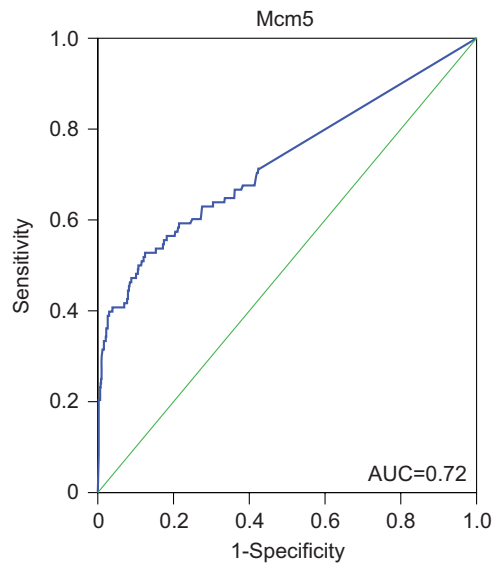
**Supplementary Material**



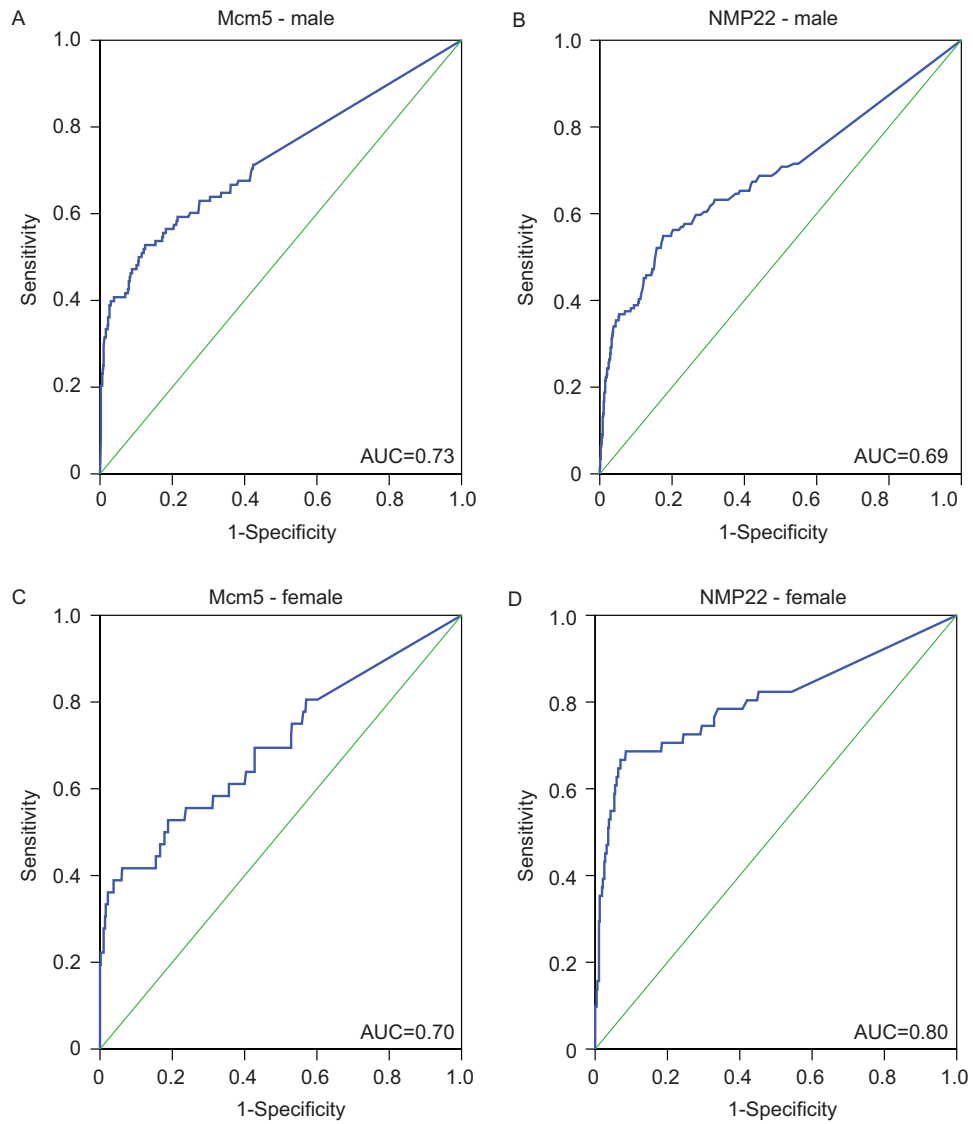
Supplementary Figure 1: Venn diagram showing the distribution of incomplete hematuria investigations amongst the 1677 recruited patients. Cytology data were deemed missing when the procedure was not performed or when there was insufficient material for complete analysis.



Supplementary Figure 2: Distribution of Mcm5 and NMP22 signals according to diagnostic group. **(A)** Plot of Mcm5 signals for all patients with a valid measurement. Mcm5 data are grouped by diagnosis subgroup. **(B)** Plot of NMP22 signals, grouped by diagnosis subgroup, for all patients with a valid measurement.

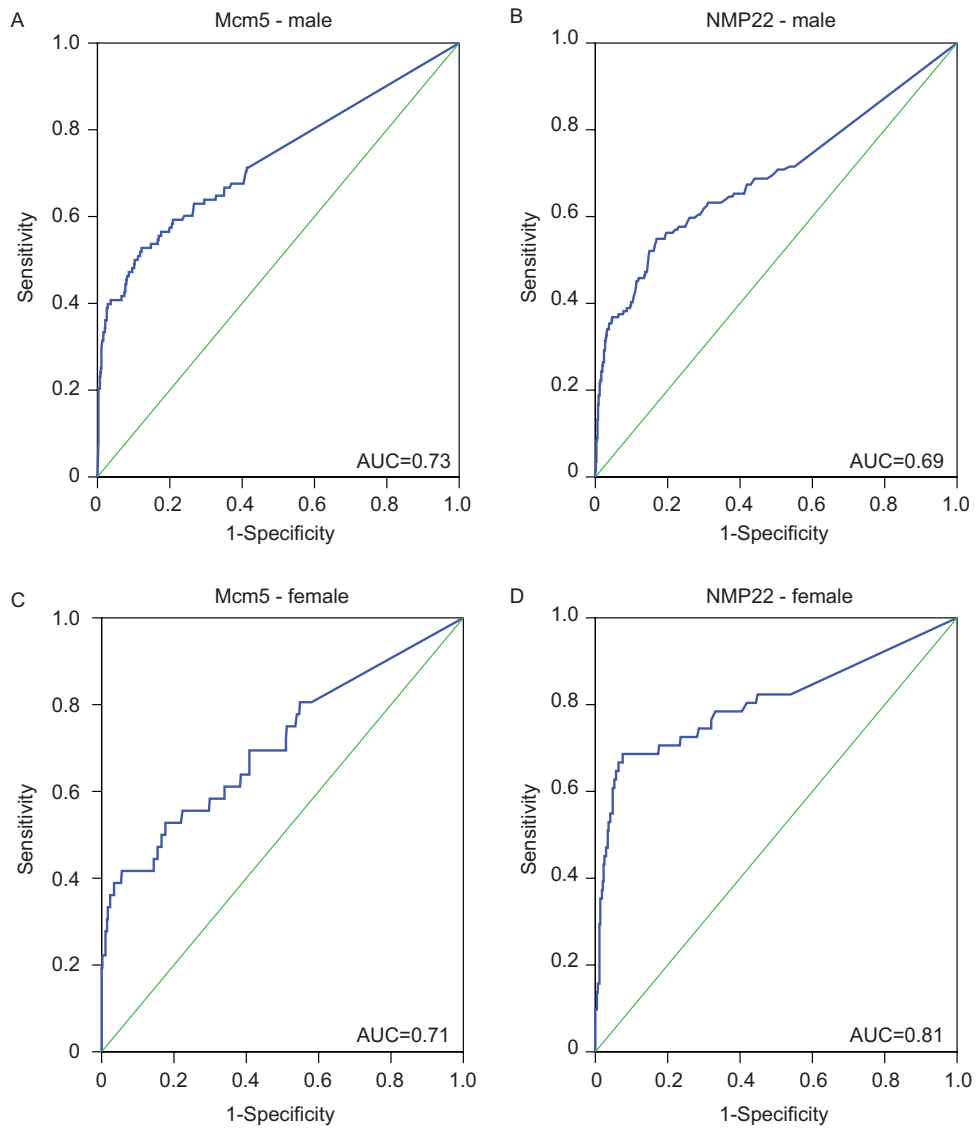


Supplementary Figure 3: ROC curve for the Mcm5 test for detection of bladder cancer in patients with clear normal findings or bladder tumors only.



Supplementary Figure 4: ROC curves for Mcm5 and NMP22 tests for detection of bladder cancer in male and female patients. (A) Mcm5 test in males. (B) NMP22 test in males. (C) Mcm5 test in females. (D) NMP22 test in females.





Supplementary Figure 5: ROC analyses of males and females, excluding patients with urinary calculi. (A) Mcm5 test in males. (B) NMP22 test in males. (C) Mcm5 test in females. (D) NMP22 test in females.

Supplementary Table 1: Patient diagnoses

	No.
Patients recruited	1677
Diagnosis	
Malignancy of bladder/upper tract	222
Clear normal	700
Other malignancies	
Gynaecological	2
Penile/testis	2
Prostate cancer	34
Renal cell carcinoma	14
Urolithiasis	
Bladder calculus	15
Renal calculus	99
Vascular calcification in kidney	1
Other benign conditions	
Benign prostatic hyperplasia	146
Nephrological	45
Prostatitis	14
Urinary tract infection	274
Miscellaneous benign	
Adult polycystic kidney disease	4
Angiomyolipoma	5
Atrophic/poorly functioning kidney	6
Balanitis	3
Bladder diverticulum	1
Catheter related	4
Chronic retention of urine	6
Epididymo-orchitis	8
Genitourinary tuberculosis	2
Hydronephrosis	1
Inverted papilloma	1
Neurogenic/pathic bladder	3
Oncocytoma	1
Normal <sup>a</sup>	4
Phimosis	1
Pyelonephritis	9
Pyelo-ureteric junction obstruction	4
Pyogenic granuloma	1
Radiation cystitis <sup>b</sup>	12
Renal transplant	3
Ureterocoele and retention of urine	1
Urethral caruncle	2
Urethral meatal stenosis	2
Urethral stricture	24
Vascular malformation of kidney	1

<sup>a</sup> Patients had a history of bladder TCC (> 5 years previously) or cyclophosphamide exposure

<sup>b</sup> Including one case with previous bladder TCC, five cases with previous prostate cancer

Supplementary Table 2: AUC values in males and females and in the groups excluding patients with urinary calculi

	Male		Female		P <sup>a</sup>
	No.	AUC (95% CI)	No.	AUC (95% CI)	
Mcm5 test					
All	910	0.73 (0.67–0.79)	541	0.70 (0.60–0.80)	0.67
Excluding urinary calculi	846	0.73 (0.67–0.79)	501	0.71 (0.61–0.81)	0.72
NMP22 test					
All	874	0.69 (0.64–0.75)	522	0.80 (0.72–0.88)	0.024
Excluding urinary calculi	812	0.69 (0.64–0.75)	488	0.81 (0.72–0.89)	0.025

Abbreviations: AUC, area under the curve; CI, confidence interval

<sup>a</sup> Chi-squared test comparing AUC values for males vs females

Supplementary Table 3: True and false negative rates of the Mcm5 and NMP22 tests, urine cytology and ultrasound by tumor grade and stage

	TNR, (95% CI)		False negative rate, (95% CI)					
	Normal (n=1307)	Grade 1 (n=13)	Grade 2 (n=88)	Grade 3 (n=36)	Stage pTa (n=81)	Stage pT1 (n=28)	Stage pT2/3/3a (n=28)	
Mcm5 test cut-point								
1000 cells/well	46 (43-49)	46 (19-75)	30 (20-40)	11 (3-26)	38 (28-50)	7 (1-24)	11 (2-28)	
1700 cells/well	64 (62-67)	62 (32-86)	40 (29-51)	17 (6-33)	51 (39-92)	11 (2-28)	18 (6-37)	
17200 cells/well	99 (98-99)	92(64 to100)	78 (68-86)	44 (28-62)	89 (80-95)	43 (24-63)	46 (28-66)	
NMP22 test cut-point								
2 U/mL	Normal (n=1201)	Grade 1 (n=25)	Grade 2 (n=112)	Grade 3 (n=51)	Stage pTa (n=109)	Stage pT1 (n=45)	Stage pT2/3/3a (n=34)	
4.5 U/mL	45 (42-48)	64 (43-82)	22 (15-21)	14 (6-26)	34 (25-44)	18 (8-32)	9 (2-24)	
100 U/mL	66 (64-69)	72 (51-88)	32 (24-42)	14 (6-26)	45 (35-55)	20 (10-35)	9 (2-24)	
	99 (98-99)	96(80 to100)	90 (83-95)	69 (54-81)	96 (91-99)	73 (58-85)	65 (46-80)	
Cytology								
All cases	Normal (n=1365)	Grade 1 (n=23)	Grade 2 (n=117)	Grade 3 (n=54)	Stage pTa (n=109)	Stage pT1 (n=46)	Stage pT2/3/3a (n=39)	
Excluding atypical	88 (86-89)	96(78 to100)	93 (87-97)	85 (73-93)	93 (86-97)	89 (76-96)	90 (76-97)	
	96 (95-97)	100 (85-100)	97 (93-99)	100 (93-100)	97 (92-99)	100 (92-100)	100 (90-100)	
Ultrasound scan								
All cases	Normal (n=1303)	Grade 1 (n=19)	Grade 2 (n=102)	Grade 3 (n=47)	Stage pTa (n=94)	Stage pT1 (n=41)	Stage pT2/3/3a (n=33)	
	84 (82-86)	53 (29-76)	50 (40-60)	26 (14-40)	51 (41-62)	44 (28-60)	21 (9-39)	

Abbreviations: CI, confidence interval; TNR, true negative rate



## Chapter 3

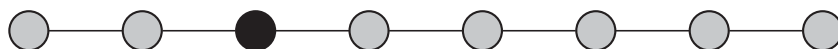
# Diagnosis of prostate cancer by detection of minichromosome maintenance 5 protein in urine sediments

TJ Dudderidge, JD Kelly, A Wollenschlaeger, O Okoturo, T Prevost, W Robson, HY Leung, GH Williams, K Stoeber

British Journal of Cancer 2010 103 (5): 701-707.

Supplementary material related to this article is available online at:

<http://www.nature.com/bjc/journal/v103/n5/supinfo/6605785s1.html>



## Diagnosis of prostate cancer by detection of minichromosome maintenance 5 protein in urine sediments

TJ Dudderidge<sup>1,2</sup>, JD Kelly<sup>1</sup>, A Wollenschlaeger<sup>3</sup>, O Okoturo<sup>3,6</sup>, T Prevost<sup>4</sup>, W Robson<sup>5</sup>, HY Leung<sup>5,7</sup>, GH Williams<sup>\*,1,3</sup> and K Stoeber<sup>1,3</sup>

<sup>1</sup>Department of Pathology and Cancer Institute, University College London, Rockefeller Building, 21 University Street, London, WC1E 6JJ, UK; <sup>2</sup>Department of Urology, Royal Marsden NHS Foundation Trust, Fulham Road, London, SW3 6JJ, UK; <sup>3</sup>Wolfson Institute for Biomedical Research, University College London, Cruciform Building, Gower Street, London, WC1E 6BT, UK; <sup>4</sup>Department of Public Health and Primary Care, Centre for Applied Medical Statistics, University of Cambridge, Institute of Public Health, Forvie Site, Robinson Way, Cambridge CB2 0SR, UK; <sup>5</sup>Urology Clinical Research Group, Newcastle upon Tyne Hospitals NHS Foundation Trust, Freeman Hospital, Newcastle upon Tyne, NE7 7DN, UK

**BACKGROUND:** The accuracy of prostate-specific antigen (PSA) testing in prostate cancer detection is constrained by low sensitivity and specificity. Dysregulated expression of minichromosome maintenance (Mcm) 2–7 proteins is an early event in epithelial multistep carcinogenesis and thus MCM proteins represent powerful cancer diagnostic markers. In this study we investigate Mcm5 as a urinary biomarker for prostate cancer detection.

**METHODS:** Urine was obtained from 88 men with prostate cancer and from two control groups negative for malignancy. A strictly normal cohort included 28 men with complete, normal investigations, no urinary calculi and serum PSA <2 ng ml<sup>-1</sup>. An expanded control cohort comprised 331 men with a benign final diagnosis, regardless of PSA level. Urine was collected before and after prostate massage in the cancer patient cohort. An immunofluorometric assay was used to measure Mcm5 levels in urine sediments. **RESULTS:** The Mcm5 test detected prostate cancer with 82% sensitivity (confidence interval (CI) = 72–89%) and with a specificity ranging from 73 (CI = 68–78%) to 93% (CI = 76–99%). Prostate massage led to increased Mcm5 signals compared with pre-massage samples (median 3440 (interquartile range (IQR) 2280 to 5220) vs 2360 (IQR <1800 to 4360); *P* = 0.009), and was associated with significantly increased diagnostic sensitivity (82 vs 60%; *P* = 0.012).

**CONCLUSIONS:** Urinary Mcm5 detection seems to be a simple, accurate and noninvasive method for identifying patients with prostate cancer. Large-scale prospective trials are now required to evaluate this test in diagnosis and screening.

*British Journal of Cancer* (2010) **103**, 701–707. doi:10.1038/sj.bjc.6605785 www.bjcancer.com

Published online 20 July 2010

© 2010 Cancer Research UK

**Keywords:** biomarker; DNA replication licensing; Mcm5; prostate cancer; PSA

Prostate-specific antigen (PSA) testing for prostate cancer has shifted the focus of diagnostic strategies from the evaluation of symptomatic men to the screening of asymptomatic men years before the disease is clinically evident. Indeed, PSA is used for informal screening, case finding, diagnosis, prognosis, staging, monitoring of treatment and identification of recurrence (Oesterling, 1991). As a result, there has been an increase in the incidence of prostate cancer and the disease is now treated at an earlier stage (Hernandez and Thompson, 2004).

However, PSA testing is constrained by low sensitivity and specificity, reflected by its low area under the receiver operating characteristic (ROC) curve (AUC = 0.678) (Thompson *et al*, 2005).

Therefore, many men undergo potentially unnecessary diagnostic prostate biopsies that are painful and associated with risks of sepsis and bleeding. PSA testing inevitably leads to the over-treatment of some men, as the biopsy pathology, clinical findings and PSA level do not adequately predict prognosis. Indeed, it has been shown that preventing one prostate cancer-related death requires between 17 and 48 radical prostatectomies (Holmberg *et al*, 2002; Schroder *et al*, 2009). Thus, more accurate, noninvasive testing methods are needed to identify life-threatening but curable disease.

The initiation of DNA replication represents a final and critical step in growth control downstream of complex and redundant oncogenic growth signalling pathways, and is therefore a potentially attractive diagnostic and therapeutic target (Williams and Stoeber, 2007). Minichromosome maintenance (Mcm) proteins 2–7, the core components of the DNA replication initiation machinery, participate in the assembly of pre-replicative complexes (pre-RCs) on chromatin in G1 phase of the cell cycle, establishing competence for initiation of DNA synthesis in the subsequent S phase (Machida *et al*, 2005; Remus and Diffley, 2009). The six Mcm proteins (MCM) constitute the DNA replicative helicase and are therefore essential for chromosomal duplication.

\*Correspondence: Professor GH Williams; E-mail: gareth.williams@ucl.ac.uk

<sup>6</sup>Current address: Department of Medicine, Imperial College London, Princes Gardens, London, SW7 1NA, UK

<sup>7</sup>Current address: Beatson Institute for Cancer Research, University of Glasgow, Garscube Estate, Switchback Road, Bearsden, Glasgow, G61 1BD, UK

Received 12 March 2010; revised 10 June 2010; accepted 16 June 2010; published online 20 July 2010



They are expressed throughout all phases of the cell division cycle, but are tightly downregulated in quiescent (G0), differentiated and senescent out-of-cycle states, and thus represent novel biomarkers of growth (Eward *et al*, 2004; Barkley *et al*, 2007; Williams and Stoeber, 2007). We and others have shown in a number of epithelial organ systems that MCMs become dysregulated and overexpressed in hyperproliferative dysplastic (preinvasive) and malignant states, resulting in exfoliation of MCM-positive tumour cells (Williams *et al*, 1998; Going *et al*, 2002; Williams and Stoeber, 2007). Moreover, the detection of exfoliated MCM-positive tumour cells in urine sediments, cervical Papanicolaou smears or gastroendoscopic-derived samples can be used in the detection of bladder, cervical, oesophageal, pancreatic and biliary tract cancers (Williams *et al*, 1998, 2004; Freeman *et al*, 1999; Stoeber *et al*, 2002; Ayaru *et al*, 2008).

We previously observed that *Mcm5* is overexpressed in prostate cancer and that raised *Mcm5* protein levels are an independent predictor of survival on multivariate analysis in patients treated with radical surgery (Meng *et al*, 2001) or androgen deprivation therapy and radiotherapy (Dudderidge *et al*, 2007). Moreover, we showed that elevated MCM expression in prostate cancer is coupled to arrested tumour differentiation and increased activation of the mitogen/extracellular-signal-regulated kinase kinase 5/extracellular signal-regulated kinase 5 (MEK/ERK5) pathway (Dudderidge *et al*, 2007). In contrast to premalignant and malignant states, MCMs are expressed at very low levels in benign prostatic tissue, with <2% of basal cells in normal and hyperplastic glands showing *Mcm2* expression (Meng *et al*, 2001; Dudderidge *et al*, 2007). These findings suggest that *Mcm 2–7* might be exploited as biomarkers for prostate cancer detection. Interestingly, in a study of *Mcm5* as a biomarker for bladder cancer, 12 patients presenting with haematuria were identified with a new diagnosis of prostate cancer. These men had higher *Mcm5* levels in urine sediments than men without malignancy ( $P < 0.001$ ). Notably, *Mcm5* was undetectable in 70 patients with benign prostatic hyperplasia (Stoeber *et al*, 2002). Taken together, these studies raise the possibility that detection of elevated levels of *Mcm5* may allow identification of prostate cancer patients with clinically significant tumours.

Urine, expressed prostatic secretions and semen could all provide suitable diagnostic material for biomarker detection of prostate cancer. Semen collection is awkward and not always possible, and the low volume of prostatic secretions restricts their use. The prostate cancer gene 3 (PCA3) test, a urinary diagnostic test for prostate cancer, uses a first-catch urine sample collected after a brief prostate massage (post-massage sample). The PCA3 assay identifies non-coding mRNA from the *PCA3* gene that is overexpressed in prostate cancer (Hessels and Schalken, 2009). The biological significance of this gene is unknown. However it seems to be a useful diagnostic tool with an AUC value for prostate cancer detection of 0.68 (Chun *et al*, 2009). Thus post-massage urine samples seem to be an effective target for prostate cancer detection.

In this pilot study we test the hypothesis that *Mcm5* levels are increased in urine sediments from men with prostate cancer compared with men with no evidence of bladder or prostate cancer. We also measure the effect of prostate massage on *Mcm5* levels.

## MATERIALS AND METHODS

### Study subjects

Patients attending urology or oncology clinics were recruited from Addenbrooke's Hospital (Cambridge, UK) and Freeman Hospital (Newcastle upon Tyne, UK). All patients gave written consent before being recruited to the study. Ethical approval was granted

locally for each institution (Cambridge Local Research Ethics Committee reference no. 00/236, Newcastle Local Research Ethics Committee reference no. 02/161). All consecutive patients with a known diagnosis of prostate cancer who attended during the study period when researchers were present were recruited and categorised into pre- and post-treatment groups. Patients undergoing investigation for prostate cancer, and who subsequently had prostate cancer identified, were also recruited to the prostate cancer cohort. Patients who refused or could not give informed consent, who had undergone recent urological instrumentation or who had current/previous urothelial cancer were excluded. Where possible, samples were obtained from patients both before and after a brief prostate massage. Pre-massage samples comprised a whole voided urine specimen. Those patients who underwent prostate massage provided a second sample. Prostate massage involved 5–10 strokes lateral to medial on each prostatic lobe. Any prostatic secretions expressed per urethra were combined with a further whole voided urine specimen. Relevant clinical data, including serum PSA and urine NMP22 concentrations, Gleason grade and Gleason score, clinical stage, imaging determined lymph node status and bone scan status, were recorded prospectively from clinical notes and pathology records.

Men comprising the control groups were recruited from haematuria clinics and only later included in the control arm if investigations met strict selection criteria intended to exclude those with coexisting genitourinary tract malignancy. A stringently selected control group was identified to only include men with negative haematuria tests and with no past history of bladder or prostate cancer. Men with PSA levels  $> 2 \text{ ng ml}^{-1}$ , NMP22 levels  $> 7 \text{ U ml}^{-1}$ , abnormal or atypical urine cytology or incomplete haematuria investigations were excluded. Men with urolithiasis were also excluded because of the known effect of urothelial trauma causing release of MCM proteins from the dividing transit compartment of the epithelium (Stoeber *et al*, 2002; Williams and Stoeber, 2007). A second, expanded control group was identified to include all men with a benign final diagnosis and no past history of cancer, regardless of PSA measurements, that is, including patients for whom no PSA measurement was available. Patients with urinary calculi, incomplete investigations (e.g., visible haematuria but no contrast imaging study) and atypical cytology but with a benign final clinical diagnosis were not excluded from this group. To approximately age match the group with prostate cancer cases, men  $< 50$  years old were excluded. Patients who refused or could not give informed consent, who had undergone recent urological instrumentation or who had current or previous urothelial cancer were excluded. Urine was provided by men in these control groups without previous prostate massage.

### Processing of urine sediments

Urine sediments were obtained by centrifuging urine samples at 1500 g for 7 min at 4 °C. The pelleted material was resuspended in storage buffer (phosphate-buffered saline (PBS), 5% bovine serum albumin, 1 M sucrose and 0.02%  $\text{NaN}_3$ ) that contained one complete EDTA-free protease inhibitor cocktail tablet (Roche Diagnostics, Burgess Hill, UK) per 50 ml of buffer. The resuspended urine sediments were stored in liquid nitrogen within 2 h of the urine samples being passed.

### Preparation of standards for immunofluorometric *Mcm5* assay

HeLa S3 cells (ATCC CCL-2.2) were cultured as exponentially growing monolayers in Dulbecco's modified Eagle medium (Invitrogen, Paisley, UK) supplemented with 10% fetal calf serum (Invitrogen),  $100 \text{ U ml}^{-1}$  penicillin and  $0.1 \text{ mg ml}^{-1}$  streptomycin in a 37 °C humidified incubator in the presence of 5%  $\text{CO}_2$ . HeLa

cells were harvested after trypsinisation and diluted with storage buffer to concentrations of 1500, 5000, 15 000, 50 000, and 150 000 cells per well. The zero-cell standard consisted of 500  $\mu$ l of storage buffer. The standards were stored in liquid nitrogen and later used to generate a standard curve for Mcm5.

### Processing of standards and clinical samples

Standards and clinical samples were thawed, and cells were isolated by centrifugation at 1500 g for 5 min at 4 °C. The supernatants were discarded, and cell pellets were washed three times with 500  $\mu$ l of PBS. Cell pellets were resuspended in 250  $\mu$ l (for those pellets with a volume approximately <200  $\mu$ l) or 500  $\mu$ l (for those pellets with a volume approximately >200  $\mu$ l) of processing buffer (PBS, 0.4% sodium dodecyl sulphate and 0.02% NaN<sub>3</sub>). Cell lysates were prepared by incubating the resuspended samples at 95 °C for 45 min. The DNA in each sample was sheared by passing the lysates through a 21-gauge needle (Terumo Europe, Leuven, Belgium), and nucleic acids were digested with DNase I (20 U ml<sup>-1</sup>; Roche Diagnostics) and RNase A (1  $\mu$ g ml<sup>-1</sup>; Roche Diagnostics) for 2 h at 37 °C. The samples were centrifuged at 15000 g for 10 min to pellet the cell debris, the supernatants were collected, and 50  $\mu$ l of each was directly used in the immunofluorometric assay.

### Immunofluorometric measurement of Mcm5 levels in urine sediments

Monoclonal antibodies (MAbs) 12A7 and 4B4 raised against His-tagged human Mcm5 were protein A-purified from hybridoma supernatants as described (Stoeber *et al*, 2002). Monoclonal antibody 4B4 was labelled with europium using a DELFIA Eu-labelling kit (PerkinElmer, Turku, Finland) according to the manufacturer's instructions. The assay was standardised using HeLa cells, and one fluorescence unit was defined as the signal generated by the Mcm5 contents of one proliferating HeLa cell, approximately 10<sup>5</sup> Mcm5 molecules (Kearsey and Labib, 1998). DELFIA research reagents were obtained from PerkinElmer. All other reagents were obtained from Sigma-Aldrich (Dorset, UK). Multibuffer was prepared from 0.2 vol 5 × DELFIA assay buffer (PerkinElmer), 0.125 vol DELFIA TSH-Ultra assay buffer (PerkinElmer) and 0.1 vol Tween 20 (Sigma-Aldrich). Immunofluorometric measurements of Mcm5 levels were performed as described (Stoeber *et al*, 2002). Standard curves were constructed from fluorescence values generated by the blank and standard wells, and the fluorescence values of the urine sediment samples were calculated with the Multicalc Advanced Immunoassay Data Management package (PerkinElmer). For immunofluorometric measurement of Mcm5 levels, assay standards, control urine sediment samples and urine sediments from prostate cancer patients were run as duplicates and the mean of the duplicate results reported. For acceptance of immunofluorometric measurements in the assay, the following coefficients of variation were required: CV <20% for results between 1500 and 5000 cells per well standard curve points; CV <15% for results between 5000 and 15 000 cells per well; and CV <10% for results of >15 000 cells per well.

### Immunoassay performance

In our analysis of patient samples, we used 1800 cells per well as the lower detection limit because the within-batch variation of the assay for cell dilutions <1800 cells per well was >20%. Samples that generated an immunofluorometric signal below that corresponding to 1800 cells per well were reported as having <1800 cells per well.

### Statistical analysis

The amplitude of the Mcm5 fluorescence signal for each patient subgroup is presented as the median value with an associated interquartile range (IQR). Test performance was evaluated by calculating sensitivity and specificity using SPSS software, version 12.0.1 (SPSS, Chicago, IL, USA). An exact 95% confidence interval (CI) for each proportion was derived assuming a binomial distribution. Pre- and post-massage Mcm5 fluorescence signals were compared using the Wilcoxon signed-rank test for paired data. The difference in test performance for pre- and post-massage samples was assessed by comparing each sensitivity figure using McNemar's test. The  $\chi^2$  tests were used to compare the sensitivity in different subgroups. All statistical tests were two tailed, and a 5% level was used to indicate statistical significance.

## RESULTS

### Prostate cancer cohort demographics

Clinical characteristics, including age, serum PSA level, stage, grade distribution and treatment status for the cancer patient cohort, are shown in Table 1. In all, 88 men with prostate cancer were recruited with a median age of 72 years (IQR 66–77 years) and a median PSA concentration of 7.8 ng ml<sup>-1</sup> (IQR 3.8–23.7 ng ml<sup>-1</sup>). The group was heterogeneous and included patients at all stages in the diagnostic and treatment pathway. The majority of patients were in clinical stage T1 (27%) and T2 (38%), with lower proportions in T3 (22%) and T4 (3%). Of the 88 prostate cancer patients, 39 were classified as 'untreated': 10 under active surveillance, 21 with newly diagnosed cancer attending for treatment decisions, 6 under investigation leading to a diagnosis of prostate cancer and 2 initially diagnosed with benign disease whose repeat biopsies showed prostate cancer. The median age of the untreated group was 69 years (IQR 65–73 years). The remaining 'treated' group included 49 patients with previous or ongoing treatment for prostate cancer, either androgen deprivation therapy, radiotherapy, chemotherapy or a combination of these treatments (Table 1). The median age of the treated patient cohort was 74 years (IQR 68–80 years), consistent with a more advanced stage of disease progression. Of the 49 treated patients, the majority were on luteinising hormone-releasing hormone (LHRH) analogues alone (31%; including patients awaiting radiotherapy), maximum androgen blockade with LHRH analogues and anti-androgens (20%) or on LHRH analogues after previous treatment with radiotherapy (24%).

### Control cohort demographics

The clinical characteristics of both control cohorts are presented in Table 2. For the strictly normal control group, 135 men with PSA measurements and complete haematuria investigations were initially recruited. Patients with a past history or investigations suggesting bladder or prostate cancer, PSA concentration >2 ng ml<sup>-1</sup>, urine NMP22 concentration >7 U ml<sup>-1</sup>, urolithiasis or visible haematuria and incomplete imaging were excluded, leaving 28 men in the control cohort. This highly selected group had a median age of 60 years (IQR 54–68 years) and a median serum PSA concentration of 0.8 ng ml<sup>-1</sup> (IQR 0.5–1.3 ng ml<sup>-1</sup>). The presenting complaints were asymptomatic nonvisible haematuria ( $n=8$ ), symptomatic nonvisible haematuria ( $n=11$ ), painless visible haematuria ( $n=6$ ), painful visible haematuria ( $n=1$ ) and haematospemia ( $n=2$ ). Normal findings were identified in 11 men. Benign prostatic hyperplasia/obstruction was identified in seven men, prostatitis in five men and urinary tract infection in five men. Thus, although this group does not reflect a normal population, it does reflect typical patients attending urology clinics for investigation, and in whom malignancy can be excluded with a high degree of certainty. For the expanded normal control group,

**Table 1** Clinical characteristics of prostate cancer patients

Characteristic	n (%) or median (IQR)
All patients	88
Age, years	72 (66–77)
PSA, ng ml <sup>-1</sup>	7.8 (3.8–23.7) <sup>a</sup>
<i>Clinical T stage</i>	
T1	24 (27)
T2	33 (38)
T3	19 (22)
T4	3 (3)
Tx	9 (10)
<i>Clinical M stage</i>	
M0	36 (41)
M1	18 (20)
Mx	34 (39)
<i>Clinical N stage</i>	
N0	38 (43)
N1	0 (0)
Nx	50 (57)
<i>Gleason score</i>	
≤6	32 (36)
7	26 (30)
8	12 (14)
9	5 (6)
10	3 (3)
Unknown	10 (11)
<i>Treatment status</i>	
Before diagnosis	2 (2)
Untreated	37 (42)
Treated	49 (56)
LHRH only	15 (31) <sup>b</sup>
Antiandrogens alone	0 (0)
Radiotherapy alone	5 (10)
Chemotherapy alone	1 (2)
LHRH + antiandrogens	10 (20)
LHRH + radiotherapy	12 (24)
Radiotherapy + antiandrogens	1 (2)
Radiotherapy + chemotherapy	1 (2)
LHRH + radiotherapy + antiandrogens	3 (6)
LHRH + radiotherapy + chemotherapy	1 (2)

Abbreviations: LHRH = luteinising hormone-releasing hormone; PSA = prostate-specific antigen; IQR = interquartile range. <sup>a</sup>N = 85. <sup>b</sup>Percentage of treated group (n = 49); rounded averages add up to < 100%.

755 men were recruited in total. In all, 331 men were identified from this group as potential controls after exclusion of men < 50 years old with either a history of bladder or prostate cancer, cancer identified during investigation or a positive NMP22 result (>7 U ml<sup>-1</sup>). The median age of this group was 68 years (IQR 59–75 years). For 55 men in this expanded cohort, PSA measurements were available. The median value was 1.8 ng ml<sup>-1</sup> (IQR 0.8–4.95 ng ml<sup>-1</sup>). The presenting complaints were asymptomatic nonvisible haematuria (n = 75), symptomatic nonvisible haematuria (n = 50), visible haematuria painless (n = 124), visible haematuria painful (n = 46), haematospermia (n = 3) and unrecorded/other (n = 33). Normal findings were identified in 154 men. Benign prostatic hyperplasia/obstruction was identified in 73, urinary calculi in 30, prostatitis in 7, urinary tract infection in 36, urethral stricture in 10, nephrological disease in 6 and other benign diagnoses in 15 men. This larger group contained men with no identifiable or previous cancer, but with the exception of a small group tested with PSA, no specific tests to exclude prostate cancer were made and thus a degree of contamination with occult tumours is to be expected.

**Table 2** Clinical characteristics of cancer-free control patients

Characteristic	n (%) or median (IQR)	
	Strictly normal	Expanded control
All patients	28	331
Age, years	60 (54–68)	68 (59–75)
PSA, ng ml <sup>-1</sup>	0.8 (0.5–1.3)	1.8 (0.8–4.95) <sup>a</sup>
<i>Initial referral</i>		
Asymptomatic nonvisible haematuria	8 (29)	75 (23)
Haematospermia	2 (7)	3 (1)
Indwelling catheter (haematuria)	0 (0)	1 (<1)
Symptomatic nonvisible haematuria	11 (39)	50 (15)
Visible haematuria, painful	1 (4)	46 (14)
Visible haematuria, painless	6 (21)	124 (37)
Unrecorded	0 (0)	32 (10) <sup>b</sup>
<i>Diagnosis on final evaluation</i>		
Normal	11 (39)	154 (47) <sup>b</sup>
Benign prostatic hyperplasia/obstruction	7 (25)	73 (22)
Nephrological	0 (0)	6 (2)
Prostatitis	5 (18)	7 (2)
Urinary calculi	0 (0)	30 (9)
Urethral stricture	0 (0)	10 (3)
Urinary tract infection	5 (18)	36 (11)
Other	0 (0)	15 (5)

Abbreviations: PSA = prostate-specific antigen; IQR = interquartile range. <sup>a</sup>N = 55, includes strictly normal patients and those with PSA levels >2 ng ml<sup>-1</sup>. <sup>b</sup>Rounded percentages do not sum to 100%.

**Table 3** Mcm5 signal for normal controls and prostate cancer patients

	n	Mcm5, median (IQR)
<i>All cancer patients</i>		
Before massage	83	2680 (<1800–4720)
After massage	60	3415 (2140–5190)
Highest Mcm5 signal	88	3560 (2430–5575)
<i>Cancer patients before and after massage</i>		
Before massage	55	2360 (<1800–4360)
After massage	55	3440 (2280–5220) <sup>a</sup>
<i>Normal controls</i>		
Strictly normal group – before massage	28	<1800 (<1800–<1800)
Expanded cohort – before massage	331	<1800 (<1800–1950)

Abbreviations: PSA = prostate-specific antigen; IQR = interquartile range; Mcm = minichromosome maintenance. <sup>a</sup>Compared with before massage, P = 0.009 (Wilcoxon's signed-rank test).

### Urinary Mcm5 detection in prostate cancer patients and normal controls

The cohort of 88 prostate cancer patients recruited for study together provided 83 pre-massage and 60 post-massage urine samples for Mcm5 immunofluorometric analysis. Table 3 and Supplementary Figure 1 show the median Mcm5 signal for pre- and post-massage urine samples, for the highest Mcm5 signal group (i.e., Mcm5 signal for pre- or post-massage urine sample, whatever the higher), and for both control groups. The median for the highest Mcm5 signal group (3560 (IQR 2430–5575)) was significantly higher compared with the strictly defined controls (<1800 (IQR <1800 to <1800); P < 0.001). Table 4 shows the sensitivity of cancer detection for pre- and post-massage samples, and for the highest Mcm5 signal group, as well as specificity values for the two control groups. In addition, 2 × 2 tables based on the highest recorded Mcm5 signal for all study participants and

patients with pre-massage data only are shown in Supplementary Tables 1 and 2, respectively. As maximum sensitivity was desired, samples were scored as Mcm5 test positive if they generated a signal above the lower threshold limit for detection of Mcm5 protein in the immunoassay (1800 cut point). Using the maximum Mcm5 value obtained for each patient (i.e., either the pre- or post-massage Mcm5 signal), the overall sensitivity was 82% (72 out of 88; CI=72–89%) and specificity was 93% (26 out of 28; CI=76–99%). The sensitivity using the pre-massage samples only was 65% (54 out of 83; CI=54–75%) and the sensitivity using the post-massage samples only was 78% (47 out of 60; CI=66–88%). Of the 26 strictly normal control patients who tested negative, 7 were diagnosed with benign prostatic hyperplasia. In a previous study we reported similar low Mcm5 signals for 70 men with benign prostatic hyperplasia, indicating that the specificity of the Mcm5 test is unaffected by this common condition (Stoeber *et al*, 2002). Interestingly, both of the strictly normal control patients who had elevated Mcm5 signals and tested positive presented with haematospermia. To consolidate our finding that Mcm5 is of diagnostic utility in prostate cancer detection, further analysis was performed using less stringent exclusion criteria to identify an expanded control cohort. The median Mcm5 signal in this group was <1800 (IQR <1800 to 1950; Table 3) and was still significantly lower than the cancer group ( $P<0.001$ ). Using this expanded control cohort, high specificity was still observed at 73% (242 out of 331; CI=68–78%; Table 4 and Supplementary

Figure 1). The false positives detected in this expanded control group (Mcm5 signal >1800) included normals without identifiable pathology (42 out of 154, 27%), urinary tract infection (10 out of 36, 28%) and urethral stricture (4 out of 10, 40%), benign prostatic hyperplasia (17 out of 73, 23%), calculi (15 out of 30, 50%), prostatitis (2 out of 7, 29%) and others (3 out of 15, 20%).

The effect of prostate massage on the Mcm5 signal and its effect on diagnostic sensitivity were also studied. From the prostate cancer cohort, 55 men provided both pre- and post-massage samples. As shown in Table 3 and Supplementary Figure 1, prostate massage led to a significant increase in median Mcm5 signal from 2360 (IQR <1800 to 4360) to 3440 (IQR 2280 to 5220;  $P=0.009$ ). The increased amplitude of the Mcm5 signal after prostate massage was associated with a significant increase in diagnostic sensitivity from 60 (CI=46–73%) to 82% (CI=69–91%;  $P=0.012$ ; Table 4).

To determine the relationship between Mcm5 signal and PSA level, prostate cancer patients were grouped by PSA concentration: <5, 5–15 and >15 ng ml<sup>-1</sup>. All three groups showed elevated Mcm5 signals and similarly high sensitivities (Table 5 and Supplementary Figure 2). Notably, when considering the highest Mcm5 signal per patient, prostate cancer patients with a low PSA level (<5 ng ml<sup>-1</sup>;  $n=26$ ) had a median Mcm5 signal of 3170 (IQR 2152–5887) and associated sensitivity of 81% (CI=61–93%), equivalent to prostate cancer patients with high PSA values (>15 ng ml<sup>-1</sup>;  $n=30$ ) who had a median Mcm5 signal of 4065 (IQR 2450–5337) and associated sensitivity of 83% (CI=65–94%;  $P=0.88$ ).

To investigate the relationship between clinical characteristics and Mcm5 signal, the cancer patient cohort was further sub-classified according to clinical stage (T1, T2 and T3/4), Gleason score (≤6, 7 and 8–10), lymph node involvement and distant metastasis. The Mcm5 signal and sensitivity of the test were not influenced by any of these clinicopathological variables (Table 5, Supplementary Table 3 and Supplementary Figures 3 and 4). Surprisingly, the overall treatment status of patients did not seem to have a major effect on the Mcm5 signal. When the sensitivities for untreated (87% (CI=73–96%)) and treated patients (78% (CI=63–88%)) were compared, no statistical difference was observed between the two ( $P=0.36$ ; Supplementary Table 4). However, considering only patients who provided a sample after prostate massage, we noted a decrease in median Mcm5 signal in those patients who underwent radiotherapy (2820 (IQR <1800 to 3960)) relative to those who did not undergo radiotherapy (3870 (IQR 2550 to 5870); Supplementary Table 4). This decrease in Mcm5 signal was associated with a significantly decreased sensitivity (54% (CI=25–81%) vs 87% (CI=70–96%);  $P=0.04$ ).

**Table 4** Sensitivity and specificity analysis of Mcm5 test performance in normal controls and prostate cancer patients

	n		% (CI)
<i>All cancer patients</i>			
Before massage	83	Sensitivity	65 (54–75)
After massage	60	Sensitivity	78 (66–88)
Highest Mcm5 signal	88	Sensitivity	82 (72–89)
<i>Cancer patients before and after massage</i>			
Before massage	55	Sensitivity	60 (46–73)
After massage	55	Sensitivity	82 (69–91) <sup>a</sup>
<i>Normal controls</i>			
Strictly normal group – before massage	28	Specificity	93 (76–99)
Expanded cohort – before massage	331	Specificity	73 (68–78)

Abbreviations: CI = confidence interval; Mcm = minichromosome maintenance. <sup>a</sup>Compared with before massage,  $P=0.012$  (McNemar's test). Sensitivity and specificity were determined using a cut point of 1800 for Mcm5 signal.

**Table 5** Mcm5 signal test sensitivity in cancer patients categorized by PSA level, clinical stage and Gleason score

	Pre-massage					Post-massage					Highest Mcm5 signal				
	n	Mcm5, median (IQR)	Sensitivity % (CI)	P (n)*	P (t) <sup>†</sup>	n	Mcm5, median (IQR)	Sensitivity % (CI)	P (n)	P (t)	n	Mcm5, median (IQR)	Sensitivity % (CI)	P (n)	P (t)
<i>PSA, ng ml<sup>-1</sup></i>															
<5	25	2180 (<1800 to 4190)	56 (34–76)	—	—	20	3170 (1874 to 5587)	75 (51–91)	—	—	26	3170 (2152 to 5887)	81 (61–93)	—	—
5–15	26	2365 (<1800 to 3947)	62 (41–80)	0.77	0.21	23	3870 (2280 to 5160)	83 (61–95)	0.65	0.96	29	3870 (2250 to 5240)	79 (60–92)	0.95	0.80
>15	29	3440 (<1800 to 5075)	72 (53–87)	0.24	—	16	3290 (1914 to 5037)	75 (48–93)	1.00	—	30	4065 (2450 to 5337)	83 (65–94)	0.88	—
<i>Clinical stage</i>															
T1	23	2460 (<1800 to 5000)	61 (39–80)	—	—	18	4485 (3210 to 7797)	94 (73–100)	—	—	24	4505 (3007 to 6900)	92 (73–99)	—	—
T2	30	2210 (<1800 to 3140)	60 (41–77)	0.98	0.70	28	2625 (<1800 to 4240)	68 (48–84)	0.08	0.06	33	2680 (2045 to 4445)	79 (61–91)	0.33	0.05
T3/4	21	3470 (<1800 to 5290)	67 (43–85)	0.75	—	9	2560 (<1800 to 4300)	67 (30–93)	0.22	—	22	3500 (<1800 to 5330)	68 (45–86)	0.10	—
<i>Gleason score</i>															
≤6	32	2310 (<1800 to 3420)	62 (44–79)	—	—	24	3800 (2887 to 5707)	87 (68–97)	—	—	32	3545 (2715 to 5707)	91 (75–98)	—	—
7	22	2125 (<1800 to 3580)	55 (32–76)	0.58	0.77	19	3660 (<1800 to 5160)	74 (49–91)	0.37	0.05	26	3375 (<1800 to 4830)	69 (48–86)	0.10	0.12
8–10	19	3530 (<1800 to 5660)	68 (43–87)	0.70	—	12	2340 (<1800 to 3212)	58 (28–85)	0.13	—	20	3255 (1942 to 5552)	75 (51–91)	0.27	—

Abbreviations: CI = confidence interval; Mcm = minichromosome maintenance; IQR = interquartile range; PSA = prostate-specific antigen. \*P-value for sensitivity, vs base category ( $\chi^2$  test). <sup>†</sup>P-value for trend across category.



## DISCUSSION

There is an urgent need for more accurate, noninvasive diagnostic testing for prostate cancer. Although serum PSA-based screening has been shown to reduce prostate cancer mortality by 20%, there is a high risk of diagnosis of clinically insignificant tumours (Schroder *et al*, 2009). Recent data from the European Randomized Study of Screening for Prostate Cancer (ERSPC) showed that 1410 men would require screening and an additional 48 cancers treated to prevent one death from prostate cancer (Schroder *et al*, 2009). Moreover, the high PSA false-positive rate observed in this study (76%) shows the high number of prostate biopsies that might be avoided if a more accurate diagnostic test was available. Crucially, the disproportionate number of cancers that must be treated to prevent one death underlines the inadequate understanding of prostate cancer biology. Future diagnostic methods must not only reduce unnecessary prostate biopsies, but also provide prognostic information to aid treatment decisions. Moreover, the ideal diagnostic marker would preferentially identify clinically significant prostate cancers with a high risk of progression.

In this study we have identified Mcm5 as a potentially important biomarker for prostate cancer detection. Principally, we have shown that Mcm5 levels are elevated in the urine cell sediments of prostate cancer patients when compared with patients without malignancy. Only two patients had an elevated Mcm5 signal in the strictly normal control group. Interestingly, both patients presented with haematuria and normal clinical investigations. This symptom is often because of prostatic calculi causing trauma to the prostatic ducts (Kumar *et al*, 2006). This would potentially expose the normal MCM-expressing proliferative compartment to the lumen of these ducts, and may thus explain the two false-positive results. Similarly, patients in the expanded haematuria control group diagnosed with bladder calculi also showed elevated Mcm5 signals. This confirms our previous findings that calculi in the genitourinary tract generate elevated Mcm5 signals in urine cell sediments (Stoeber *et al*, 2002). Importantly, the 73 patients with BPH included in this study did not show elevated Mcm5 signals compared with those controls without pathology. Similarly, 70 patients with BPH analysed as part of a previous Mcm5 bladder cancer trial did not show elevated Mcm5 levels (Stoeber *et al*, 2002). This is consistent with the fact that MCM expression levels in hyperplastic glands are very low (<2% of basal cells), similar to those observed in normal prostatic tissue (Meng *et al*, 2001; Dudderidge *et al*, 2007). Notably, prostatitis was associated with an elevated Mcm5 signal.

A reduction in specificity of the Mcm5 test, from 93 to 73%, was observed when using the expanded control cohort. Although this measure of specificity was derived from a much larger population, the PSA values were unknown for the majority. This expanded control cohort is therefore likely to include occult prostate cancers. Indeed, if one considers that the prevalence of prostate cancer in the Prostate Cancer Prevention Trial was 20.7% in the 55- to 59-year-old group (in a group originally comprising patients with normal digital rectal examination and PSA <3 ng ml<sup>-1</sup>; Thompson *et al*, 2003), one might expect a significant number of occult prostate cancers to be included within our expanded control population. Interestingly, the Mcm5 false-positive rate in the normal population without detectable pathology was 27%. It will therefore be of interest in future studies to determine what percentage of these cases might represent occult prostate cancers.

## REFERENCES

- Ayaru L, Stoeber K, Webster GJ, Hatfield AR, Wollenschlaeger A, Okoturo O, Rashid M, Williams G, Pereira SP (2008) Diagnosis of pancreaticobiliary malignancy by detection of minichromosome maintenance protein 5 in bile aspirates. *Br J Cancer* **98**: 1548–1554
- Barkley LR, Hong HK, Kingsbury SR, James M, Stoeber K, Williams GH (2007) Cdc6 is a rate-limiting factor for proliferative capacity during HL60 cell differentiation. *Exp Cell Res* **313**: 3789–3799

In the context of prostate cancer detection, we have also established the importance of prostate massage in the preparation of urine samples for Mcm5 testing. This brief procedure is well tolerated by patients in the urology clinic and is an integral part of their clinical assessment. Little variation from standard examination is required to optimise sample quality. We have shown that massage not only increased Mcm5 signals in urine sediments, but it also led to significantly increased diagnostic sensitivity. These findings require verification in a larger study with all patients undergoing pre- and post-massage testing.

It is interesting to note that there was no major reduction in Mcm5 signals after medical therapeutic intervention. We have previously shown in normal tissues and tumours that cells arrested 'in cycle' can maintain MCM protein expression, designated as 'licensed' cells with proliferative potential (Stoeber *et al*, 2001; Dudderidge *et al*, 2005; Williams and Stoeber, 2007). Persistence of elevated Mcm5 signals in the urine sediments of treated patients suggests that there has been no significant reduction in tumour cell volume, and this may contribute to relapse after such medical therapeutic interventions. Disease progression could be triggered by the overriding of DNA damage cell cycle checkpoints or, alternatively, through the establishment of growth-independent (autonomous) cancer cell cycles.

Prostate-specific antigen is primarily an organ-specific marker and its elevation in prostate cancer is because of the leakage of a physiological protein into the blood, resulting from the disruption of the basement membrane (Lilja *et al*, 2008). Thus, PSA is not an ideal tumour marker as it is also elevated in other prostatic diseases that cause increased permeability of the basement membrane, including BPH and prostatitis (Lilja *et al*, 2008). In contrast, Mcm5 detection can be regarded as a cancer-specific test. Therefore, the combination of a cancer-specific test in Mcm5 with a prostate-specific test in PSA may provide an improved algorithm for prostate cancer detection.

Although this pilot study has identified Mcm5 as a new biomarker for prostate cancer detection, it is not yet clear whether the test will be able to specifically identify clinically significant cancers. Comparable sensitivities and Mcm5 signals were observed between low-grade, low-stage and high-grade, advanced-stage tumours. However, this is a heterogeneous patient cohort, in which many patients have undergone therapeutic intervention. Trials on a conventional diagnostic untreated patient cohort will be required to address this question. Future studies should also evaluate the combination and comparison of serum PSA, urinary PCA3 and Mcm5, and assess the use of a combined predictive biomarker algorithm that may allow identification of patients in whom prostate biopsy can be safely avoided.

## ACKNOWLEDGEMENTS

We thank Mr Andrew Doble and Dr Simon Russell for providing patient resources, Pam de Clive-Lowe and Julie Lynch for sample collection, processing and management, and Diane Walia for data entry and spreadsheet management. Kai Stoeber and Gareth Williams are supported by CRUK grants C428/A6263 and C428/A3441.

Supplementary Information accompanies the paper on British Journal of Cancer website (<http://www.nature.com/bjc>)

- Chun FK, de la Taille A, van PH, Marberger M, Stenzl A, Mulders PF, Huland H, Abbou CC, Stillebroer AB, van Gils MP, Schalken JA, Fradet Y, Marks LS, Ellis W, Partin AW, Haese A (2009) Prostate cancer gene 3 (PCA3): development and internal validation of a novel biopsy nomogram. *Eur Urol* **56**(4): 659–667
- Dudderidge TJ, McCracken SR, Loddo M, Fanshawe TR, Kelly JD, Neal DE, Leung HY, Williams GH, Stoeber K (2007) Mitogenic growth signalling,

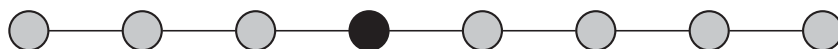
- DNA replication licensing, and survival are linked in prostate cancer. *Br J Cancer* **96**: 1384–1393
- Dudderidge TJ, Stoeber K, Loddo M, Atkinson G, Fanshawe T, Griffiths DF, Williams GH (2005) Mcm2, Geminin, and Ki67 define proliferative state and are prognostic markers in renal cell carcinoma. *Clin Cancer Res* **11**: 2510–2517
- Eward KL, Obermann EC, Shreeram S, Loddo M, Fanshawe T, Williams C, Jung HI, Prevost AT, Blow JJ, Stoeber K, Williams GH (2004) DNA replication licensing in somatic and germ cells. *J Cell Sci* **117**: 5875–5886
- Freeman A, Morris LS, Mills AD, Stoeber K, Laskey RA, Williams GH, Coleman N (1999) Minichromosome maintenance proteins as biological markers of dysplasia and malignancy. *Clin Cancer Res* **5**: 2121–2132
- Going JJ, Keith WN, Neilson L, Stoeber K, Stuart RC, Williams GH (2002) Aberrant expression of minichromosome maintenance proteins 2 and 5, and Ki-67 in dysplastic squamous oesophageal epithelium and Barrett's mucosa. *Gut* **50**: 373–377
- Hernandez J, Thompson IM (2004) Prostate-specific antigen: a review of the validation of the most commonly used cancer biomarker. *Cancer* **101**: 894–904
- Hessels D, Schalken JA (2009) The use of PCA3 in the diagnosis of prostate cancer. *Nat Rev Urol* **6**: 255–261
- Holmberg L, Bill-Axelsson A, Helgesen F, Salo JO, Folmerz P, Haggman M, Andersson SO, Spangberg A, Busch C, Nordling S, Palmgren J, Adami HO, Johansson JE, Norlen BJ (2002) A randomized trial comparing radical prostatectomy with watchful waiting in early prostate cancer. *N Engl J Med* **347**: 781–789
- Kearsey SE, Labib K (1998) MCM proteins: evolution, properties, and role in DNA replication. *Biochim Biophys Acta* **1398**: 113–136
- Kumar P, Kapoor S, Nargund V (2006) Haematospermia – a systematic review. *Ann R Coll Surg Engl* **88**: 339–342
- Lilja H, Ulmert D, Vickers AJ (2008) Prostate-specific antigen and prostate cancer: prediction, detection and monitoring. *Nat Rev Cancer* **8**: 268–278
- Machida YJ, Hamlin JL, Dutta A (2005) Right place, right time, and only once: replication initiation in metazoans. *Cell* **123**: 13–24
- Meng MV, Grossfeld GD, Williams GH, Dilworth S, Stoeber K, Mulley TW, Weinberg V, Carroll PR, Tlsty TD (2001) Minichromosome maintenance protein 2 expression in prostate: characterization and association with outcome after therapy for cancer. *Clin Cancer Res* **7**: 2712–2718
- Oesterling JE (1991) Prostate specific antigen: a critical assessment of the most useful tumor marker for adenocarcinoma of the prostate. *J Urol* **145**: 907–923
- Remus D, Diffley JF (2009) Eukaryotic DNA replication control: lock and load, then fire. *Curr Opin Cell Biol* **21**: 771–777
- Schroder FH, Hugosson J, Roobol MJ, Tammela TL, Ciatto S, Nelen V, Kwiatkowski M, Lujan M, Lilja H, Zappa M, Denis LJ, Recker F, Berenguer A, Maattanen L, Bangma CH, Aus G, Villers A, Rebillard X, van der Kwast T, Blijenberg BG, Moss SM, de Koning HJ, Auvinen A (2009) Screening and prostate-cancer mortality in a randomized European study. *N Engl J Med* **360**: 1320–1328
- Stoeber K, Swinn R, Prevost AT, de Clive-Lowe P, Halsall I, Dilworth SM, Marr J, Turner WH, Bullock N, Doble A, Hales CN, Williams GH (2002) Diagnosis of genito-urinary tract cancer by detection of minichromosome maintenance 5 protein in urine sediments. *J Natl Cancer Inst* **94**: 1071–1079
- Stoeber K, Tlsty TD, Happerfield L, Thomas GA, Romanov S, Bobrow L, Williams ED, Williams GH (2001) DNA replication licensing and human cell proliferation. *J Cell Sci* **114**: 2027–2041
- Thompson IM, Ankerst DP, Chi C, Lucia MS, Goodman PJ, Crowley JJ, Parnes HL, Coltman Jr CA (2005) Operating characteristics of prostate-specific antigen in men with an initial PSA level of 3.0 ng/ml or lower. *JAMA* **294**: 66–70
- Thompson IM, Goodman PJ, Tangen CM, Lucia MS, Miller GJ, Ford LG, Lieber MM, Cespedes RD, Atkins JN, Lippman SM, Carlin SM, Ryan A, Szczepanek CM, Crowley JJ, Coltman Jr CA (2003) The influence of finasteride on the development of prostate cancer. *N Engl J Med* **349**: 215–224
- Williams GH, Romanowski P, Morris L, Madine M, Mills AD, Stoeber K, Marr J, Laskey RA, Coleman N (1998) Improved cervical smear assessment using antibodies against proteins that regulate DNA replication. *Proc Natl Acad Sci USA* **95**: 14932–14937
- Williams GH, Stoeber K (2007) Cell cycle markers in clinical oncology. *Curr Opin Cell Biol* **19**: 672–679
- Williams GH, Swinn R, Prevost AT, de Clive-Lowe P, Halsall I, Going JJ, Hales CN, Stoeber K, Middleton SJ (2004) Diagnosis of oesophageal cancer by detection of minichromosome maintenance 5 protein in gastric aspirates. *Br J Cancer* **91**: 714–719

## Chapter 4

# Diagnosis of pancreaticobiliary malignancy by detection of minichromosome maintenance protein 5 in bile aspirates

L Ayaru, K Stoeber, GJ Webster, ARW Hatfield, A Wollenschlaeger, O Okoturo, M Rashid, GH Williams, SP Pereira

British Journal of Cancer 2008 98 (9): 1548-1554.



## Diagnosis of pancreaticobiliary malignancy by detection of minichromosome maintenance protein 5 in bile aspirates

L Ayaru<sup>1</sup>, K Stoeber<sup>2,3</sup>, GJ Webster<sup>4</sup>, ARW Hatfield<sup>4</sup>, A Wollenschlaeger<sup>3</sup>, O Okoturo<sup>2</sup>, M Rashid<sup>3</sup>, G Williams<sup>\*,2,3</sup> and SP Pereira<sup>\*,1,4</sup>

<sup>1</sup>The Institute of Hepatology, University College London, London, UK; <sup>2</sup>Wolfson Institute for Biomedical Research, University College London, London, UK; <sup>3</sup>Department of Pathology, University College London, London, UK; <sup>4</sup>Department of Gastroenterology, University College London Hospitals NHS Foundation Trust, London, UK

Biliary brush cytology is the standard method of sampling a biliary stricture but has a low sensitivity for the detection of malignancy. We have previously shown that minichromosome maintenance (MCM) replication proteins (Mcm2–7) are markers of dysplasia and have utilised these novel biomarkers of growth for the diagnosis of cervical and bladder cancer. We aimed to determine if MCM proteins are dysregulated in malignant pancreaticobiliary disease and if levels in bile are a sensitive marker of malignancy. In 30 tissue specimens from patients with malignant/benign biliary strictures, we studied Mcm2 and -5 expression by immunohistochemistry. Bile samples were also collected prospectively at endoscopic retrograde cholangiopancreatography from 102 consecutive patients with biliary strictures of established ( $n = 42$ ) or indeterminate aetiology ( $n = 60$ ). Patients with indeterminate strictures also underwent brush cytology as part of standard practice. Bile sediment Mcm5 levels were analysed using an automated immunofluorometric assay. In benign biliary strictures, Mcm2 and -5 protein expression was confined to the basal epithelial proliferative compartment – in contrast to malignant strictures where expression was seen in all tissue layers. The percentage of nuclei positive for Mcm2 was higher in malignant tissue (median 76.5%, range 42–92%) than in benign tissue (median 5%, range 0–33%) ( $P < 0.0005$ ), with similar results for Mcm5. Minichromosome maintenance protein 5 levels in bile were significantly more sensitive than brush cytology (66 vs 20%;  $P = 0.004$ ) for the detection of malignancy in patients with an indeterminate stricture, with a comparable positive predictive value (97 vs 100%;  $P = ns$ ). In this study, we demonstrate that Mcm5 in bile detected by a simple automated test is a more sensitive indicator of pancreaticobiliary malignancy than routine brush cytology.

*British Journal of Cancer* (2008) **98**, 1548–1554. doi:10.1038/sj.bjc.6604342 www.bjcancer.com

Published online 15 April 2008

© 2008 Cancer Research UK

**Keywords:** pancreatic cancer; biliary tract cancer; biliary stricture; MCM

The diagnosis of pancreatic and biliary tract cancer at an early stage of disease remains difficult and there are currently no established methods of surveillance for biliary tract cancer in patients with primary sclerosing cholangitis (PSC). Current diagnostic modalities include serum tumour markers and imaging but are not specific enough to allow for confident confirmation of malignancy especially in its early stages and therefore cytological/biopsy specimens are usually acquired from biliary strictures/masses (Lee, 2006). Brush cytology is the most commonly used method of sampling a biliary stricture (De Bellis *et al*, 2002a) as it

is relatively easy to perform, does not compromise resection margins in potentially resectable cases and has a high specificity (96–100%) for malignancy. However, cytology has a low sensitivity (9–57%) (de Bellis *et al*, 2002b; Baron *et al*, 2004; Harewood *et al*, 2004; Moreno Luna *et al*, 2006) for the detection of malignancy, which is even lower if cells are acquired from bile aspirates (6–32%) (De Bellis *et al*, 2002a). The poor detection rate may stem from a number of factors, including the desmoplastic nature of biliary tract cancers, failure to obtain an adequate cellular yield and morphological changes induced by inflammation and necrosis. Furthermore, to some extent, the interpretation of cytological specimens is subjective and observer-dependent and more accurate quantitative tests would be desirable.

Despite the detection of several molecular genetic alterations in pancreatic and biliary tract cancer, their reported low frequency in biological samples has limited their usefulness as diagnostic markers (Gress, 2004). For example, neither K-Ras nor p53 mutational analysis has been shown to be superior to conventional cytopathology for the diagnosis of pancreaticobiliary tumours (Khan *et al*, 2005).

The initiation of DNA replication represents a final and critical step in growth regulation and lies downstream at the convergence

\*Correspondence: Dr S Pereira, The Institute of Hepatology, Royal Free and University College, Medical School, University College London, 69–75 Chenies Mews, London WC1E 6HX, UK;

E-mail: stephen.pereira@ucl.ac.uk or

Professor G Williams, Department of Pathology, Royal Free and University College, Medical School, University College London, Rockefeller Building, University Street, London WC1E 6JJ, UK;

E-mail: gareth.williams@ucl.ac.uk

Received 12 December 2007; revised 10 March 2008; accepted 10 March 2008; published online 15 April 2008



point of growth regulatory pathways (Williams and Stoeber, 1999). Minichromosome maintenance proteins (Mcm2–7) participate in the assembly of prereplicative complexes to establish competence for initiation of DNA synthesis (DNA replication licensing). All six Mcm proteins are essential for replication, are present in all phases of the proliferative cell cycle but are tightly downregulated in the quiescent, terminally differentiated and senescent ‘out-of-cycle’ states. The presence of one protein reflects the presence of the other five as all six are loaded together onto DNA as a heterohexamer on exit from metaphase (Blow and Hodgson, 2002). We have shown that these biomarkers detect, in addition to actively proliferating cells, cells with growth potential (Stoeber *et al.*, 2001). We have also shown that dysregulation of MCM proteins is an early event in epithelial carcinogenesis, which occurs in a wide range of preneoplastic and neoplastic states (Freeman *et al.*, 1999) resulting in exfoliation of MCM-positive tumour cells. Moreover, we have utilised these novel biomarkers of growth as diagnostic markers of cervical, genitourinary tract and oesophageal cancer (Williams *et al.*, 1998, 2004; Stoeber *et al.*, 1999, 2002).

On the basis of these data in other solid-organ tumours, we proposed that detection of MCM proteins in exfoliated tumour cells might be a potentially sensitive indicator of pancreaticobiliary neoplasia. Here we describe a novel automated liquid-phase immunofluorometric assay to quantify Mcm5 levels in biliary aspirates obtained from patients undergoing endoscopic retrograde cholangiopancreatography (ERCP) for the diagnosis and treatment of biliary strictures.

## METHODS

### Patients

Between 2004 and 2006, 113 consecutive patients were invited to participate in the study for evaluation of indeterminate, or established, benign and malignant biliary tract strictures. Seven patients were excluded due to inability to sedate the patient adequately ( $n=3$ ), bile not aspirated ( $n=2$ ), ampulla not identified ( $n=1$ ) or patient did not agree to participate in the study ( $n=1$ ). A total of 106 patients underwent ERCP with aspiration of bile for Mcm5 analysis and parallel biliary brush cytology obtained as part of routine diagnostic practice in indeterminate strictures. Four patients were excluded after bile collection as we did not have access to sufficient follow-up information to be confident of a diagnosis. Therefore, a total of 102 patients were included in the study. A diagnosis of malignancy was made by positive cytology/biopsy or evidence of disease progression on imaging. Benign disease was established by negative pathology and a median of 39 (range 21–48) months clinical follow-up. The study was approved by the Joint UCLH/UCL ethical committee and all patients gave written informed consent.

### Brush cytology of biliary strictures

If a stricture of indeterminate aetiology was present at ERCP, biliary brush cytology was collected by standard technique. A wire-guided sheathed cytology brush (Combocath, Microinvasive; Boston Scientific, Notick, MA, USA) was advanced across the stricture several times before being resheathed and the sheathed brush withdrawn from the endoscope. The cytology specimen was then transferred immediately to glass slides by smearing the cellular material from the brush directly onto two slides. These were fixed and later stained for malignant cells using the standard Papanicolaou technique for smears. Brush cytology samples were analysed by expert cytopathologists within the context of a multidisciplinary cancer review meeting. Cytology was classified as malignant or no definitive evidence of malignancy (highly suspicious, low-grade dysplasia, inflammatory, normal).

### Immunohistochemistry

Formalin-fixed archival blocks were selected from the files at University College London Hospital. Sections ( $4\mu\text{m}$ ) were cut using a sledge microtome and placed onto Superfrost Plus slides. After drying the slides overnight at  $60^\circ\text{C}$ , sections were deparaffinised in xylene and rehydrated in water. Antigen retrieval was performed by pressure cooking sections in  $0.1\text{mmol l}^{-1}$  citrate buffer (pH 6.0) at 15 p.s.i. (103.4 kPa) for 2 min.

Tissue sections cut on to Superfrost Plus slides were stained manually or using a standard protocol, as described below. Following antigen retrieval, the slides were washed thrice (using Tris buffered saline with 0.1% Tween 20 for this and subsequent washes). Endogenous peroxidase activity was quenched with peroxidase-blocking solution (DAKO, Ely, UK) for 15 min. Sections were incubated with primary antibody for 45 min. Mouse anti-human monoclonal Mcm2 and rabbit anti-human polyclonal Mcm5 antibodies were obtained from BD Transduction Laboratories (Lexington, KY, USA). The slides were incubated with the secondary antibody for 2 h and developed with 3,3-diaminobenzidine for 10 min. Slides were then counterstained with Mayer’s haematoxylin, differentiated in 1% acid alcohol, dehydrated and cleared in xylene. Coverslips were applied with Leica CV Mount (Leica, Nussloch, Germany). Incubation without the primary antibody was used as a negative control and colonic epithelial sections were used as positive controls. Those sections mounted on DAKO ChemMate capillary gap slides were stained using the DAKO TechMate 500 immunostainer (DAKO, Cambridge, UK). Microscopic images were acquired with an Olympus BX51 light microscope/CCD camera setup and ANALYSIS image-capturing software (Soft Imaging Systems GmbH, Munster, Germany). A semiquantitative determination of the extent of staining was obtained by calculating a labelling index for each protein stained. At least 200 epithelial nuclei were assessed per case. Results were expressed as a percentage of positively stained nuclei out of the total number of nuclei counted in representative microscopic fields. The median and range of labelling indices were calculated.

### Bile aspirate collection and storage

After biliary brushing, 5–10 ml of bile was aspirated from directly above the stricture via a standard ERCP catheter. Storage buffer (10 × phosphate-buffered saline (PBS), 5% bovine serum albumin, 1 M sucrose, 0.2%  $\text{NaN}_3$ ) containing one complete mini EDTA-free protease inhibitor cocktail tablet (Roche Diagnostics Ltd, Lewes, East Sussex, UK) per 10 ml of buffer was added to bile aspirates at one-tenth aspirate volume and mixed with the sample. Bile aspirates in storage buffer were transferred into 15 ml cryovials, placed in dry ice and stored at  $-80^\circ\text{C}$  within 6 h.

### Processing of standards and bile aspirates

Aspirates were analysed in a blinded manner for immunofluorometric Mcm5 detection. Standards for the immunofluorometric Mcm5 assay were prepared by serial dilution of lysates from asynchronous HeLa S3 cultures to 1500, 5000, 15 000, 50 000 and 150 000 cells per well. Standards and bile samples were processed as described previously (Stoeber *et al.*, 2002). Briefly, standards and clinical samples were thawed, and the cells were isolated by centrifugation at 1500 g for 5 min at  $4^\circ\text{C}$ . The supernatants were discarded, and the cell pellets were washed three times with  $500\mu\text{l}$  of PBS. Cell pellets were resuspended in  $250\mu\text{l}$  of processing buffer (PBS, 0.4% sodium dodecyl sulphate (SDS), 0.02%  $\text{NaN}_3$ ). Cell lysates were prepared by incubating the resuspended samples at  $95^\circ\text{C}$  for 45 min. The DNA in each sample was sheared by passing the lysates through a 21-gauge needle (Terumo Europe NV, Leuven, Belgium), and nucleic acids were digested with DNase I ( $20\text{U ml}^{-1}$ ; Roche Diagnostics) and RNase A ( $1\text{mg ml}^{-1}$ ;

Sigma-Aldrich UK Ltd, Dorset, UK) for 2 h at 37°C. The samples were centrifuged at 15 000 g for 10 min to pellet the cell debris, the supernatants were collected and 50 µl of each was directly used in the immunofluorometric assay.

**Automated immunofluorometric measurement of Mcm5 levels in bile aspirates**

Monoclonal antibodies (MAbs) 12A7 and 4B4 raised against His-tagged human Mcm5 were protein A-purified from hybridoma supernatants as described previously (Stoeber *et al*, 2002). Protein A-purified MAb 4B4 was labelled with europium using a DELFIA Eu-labelling kit (Perkin-Elmer Life Science, Wallac Oy, Turku, Finland) according to the manufacturer’s instructions. The assay was standardised using HeLa cells as described above and previously (Stoeber *et al*, 2002), and one fluorescence unit was defined as the signal generated by the Mcm5 contents of one proliferating HeLa S3 cell, approximately 10<sup>5</sup> Mcm5 molecules (Kearsey and Labib, 1998). DELFIA research reagents were obtained from Perkin-Elmer Life Science. Multibuffer was prepared from 0.2 vol 5 × DELFIA assay buffer (Perkin-Elmer), 0.125 vol DELFIA TSH-Ultra assay buffer (Perkin-Elmer) and 0.1 vol Tween 20 (Sigma). All other reagents were obtained from Sigma-Aldrich. Immunofluorometric measurements of Mcm5 levels were performed as described previously (Stoeber *et al*, 2002). Standard curves were constructed from fluorescence values generated by the blank and standard wells, and the fluorescence values of the bile aspirate samples were calculated with the Multicalc Advanced Immunoassay Data Management package (Perkin-Elmer Life Science). The reliability of the test was maintained by assaying the Mcm5 content of a known number of HeLa cells as an internal standard when bile samples were assayed.

For immunofluorometric measurement of Mcm5 levels, assay standards, control samples and bile aspirate samples were run as duplicates and the mean of the duplicate results reported. For acceptance of immunofluorometric measurements in the assay, the following coefficients of variations were required: CV < 20% for results between 1500 and 5000 cells per well standard curve points; CV < 15% for results between 5000 and 15 000 cells per well; and CV < 10% for results > 15 000 cells per well. On completion of the study, patient data were decoded and the immunofluorometric signals compared with biliary brushing results.

**Immunoassay performance**

In our analysis, we used 1000 cells per well as the lower detection limit because the within-batch coefficient of variation of the assay was less than 25% in all samples with cell dilutions above 1000 cells per well, but in only one-quarter of samples below this limit. Samples that generated a fluorescence signal below that corresponding to 1000 cells per well were reported as having fewer than 1000 cells per well.

**Statistical analysis**

Sensitivity and specificity characteristics of the immunofluorometric Mcm5 test for the detection of pancreaticobiliary malignancy were presented as a receiver operating characteristics (ROC) curve. The area under the nonparametric ROC curve was used to assess the overall accuracy of the test. Two cut points were used to demonstrate test performance under different circumstances as follows: (i) at the lower detection limit of the assay (i.e. 1000 cells per well), where sensitivity of the test was maximal and (ii) where specificity was 100% (i.e. 1780 cells per well). An exact 95% confidence interval (CI) for each proportion, including sensitivity, specificity and predictive values of Mcm5 and cytology, was derived assuming a binomial distribution using Graph Pad Prism 4

(Graph Pad Software, Inc., San Diego, CA, USA) and/or SPSS software, version 11.5 (SPSS Inc., Chicago, IL, USA).

The sensitivity determined for biliary brush cytology was compared with that of the immunofluorometric Mcm5 test using McNemar’s test for paired proportions. The level of the signal was compared between patient groups using the Mann–Whitney U-test. All statistical tests were two-tailed, and a 5% level was used to indicate statistical significance.

**RESULTS**

**MCM proteins are dysregulated in malignant pancreaticobiliary disease**

The pattern of Mcm2 and -5 protein expression was assessed by immunohistochemistry in morphologically normal, benign and malignant biliary and pancreatic tissue derived from biopsies of masses associated with biliary strictures (Table 1) (Figure 1A–D).

As a positive control for experiments on pancreaticobiliary tissues, the pattern of Mcm2 and -5 protein expression was assessed in the colonic crypt as we have described previously (Stoeber *et al*, 2001). There was nuclear staining of 70 and 74% of cells in the lower third of colonic crypts for Mcm2 and Mcm5 respectively, and less than 5% in the upper third (Figure 2A). In the normal ampulla, which has glands similar to the colon, the expression of MCM proteins was limited to the basal proliferative epithelial compartment (Figure 2B).

The expression of Mcm2 and Mcm5 (not shown) was extremely low in normal pancreas and bile duct (<5% positively stained nuclei), in keeping with previous observations that reduced proliferative capacity in stable tissues (e.g., liver and thyroid) is coupled to repression of origin licensing through downregulation of MCM helicase subunits (Stoeber *et al*, 2001). In contrast, in pancreatic cancer, ampullary carcinoma and cholangiocarcinoma, high levels of Mcm2 and -5 expression were seen in all tissue layers indicative of cell-cycle re-entry (Stoeber *et al*, 1998, 2001; Wharton *et al*, 2001). The percentage of nuclei positive for Mcm2 was higher in malignant tissue (median 76.5%, range 42–92%) than that in benign tissue (median 5%, range 0–33%) (*P* < 0.0005) (Figure 3). Similarly, the percentage of nuclei positive for Mcm5 was higher in malignant strictures (median 91%, range 84–95%, *n* = 5) than in benign strictures (median 4%, range 3–8%, *n* = 5) (not shown).

**Mcm5 in bile aspirates compared with routine brush cytology to diagnose pancreaticobiliary malignancy**

Bile aspirates were acquired from 102 patients with biliary strictures of established (*n* = 42) or indeterminate aetiology (*n* = 60) and the final diagnoses are shown in Table 2. The median age of the patients was 67 years (33–103 years; M:F 1 : 1). A final diagnosis of malignancy was eventually made in 44/60 patients with indeterminate strictures established by brush cytology

**Table 1** Mcm2 expression in masses associated with biliary strictures

Tissue	Cases ( <i>n</i> = 30)	Mcm2 % (range)
Normal pancreas	4	3.5 (0–9.9)
Inflammatory biliary epithelium	5	6 (0–16)
Benign ampulla <sup>a</sup>	3	26 (16–38)
Chronic pancreatitis	3	5.5 (0–14)
Pancreatic cancer	5	80 (30–91)
Ampullary cancer	5	56 (40–75)
Cholangiocarcinoma	5	86 (80–92)

Abbreviation: Mcm2 = minichromosome maintenance protein 2. <sup>a</sup>Normal ampulla *n* = 1, ampulla with chronic inflammation *n* = 1, villous adenoma with low-grade dysplasia *n* = 1.

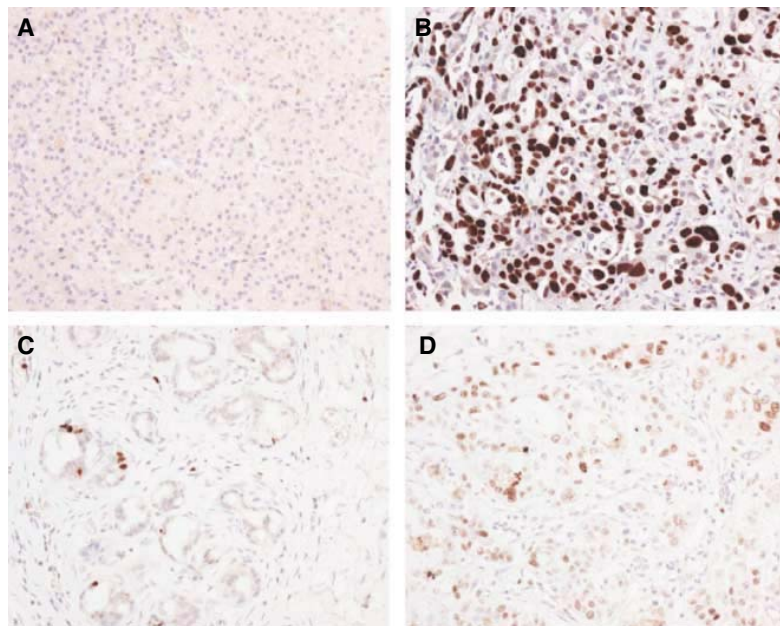


**Figure 1** Minichromosome maintenance protein 2 expression in benign and neoplastic pancreaticobiliary diseases. **(A)** Normal pancreas showing absence of MCM2 expression. **(B)** Moderately to poorly differentiated pancreatic adenocarcinoma showing high levels of MCM2 expression. Occasional viable MCM2-negative cells are present. **(C)** Section of a benign hilar stricture showing occasional MCM2-positive cells at the base of glands. **(D)** Moderately to poorly differentiated cholangiocarcinoma showing high levels of MCM2 expression. MCM2 = minichromosome maintenance protein 2.

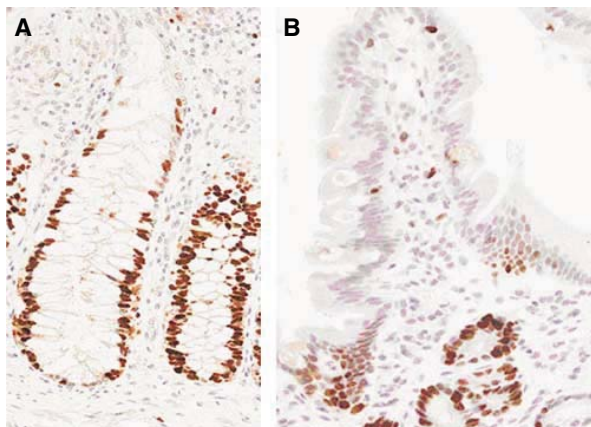


**Figure 2** Immunohistochemistry for MCM5 in the **(A)** colonic crypt and **(B)** ampulla. At the base of epithelium, nuclei of epithelial cells are positive for MCM5 (dark brown) in contrast to surface of epithelium where cells do not express MCM5. MCM5 = minichromosome maintenance protein 5.

( $n=9$ ), endoscopic ultrasound-fine-needle aspiration (EUS-FNA) ( $n=1$ ), intraductal biopsy ( $n=7$ ), percutaneous biopsy ( $n=16$ ), resection specimens ( $n=3$ ) or clinical course ( $n=8$ ). Two brush cytology specimens were highly suspicious for malignancy and a final diagnosis of cancer was made in both. First (i) endoscopic biopsy performed at the time of brush cytology ( $n=20$ ), (ii) percutaneous biopsy ( $n=9$ ) or (iii) EUS-FNA ( $n=1$ ) performed on a separate occasion was obtained in 30/44 patients with eventual diagnoses of malignant strictures and was positive for cancer in 13/30 (43%). Fourteen patients with final diagnoses of malignant strictures underwent a second biopsy/EUS-FNA, which was positive for cancer in 11/14 (79%). Twenty-four out of

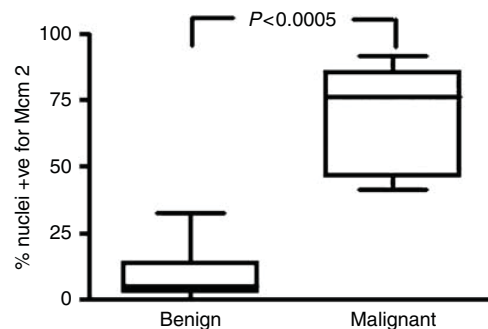


**Figure 3** Box-and-whisker plot of range 25th–75th percentile and median MCM2 expression in benign and malignant biliary strictures. MCM2 = minichromosome maintenance protein 2.

forty-four (55%) patients underwent at least two separate attempts (range 1–3) at tissue acquisition before malignancy was confirmed. Benign disease was confirmed by negative pathology during a mean of 36 (range 21–48) months follow-up.

The performance of the immunofluorometric MCM5 assay as a diagnostic test for pancreaticobiliary malignancy in patients with indeterminate strictures is shown as an ROC curve (Figure 4). The test discriminated with high accuracy between patients with and without malignancy, as demonstrated by an area under the ROC curve of 0.80 (95% CI 0.70–0.91), which was significantly larger than the area predicted by the null hypothesis (0.5) ( $P<0.0004$ ). In other words, a randomly selected patient with pancreaticobiliary malignancy would have an 80% probability of having an immunofluorometric MCM5 value that is greater than that for a randomly selected patient without malignancy. Three patients with malignant strictures had bile samples aspirated on two separate occasions and the mean fluorescence differed by <math><5\%</math>.



Evaluation of the test in comparison with brush cytology in the 60 patients with indeterminate strictures at the time of sample collection is shown in Table 3 at two different performance levels: (i) 1000 cells per well (lower detection limit of the assay) and (ii) 1780 cells per well (high specificity). At the 1000-cell cut point, the test had 66% (29/44) sensitivity and 97% (29/30) positive predictive value. The Mcm5 test detected 20/44 (45%) additional cases of cancer that were not detected by brush cytology. At the

1780 cut point, the test had 43% sensitivity and 100% positive predictive value. The sensitivity and specificity of the Mcm5 test at the 1000-cell cut point in strictures with established diagnoses were 62 and 92%, respectively. In patients with a final diagnosis of a benign stricture, 3/39 (gallstones  $n=1$ , PSC  $n=2$ ) had biliary Mcm5 values greater than 1000 cells per well.

The performance of the immunofluorometric Mcm5 test according to selected final diagnoses is shown in Table 4. The Mcm5 immunofluorometric signal for patients with bile duct stones with or without cholangitis (median <1000) was not higher than that for other patients negative for malignancy, where the median signal was also below the lower detection limit of 1000 cells per well (Mann-Whitney  $U$ -test,  $P=0.78$ ). Significant differences were detected between those samples from patients with cholangiocarcinoma (median 1070,  $P=0.03$ ) or pancreatic cancer (median 1490,  $P=0.003$ ) and those with inflammatory strictures (median <1000). The level of signal was not significantly different ( $P=0.16$ ) between cholangiocarcinoma and pancreatic cancer.

**Table 2** Final diagnosis of bile duct strictures in study of Mcm5 test in bile aspirates

Stricture	Established diagnoses (n = 42)	Final diagnoses of indeterminate strictures (n = 60)	Total (n = 102)
<i>Malignant</i>	18	44	62
Cholangiocarcinoma	12	15	27
Pancreatic cancer	4	19	23
Ampullary carcinoma	0	4	4
Mucinous tumours	2	2	3
Hepatocellular carcinoma	0	1	1
Lymphoma	0	1	1
Metastases to bile duct	0	1	1
Neuroendocrine tumour	0	1	1
<i>Benign</i>	24	16	40
Gallstones	9	5	14
Primary sclerosing cholangitis	6	3	9
Chronic pancreatitis	3	2	5
Autoimmune pancreatitis	0	3	3
Idiopathic	3	1	4
Postoperative	2	1	3
Papillary stenosis	0	0	1
Ampullary adenoma	0	1	1

Abbreviation: Mcm5 = minichromosome maintenance protein 5.

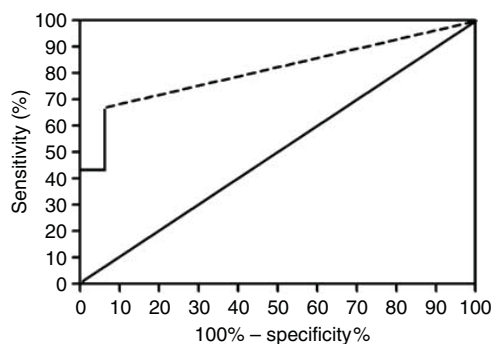


**Figure 4** Receiver operating characteristic curve of immunofluorometric Mcm5 test. The jagged curve (solid line) is the nonparametric ROC curve. The diagonal line is the reference line. Area under the curve is 80% (95% CI 70–91). Mcm5 = minichromosome maintenance protein 5; ROC = receiver operating characteristic.

**DISCUSSION**

In patients who present with a pancreaticobiliary stricture of indeterminate origin, biliary brush cytology is the most commonly used invasive technique to distinguish benign from malignant disease. The technique offers the clinician almost definitive diagnostic certainty when positive for malignancy (specificity 96–100%) but has a poor ability to detect malignancy (sensitivity 18–57%) (de Bellis *et al*, 2002b; Baron *et al*, 2004; Harewood *et al*, 2004; Moreno Luna *et al*, 2006).

This proof of principle study has shown that the sensitivity of the automated immunofluorometric Mcm5 test on bile aspirates for detecting pancreaticobiliary malignancy was superior (four times more at the 1000 cells per well cut point) to that of brush cytology, while maintaining a high specificity. The high positive predictive value for malignancy of this test in this group of patients is of particular importance as a positive test would allow the clinician to make treatment recommendations with a high degree of certainty. We have previously shown that the Mcm5 immunofluorometric test is an accurate test for bladder, prostate and oesophageal cancer (Stoeber *et al*, 2002; Williams *et al*, 2004), and

**Table 4** Immunofluorometric Mcm5 test performance in patient groups

Patient group	Group size (N)	Median signal	Interquartile range
<i>Negative for cancer</i>	40	<1000	<1000–<1000
Gallstones	15	<1000	<1000–<1000
Chronic inflammation <sup>a</sup>	14	<1000	<1000–<1000
<i>All cancers</i>	62	1198	<1000–3495
Cholangiocarcinoma	27	1070	<1000–2060
Pancreatic cancer	23	1490	<1000–5340

Abbreviation: Mcm5 = minichromosome maintenance protein 5. <sup>a</sup>Primary sclerosing cholangitis and chronic pancreatitis.

**Table 3** Comparison of the Mcm5 immunofluorometric assay in bile aspirates with brush cytology for the diagnosis of pancreaticobiliary malignancy

	Sensitivity (95% CI)	Specificity (95% CI)	PPV (95% CI)	NPV (95% CI)	Area under curve (95% CI)
Mcm5 cutoff point > 1000	66% (50–79) <sup>a</sup>	94% (70–100) <sup>b</sup>	97% (90–100)	50% (32–68)	80% (70–91)
Mcm5 cutoff point > 1780	43% (29–57)	100%	100%	39% (24–53)	72% (58–85%)
Brush cytology	20% (7–35) <sup>a</sup>	100% <sup>b</sup>	100%	31% (18–44)	60% (40–76)

Abbreviations: Mcm5 = minichromosome maintenance protein 5; NPV = negative predictive value; PPV = positive predictive value. <sup>a</sup> $P=0.004$  for sensitivity Mcm5 vs cytology <sup>b</sup> $P$  = not significant.

here we show its utility for the diagnosis of pancreatic and biliary tract cancer. Taken together, these studies indicate that the MCM5 immunofluorometric assay is a robust test to detect exfoliated malignant cells in body fluids. Moreover, as these malignancies are associated with different sets of genetic mutations leading to uncontrolled cell proliferation, this study provides further evidence supporting the hypothesis that the convergence point of growth regulatory pathways that control cell proliferation is the initiation of genome replication in which the MCM complex plays an essential part.

The median level of expression of MCM5 in malignant bile samples was lower than that we detected in urine and oesophageal aspirates obtained from patients with bladder and oesophageal cancer respectively (Stoeber *et al*, 2002; Williams *et al*, 2004). The absolute values obtained are however not the most important factor in determining the usefulness of the test but whether a cutoff point can be obtained that helps to distinguish between benign and malignant bile duct strictures by a clinically important margin, which this test did in the population studied.

Importantly, inflammatory strictures secondary to PSC and chronic pancreatitis, which are particularly difficult to distinguish from malignant disease with conventional imaging (Lazaridis and Gores, 2005; Hamer and Feuerbach, 2006), had median biliary MCM5 values below the detection limit of the assay. Benign/normal tissues did express MCM proteins at low levels (median 5% of cells stained by immunohistochemistry), but as the cells are located in the basal epithelium they were probably not exfoliated in bile in large numbers and therefore not detected by the immunofluorometric test. Interestingly, patients with bile duct stones and cholangitis – who might be expected to have ulceration and exposure of the stem-transit compartment of biliary epithelium to bile – also had a median MCM5 level in bile below the detection limit of the assay, reflecting low shedding of reactive MCM5-positive cells. This was in contrast to our previous data in patients with renal calculi and oesophageal ulceration, where the test detected positive cells in urine and luminal secretions, though of a magnitude below that of patients with urothelial or oesophageal carcinoma (Stoeber *et al*, 2002; Williams *et al*, 2004).

The immunofluorometric MCM5 level results in bile were corroborated by immunohistochemistry data, which showed that the percentage of nuclei positive for MCM2 and -5 was higher in malignant strictures than benign strictures. To date, we have performed immunohistochemistry on more samples using anti-MCM2 than anti-MCM5 antibodies. The MCM complex consists of six proteins, all of which are necessary to support initiation of replication. By detecting the presence of one protein, one can infer the presence of the other five. However, to verify this we tested 10 cases for both MCM5 and MCM2, which showed a similar % of nuclei positive for MCM proteins.

The molecular diagnosis of pancreaticobiliary malignancies has been the subject of intensive investigation (Gress, 2004), but to date few such tests have been developed and incorporated into routine clinical practice. A recent study of fluorescence *in situ* hybridisation to detect chromosomal abnormalities in biliary brush cytology samples demonstrated results comparable to our study with a sensitivity of 59–70% and specificity of 86–100% for the diagnosis of pancreaticobiliary malignancy compared with a

sensitivity of 4–20% for conventional brush cytology (Moreno Luna *et al*, 2006).

The sensitivity of biliary brush cytology (20%) in our study is at the lower end of the range in the published literature although other published studies (Baron *et al*, 2004; Harewood *et al*, 2004; Moreno Luna *et al*, 2006) have reported similar sensitivities of around 20%. One possible explanation is that patients referred to our centre had small volume, difficult to diagnose tumours, as demonstrated by the fact that the majority of the first cytology/biopsy episodes of malignant strictures were negative for cancer. Bile duct forceps biopsy (Jailwala *et al*, 2000), EUS-guided FNA of strictures (Fritscher-Ravens *et al*, 2004) or a cytopathologist within the endoscopy room to immediately analyse samples (De Bellis *et al*, 2002a) can all independently add to the detection rate of brush cytology. However, intraductal biopsy, which often requires a biliary sphincterotomy (Ponchon *et al*, 1995), and EUS-guided FNA of strictures are technically challenging procedures with a higher risk of complications than brush cytology and therefore are not usual practice in our unit or at other centres (Lee, 2006) when acquiring tissue for the first time. The advantage of the immunofluorometric test is that it is based on bile aspirates, which is technically easier to acquire than all of the methods mentioned.

The sensitivity of the MCM5 test depends in part on the cellularity of bile, which can be acellular in up to 30% of samples (Mansfield *et al*, 1997), so that the sensitivity of bile aspirate MCM5 cannot be expected to reach 100%. In contrast, the cellularity of brush cytology is much greater than bile aspirates and we are currently assessing whether cells derived from brush cytology will further improve the sensitivity of the MCM5 test. As all cancer tissues studied expressed MCM proteins, a sensitivity approaching 100% with cells derived from brush cytology applied to the immunofluorometric MCM5 test is theoretically achievable. Future work will aim to replicate these results in a new cohort of patients and also examine the utility of this test in distinguishing PSC from cholangiocarcinoma and chronic pancreatitis from pancreatic cancer in a larger number of patients.

In conclusion, we have demonstrated that immunofluorometric detection of MCM5 in bile aspirates is a sensitive and specific diagnostic test for pancreaticobiliary malignancy. The test detects a variety of cancer types including those often missed by biliary brush cytology. This simple method for detecting pancreaticobiliary malignancy is now automated allowing for easy translation into a clinical diagnostic test.

## ACKNOWLEDGEMENTS

We thank Fiona Tulloch and Keith Burling for technical assistance with the immunofluorometric MCM5 test. This work was supported by grants from the British Liver Trust (with thanks to the Brian Mercer Trust), UCLH Charities and the RF&UCL Medical School, and a Cancer Research UK programme grant. The work was undertaken at UCLH/UCL, which received a proportion of funding from the Department of Health's National Institute for Health Research (NIHR) Biomedical Research Centres funding scheme.

## REFERENCES

- Baron TH, Harewood GC, Rumalla A, Pochron NL, Stadheim LM, Gores GJ, Therneau TM, De Groen PC, Sebo TJ, Salomao DR, Kipp BR (2004) A prospective comparison of digital image analysis and routine cytology for the identification of malignancy in biliary tract strictures. *Clin Gastroenterol Hepatol* 2: 214–219
- Blow JJ, Hodgson B (2002) Replication licensing—defining the proliferative state? *Trends Cell Biol* 12: 72–78
- De Bellis M, Sherman S, Fogel EL, Cramer H, Chappo J, McHenry Jr L, Watkins JL, Lehman GA (2002a) Tissue sampling at ERCP in suspected malignant biliary strictures (Part 1). *Gastrointest Endosc* 56: 552–561

- de Bellis M, Sherman S, Fogel EL, Cramer H, Chappo J, McHenry Jr L, Watkins JL, Lehman GA (2002b) Tissue sampling at ERCP in suspected malignant biliary strictures (Part 2). *Gastrointest Endosc* **56**: 720–730
- Freeman A, Morris LS, Mills AD, Stoeber K, Laskey RA, Williams GH, Coleman N (1999) Minichromosome maintenance proteins as biological markers of dysplasia and malignancy. *Clin Cancer Res* **5**: 2121–2132
- Fritscher-Ravens A, Broering DC, Knoefel WT, Rogiers X, Swain P, Thonke F, Bobrowski C, Topalidis T, Soehendra N (2004) EUS-guided fine-needle aspiration of suspected hilar cholangiocarcinoma in potentially operable patients with negative brush cytology. *Am J Gastroenterol* **99**: 45–51
- Gress TM (2004) Molecular diagnosis of pancreaticobiliary malignancies in brush cytologies of biliary strictures. *Gut* **53**: 1727–1729
- Hamer OW, Feuerbach S (2006) How useful is integrated PET and CT for the management of pancreatic cancer? *Nat Clin Pract Gastroenterol Hepatol* **3**: 74–75
- Harewood GC, Baron TH, Stadheim LM, Kipp BR, Sebo TJ, Salomao DR (2004) Prospective, blinded assessment of factors influencing the accuracy of biliary cytology interpretation. *Am J Gastroenterol* **99**: 1464–1469
- Jailwala J, Fogel EL, Sherman S, Gottlieb K, Flueckiger J, Bucksot LG, Lehman GA (2000) Triple-tissue sampling at ERCP in malignant biliary obstruction. *Gastrointest Endosc* **51**: 383–390
- Kearsey SE, Labib K (1998) MCM proteins: evolution, properties, and role in DNA replication. *Biochim Biophys Acta* **1398**: 113–136
- Khan SA, Thomas HC, Davidson BR, Taylor-Robinson SD (2005) Cholangiocarcinoma. *Lancet* **366**: 1303–1314
- Lazaridis KN, Gores GJ (2005) Cholangiocarcinoma. *Gastroenterology* **128**: 1655–1667
- Lee JG (2006) Brush cytology and the diagnosis of pancreaticobiliary malignancy during ERCP. *Gastrointest Endosc* **63**: 78–80
- Mansfield JC, Griffin SM, Wadehra V, Matthewson K (1997) A prospective evaluation of cytology from biliary strictures. *Gut* **40**: 671–677
- Moreno Luna LE, Kipp B, Halling KC, Sebo TJ, Kremers WK, Roberts LR, Barr Fritcher EG, Levy MJ, Gores GJ (2006) Advanced cytologic techniques for the detection of malignant pancreaticobiliary strictures. *Gastroenterology* **131**: 1064–1072
- Ponchon T, Gagnon P, Berger F, Labadie M, Liaras A, Chavaillon A, Bory R (1995) Value of endobiliary brush cytology and biopsies for the diagnosis of malignant bile duct stenosis: results of a prospective study. *Gastrointest Endosc* **42**: 565–572
- Stoeber K, Halsall I, Freeman A, Swinn R, Doble A, Morris L, Coleman N, Bullock N, Laskey RA, Hales CN, Williams GH (1999) Immunoassay for urothelial cancers that detects DNA replication protein Mcm5 in urine. *Lancet* **354**: 1524–1525
- Stoeber K, Mills AD, Kubota Y, Krude T, Romanowski P, Marheineke K, Laskey RA, Williams GH (1998) Cdc6 protein causes premature entry into S phase in a mammalian cell-free system. *EMBO J* **17**: 7219–7229
- Stoeber K, Swinn R, Prevost AT, de Clive-Lowe P, Halsall I, Dilworth SM, Marr J, Turner WH, Bullock N, Doble A, Hales CN, Williams GH (2002) Diagnosis of genito-urinary tract cancer by detection of minichromosome maintenance 5 protein in urine sediments. *J Natl Cancer Inst* **94**: 1071–1079
- Stoeber K, Tlsty TD, Happerfield L, Thomas GA, Romanov S, Bobrow L, Williams ED, Williams GH (2001) DNA replication licensing and human cell proliferation. *J Cell Sci* **114**: 2027–2041
- Wharton SB, Chan KK, Anderson JR, Stoeber K, Williams GH (2001) Replicative Mcm2 protein as a novel proliferation marker in oligodendrogliomas and its relationship to Ki67 labelling index, histological grade and prognosis. *Neuropathol Appl Neurobiol* **27**: 305–313
- Williams G, Stoeber K (1999) Clinical applications of a novel mammalian cell-free DNA replication system. *Br J Cancer* **80**(Suppl 1): 20–24
- Williams GH, Romanowski P, Morris L, Madine M, Mills AD, Stoeber K, Marr J, Laskey RA, Coleman N (1998) Improved cervical smear assessment using antibodies against proteins that regulate DNA replication. *Proc Natl Acad Sci USA* **95**: 14932–14937
- Williams GH, Swinn R, Prevost AT, De Clive-Lowe P, Halsall I, Going JJ, Hales CN, Stoeber K, Middleton SJ (2004) Diagnosis of oesophageal cancer by detection of minichromosome maintenance 5 protein in gastric aspirates. *Br J Cancer* **91**: 714–719

## Chapter 5

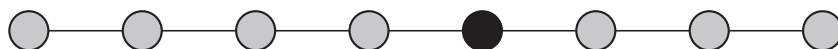
# DNA replication licensing factors and aneuploidy are linked to tumor cell cycle state and clinical outcome in penile carcinoma

OJ Kayes, M Loddo, N Patel, P Patel, S Minhas, G Ambler, A Freeman, A Wollenschlaeger, DJ Ralph, K Stoeber, GH Williams

Clinical Cancer Research 2009 15 (23): 7335-7344.

Supplementary material related to this article is available online at:

<http://clincancerres.aacrjournals.org/content/15/23/7335/suppl/DC1>





## DNA Replication Licensing Factors and Aneuploidy Are Linked to Tumor Cell Cycle State and Clinical Outcome in Penile Carcinoma

Oliver J. Kayes,<sup>1,4</sup> Marco Loddo,<sup>1,3</sup> Nimish Patel,<sup>1</sup> Pranav Patel,<sup>1</sup> Suks Minhas,<sup>4</sup> Gareth Ambler,<sup>2,5</sup> Alex Freeman,<sup>1</sup> Alex Wollenschlaeger,<sup>3</sup> David J. Ralph,<sup>4</sup> Kai Stoeber,<sup>1,3</sup> and Gareth H. Williams<sup>1,3</sup>

**Abstract Purpose:** The DNA replication licensing machinery is integral to the control of proliferation, differentiation, and maintenance of genomic stability in human cells. We have analyzed replication licensing factors (RLF), together with DNA ploidy status, to investigate their role in progression of penile squamous cell carcinoma and to assess their utility as novel prognostic tools.

**Experimental Design:** In a cohort of 141 patients, we linked protein expression profiles of the standard proliferation marker Ki67 and the RLFS Mcm2 and geminin to clinicopathologic variables, ploidy status, and clinical outcome.

**Results:** Increased Ki67, Mcm2, and geminin levels were each significantly associated with arrested tumor differentiation ( $P < 0.0001$ ) and aneuploidy ( $P \leq 0.01$ ). Accelerated cell cycle progression was linked to increasing tumor size, stage, and depth of invasion. Aneuploid tumors significantly correlated with tumor grade ( $P < 0.0001$ ). Biomarker expression and DNA ploidy status were significant predictors of locoregional disease progression [Mcm2 ( $P = 0.02$ ), geminin ( $P = 0.02$ ), Ki67 ( $P = 0.03$ ), and aneuploidy ( $P = 0.03$ )] in univariate analysis. Importantly, aneuploidy was a strong independent prognosticator for overall survival (hazard ratio, 4.19; 95% confidence interval, 1.17-14.95;  $P = 0.03$ ). Used in conjunction with conventional pathologic information, multiparameter analysis of these variables can stratify patients into low- or high-risk groups for disease progression (Harrell's c-index = 0.88).

**Conclusions:** Our findings suggest that RLFS and tumor aneuploidy may be used as an adjunct to conventional prognostic indicators, identifying men at high risk of disease progression. Our results also identify the DNA replication initiation pathway as a potentially attractive therapeutic target in penile squamous cell carcinoma. (Clin Cancer Res 2009;15(23):7335-44)

Penile carcinoma is a rare cancer in the Western world with an incidence of 0.1 to 0.9 per 100,000 males. However, there is notable geographic variation with much higher incidences in Africa, Asia, and South America (1). Patients with penile squamous cell carcinoma (PeSCC) represent the largest subgroup (98% of all cases) and typically present with primary lesions

on the glans, foreskin, or shaft of the penis (2). Locoregional lymph node status is currently the most powerful prognostic indicator identified in penile cancer. Early radical inguinal lymphadenectomy has been shown to convey a distinct survival benefit (3-6), but this surgical technique is limited by its associated high rates of morbidity and mortality (7). Furthermore, controversy exists over patient selection for both radical surgical and chemotherapeutic interventions. Treatment selection is currently based on the patient's age and health status and clinical lymph node stage, together with conventional prognostic factors including histologic grade, tumor-node-metastasis stage, and depth of invasion (8, 9). However, a proportion of men will be incorrectly staged using these algorithms and potentially inappropriately treated (10). Therefore, it is imperative to isolate novel biomarkers in patients with poor prognostic characteristics to identify high-risk patients and facilitate treatment stratification.

Tumors acquire a growth advantage over normal tissues through a variety of mechanisms, including acquisition of aneuploidy and dysregulation of the mechanisms that control cellular proliferation. The DNA replication licensing pathway has emerged as a powerful downstream mechanism for controlling the proliferative state of cells and ensures that DNA is replicated once and only once per cell cycle, thus maintaining genomic

**Authors' Affiliations:** Departments of <sup>1</sup>Pathology and <sup>2</sup>Statistical Science and <sup>3</sup>Wolfson Institute for Biomedical Research, University College London; <sup>4</sup>Department of Urology and <sup>5</sup>Joint University College London Hospitals/University College London Biomedical Research Unit, University College Hospital London, London, United Kingdom  
Received 4/8/09; revised 8/13/09; accepted 8/31/09; published OnlineFirst 11/17/09.

The costs of publication of this article were defrayed in part by the payment of page charges. This article must therefore be hereby marked *advertisement* in accordance with 18 U.S.C. Section 1734 solely to indicate this fact.

**Note:** Supplementary data for this article are available at Clinical Cancer Research Online (<http://clincancerres.aacrjournals.org/>).

**Requests for reprints:** Kai Stoeber, Department of Pathology, University College London, Rockefeller Building, University Street, London WC1E 6BT, United Kingdom. Phone: 44-20-7679-6302; Fax: 44-20-8377-4408; E-mail: k.stoeber@ucl.ac.uk.

© 2009 American Association for Cancer Research.  
doi:10.1158/1078-0432.CCR-09-0882

### Translational Relevance

Penile cancer is a rare malignancy associated with poor survival outcomes for patients with advanced disease states. Identifying patients who will benefit from aggressive therapeutic strategies remains problematic. The delineation of novel effective molecular targets capable of delivering powerful prognostic information as well as defining new therapeutic targets in this clinical setting is challenging. In this study we show that dysregulation of the DNA replication licensing pathway is intricately linked to tumor progression and aneuploidy. Using a panel of cell cycle biomarkers, we have identified key “proliferation signatures” that reflect aggressive cell cycle phenotypes linked to poorer clinical outcomes. Integration of these biomarkers with conventional clinicopathologic parameters in a novel predictive model has potential to facilitate identification of those patients most likely to benefit from radical surgical and chemotherapeutic interventions.

stability (11, 12). During late mitosis and early G<sub>1</sub> phase, the replication licensing factors (RLF) ORC, Cdc6, Cdt1, and Mcm2-7 assemble into prereplicative complexes, which render replication origins “licensed” for DNA synthesis. During S phase, Cdc7 kinase and cyclin-dependent kinases induce a conformational change in the prereplicative complex, resulting in recruitment of additional initiator proteins that collectively promote DNA unwinding and recruitment of DNA polymerases (13, 14). During S-G<sub>2</sub>-M phases, the presence of the licensing repressor protein geminin prevents inappropriate reinitiation events at origins that have already been activated (15, 16). Recent studies suggest that dysregulation of replication licensing in early tumorigenesis may arise as a consequence of oncogene-induced cell proliferation, which can cause either underreplication or overreplication of chromosomal DNA and therefore contribute to the development of aneuploidy commonly seen during multistep tumor progression to an aggressive cancer phenotype (17).

Mcm2-7 (MCM) proteins are expressed throughout the cell cycle (G<sub>1</sub>-S-G<sub>2</sub>-M) but are tightly downregulated during exit into out-of-cycle quiescent (G<sub>0</sub>), differentiated, or senescent states (11, 12, 14, 18–21). Thus, the MCM proteins represent novel biomarkers of growth and have been confirmed as powerful markers for cancer detection and prognostication in a wide range of tumor types (11, 17, 22). Moreover, expression profiling of MCM together with Ki67 (standard proliferation marker) and geminin (biomarker of S-G<sub>2</sub>-M progression) allows cells in out-of-cycle states to be distinguished from those residing in cycle and can assign cells to G<sub>1</sub> and S-G<sub>2</sub>-M phase (23, 24). Mcm2-7 protein expression also identifies noncycling cells with proliferative potential. The Mcm2/Ki67 ratio therefore defines the proportion of cells that are licensed to proliferate. Consequently, the higher the Mcm2/Ki67 ratio, the greater the proportion of cells that reside in a licensed noncycling state (11, 23–27). Because Ki67 is present throughout the cell cycle in proliferating cells, the “geminin/Ki67” ratio may be used as an indicator of the relative length of G<sub>1</sub> phase and the rate of

cell cycle progression (11, 23–27). Similarly, the “Ki67-geminin” labeling index (LI) can be used to identify the numbers of cells transiting G<sub>1</sub> phase (27–29). This information is valuable for determining the cell cycle kinetics of dynamic tumor cell populations and is of prognostic significance (11, 23–27).

Complex signaling pathways interlinked with redundant growth-regulatory mechanisms contribute to the diverse and heterogeneous effects of oncogenic mutations observed in diverse tumor types (30). Attempts to formulate improved biomarkers for cancer detection and progression alongside the development of novel chemotherapeutic agents against these new molecular targets have met with limited success to date (31). Targeting the DNA replication licensing pathway, which acts as an integration point for upstream mitogenic signaling pathways, is an attractive alternative approach to the identification of new prognostic and predictive markers (11). In light of the biological, prognostic, and therapeutic implications of these cell cycle regulators in tumorigenesis, we have investigated their role in the progression of penile carcinoma. We have used multiparameter analysis of Mcm2, geminin, and Ki67 to study the cell cycle kinetics of this tumor type *in vivo* and how deregulation of the replication licensing pathway is linked to acquisition of aneuploidy and clinical outcome. Our findings provide new insights into the biological mechanisms involved in tumor progression of penile carcinoma and how these novel biomarkers of growth might be exploited to predict the *in vivo* behavior of this rare tumor type.

### Materials and Methods

**Study cohort.** From January 1988 to January 2007, 141 patients were diagnosed with carcinoma *in situ* or invasive squamous cell carcinoma of the penis. All patients had been treated within the North London Cancer Network and histologic specimens were reviewed by a uro-oncology pathologist at diagnosis. Paraffin wax-embedded tissue specimens were retrieved from the pathology archives for all patients and clinical information was sourced from hospital medical records. Local research ethics committee approval for the study was obtained from the joint University College London/University College London Hospitals Committees on the Ethics of Human Research. Excised tumors were histologically staged using the revised tumor-node-metastasis system criteria 2002 (32). Pathologic variables of the primary tumor included grade, local stage, subtype, extent (unifocal/multifocal), tumor size, depth of invasion, and lymphovascular invasion. All pathologic parameters were recorded by a specialist uro-oncology pathologist and independently reviewed by a second pathologist. Tumor grade was defined using Broders' classification (33): well differentiated (grade 1), moderately differentiated (grade 2), and poorly differentiated (grade 3). Tumor size was defined as the maximal dimension and depth of invasion measured from adjacent normal epithelium to the deepest invasive point. Lymphovascular invasion was determined microscopically and confirmed using antibodies against endothelial markers CD33 and CD34. Lymph node status was confirmed following pathologic review of inguinal and pelvic lymph node specimens attained through prophylactic or delayed lymphadenectomy. Patients who entered into surveillance programs without lymph node surgery were classified as negative after 2 y without disease presentation. Twelve patients with carcinoma *in situ* were removed from most analyses and 11 patients were lost to follow-up. Therefore, 118 patients were included in the long-term follow-up survival study. The median follow-up time was 20 mo (range, 0.8–162.4 mo). Table 1 summarizes the clinicopathologic characteristics of the patients. The mean age of all patients at the time of diagnosis was 62 y (range, 27–87 y).

**Table 1.** Patient characteristics

	Frequency (%)
Age (y)	
Mean	62.7
Range	27-86
Grade	
1	26 (18)
2	54 (38)
3	49 (35)
Tumor stage	
I	60 (47)
II	55 (43)
III	12 (9)
IV	2 (1)
Subtype	
Standard PeScC	87 (68)
Basaloid	7 (5)
Warty/verrucous	6 (4)
Papillary	18 (14)
Mixed	11 (9)
Tumor extent	
Unifocal	101 (78)
Multifocal	28 (22)
Vascular invasion	
Negative	101 (78)
Positive	28 (22)
Size (cm)	
≤2	45 (35)
>2	60 (47)
Unknown	14 (11)
Depth invasion (mm)	
≤5	58 (45)
6-10	27 (21)
11-20	17 (13)
>20	11 (9)
Unknown	16 (12)
Nodal stage	
0	59 (46)
1	12 (9)
2	15 (12)
3	9 (7)
Unknown	34 (26)
Lymph node metastases	
Negative	59 (46)
Positive	37 (28)
Surveillance	20 (16)
Unknown	13 (10)
Distant metastases	
Negative	96 (74)
Positive	16 (12)
Unknown	17 (14)
Penile cancer death	
Alive	92 (71)
Dead	26 (20)
Unknown	11 (9)
Survival follow-up (mo)	
Median	20.1
Range	1-160

NOTE:  $n = 129$ .

**Antibodies.** Affinity-purified rabbit polyclonal antibody against full-length human geminin was previously generated and validated (14, 34). Ki67 monoclonal antibody (clone MIB-1) was obtained from DAKO and Mcm2 monoclonal antibody (clone 46) was from BD Transduction Laboratories. The specificity of Ki67 and Mcm2 monoclonal antibody has been extensively studied and validated in previous studies (24, 25, 27).

**Immunohistochemistry.** Consecutive serial sections were cut from each paraffin-embedded tissue block representative of the tumor. Three-micrometer sections were cut onto Superfrost Plus slides (Leica Microsystems), dewaxed in xylene, and rehydrated through graded alcohol to water. For antigen retrieval, slides were pressure cooked in 0.1 mol/L citrate buffer (pH 6.0) at 103 kPa for 2.5 min. Tissue sections were immunostained using the Bond Polymer Define Detection kit and Bond-X automated system (Leica) according to the manufacturer's instructions. Primary antibodies were applied at the following dilutions: Ki67 (1:70), Mcm2 (1:1,000), and geminin (1:500). Coverslips were applied with Pertex mounting medium (CellPath). Incubation without the primary antibody was used as a negative control and colonic epithelial sections were used as positive controls.

**Protein expression profile analysis.** Protein expression analysis was done by determining the LI of the markers in each tumor, as previously described (23-27, 35). Consecutive serial sections cut from the same formalin-fixed, paraffin-embedded tissue block were used to stain for the markers. Slides were evaluated at  $\times 100$  magnification to select the advancing edge of the tumor. Selected areas at the advancing edge plus three to five adjacent fields perpendicular to the advancing front moving progressively toward the center of the tumor were image captured at  $\times 400$  magnification with a charge-coupled device camera and AnalySIS image analysis software (SIS). Images were subsequently printed for quantitative analysis, which was undertaken with the observer unaware of the clinicopathologic variables. Both positive and negative cells within the field were counted and any stromal or inflammatory cells were excluded. A minimum of 500 cells was counted for each case. The LI was calculated using the following formula:  $LI = \text{number of positive cells} / \text{total number of cells} \times 100$ . Normal foreskin and colon specimens were used as external controls. Normal adjacent epithelium acted as an additional internal control. Reassessment of 10 randomly selected cases by an independent assessor showed high levels of agreement.

**DNA image cytometry.** For each case, one 40- $\mu\text{m}$  section of formalin-fixed, paraffin-embedded tissue, obtained from the same block as that assessed for immunohistochemistry, was used to prepare a suspension of nuclei. Sections were deparaffinized in xylene, rehydrated through decreasing alcohol gradient, and washed twice in PBS. Rehydrated tissue sections were incubated at 37°C in a shaker water bath for 2 h in the presence of 20 mg/mL bacterial proteinase type XXIV (Sigma). Chilled PBS was added to stop enzymatic digestion and the suspension of nuclei was filtered through a nylon mesh filter and centrifuged at 1500 rpm for 5 min. The supernatant was then discarded and the pellet was resuspended in 3 mL of fresh PBS. A volume of 100  $\mu\text{L}$  of the suspension was cytospun at 1500 rpm for 5 min to prepare a monolayer on a Superfrost Plus slide (Visions Biosystems). The density of the nuclear preparation on the slide was checked under a light microscope and an adjusted volume of the suspension was cytospun if correction of the density was required. The monolayer preparations were air dried and fixed overnight in 4% formaldehyde. After washing in distilled water, slides were incubated in 5 mol/L HCl for 1 h at room temperature for hydrolysis. Slides were then rinsed in distilled water and incubated in Feulgen-Schiff's solution for 2 h in the dark. Finally, the slides were washed in running tap water for 10 min, dehydrated in increasing alcohol gradient, cleared in xylene, and coverslipped.

The Fairfield DNA Ploidy System (Fairfield Imaging) was used for image processing, analysis, and classification. This consisted of a Zeiss Axioplan microscope equipped with a 40/0.75 objective lens (Zeiss), a 546-nm green filter, and a black and white high-resolution digital camera (C4742-95; Hamamatsu Photonics K.K.) with 1024  $\times$  1024 pixels at 10 bits per pixel. The integrated absorbance of each nucleus was calculated based on measurements of absorbance and area. Background absorbance was measured and corrected for each nucleus. At least 1,000 nuclei were scanned for each case and stored in galleries, which were then edited to discard spliced, overlapping, and pyknotic nuclei. A minimum of 300 tumor nuclei per case was used by Histogram Draftsman



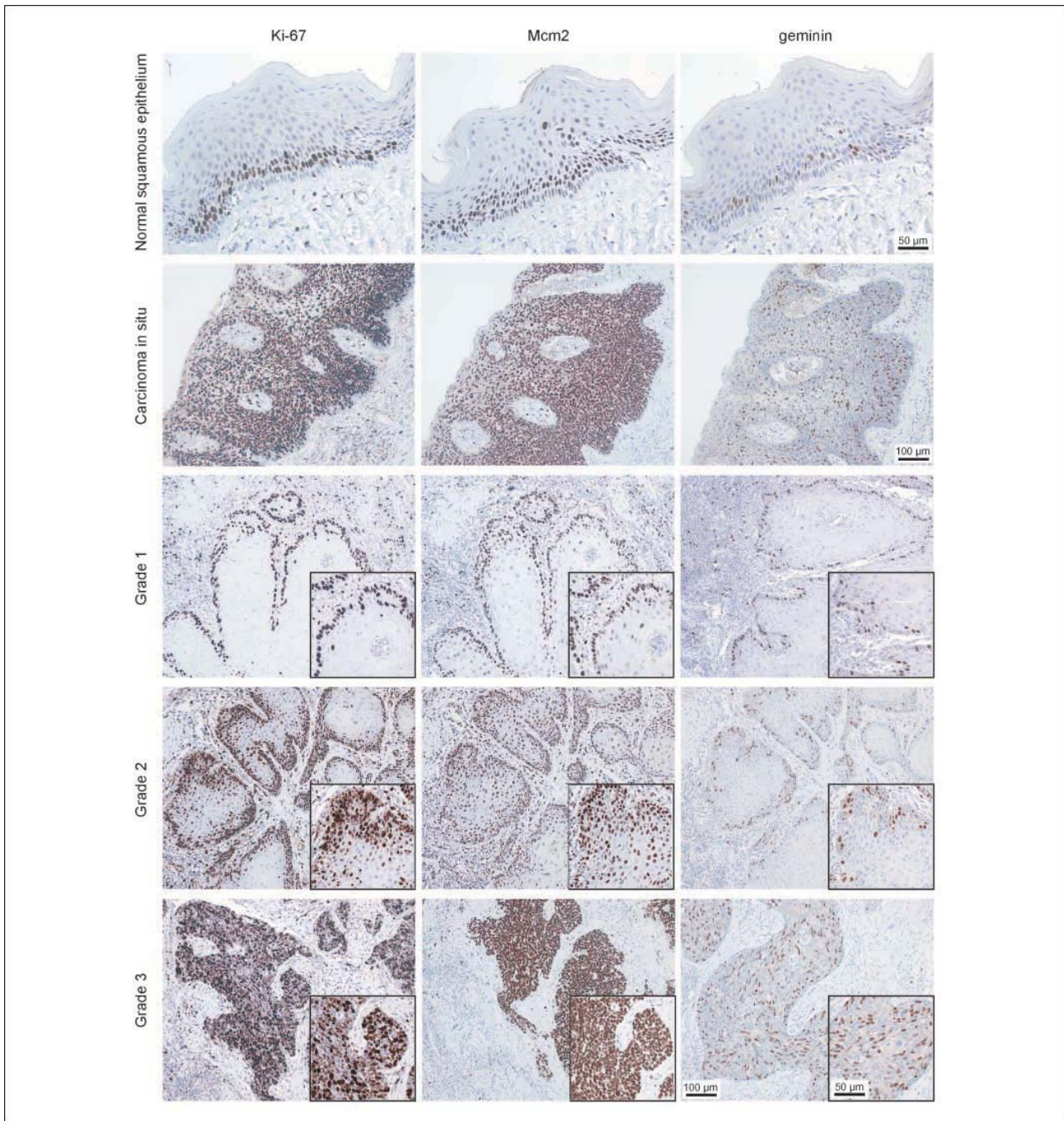


**Fig. 1.** Photomicrographs of paraffin wax-embedded tissue sections of representative normal squamous epithelium, carcinoma *in situ*, and PeScc (grades 1-3) immunohistochemically stained with antibodies to Ki67, Mcm2, and geminin. Magnification,  $\times 200$ . Inset shows immunostaining at high magnification ( $\times 400$ ).

1.4 (Fairfield Imaging) to create the histograms. Lymphocytes and plasma cells were included as diploid internal controls and sections of high-grade bladder cancer and normal foreskin tissue as external controls for aneuploid and diploid populations, respectively.

Ploidy histograms were constructed for 121 cases, with 9 cases not linked to survival data. Twenty specimens could not be fully processed due to insufficient or poor-quality tissue material. Histograms were classified according to the following previously published criteria

(36): The tumor was classified as diploid if only one  $G_0$ - $G_1$  peak (2c) was present, the number of nuclei in the  $G_2$  (4c) peak did not exceed 10% of the total number of nuclei, and the number of nuclei with a DNA content exceeding 5c did not exceed 1%. A tumor was defined as tetraploid when a peak in the 4c position was present together with a peak in the 8c position or the fraction of nuclei in the 4c region exceeded 10% of the total number of nuclei. A tumor was defined as polyploid when a peak in the 8c position was present together with a peak

**Table 2.** Relationship between biomarker expression and tumor differentiation

	Grade 1 (n = 26)	Grade 2 (n = 54)	Grade 3 (n = 49)	P*
Mcm2	53 (34-65) <sup>†</sup>	75 (61-84)	86 (74-95)	<0.0001
Ki67	39 (27-55)	66 (51-77)	75 (60-87)	<0.0001
Geminin	10 (9-17)	20 (14-24)	21 (17-29)	<0.0001
Mcm2/Ki67 <sup>‡</sup>	1.20 (1.09-1.39)	1.13 (1.04-1.21)	1.10 (1.04-1.22)	0.09
Geminin/Ki67 <sup>§</sup>	0.30 (0.20-0.34)	0.30 (0.23-0.35)	0.30 (0.25-0.38)	0.22
Ki67-geminin <sup>  </sup>	28 (22-39)	46 (39-54)	50 (43-61)	<0.0001

NOTE: Labeling index (expressed as percentages). n = 129.

\*Jonckheere-Terpstra test.

<sup>†</sup>Median (interquartile range).

<sup>‡</sup>Mcm2/Ki67 indicates the ratio of licensed to actively proliferating cells.

<sup>§</sup>Geminin/Ki67 ratio indicates the relative length of G<sub>1</sub> phase.

<sup>||</sup>Ki67-geminin represents the percentage of cells that are transiting G<sub>1</sub>.

in the 16c position. The tumor was defined as aneuploid when non-euploid peaks were present or the number of nuclei with a DNA content exceeding 5c/9c, not representing euploid populations, exceeded 1%. The histograms were classified by two independent assessors with a high level of agreement and without knowledge of the clinicopathologic variables. For the purposes of statistical analysis, tetraploid and polyploid tumors were grouped together with aneuploid tumors.

**Statistical analysis.** Relationships between biomarker expression and other factors were assessed using the Mann-Whitney U, Kruskal-Wallis, and Jonckheere-Terpstra tests. Data were summarized as the median value and interquartile range of LIs observed across the cohort. Multivariable analyses for lymph node status were carried out in three steps using logistic regression: (a) all factors were assessed separately and those with P < 0.05 were retained, (b) remaining pathologic and biomarker factors were entered into two separate models and backward elimination was applied with P = 0.05, and (c) remaining factors were entered into a single model and backward elimination was applied to produce a final model. Multivariable analyses for overall survival were carried out in a similar fashion using Cox's proportional hazards model. The discriminatory ability of this model was quantified using Harrell's c-index (37), which is analogous to the receiver operating characteristic area and gives the probability that two randomly selected patients have concordant predictions and survival times. The c-index takes values between 0.5 (random predictions) and 1 (perfect concor-

dance). Patients were divided into tertile model-based risk groups and labeled as low, medium, and high risk for disease progression. Patients with incomplete data were excluded from multivariable analyses. All tests were two sided and used a significance level of 0.05 with 95% confidence intervals (95% CI), and no allowances were made for multiple hypothesis testing. All analyses were done using Stata 10 for Windows (StataCorp).

**Results**

**RLF expression in normal, dysplastic, and malignant penile squamous epithelium.** Protein expression profiles for Mcm2, Ki67, and geminin were determined in benign, dysplastic, and malignant lesions of the penis (Fig. 1) using previously characterized monospecific antibodies against Mcm2, geminin, and Ki67 (14, 25, 34). In normal penile squamous epithelium, Mcm2, geminin, and Ki67 expression was restricted to the basal and suprabasal layers forming the transit-amplifying compartment. Cells in the superficial layers showed a fully differentiated phenotype with flattened morphology and showed low Mcm2, Ki67, and geminin LIs (<4%). In striking contrast, dysplastic lesions showed very high replication Mcm2, geminin, and Ki67

**Fig. 2.** The median (solid black line), interquartile range (boxed), and range (enclosed by lines) of Mcm2, Ki67, and geminin expression are shown according to tumor grade (outlying cases are shown by isolated points). The mean and interquartile range of Mcm2 and Ki67 levels increase with increasing grade compared with geminin.

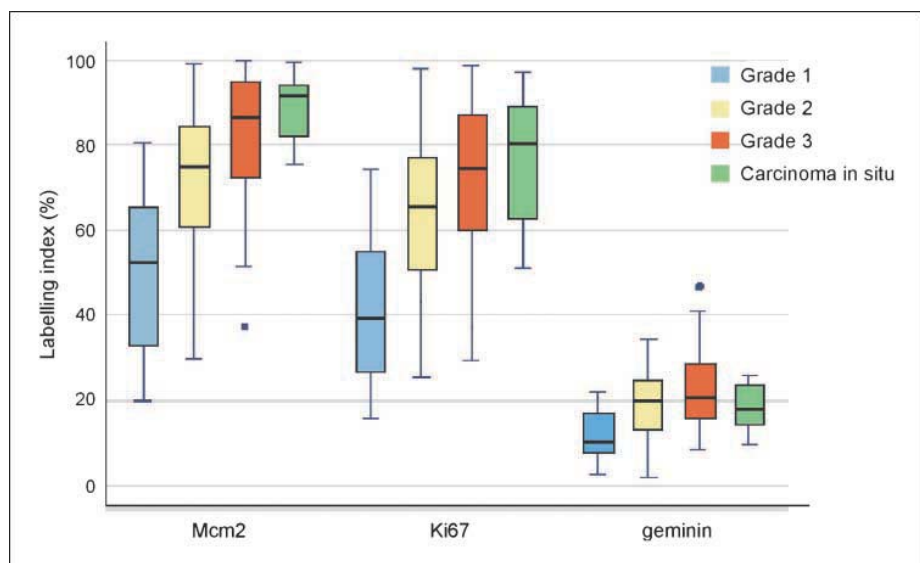


**Table 3.** Relationship between biomarker expression and clinicopathologic variables

	<i>n</i>	Mcm2	Ki67	Geminin	Mcm2/Ki67*	Geminin/Ki67 <sup>†</sup>	Ki67-geminin <sup>‡</sup>
<b>Tumor stage</b>							
T1	60	72 (57-91) <sup>§</sup>	62 (48-76)	16 (10-23)	1.11 (1.03-1.24)	0.27 (0.20-0.35)	45 (39-53)
T2	55	78 (63-90)	67 (51-83)	20 (12-26)	1.14 (1.06-1.26)	0.30 (0.25-0.39)	44 (31-59)
T3+4	14	78 (60-83)	66 (53-76)	20 (16-25)	1.14 (1.07-1.24)	0.33 (0.31-0.36)	44 (39-47)
<i>p</i> <sup>  </sup>		0.39	0.72	0.05	0.38	0.02	0.59
<b>Lymph node metastases</b>							
Absent	59	74 (59-83)	63 (47-77)	18 (11-24)	1.11 (1.04-1.22)	0.30 (0.24-0.37)	45 (29-53)
Present	37	82 (67-94)	70 (60-85)	23 (17-28)	1.10 (1.04-1.17)	0.33 (0.27-0.36)	50 (39-58)
<i>p</i> <sup>  </sup>		0.02	0.04	<0.01	0.56	0.30	0.10
<b>Distant metastases</b>							
Absent	96	75 (59-85)	65 (50-78)	18 (11-25)	1.12 (1.04-1.23)	0.30 (0.23-0.36)	45 (34-53)
Present	16	82 (72-93)	69 (60-83)	23 (15-27)	1.10 (1.06-1.16)	0.30 (0.27-0.36)	54 (39-58)
<i>p</i> <sup>  </sup>		0.09	0.16	0.14	0.83	0.56	0.23
<b>Subtype</b>							
Standard PeScc	87	74 (61-86)	60 (50-75)	18 (13-24)	1.14 (1.06-1.25)	0.30 (0.24-0.36)	44 (31-53)
Papillary	18	80 (61-95)	75 (53-86)	22 (14-28)	1.09 (1.03-1.20)	0.30 (0.25-0.36)	49 (39-62)
Basaloid	7	90 (81-99)	76 (64-87)	25 (15-28)	1.14 (1.02-1.27)	0.26 (0.24-0.38)	52 (49-54)
Verrucous + warty	6	38 (23-51)	31 (24-45)	7 (4-12)	1.22 (1.14-1.43)	0.26 (0.11-0.36)	23 (21-35)
Mixed	11	81 (71-98)	68 (55-91)	17 (11-28)	1.09 (1.04-1.22)	0.26 (0.16-0.32)	47 (39-61)
<i>p</i> <sup>**</sup>		<0.01	<0.01	0.03	0.59	0.70	<0.01
<b>Size (cm)</b>							
≤2	45	71 (57-78)	60 (47-69)	17 (9-21)	1.14 (1.04-1.24)	0.25 (0.18-0.34)	44 (33-49)
>2	60	81 (64-94)	71 (54-84)	22 (15-28)	1.12 (1.06-1.20)	0.31 (0.27-0.38)	46 (35-58)
<i>p</i> <sup>  </sup>		<0.01	0.02	<0.001	0.82	<0.01	0.18
<b>Depth of invasion (mm)</b>							
≤5	58	74 (61-92)	60 (49-76)	17 (10-22)	1.14 (1.04-1.27)	0.27 (0.20-0.35)	45 (36-57)
6-10	27	76 (58-88)	70 (46-83)	20 (9-29)	1.10 (1.07-1.19)	0.29 (0.24-0.42)	44 (31-54)
10-20	17	74 (60-83)	67 (55-76)	21 (14-24)	1.10 (1.00-1.16)	0.32 (0.29-0.35)	46 (39-55)
≥20	11	82 (71-94)	70 (61-84)	22 (17-28)	1.12 (1.06-1.24)	0.35 (0.28-0.41)	47 (39-57)
<i>p</i> <sup>  </sup>		0.82	0.25	0.02	0.31	0.03	0.82

NOTE: LI (expressed as percentages). *n* = 129.

\*Mcm2/Ki67 indicates the ratio of licensed to actively proliferating cells.

<sup>†</sup>Geminin/Ki67 indicates the relative length of G<sub>1</sub> phase.

<sup>‡</sup>Ki67-geminin represents the percentage of cells that are transiting G<sub>1</sub>.

<sup>§</sup>Median (interquartile range).

<sup>||</sup>Jonckheere-Terpstra test.

<sup>††</sup>Mann-Whitney test.

<sup>\*\*</sup>Kruskal-Wallis test.

expression throughout the full thickness of the epithelium, reflecting an expanded proliferative compartment and arrested differentiation (Fig. 1). As expected, penile cancers showed high levels of Mcm2, geminin, and Ki67 expression, indicative of a hyperproliferative state (Fig. 1).

**Relationship between RLF expression, DNA ploidy, and clinicopathologic characteristics.** Mcm2, geminin, and Ki67 LIs were highly significantly associated with tumor grade, with more poorly differentiated tumors showing a higher LI (all *P* < 0.0001; Table 2). Median Mcm2 expression was greater than median Ki67 expression, with both biomarkers mapped over a broad range within each tumor grade (Fig. 2). Mcm2 and Ki67 levels were higher than geminin expression in these tumors, reflecting the lower growth fraction identified by geminin, which is only present during S-G<sub>2</sub>-M (14). There was strong correlation between all biomarkers tested, highlighted by the high concordance between Mcm2 and Ki67 LIs (Pearson coefficient  $\rho$  = 0.87), consistent with their linkage to the cell division cycle. The Ki67-geminin score was associated with an increase in tumor grade (*P* < 0.0001), indicative of an increase in the number of cells transiting G<sub>1</sub> phase (11, 27). Thus, the proportion of tumor cells actively cycling increases with increasing grade. There was little evidence, however, of an increase in

the geminin/Ki67 ratio with increasing grade. This ratio is an indicator of the relative length of G<sub>1</sub> phase, and the results suggest that increased recruitment of cells into the cell division cycle was not linked to accelerated cell cycle progression as seen in other tumor types (e.g., epithelial ovarian cancer; ref. 25). There was evidence of a trend for decreasing "Mcm2/Ki67" ratio with increasing grade (*P* = 0.09), reflecting a shift in the proportion of nonproliferating cells that are licensed for DNA replication in well-differentiated tumors to a population of actively cycling cells in poorly differentiated tumors (25–27, 34).

We observed an association between both high geminin LI and an increase in the geminin/Ki67 ratio with advanced tumor growth. An increase in these indices is indicative of accelerated cell cycle transit and was linked to increasing tumor stage (geminin, *P* = 0.05; geminin/Ki67, *P* = 0.02) and depth of invasion (geminin, *P* = 0.02; geminin/Ki67, *P* = 0.03; Table 3). Furthermore, we noted a significant association between increased biomarker expression and geminin/Ki67 ratio with increasing tumor size (Mcm2, *P* < 0.01; Ki67, *P* = 0.02; geminin, *P* < 0.001; geminin/Ki67, *P* < 0.01; Table 3). Thus, larger tumors contain a greater proportion of cycling cells and this increased growth fraction is also coupled to accelerated cell cycle transit. Interestingly, a strong



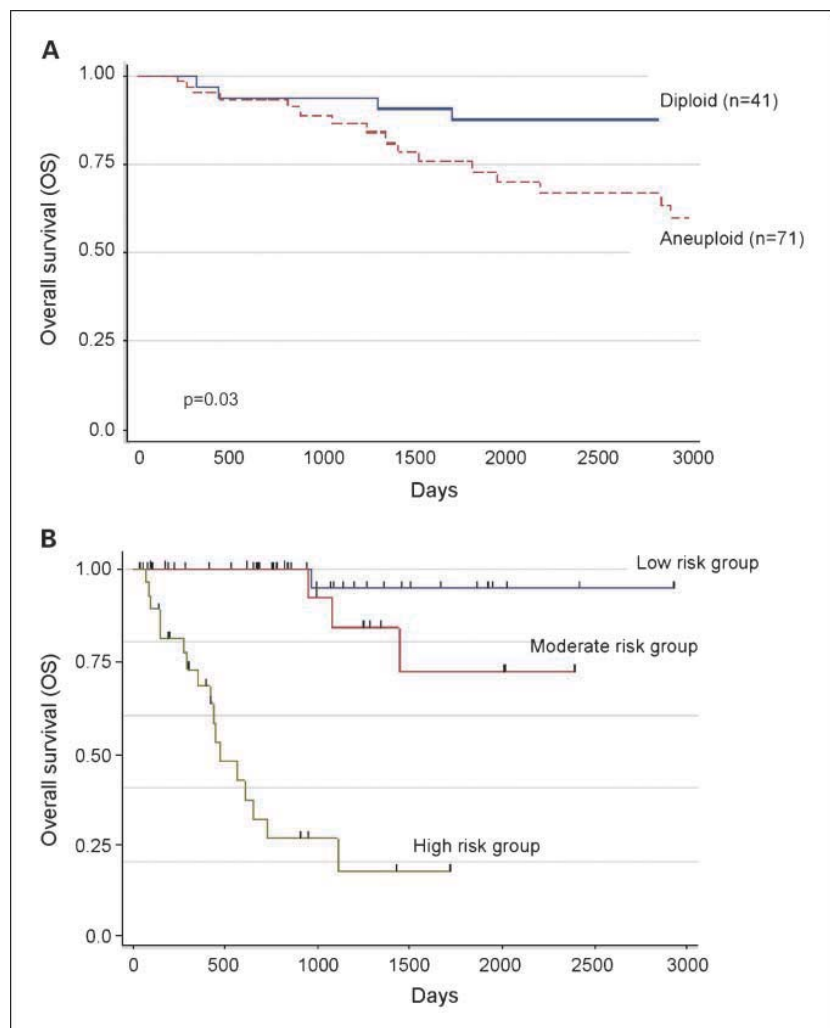
association was found for increased Mcm2, Ki67, and geminin expression with aggressive tumor subtypes (Table 3). Previous research has shown that verrucous and warty tumors behave in a biologically indolent fashion with low risk for disease progression compared with more aggressive variants, such as papillary and basaloid tumors, which are associated with poorer clinical outcomes (38). We observed that low-risk tumors were significantly associated with lower Ki67 and RLF expression, with the lower geminin and Ki67-geminin scores indicating smaller numbers of cells transiting S-G<sub>2</sub>-M and G<sub>1</sub> phase, respectively, when compared with aggressive papillary and basaloid tumors. The subtypes associated with poorer clinical outcome therefore displayed a more aggressive cell cycle phenotype.

We next sought to investigate the relationship between RLF expression, anaplasia (arrested differentiation), and tumor DNA ploidy in our study cohort. Tumors showing increasing anaplasia also strongly exhibited aneuploidy as determined by image cytometry ( $P < 0.0001$ ; Supplementary Table S1; Supplementary Fig. S1), suggesting that arrested differentiation and aneuploidy are linked in PeSCC. Moreover, the subset of aneuploid tumors was significantly linked to increased Mcm2, geminin, and Ki67 expression ( $P \leq 0.01$ ); a decreased Mcm2/Ki67

ratio ( $P = 0.03$ ); and increased Ki67-geminin score ( $P = 0.01$ ; Supplementary Table S2), indicating an increased proportion of actively cycling tumor cells in aneuploid tumors compared with diploid tumors. Interestingly, further analysis revealed a significant association between aneuploidy and the development of distant metastases ( $P = 0.04$ ).

To investigate the correlation of RLF expression and locoregional disease progression, protein expression profiles for each biomarker were compared with lymph node status (positive/negative) using logistic regression. Ninety-six men with recorded outcomes for these variables were analyzed, with 37 men (38.5%) identified with positive locoregional disease. In univariate analysis, Mcm2 ( $P = 0.02$ ), geminin ( $P = 0.02$ ), and Ki67 ( $P = 0.03$ ) expression were all significant predictors of nodal status. Tumor grade ( $P = 0.02$ ) and stage ( $P < 0.01$ ), presence of vascular invasion ( $P = 0.04$ ), and ploidy status ( $P = 0.03$ ) were also predictive of nodal status, with poorly differentiated tumors [odds ratio (OR), 8.76; 95% CI, 1.80-42.73], high-stage disease (OR, 4.80; 95% CI, 1.81-12.74), presence of vascular invasion (OR, 2.66; 95% CI, 1.04-6.75), and aneuploidy (OR, 2.96; 95% CI, 1.09-8.01) closely linked to advanced disease with regional lymph node involvement. Multivariate analyses were

**Fig. 3.** Kaplan-Meier survival curves showing cumulative overall survival across the whole series. **A**, aneuploid tumors show significantly poorer overall survival (HR, 4.19; 95% CI, 1.17-14.95;  $P = 0.03$ ; log-rank test  $P < 0.004$ ). **B**, tertile risk groups based on calculated prognostic index (low-risk prognostic index  $< 4.4$ ; intermediate risk  $4.4 <$  prognostic index  $< 6.2$ ; high-risk prognostic index  $> 6.2$ ) using independent predictive factors for overall survival (Harrell's c-index = 0.88; log-rank test  $P < 0.001$ ).





used to construct a final model using these factors. After backward elimination, biomarker information (Mcm2, Ki67, or geminin LI), vascular invasion, and ploidy status were excluded from the final analysis. Tumor grade ( $P = 0.006$ ) and local stage ( $P = 0.003$ ) were independent predictors of positive lymph node disease (Supplementary Table S3). The area under the receiver operating characteristic curve for this model was 0.78 (95% CI, 0.69–0.87). Although all biomarkers were predictive markers in univariate analysis, no single biomarker was a significant predictor after adjustment for grade and stage. This is due in part to the significant associations between biomarker LI and tumor grade and stage, making it difficult to separate their independent effects.

**RLF expression, DNA ploidy, tumor characteristics, and overall survival.** Next, we investigated the survival time for patients with PeScc using Cox's proportional hazards model. The study group for the analysis included 118 men with a recorded survival time. Of these, 26 patients were dead (22%) and 92 were alive (78%) at the time of analysis. Univariate analysis showed that Mcm2 ( $P = 0.02$ ) and Ki67 ( $P = 0.04$ ) expression and Ki67-geminin score ( $P = 0.03$ ) were all significantly associated with overall survival. Age ( $P = 0.002$ ), tumor stage ( $P = 0.02$ ), depth of invasion ( $P < 0.0001$ ), tumor multifocality ( $P = 0.002$ ), vascular invasion ( $P = 0.04$ ), and ploidy status ( $P = 0.008$ ) were also predictive of overall survival outcomes. Advanced age [hazard ratio (HR), 1.05 per year; 95% CI, 1.02–1.1], higher-stage tumors (HR, 3.89; 95% CI, 1.52–9.99), multifocal tumors (HR, 3.69; 95% CI, 1.63–8.32), increased depth of invasion (HR, 1.045; 95% CI, 1.025–1.064), presence of vascular invasion (HR per mm, 2.23; 95% CI, 1.02–4.87), and aneuploidy (HR, 4.28; 95% CI, 1.46–12.58) were associated with a significantly shorter overall survival time. It was also noted that lymph node status (negative or positive) was an excellent prognostic factor on univariate analysis (HR, 11.07; 95% CI, 3.74–32.71), in keeping with previous reports (5, 6). Notably, tumor grade failed to predict outcome in this series ( $P = 0.28$ ), emphasizing the limitations with current grading systems. Multivariate analyses were used to construct a final model involving 84 patients (Supplementary Tables S3–S7). Backward elimination resulted in the exclusion of biomarker information (Mcm2, Ki67, or geminin LI), vascular invasion, local tumor stage, and depth of invasion from the final model. However, age ( $P = 0.004$ ), lymph node status ( $P < 0.001$ ), tumor multifocality ( $P = 0.002$ ), and aneuploidy ( $P = 0.03$ ) were identified as independent predictors of overall survival (Supplementary Table S8). We quantified the discriminatory ability of this model using Harrell's c-index. In isolation, these predictors have c-index values of 0.77 (lymph node status), 0.68 (age), 0.65 (aneuploidy), and 0.64 (multifocality). The multivariable model has a c-index of 0.88. Kaplan-Meier curves (Fig. 3) show the survival advantages between patients with diploid versus aneuploid tumors and between tertile risk groups derived by splitting the patients into equal-sized groups based on their predicted risk from the model. Of the 26 deaths analyzed, 24 were cancer specific. We applied the same modeling methodology to cancer-specific survival, resulting in the same predictors having univariable associations that were significant at the 5% level. The same biomarker model was then selected (Mcm2 only) but ploidy status was omitted from the pathologic model (lymph node metastases, age, and extent were selected). The final model omitted Mcm2

(as before), leaving the predictors lymph node metastases, age, and extent (for HRs and  $P$  values for this model, see Supplementary Table S9).

## Discussion

In this study, we have assessed the utility of Mcm2 and geminin, alongside DNA ploidy status, as novel biological predictors of outcome in men with PeScc. Our results show that Mcm2 and geminin LIs and aneuploidy are prognostic indicators and predictors of locoregional metastasis. The inverse relationship between RLF expression and differentiation status recapitulates our findings in the *in vitro* HL60 monocyte/macrophage differentiation model system (18) and has been noted in several other malignancies (25–28, 34, 35, 39–46). This relationship reflects the mutually antagonistic circuits that control cell proliferation and differentiation in human cells and highlights the potential clinical utility of RLFs for improving current tumor grading systems (33). Our data show that analysis of RLFs and ploidy status in primary biopsy material from PeScc can provide important additional prognostic information and identify those tumors with an aggressive cell cycle phenotype, the latter characterized by an increased growth fraction [i.e., an increase in the numbers of cells traversing  $G_1$  (Ki67-geminin score) and S-G<sub>2</sub>-M phases (geminin LI)] and accelerated cell cycle transit (geminin/Ki67 LI; refs. 11, 25, 26, 28, 34). Notably, the aggressive tumor cell cycle phenotype was linked to increasing tumor size, stage, and depth of invasion and to morphologic subtypes associated with an adverse prognosis. The aggressive cell cycle phenotype was also linked to tumor ploidy status, suggesting that dysregulation of the DNA replication licensing pathway and cell cycle machinery is linked to the development of aneuploidy in PeScc. In addition, Mcm2, Ki67, and geminin LIs and aneuploidy were identified as significant predictors of locoregional metastasis, and aneuploidy was identified as a predictor of distant metastasis.

We have previously shown in the HL60 monocyte/macrophage differentiation model system that loss of proliferative capacity and cell cycle withdrawal following engagement of the somatic differentiation program is tightly coupled to downregulation of core constituents of the DNA replication licensing machinery, including the Mcm2-7 proteins (11, 18). This coupling between loss of proliferative capacity, cell cycle withdrawal, downregulation of the Mcm2-7 helicase complex, and differentiation has been observed in anal, bladder, cervical, colonic, esophageal, oral, pancreatic, and prostatic epithelia (28, 35, 39, 41, 42, 45–50). In normal stratified squamous penile epithelium, we observed downregulation of RLFs as cells exit the cell cycle and engage the somatic differentiation program. This seems to be a ubiquitous mechanism for lowering the proliferative capacity of cells in stem-transit–differentiating self-renewing tissue systems (11, 14, 18–20). In contrast, block to the differentiation program (arrested differentiation) that characterizes dysplastic (preinvasive) lesions is associated with persistent expression of MCM proteins even in surface epithelial layers, indicative of cells failing to withdraw from the cell cycle (11, 14, 18, 20, 45). As previously observed for dysplastic lesions of the cervix, esophagus, bladder, oral, and anal mucosa, high-level MCM expression was detected in penile dysplasia (11, 28, 35, 41, 42, 45, 48, 49). Surface sampling of penile lesions followed by immunoprecipitation

analysis for MCM proteins could therefore provide a rapid method for distinguishing benign hyperplastic lesions from dysplasia. This approach has already been exploited in screening for cervical cancer and detection of esophageal, lung, bladder, anal, and oral dysplasia (11, 42, 45).

Predictive nomograms for lymph node involvement and cancer-specific survival in PeSCC using traditional histopathologic information alone have been developed but require prospective validation (51, 52). In our study, Mcm2 and Ki67 IIs, Ki67-geminin score, age, tumor stage, depth of invasion, tumor extent, vascular invasion, and nodal and ploidy status were all identified as predictors of overall survival, with lymph node status, tumor extent, and ploidy status identified as independent predictors of overall survival. Interestingly, we have shown that these parameters can be incorporated into a simple prediction model to stratify patients into high-, intermediate-, and low-risk groups for disease progression in PeSCC. Notably, the multivariable model suggests that low-risk patients are at minimal risk of disease progression compared with men assigned to moderate- or high-risk groups. This is highlighted by overall survival rates at 3 years of 97%, 93%, and 27%, and 5-year survival figures of 97%, 72%, and 18%,

for low-, moderate-, and high-risk men, respectively. This provides a potentially powerful approach for early treatment stratification of patients, with low-risk patients assigned to surveillance programs, and targeting of high-risk patients with radical surgical and adjuvant chemotherapeutic interventions. Further studies in additional patient cohorts are now warranted to confirm the predictive power of this model in the risk stratification of PeSCC.

Inhibition of the DNA replication initiation machinery has been shown to provoke a cancer cell-specific apoptotic response as a result of the loss or impairment of a putative checkpoint for replication-competent origins during tumorigenesis (17, 53). Here, we have shown that increasing dysregulation of the DNA replication licensing pathway is linked to emergence of an aggressive cell cycle phenotype that affects the *in vivo* behavior of this tumor type. The DNA replication licensing pathway therefore seems to be also a potentially attractive therapeutic target in PeSCC.

### Disclosure of Potential Conflicts of Interest

No potential conflicts of interest were disclosed.

### References

- Parkin DM, Muir CS. Cancer incidence in five continents. Comparability and quality of data. IARC Sci Publ 1992;120:45-173.
- Burgers JK, Badalament RA, Drago JR. Penile cancer. Clinical presentation, diagnosis, and staging. Urol Clin North Am 1992;19:247-56.
- Horenblas S, van TH, Delemarre JF, Moonen LM, Lustig V, van Waardenburg EW. Squamous cell carcinoma of the penis. III. Treatment of regional lymph nodes. J Urol 1993;149:492-7.
- Kroon BK, Horenblas S, Lont AP, Tanis PJ, Gallee MP, Nieweg OE. Patients with penile carcinoma benefit from immediate resection of clinically occult lymph node metastases. J Urol 2005; 173:816-9.
- Ravi R. Correlation between the extent of nodal involvement and survival following groin dissection for carcinoma of the penis. Br J Urol 1993; 72:817-9.
- Ornellas AA, Kinchin EW, Nobrega BL, Wisnesky A, Koifman N, Quirino R. Surgical treatment of invasive squamous cell carcinoma of the penis: Brazilian National Cancer Institute long-term experience. J Surg Oncol 2008;97:487-95.
- Ravi R. Morbidity following groin dissection for penile carcinoma. Br J Urol 1993;72:941-5.
- Solsona E, Algaba F, Horenblas S, Pizzocaro G, Windahl T. EAU guidelines on penile cancer. Eur Urol 2004;46:1-8.
- Velazquez EF, Cubilla AL. Penile squamous cell carcinoma: anatomic, pathologic and viral studies in Paraguay (1993-2007). Anal Quant Cytol Histol 2007;29:185-98.
- Hegarty PK, Kayes O, Freeman A, Christopher N, Ralph DJ, Minhas S. A prospective study of 100 cases of penile cancer managed according to European Association of Urology guidelines. BJU Int 2006;98:526-31.
- Williams GH, Stoeber K. Cell cycle markers in clinical oncology. Curr Opin Cell Biol 2007;19: 672-9.
- Blow JJ, Hodgson B. Replication licensing—defining the proliferative state? Trends Cell Biol 2002;12:72-8.
- Bell SP, Dutta A. DNA replication in eukaryotic cells. Annu Rev Biochem 2002;71:333-74.
- Eward KL, Obermann EC, Shreeram S, et al. DNA replication licensing in somatic and germ cells. J Cell Sci 2004;117:5875-86.
- Wohlschlegel JA, Kutok JL, Weng AP, Dutta A. Expression of geminin as a marker of cell proliferation in normal tissues and malignancies. Am J Pathol 2002;161:267-73.
- Blow JJ, Dutta A. Preventing re-replication of chromosomal DNA. Nat Rev Mol Cell Biol 2005; 6:476-86.
- Blow JJ, Gillespie PJ. Replication licensing and cancer—a fatal entanglement? Nat Rev Cancer 2008;8:799-806.
- Barkley LR, Hong HK, Kingsbury SR, James M, Stoeber K, Williams GH. Cdc6 is a rate-limiting factor for proliferative capacity during HL60 cell differentiation. Exp Cell Res 2007;313: 3789-99.
- Kingsbury SR, Loddo M, Fanshawe T, et al. Repression of DNA replication licensing in quiescence is independent of geminin and may define the cell cycle state of progenitor cells. Exp Cell Res 2005;309:56-67.
- Stoeber K, Tlsty TD, Happerfield L, et al. DNA replication licensing and human cell proliferation. J Cell Sci 2001;114:2027-41.
- Stoeber K, Mills AD, Kubota Y, et al. Cdc6 protein causes premature entry into S phase in a mammalian cell-free system. EMBO J 1998;17: 7219-29.
- Baldwin P, Laskey R, Coleman N. Translational approaches to improving cervical screening. Nat Rev Cancer 2003;3:217-26.
- Kulkarni AA, Kingsbury SR, Tudzarova S, et al. Cdc7 kinase is a predictor of survival and a novel therapeutic target in epithelial ovarian carcinoma. Clin Cancer Res 2009;15:2417-25.
- Loddo M, Kingsbury SR, Rashid M, et al. Cell-cycle-phase progression analysis identifies unique phenotypes of major prognostic and predictive significance in breast cancer. Br J Cancer 2009;100:959-70.
- Kulkarni AA, Loddo M, Leo E, et al. DNA replication licensing factors and aurora kinases are linked to aneuploidy and clinical outcome in epithelial ovarian carcinoma. Clin Cancer Res 2007; 13:6153-61.
- Shetty A, Loddo M, Fanshawe T, et al. DNA replication licensing and cell cycle kinetics of normal and neoplastic breast. Br J Cancer 2005;93:1295-300.
- Dudderidge TJ, Stoeber K, Loddo M, et al. Mcm2, geminin, and Ki67 define proliferative state and are prognostic markers in renal cell carcinoma. Clin Cancer Res 2005;11:2510-7.
- Dudderidge TJ, McCracken SR, Loddo M, et al. Mitogenic growth signalling, DNA replication licensing, and survival are linked in prostate cancer. Br J Cancer 2007;96:1384-93.
- Wharton SB, Maltby E, Jellinek DA, et al. Subtypes of oligodendroglioma defined by 1p,19q deletions, differ in the proportion of apoptotic cells but not in replication-licensed non-proliferating cells. Acta Neuropathol 2007;113:119-27.
- Bild AH, Potti A, Nevins JR. Linking oncogenic pathways with therapeutic opportunities. Nat Rev Cancer 2006;6:735-41.
- Ludwig JA, Weinstein JN. Biomarkers in cancer staging, prognosis and treatment selection. Nat Rev Cancer 2005;5:845-56.
- Sobin LH, Wittekind C. TNM classification of malignant tumors. Oxford (UK): Wiley; 2002.
- Broders AC. Squamous-cell epithelioma of the skin: a study of 256 cases. Ann Surg 1921;73: 141-60.
- Wharton SB, Hibberd S, Eward KL, et al. DNA replication licensing and cell cycle kinetics of oligodendroglial tumours. Br J Cancer 2004;91: 262-9.
- Meng MV, Grossfeld GD, Williams GH, et al. Minichromosome maintenance protein 2 expression in prostate: characterization and association with outcome after therapy for cancer. Clin Cancer Res 2001;7:2712-8.
- Haroske G, Giroud F, Reith A, Bocking A. 1997 ESACP consensus report on diagnostic DNA image cytometry. Part I: basic considerations and recommendations for preparation, measurement and interpretation. European Society for Analytical Cellular Pathology. Anal Cell Pathol 1998;17: 189-200.
- Harell FE. Regression modeling strategies. Guildford (UK): Springer; 2001.
- Cubilla AL, Reuter VE, Gregoire L, et al. Basaloid squamous cell carcinoma: a distinctive human

- papilloma virus-related penile neoplasm: a report of 20 cases. *Am J Surg Pathol* 1998;22:755–61.
39. Ayaru L, Stoeber K, Webster GJ, et al. Diagnosis of pancreaticobiliary malignancy by detection of minichromosome maintenance protein 5 in bile aspirates. *Br J Cancer* 2008;98:1548–54.
40. Chatrath P, Scott IS, Morris LS, et al. Aberrant expression of minichromosome maintenance protein-2 and Ki67 in laryngeal squamous epithelial lesions. *Br J Cancer* 2003;89:1048–54.
41. Freeman A, Morris LS, Mills AD, et al. Minichromosome maintenance proteins as biological markers of dysplasia and malignancy. *Clin Cancer Res* 1999;5:2121–32.
42. Going JJ, Keith WN, Neilson L, Stoeber K, Stuart RC, Williams GH. Aberrant expression of minichromosome maintenance proteins 2 and 5, and Ki-67 in dysplastic squamous oesophageal epithelium and Barrett's mucosa. *Gut* 2002;50:373–7.
43. Gonzalez MA, Pinder SE, Callagy G, et al. Minichromosome maintenance protein 2 is a strong independent prognostic marker in breast cancer. *J Clin Oncol* 2003;21:4306–13.
44. Obermann EC, Eward KL, Dogan A, et al. DNA replication licensing in peripheral B-cell lymphoma. *J Pathol* 2005;205:318–28.
45. Williams GH, Romanowski P, Morris L, et al. Improved cervical smear assessment using antibodies against proteins that regulate DNA replication. *Proc Natl Acad Sci U S A* 1998;95:14932–7.
46. Williams GH, Swinn R, Prevost AT, et al. Diagnosis of oesophageal cancer by detection of minichromosome maintenance 5 protein in gastric aspirates. *Br J Cancer* 2004;91:714–9.
47. Stoeber K, Halsall I, Freeman A, et al. Immunoassay for urothelial cancers that detects DNA replication protein Mcm5 in urine. *Lancet* 1999;354:1524–5.
48. Stoeber K, Swinn R, Prevost AT, et al. Diagnosis of genito-urinary tract cancer by detection of minichromosome maintenance 5 protein in urine sediments. *J Natl Cancer Inst* 2002;94:1071–9.
49. Scarpini C, White V, Muralidhar B, et al. Improved screening for anal neoplasia by immunocytochemical detection of minichromosome maintenance proteins. *Cancer Epidemiol Biomarkers Prev* 2008;17:2855–64.
50. Torres-Rendon A, Roy S, Craig GT, Speight PM. Expression of Mcm2, geminin and Ki67 in normal oral mucosa, oral epithelial dysplasias and their corresponding squamous-cell carcinomas. *Br J Cancer* 2009;100:1128–34.
51. Ficarra V, Zattoni F, Artibani W, et al. Nomogram predictive of pathological inguinal lymph node involvement in patients with squamous cell carcinoma of the penis. *J Urol* 2006;175:1700–4.
52. Kattan MW, Ficarra V, Artibani W, et al. Nomogram predictive of cancer specific survival in patients undergoing partial or total amputation for squamous cell carcinoma of the penis. *J Urol* 2006;175:2103–8.
53. Jackson PK. Stopping replication, at the beginning. *Nat Chem Biol* 2008;4:331–2.



## Chapter 6

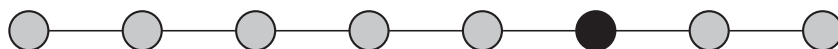
# Molecular architecture of the DNA replication origin activation checkpoint

S Tudzarova, MWB Trotter, A Wollenschlaeger, C Mulvey, J Godovac-Zimmermann, GH Williams, K Stoeber

EMBO Journal 2010 29 (19): 3381-3394.

Supplementary material related to this article is available online at:

<http://www.nature.com/emboj/journal/v29/n19/extref/emboj2010201s1.pdf>



## Molecular architecture of the DNA replication origin activation checkpoint

Slavica Tudzarova<sup>1</sup>, Matthew WB Trotter<sup>2</sup>, Alex Wollenschlaeger<sup>1</sup>, Claire Mulvey<sup>3</sup>, Jasminka Godovac-Zimmermann<sup>3</sup>, Gareth H Williams<sup>1,4,\*</sup> and Kai Stoeber<sup>1,4</sup>

<sup>1</sup>Wolfson Institute for Biomedical Research, University College London, London, UK, <sup>2</sup>Anne McLaren Laboratory for Regenerative Medicine and Department of Surgery, University of Cambridge, Cambridge, UK, <sup>3</sup>Division of Medicine, Centre for Molecular Medicine, University College London, London, UK and <sup>4</sup>Research Department of Pathology and UCL Cancer Institute, University College London, London, UK

**Perturbation of DNA replication initiation arrests human cells in G1, pointing towards an origin activation checkpoint. We used RNAi against Cdc7 kinase to inhibit replication initiation and dissect this checkpoint in fibroblasts. We show that the checkpoint response is dependent on three axes coordinated through the transcription factor FoxO3a. In arrested cells, FoxO3a activates the ARF-Hdm2-p53→p21 pathway and mediates p15<sup>INK4B</sup> upregulation; p53 in turn activates expression of the Wnt/β-catenin signalling antagonist Dkk3, leading to Myc and cyclin D1 downregulation. The resulting loss of CDK activity inactivates the Rb-E2F pathway and overrides the G1-S transcriptional programme. Fibroblasts concomitantly depleted of Cdc7/FoxO3a, Cdc7/p15, Cdc7/p53 or Cdc7/Dkk3 can bypass the arrest and proceed into an abortive S phase followed by apoptosis. The lack of redundancy between the checkpoint axes and reliance on several tumour suppressor proteins commonly inactivated in human tumours provides a mechanistic basis for the cancer-cell-specific killing observed with emerging Cdc7 inhibitors.**

*The EMBO Journal* (2010) **29**, 3381–3394. doi:10.1038/emboj.2010.201; Published online 20 August 2010

**Subject Categories:** signal transduction; genome stability & dynamics

**Keywords:** cell cycle; checkpoint; Dkk3; DNA replication origin; FoxO3A

### Introduction

An estimated 30 000 replication origins are spread along human chromosomes and it is understood that chromatin structure, adjacent sites of transcription and epigenetic parameters all affect origin selection (Mechali, 2001; Biamonti *et al.*, 2003). Initiation of DNA replication is a two-step process. In early G1, the origin recognition complex (ORC)

cooperates with Cdc6 and Cdt1 in loading the Mcm2–7 helicase to form a ‘licensed’ pre-replicative complex (pre-RC). In late G1, the origin is ‘fired’ by CDKs and Cdc7/Dbf4 kinase. Cdc7 phosphorylates the Mcm2, 4 and 6 subunits, thereby inducing a conformational change that stimulates MCM helicase activity and exposes a domain of Mcm5 required for Cdk2-dependent loading of Cdc45 and the replisome containing RPA, PCNA and DNA polymerase  $\alpha$ -primase (Sclafani and Holzen, 2007). In addition to its highly conserved function in origin firing, other, less well understood, functions have been reported for Cdc7 kinase. These include activation of the ATR-Chk1 pathway in response to DNA damage and DNA replication stress (Takeda *et al.*, 1999; Costanzo *et al.*, 2003; Dierov *et al.*, 2004; Tenca *et al.*, 2007; Kim *et al.*, 2008), cohesin loading onto chromatin required for chromosomal segregation in mitosis (Takahashi *et al.*, 2008), regulation of exit from mitosis (Miller *et al.*, 2009) and double-strand break formation during meiotic recombination (Matos *et al.*, 2008).

As the two-step-replication model excludes the formation of replication-competent origins once S phase has started, it has been argued on the basis of experimental evidence that a putative cell cycle checkpoint could delay progression from G1 into S phase if replication initiation is perturbed (Blow and Gillespie, 2008). In breast epithelial cells, for example, RNAi against *ORC2* impairs DNA replication, causing G1 arrest with low cyclin E-Cdk2 activity (Machida *et al.*, 2005). Inhibition of pre-RC assembly by overexpressing a stable form of geminin causes G1 arrest associated with low CDK activity in fibroblasts (Shreeram *et al.*, 2002). Blocking activation of the MCM helicase through RNAi against *CDC7* also causes G1 arrest in fibroblasts and leads to elevated p53 levels, p21 induction and hypo-phosphorylated Rb (Montagnoli *et al.*, 2004). These findings, therefore, suggest that somatic cells can respond directly to impairment of the DNA replication initiation machinery by blocking S phase entry (Blow and Gillespie, 2008). In contrast, inhibition of origin licensing or firing has been shown to cause apoptotic cell death in a range of different cancer cell lines. This is thought to arise as a result of transformed cells entering S phase with inadequate numbers of competent origins to complete chromosomal replication, arguing for loss of the putative origin activation checkpoint in cancer. As only a limited number of replication forks can be established when replication initiation is perturbed, it is plausible that apoptosis is triggered as a result of fork stalling/collapse in cancer cells with active intra S phase checkpoint mechanisms or mitotic catastrophe arising from partially replicated chromosomes in more transformed cells (Blow and Gillespie, 2008).

The cancer-cell-specific killing reported for emerging pharmacological Cdc7 inhibitors, while normal cells undergo a non-genotoxic G1 arrest, has generated widespread interest in small molecule inhibitors of the DNA replication initiation machinery (Jackson, 2008; Montagnoli *et al.*, 2008; Swords *et al.*, 2010). However, very little is known about the

\*Corresponding author. Wolfson Institute for Biomedical Research, University College London, The Cruciform Building, Gower Street, London WC1E 6BT, UK. Tel.: +44 20 7679 6304; Fax: +44 20 7388 4408; E-mail: gareth.williams@ucl.ac.uk

Received: 29 March 2010; accepted: 27 July 2010; published online: 20 August 2010



molecular architecture and circuitry of the proposed origin activation checkpoint on which tumour specificity is dependent. Here, we have used RNAi against *CDC7* to inhibit replication initiation and elucidate the molecular architecture of the checkpoint in human fibroblasts.

## Results

### ***Cdc7* depletion in IMR90 fibroblasts causes cell cycle arrest in G1**

We set out to determine whether *Cdc7* depletion can activate a checkpoint response to impaired DNA replication initiation by transfecting IMR90 cells with three different siRNAs with sequences corresponding to the *CDC7* cDNA. Notably, two of the *CDC7* siRNAs have been characterized in a previous study (Montagnoli *et al.*, 2004), whereas the third has been validated by the manufacturer (Ambion, Warrington, UK) (Supplementary Table 1 and Supplementary Figure 1A–D). All three oligos efficiently reduced *CDC7* mRNA levels (Supplementary Figure 1B). On the basis of the highest knock-down score and consistency in replicate experiments (Supplementary Figure 1B–D), oligo *CDC7*-A (referred to here as ‘*CDC7*-siRNA’) was used for all experiments shown, except those in which siRNA specificity was shown with an alternative siRNA (oligo *CDC7*-B).

Relative to control-siRNA (CO), transfection of IMR90 cells with *CDC7*-siRNA reduced *CDC7* mRNA levels by 65% 48 h post-transfection, by 85% at 72 h and by >95% at 96 h (Figure 1A). Correspondingly, in whole cell extracts (WCE), *Cdc7* protein levels started to fall by 24 h and were undetectable from 48 h until 120 h post-transfection (Figure 1B). Consistent with efficient *Cdc7* depletion, we noted a decrease in total Mcm2 protein levels and a shift from hyper-phosphorylated to slower migrating, hypo-phosphorylated Mcm2 isoforms (Montagnoli *et al.*, 2004) (Figure 1B). Downregulation of *Cdc7* expression caused a cessation of cell proliferation with cell numbers reaching a plateau 48 h post-transfection (Figure 1C). The majority of *CDC7*-siRNA-transfected cells accumulated with G1 DNA content. Although a small fraction of cells showed a G2/M DNA content, cells with less than 2C DNA content were not detected (Figure 1D), indicating that *Cdc7*-depleted cells remained viable. In cells that were synchronized by release from double thymidine block and directly transfected with *CDC7*-siRNA, the majority of cells again showed a G1 DNA content (90%), whereas the small G2/M peak noted for asynchronous cells (9%) was lost with remaining cells equally distributed between the S and G2/M fractions (5% each) (Figure 1E). To provide further evidence that *Cdc7* depletion is causing a G1 arrest, cells were transfected with *CDC7*-siRNA and control-siRNA, pulsed with BrdU and immunostained with anti-BrdU antibodies. In keeping with the cell cycle profile, the percentage of BrdU-incorporating cells dropped from 22% in cells transfected with control-siRNA (23% in untreated cells) to 2% in *Cdc7*-depleted cells (Figure 1F). Interestingly, 6 days after transfection with *CDC7*-siRNA, IMR90 cells re-expressed *Cdc7* and resumed cell proliferation, showing a degree of confluency seen in control cells (Supplementary Figure 1E–G).

To control for siRNA specificity, we studied an alternative *CDC7*-siRNA (oligo *CDC7*-B; Supplementary Table 1 and Supplementary Figure 1B and C) targeting a different

region of the transcript. Oligos *CDC7*-B and *CDC7*-A showed comparable gene silencing efficacy (mRNA and protein reduction) and induced similar phenotypic effects (accumulation of cells with G1 DNA content) (Figure 1; Supplementary Figure 2A and B). Moreover, rescue experiments were performed in which the RNAi effect was reversed through expression of a *CDC7* gene variant refractory to silencing by oligo *CDC7*-A. Under these conditions, IMR90 cells were able to recover from the cell cycle arrest caused by *Cdc7* depletion, as shown by flow cytometry and BrdU-incorporation data strongly resembling those of control cells (Supplementary Figure 3A–C). We, therefore, reasoned that *CDC7* oligos A and B are equivalent and that the cell cycle arrest phenotype directly correlates with *Cdc7* depletion and is unlikely to be due to concomitant non-specific downregulation of an unknown gene (off-target effects). Taken together, these data show that after *Cdc7* depletion diploid human fibroblasts arrest cell cycle progression in G1, remaining in a non-proliferative state from which they can re-enter the cell cycle after *Cdc7* levels have been restored.

### ***CDK activity and replication initiation factors are downregulated in response to Cdc7 depletion***

The Mcm2–7-replicative helicase is an important target for S phase-promoting kinases during origin activation, and the Mcm2 subunit, in particular, has been shown to be a substrate for both CDK and *Cdc7*. Phosphosites have been mapped in the N-terminal tail of Mcm2 for *Cdc7* (Ser-40, Ser-53 and Ser-108) and Cdk2 (Ser-13, Ser-27 and Ser-41) *in vitro* and *in vivo* (Montagnoli *et al.*, 2006). To test whether the *Cdc7*-depletion-induced checkpoint response involves downregulation of S phase-promoting CDK activity, we transfected IMR90 cells with *CDC7*-siRNA and studied Mcm2 phosphorylation at the mapped CDK and *Cdc7* phosphosites. In keeping with a previous study (Montagnoli *et al.*, 2004), *Cdc7* depletion caused a decrease in Mcm2 levels and reduced the electrophoretic mobility of the protein in polyacrylamide gels, showing the presence of hypo-phosphorylated Mcm2 isoforms (Figure 2A). Although Mcm2 total protein levels consistently dropped in *Cdc7*-depleted cells, the extent of Mcm2 reduction varied between experiments. The average reduction in the intensity of Mcm2 protein bands (relative to control-siRNA-transfected cells) was 45% at 48 h, 62% at 96 h and 76% at 120 h post-transfection (Image J densitometry analysis). Mcm2 Ser-40/41 and Ser-53 phosphorylation was abolished when *Cdc7* kinase was downregulated (48–120 h post-transfection), whereas phosphorylation at the CDK phosphosites Ser-27 and Ser-41 was significantly reduced after 96 h (Figure 2A). To confirm the loss of CDK activity in *Cdc7*-depleted cells, we carried out *in vitro* kinase assays with immunoprecipitated Cdk2 (Figure 2B). As expected, *in vitro* phosphorylated, recombinant truncated Rb protein was detected with an anti-Thr-821-phosphorylated Rb antibody in IMR90 and MDA-MB231 breast cancer cells (controls), but not in IMR90 cells transfected with *CDC7*-siRNA or treated with the CDK inhibitor roscovitine.

The decline in Mcm2 levels in *Cdc7*-depleted cells (Figure 2A) raises the possibility that perturbation of origin activation may result in downregulation of replication initiation factors and/or affect the stability on chromatin of pre-RCs already formed. To address this question, IMR90



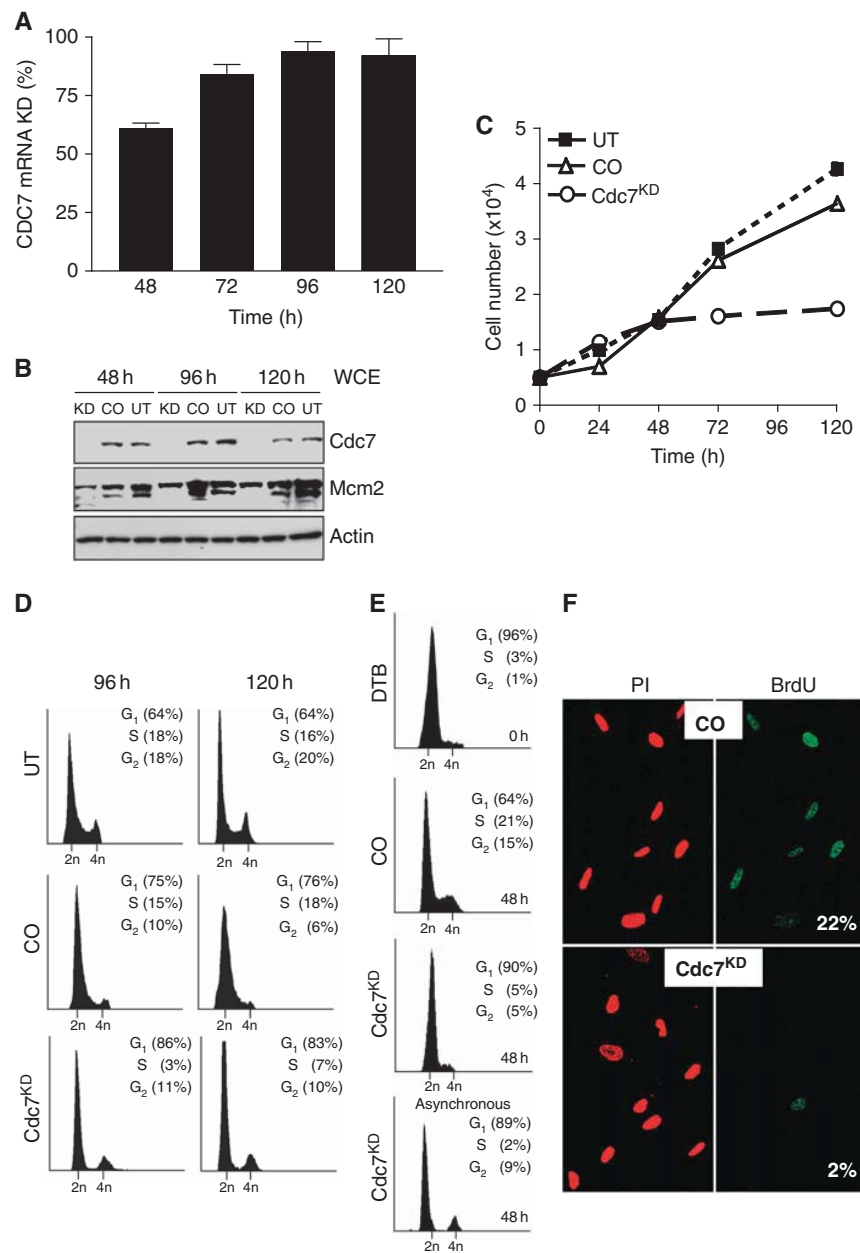


**Figure 1** Cdc7 depletion in IMR90 fibroblasts causes cell cycle arrest in G1. **(A)** Time course of CDC7 mRNA knock-down (KD) in IMR90 cells relative to cells transfected with control-siRNA (CO). **(B)** Whole cell extracts (WCE) prepared from untreated (UT), CO and Cdc7<sup>KD</sup> cells were analysed by immunoblotting with the indicated antibodies ( $\beta$ -actin—loading control). **(C)** At the indicated time points, cell number was measured in UT, CO and Cdc7<sup>KD</sup> cell populations. **(D)** DNA content of UT, CO and Cdc7<sup>KD</sup> cells at 96 and 120 h post-transfection. **(E)** DNA content of double thymidine-arrested cells (DTB), CO and Cdc7<sup>KD</sup> cells 48 h after release from double thymidine block and transfection, and asynchronous Cdc7<sup>KD</sup> cells 48 h post-transfection. **(F)** At 96 h post-transfection, cells were pulsed for 2 h with BrdU, fixed and detected with an FITC-conjugated anti-BrdU antibody. DNA was stained with propidium iodide (PI). Numbers show the percentage of cells incorporating BrdU.

cells transfected with CDC7- and control-siRNAs were biochemically fractionated into WCE and chromatin-bound fractions (CBF) and immunoblotted with antibodies against replication initiation factors (Figure 2C). Orc4 levels in untreated and siRNA-transfected cells did not vary over the course of the experiment. On the contrary, in Cdc7 depleted, but not control cells, protein levels of Cdc6, Cdt1, Mcm2, Dbf4, Mcm10 and Cdc45 were significantly downregulated, whereas levels of these replication initiation factors

associated with chromatin were also reduced. Notably, the DNA polymerase processivity factor PCNA was undetectable in CBF from Cdc7-depleted cells (Figure 2C).

Next, we sought to establish whether the Cdc7-depletion-induced checkpoint response involves any known cell cycle regulators of the G1-S transition. Compared with control cells, at 96 h post-transfection Cdc7-depleted cells showed a marked increase in cyclin E levels, whereas cyclin A levels were reduced below the detection limit (Figure 2D). The loss

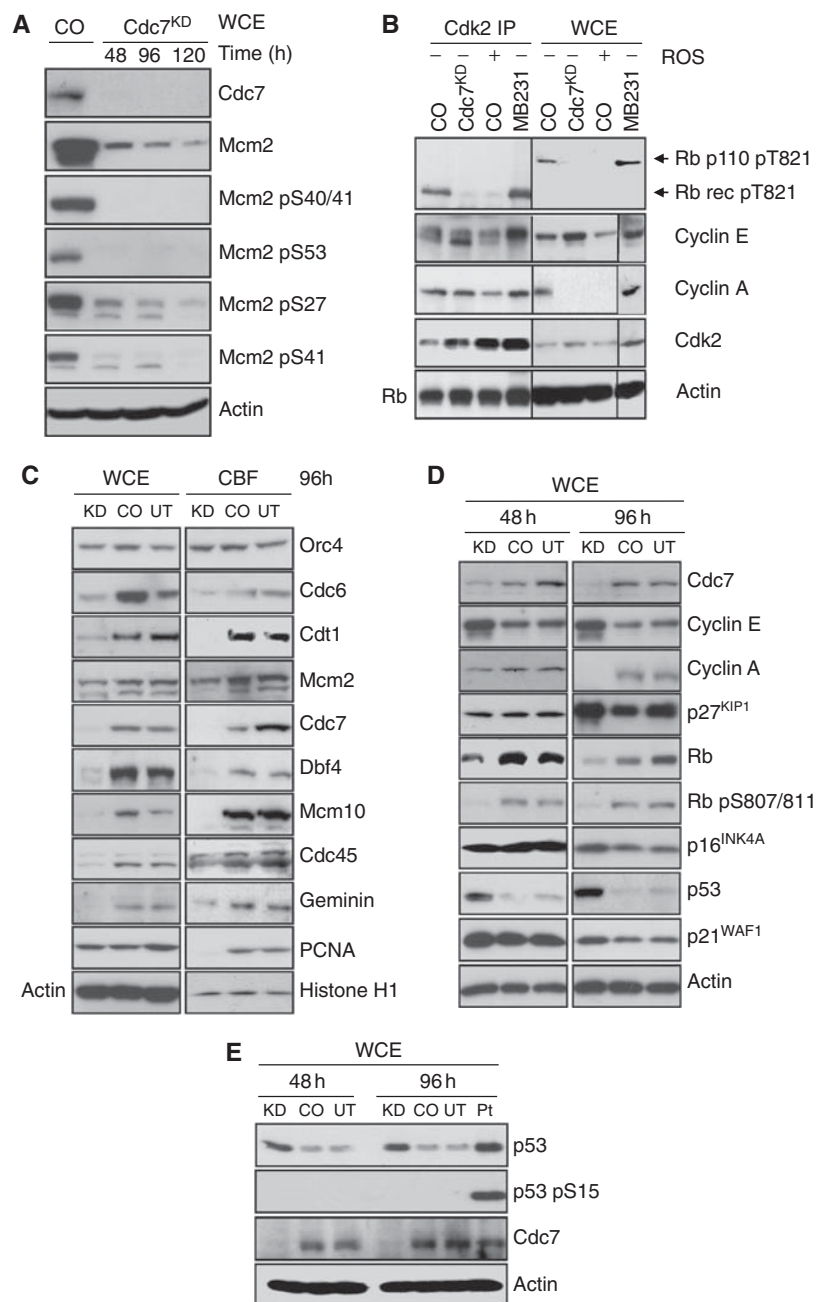


**Figure 2** CDK activity and replication initiation factors are downregulated in response to Cdc7 depletion. **(A)** WCE prepared from IMR90 cells transfected with control-siRNA (CO) and CDC7-siRNA (Cdc7<sup>KD</sup>) were analysed by immunoblotting with the indicated antibodies ( $\beta$ -actin—loading control). **(B)** WCE prepared from CO and Cdc7<sup>KD</sup> cell populations and from CO cells treated with 200  $\mu$ M roscovitine (ROS) for 24 h (negative control) and MDA-MB231 breast cancer cells (positive control) were immunoprecipitated with anti-cyclin A and anti-cyclin E antibodies. Cdk2 immunoprecipitates (Cdk2 IP) were subjected to an *in vitro* kinase assay using recombinant truncated Rb protein (p56) as substrate. *In vitro* phosphorylation was detected with a specific anti-Rb-phospho-Thr-821 antibody. Note that lanes 1–8 were run on the same polyacrylamide gel and proteins transferred to the same PVDF membrane by semi-dry electroblotting. The membrane was subsequently cut as indicated for optimized immunodetection. **(C)** WCE and chromatin-bound protein fractions (CBF) prepared from untreated (UT), CO and Cdc7<sup>KD</sup> cells (96 h post-transfection) were analysed by immunoblotting with the indicated antibodies ( $\beta$ -actin and histone H1—loading controls). **(D)** WCE from UT, CO and Cdc7<sup>KD</sup> cells (48 and 96 h post-transfection) were analysed by western blotting with the indicated antibodies ( $\beta$ -actin—loading control). **(E)** WCE from UT, CO and Cdc7<sup>KD</sup> cells (48 and 96 h post-transfection) and from cells treated for 24 h with 17  $\mu$ M cisplatin (Pt) were analysed by western blotting with the indicated antibodies ( $\beta$ -actin—loading control).

of cyclin A (Figure 2D) and lack of chromatin-bound PCNA (Figure 2C) further support the notion of a late G1 arrest in Cdc7-depleted cells. The Cdc7-depleted cells also showed early loss of Rb phosphorylation at Ser-807/811, thought to

be either Cdk4 or Cdk2 phosphorylation sites (Connell-Crowley *et al.*, 1997; Chi *et al.*, 2008), slightly raised p16 levels, p53 stabilization and increased levels of p21 (Figure 2D). Phosphorylation of p53 at Ser-15 (Figure 2E)

and Chk1 at Ser-345 (Supplementary Figure 4) was not detected in Cdc7-depleted or control cells, indicating that the ATM/ATR checkpoint pathways were not activated. These results show that Cdc7 depletion results in down-regulation of replication initiation factors and low CDK activity, consistent with the observed increase in p21 levels and the appearance of hypo-phosphorylated Rb.

#### ***Cdc7 depletion affects expression of genes required for cell cycle progression and proliferation***

To investigate signalling pathways affected by *CDC7* knock-down, we performed gene expression microarray (GEM) analysis on samples prepared from IMR90 cells transfected with *CDC7*-siRNA and control-siRNA (84 h post-transfection; see Supplementary Materials and Methods). Differentially regulated genes were analysed according to their membership of Kyoto Encyclopedia of Genes and Genomes human signalling pathways (Supplementary Table 2). The overall expression profile of genes in the cell cycle cluster was significantly altered between control cells and Cdc7-depleted cells ( $P < 0.0001$ ). Genes encoding Cdc6 and Mcm2-7, a number of mitosis regulatory factors, A-, B- and D-type cyclins, and Cdk1 and Cdk6 were all significantly downregulated in Cdc7-depleted cells, whereas *CDKN2B* (p15<sup>INK4B</sup>) was strongly upregulated (Supplementary Figure 5A). Genes in the p53 network cluster were also found to be differentially regulated ( $P < 0.0001$ ; Supplementary Figure 5B). The DNA damage checkpoint kinases ATM and ATR were strongly downregulated in Cdc7-depleted cells (Supplementary Figure 5B), consistent with the absence of p53 phosphorylation at Ser-15 (Figure 2E) and Chk1 phosphorylation at Ser-345 (Supplementary Figure 4). Although the pro-apoptotic genes *BAX* and *FAS* were upregulated, caspase 9 (*CASP9*) and caspase 3 (*CASP3*) were downregulated (Supplementary Figure 5B), suggesting that Cdc7 depletion may sensitize fibroblasts to pro-apoptotic signals, but does not activate the cell death effector machinery. Among p53-target genes, *SIAH1*, known to ubiquitinate  $\beta$ -catenin (Matsuzawa and Reed, 2001), and *Dickkopf* homolog 3 (*DKK3*), which blocks  $\beta$ -catenin accumulation in the nucleus (Wei *et al.*, 2006; Lee *et al.*, 2009), were strongly upregulated (Supplementary Figure 5B and C), pointing towards possible coupling between the p53 network and Wnt/ $\beta$ -catenin signalling pathway after *CDC7* knock-down. This supposition was further supported by the notion that the overall expression profile of genes in the Wnt-signalling cluster was significantly altered between control and Cdc7-depleted cells ( $P = 0.014$ ; Supplementary Table 2; Supplementary Figure 5C). The GEM data indicate that the Cdc7-depletion-induced checkpoint overrides the transcriptional programme in a way that tilts the balance in favour of cell cycle arrest and reduced competency for cell proliferation. The GEM data used here may be found in the Array Express data repository (<http://www.ebi.ac.uk/arrayexpress>) under accession number E-MEXP-2115.

#### ***The Cdc7-depletion-induced checkpoint is p53 dependent***

As the ATM/ATR checkpoint pathway does not appear to be active in Cdc7-depleted cells, we reasoned that the balance between Hdm2 and p14<sup>ARF</sup> may constitute the main mechanism for controlling p53 levels. Immunoblot analysis of nuclear extracts (NEs) prepared from Cdc7-depleted cells

confirmed an increase in ARF levels, which correlated with loss of Hdm2 and p53 stabilization (Supplementary Figure 6A). Hdm2 protein was also not detectable in nucleolar subfractions prepared from Cdc7-depleted cells (data not shown). In keeping with the biochemical data, Cdc7-depleted cells showed strong ARF immunostaining compared with control cells (Supplementary Figure 6B). Hdm2 transcript levels increased two-fold in Cdc7-depleted cells relative to control-transfected cells 72 h post-transfection and were comparable at later time points, arguing against transcriptional downregulation of Hdm2 because of siRNA off-target effects (Supplementary Figure 7). A previous study in dermal fibroblasts showed that the Cdc7-depletion-induced checkpoint is dependent on p53 (Montagnoli *et al.*, 2004). To confirm an active function for p53 in our experimental system, we used RNAi to downregulate p53 in IMR90 cells previously arrested by Cdc7 depletion (Supplementary Figure 8A). Notably, whereas Mcm2 phosphorylation at Ser-27 was abolished in Cdc7-depleted cells, phosphorylation at this mapped Cdk2 phosphosite was detectable in doubly depleted Cdc7/p53 cells. On the contrary, Mcm2 phosphorylation at the mapped Cdc7 phosphosite was strongly reduced in both Cdc7- and Cdc7/p53-depleted cells (Supplementary Figure 9). These data show that S phase-promoting CDK activity was restored in doubly depleted Cdc7/p53 cells. In keeping with the findings reported by Montagnoli *et al.*, doubly depleted Cdc7/p53 cells failed to arrest cell cycle progression and instead progressed through S/G2 (Supplementary Figure 6C and D). Failure to elicit the Cdc7-depletion-induced checkpoint under *CDC7* and *P53* double knock-down conditions, however, eventually resulted in apoptotic cell death (Supplementary Figure 6E and F). Interestingly, cytoplasmic protein fractions prepared from doubly depleted Cdc7/p53 cells revealed reduced levels of the  $\beta$ -catenin antagonist Dkk3 (Supplementary Figure 6G), supporting the notion of possible coupling between the p53 network and Wnt/ $\beta$ -catenin signalling pathway after Cdc7 depletion (Supplementary Table 2 and Supplementary Figure 5B and C). Note that in keeping with a previous report (Hsieh *et al.*, 2004), peptide blocking and N-glycanase treatment identified the different bands detected with Dkk3 antibody as N-glycosylated Dkk3 isoforms (Supplementary Figure 10).

#### ***The Cdc7-depletion-induced checkpoint is dependent on p53 activity upstream of Wnt/ $\beta$ -catenin signalling antagonist Dkk3 to downregulate Myc and cyclin D1 expression***

Dkk3 is known to block nuclear accumulation of  $\beta$ -catenin (Lee *et al.*, 2009), resulting in downregulation of its downstream targets including *CCND1* (cyclin D1) and *MYC* (Clevers, 2006). As *DKK3* upregulation in Cdc7-depleted cells is dependent on p53 (Supplementary Figures 5C and 6G), we reasoned that p53 may affect cell cycle progression by indirectly blocking Wnt/ $\beta$ -catenin signalling. Indeed, immunoblot analysis of cytoplasmic fraction (CF) and NE prepared from Cdc7-depleted cells showed reduced nuclear  $\beta$ -catenin and low Myc and cyclin D1 levels in conjunction with an increase in the inducible, faster migrating isoform of Dkk3 (Figure 3A). Consistent with the biochemical data, Cdc7-depleted cells showed only weak Myc and cyclin D1 immunostaining compared with control cells (Figure 3B). Notably, inducible Dkk3 expression and reduced nuclear

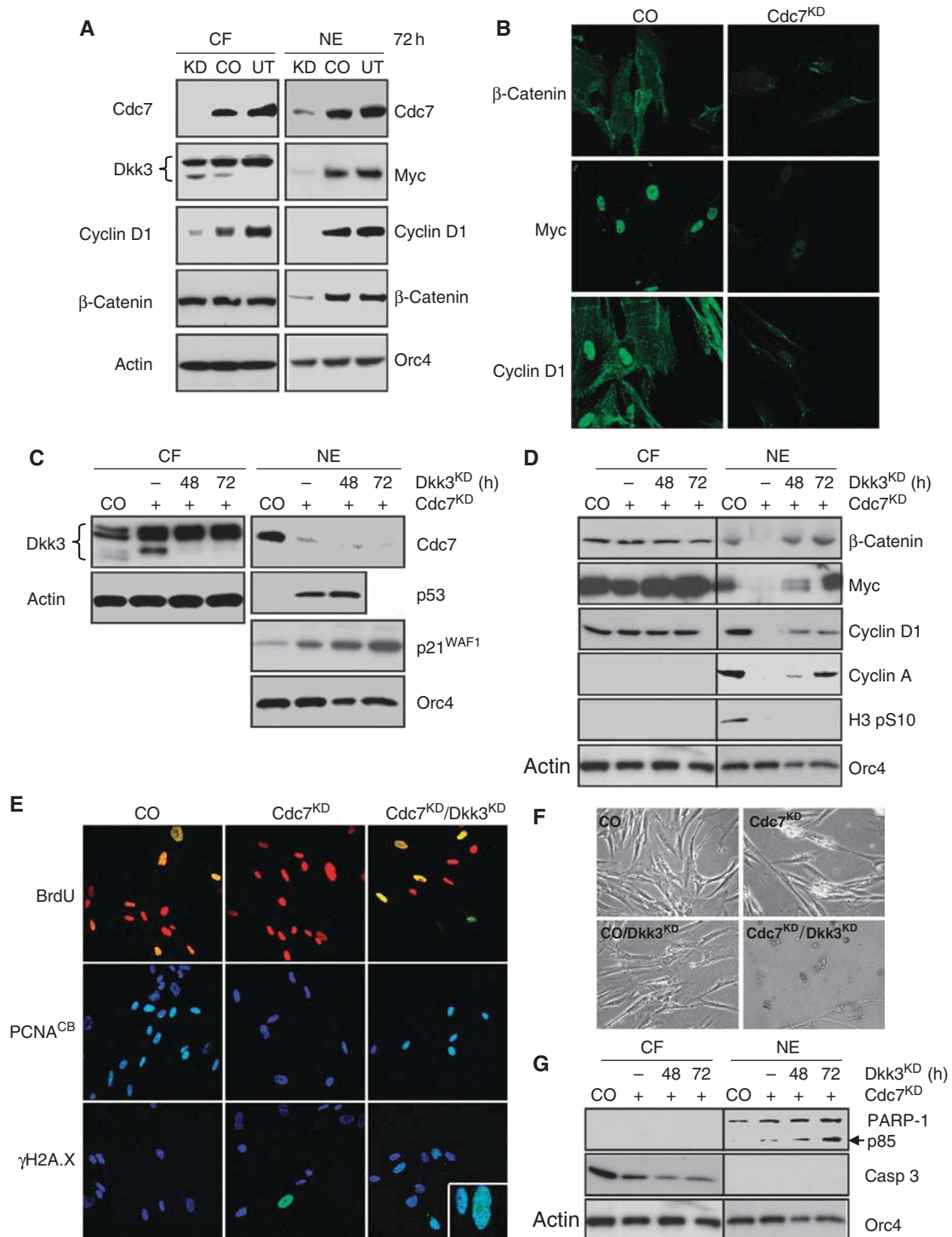


**Figure 3** p53-dependent upregulation of Wnt/β-catenin signalling antagonist Dkk3 is required for Cdc7-depletion-induced cell cycle arrest. (A) Cytoplasmic protein fractions (CF) and crude nuclear extracts (NE) from untreated (UT), control-siRNA (CO) and CDC7-siRNA (Cdc7<sup>KD</sup>)-transfected IMR90 cells (72 h post-transfection) were analysed by immunoblotting with the indicated antibodies (β-actin and Orc4—loading controls). (B) At the same time point, CO and Cdc7<sup>KD</sup> cells were fixed and β-catenin, Myc and cyclin D1 detected by indirect immunofluorescence using a fluorescein-labelled secondary antibody. (C, D) CF and NE samples prepared from CO, Cdc7<sup>KD</sup> and doubly depleted Cdc7/Dkk3 (Cdc7<sup>KD</sup>/Dkk3<sup>KD</sup>) cells 48 and 72 h post-transfection were analysed by immunoblotting with the indicated antibodies. (E) 72 h post-transfection CO, Cdc7<sup>KD</sup> and Cdc7<sup>KD</sup>/Dkk3<sup>KD</sup> cells were pulsed for 2 h with BrdU, fixed and detected with an FITC-conjugated anti-BrdU antibody. Chromatin-bound PCNA and γH2A.X (inset: higher magnification) were detected by indirect immunofluorescence with anti-PCNA and anti-γH2A.X antibodies and a fluorescein-labelled secondary antibody. DNA was stained with propidium iodide (BrdU) or DAPI (PCNA and γH2A.X). Apoptotic cell death was detected in doubly depleted Cdc7<sup>KD</sup>/Dkk3<sup>KD</sup> cells by (F) phase contrast microscopy and by (G) immunoblot analysis of CF and NE with the indicated antibodies (β-actin and Orc4—loading controls).



$\beta$ -catenin and cyclin D1 protein levels were not detected in IMR90 cells arrested through specific activation of the p53 pathway by low dose actinomycin D (Choong *et al.*, 2009) (Supplementary Figure 11), further supporting a close relationship between p53-dependent *Dkk3* upregulation and DNA replication control.

To directly test whether the p53  $\rightarrow$  Dkk3- $\beta$ -catenin axis is essential for the checkpoint response, we downregulated *Dkk3* through RNAi in IMR90 cells previously arrested by *Cdc7* depletion (Supplementary Figure 8B). Immunoblot analysis of CF and NE prepared at 48 and 72 h post-transfection shows loss of the inducible form of *Dkk3* in the *Cdc7*-depleted background and confirms maintenance of elevated p53 and p21 levels (Figure 3C). Note that downregulation of the slower migrating, heavily glycosylated *Dkk3* isoforms (upper bands) only occurs at later time points (Supplementary Figure 10B and C). *Cdc7* depletion alone diminished the pool of nuclear  $\beta$ -catenin and reduced Myc and cyclin D1 levels (Figure 3D). As expected, this resulted in G1 arrest as shown by cells failing to incorporate BrdU (Figure 3E), loss of chromatin-bound PCNA (Figure 3E) and cyclin A and histone H3 Ser-10 phosphorylation becoming undetectable (Figure 3D). Importantly, in doubly depleted *Cdc7/Dkk3* cells, nuclear levels of  $\beta$ -catenin, Myc and cyclin D1 were restored 72 h post-transfection (Figure 3D). In contrast to *Cdc7*-depleted cells, doubly depleted *Cdc7/Dkk3* cells did not arrest in G1 and instead progressed into S phase, as shown by high levels of chromatin-bound PCNA (Figure 3E), BrdU incorporation (Figure 3E), cyclin A detection (Figure 3D) and flow cytometry (Supplementary Figure 12C). Notably, doubly depleted *Cdc7/Dkk3* cells exhibited  $\gamma$ H2A.X immunostaining indicative of double-strand breaks (Figure 3E) and did not appear to progress to G2/M as shown by the lack of histone H3 Ser-10 phosphorylation (Figure 3D). Induction of apoptosis in doubly depleted *Cdc7/Dkk3* cells was confirmed morphologically (Figure 3F), through detection of caspase 3 activation and PARP-1 cleavage (Figure 3G), and by flow cytometric detection of cells with less than 2C DNA content (Supplementary Figure 12C). These results show that *Dkk3*-mediated downregulation of Myc and cyclin D1, critical components of the cell cycle engine required for progression through G1 phase, is essential for a functioning origin activation checkpoint.

**The Forkhead transcription factor FoxO3a coordinates the ARF/Hdm2/p53  $\rightarrow$  p21, p53  $\rightarrow$  Dkk3- $\beta$ -catenin and p15<sup>INK4B</sup>-cyclin D-CDK axes of the origin activation checkpoint**

*Cdc7*-depleted IMR90 cells showed six-, seven- and four-fold increases in *CDKN2A* (ARF), *CDKN2B* (p15) and *CDKN1B* (p27) mRNA transcript levels (Supplementary Figure 13A). As FoxO3a can mediate the expression of all three of these cell cycle regulatory genes in response to different stimuli (Brunet *et al.*, 1999; Bouchard *et al.*, 2007; Katayama *et al.*, 2008), we hypothesized that this transcription factor could represent an important node in the *Cdc7*-depletion-induced origin activation checkpoint. Immunoblot analysis showed a pool of FoxO3a present in the cytoplasm of untreated control cells and revealed nuclear accumulation of FoxO3a in *Cdc7*-depleted cells (Figure 4A). Concurrent with the nuclear accumulation of FoxO3a in *Cdc7*-depleted cells, we noted an increase in nuclear ARF, p53 and p21 levels and in nuclear

and cytoplasmic p15 and p27 levels (Figure 4A). Protein levels of these cell cycle regulators were not raised and *Dkk3* expression was not induced in synchronized late G1 phase control-transfected IMR90 cells or in the G1 DNA content fraction collected by one-way sorting of propidium iodide (PI)-stained control cells (Supplementary Figure 14). Hence, the observed increase in checkpoint protein levels is not an indirect consequence of cell cycle position. Co-knock-down of *CDC7* and *FOXO3A* (Supplementary Figure 8C) reduced *CDKN2A* mRNA levels by 89%, *CDKN2B* levels by 85% and *CDKN1B* levels by 50% compared with *CDC7* knock-down alone (Supplementary Figure 13B). Concordantly, ARF became undetectable by western blotting and p53, p15, p21 and p27 were reduced to background levels seen in untreated control cells (Figure 4A). When expression of these proteins was compared in *Cdc7*-depleted and oxidatively stressed cells (note that reactive oxygen species are known regulators of FoxO family members), p53, p21, p15 and p27 upregulations were found in both cell populations, whereas increased ARF levels and inducible *Dkk3* expression were restricted to *Cdc7*-depleted cells (Supplementary Figure 15). This suggests that inducible ARF and *Dkk3* expression are more specific events associated with DNA replication control, whereas p15 and p27 upregulation in *Cdc7*-depleted-arrested cells overlaps with a common FoxO-induced cell cycle arrest pathway. Taken together, these expression profiles support the supposition that triggered by impaired origin activation FoxO3a may, either directly through transcriptional mechanisms or indirectly, mediate the expression of *Dkk3*, INK4 and CIP/KIP CDK inhibitors.

We reasoned that if the origin activation checkpoint is dependent on FoxO3a, doubly depleted *Cdc7/FoxO3a* cells should bypass the cell cycle blockade and progress into S phase. As predicted, flow cytometric analysis of doubly depleted *Cdc7/FoxO3a* cells 48 h post-transfection revealed a small S phase population, a marginally increased fraction of cells with G2/M DNA content and a large population of cells with less than 2C DNA content (Figure 4B). The notion that doubly depleted *Cdc7/FoxO3a* cells had progressed into S phase was further supported by positive immunostaining for chromatin-bound PCNA and detection of BrdU incorporation (Figure 4C). Notably, doubly depleted *Cdc7/FoxO3a* cells incorporated only low levels of BrdU into DNA (Figure 4C, insert) and showed strong immunostaining of the  $\gamma$ H2A.X surrogate marker for DNA fragmentation (Figure 4C). Induction of apoptosis was confirmed by flow cytometry (Figure 4B), morphologically (Figure 4D), and through detection of caspase 3 activation and PARP-1 cleavage (Figure 4E).

In *Cdc7*-depleted cells, p15 expression is strongly upregulated at both transcriptional (Supplementary Figure 13A) and protein level (Figure 5A and B). By binding to and inhibiting cyclin D-CDK4/6 complexes, p15 may inactivate the CDK-Rb-E2F pathway in *Cdc7*-depleted cells, which could be critical for shifting the balance between growth-promoting and anti-proliferative signals in favour of cell cycle arrest. To address this question, we downregulated p15 in IMR90 cells previously arrested by *Cdc7* depletion (Supplementary Figure 8D). Immunoblot analysis shows knock-down of p15 expression in the *Cdc7*-depleted background (Figure 5C). In contrast to *Cdc7*-depleted cells arresting in G1, doubly depleted *Cdc7/p15* cells entered S phase despite elevated p53 and p21 levels as shown by flow cytometry (Supplementary Figure 12D),

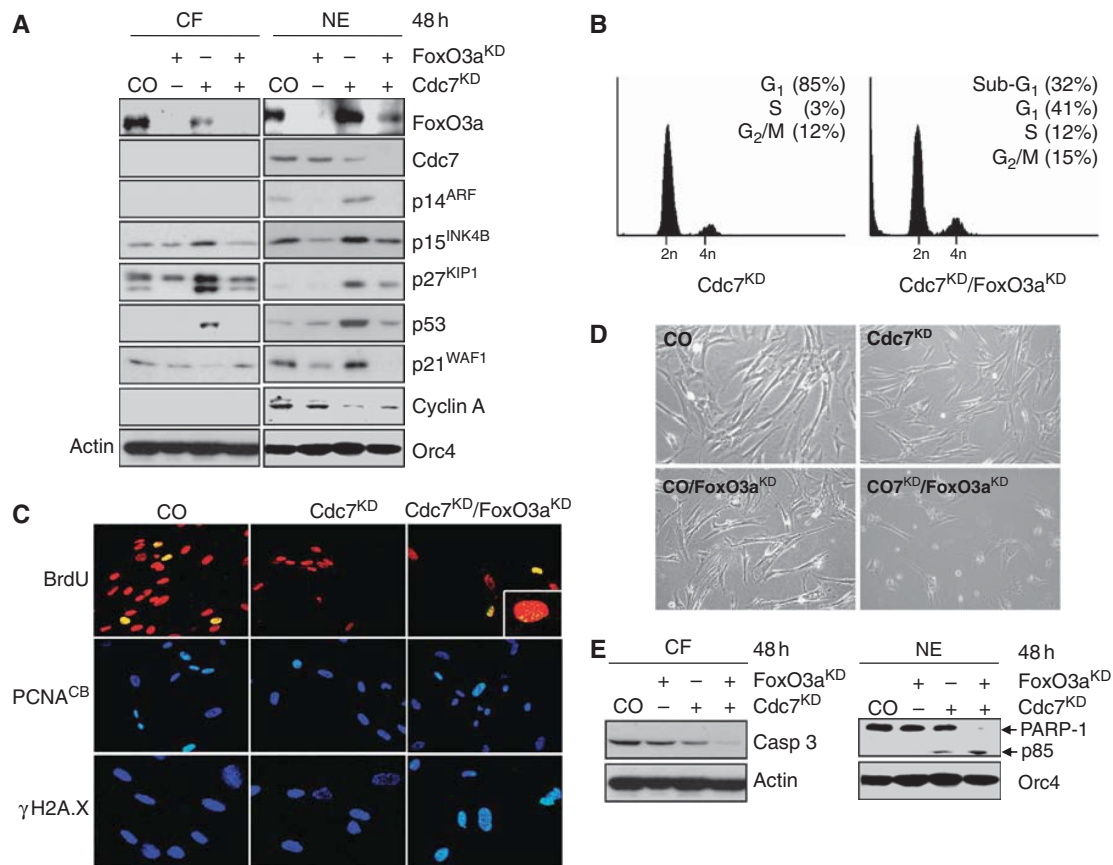


**Figure 4** FoxO3a-mediated upregulation of ARF and CDK inhibitors is an essential step for arresting cell cycle progression in Cdc7-depleted cells. (A) Cytoplasmic protein fractions (CF) and crude nuclear extracts (NE) prepared from CO, FoxO3a<sup>KD</sup>, Cdc7<sup>KD</sup> and doubly depleted Cdc7/FoxO3a (Cdc7<sup>KD</sup>/FoxO3a<sup>KD</sup>) IMR90 cells 48 h post-transfection were analysed by immunoblotting with the indicated antibodies (β-actin and Orc4—loading controls). Note that the faster migrating band represents the hypo-phosphorylated, active form of p27 and the slower migrating band its hyper-phosphorylated inactive form (Rodier *et al.*, 2001; Chopra *et al.*, 2002) (B) DNA content of Cdc7<sup>KD</sup> and Cdc7<sup>KD</sup>/FoxO3a<sup>KD</sup> cells 48 h post-transfection. (C) 48 h post-transfection CO, Cdc7<sup>KD</sup> and Cdc7<sup>KD</sup>/FoxO3a<sup>KD</sup> cells were pulsed for 2 h with BrdU, fixed and detected with an FITC-conjugated anti-BrdU antibody (inset: higher magnification). Chromatin-bound PCNA and γH2A.X were detected as described in the legend to Figure 3. Apoptotic cell death was detected 48 h post-transfection in doubly depleted Cdc7<sup>KD</sup>/FoxO3a<sup>KD</sup> cells (D) by phase contrast microscopy and (E) by immunoblot analysis of CF and NE with the indicated antibodies (β-actin and Orc4—loading controls).

chromatin-bound PCNA and BrdU incorporation (Figure 5D), and increased cyclin A detection (Figure 5C). Doubly depleted Cdc7/p15 cells also exhibited replication stress in the form of strong γH2A.X immunostaining (Figure 5D) and induced apoptosis as confirmed by flow cytometry (Supplementary Figure 12D), morphologically (Figure 5E), and through detection of caspase activation and PARP-1 cleavage (Figure 5F). Importantly, single knock-down control experiments showed that p15, FoxO3a, Dkk3 or p53 depletion alone does not cause strong S phase stimulation or apoptosis in this experimental system (Supplementary Figure 16).

Cdc7 depletion with an alternative CDC7-siRNA (oligo CDC7-B) triggered the same molecular changes in the described checkpoint pathways as CDC7 knock-down with oligo CDC7-A (Supplementary Figure 2C). The cell cycle arrest phenotype was reversed through expression of a CDC7 gene variant refractory to silencing by oligo CDC7-A (Supplementary Figure 3D and E). Moreover, the arrested phenotype was fully reproducible in a different fibroblast strain (Supplementary Figure 17). These control experiments further reinforce our findings and argue against RNAi off-target effects.

It can be postulated that if the checkpoint pathways elucidated here for Cdc7-depleted cells are manifested by impaired origin activation, these pathways should be similarly activated by depletion of other replication initiation proteins. To address this question, we compared the cellular response to Cdc7 depletion in IMR90 cells with the response caused by RNAi against *ORC2*, an origin licensing factor that acts upstream of Cdc7 in the DNA replication initiation pathway. Indeed, *ORC2* knock-down led to an accumulation of cells with G1 DNA content (Supplementary Figure 18A and B). As expected, immunoblotting revealed changes in protein levels and subcellular localization of FoxO3a, ARF, p15, p21, p27, p53 and Dkk3 similar to those found in Cdc7-depleted cells (Supplementary Figure 18C). Moreover, CDK activity, determined indirectly through Mcm2 phosphorylation at the Cdk2 phosphosite Ser-27, was reduced and cyclin D1 down-regulated in *Orc2*-depleted cells (Supplementary Figure 18C). Thus, at least partially overlapping checkpoint pathways appear to be activated by targeting either *CDC7* or *ORC2*, reinforcing the conclusion that the Cdc7-depletion-induced checkpoint is triggered by impaired origin activation.



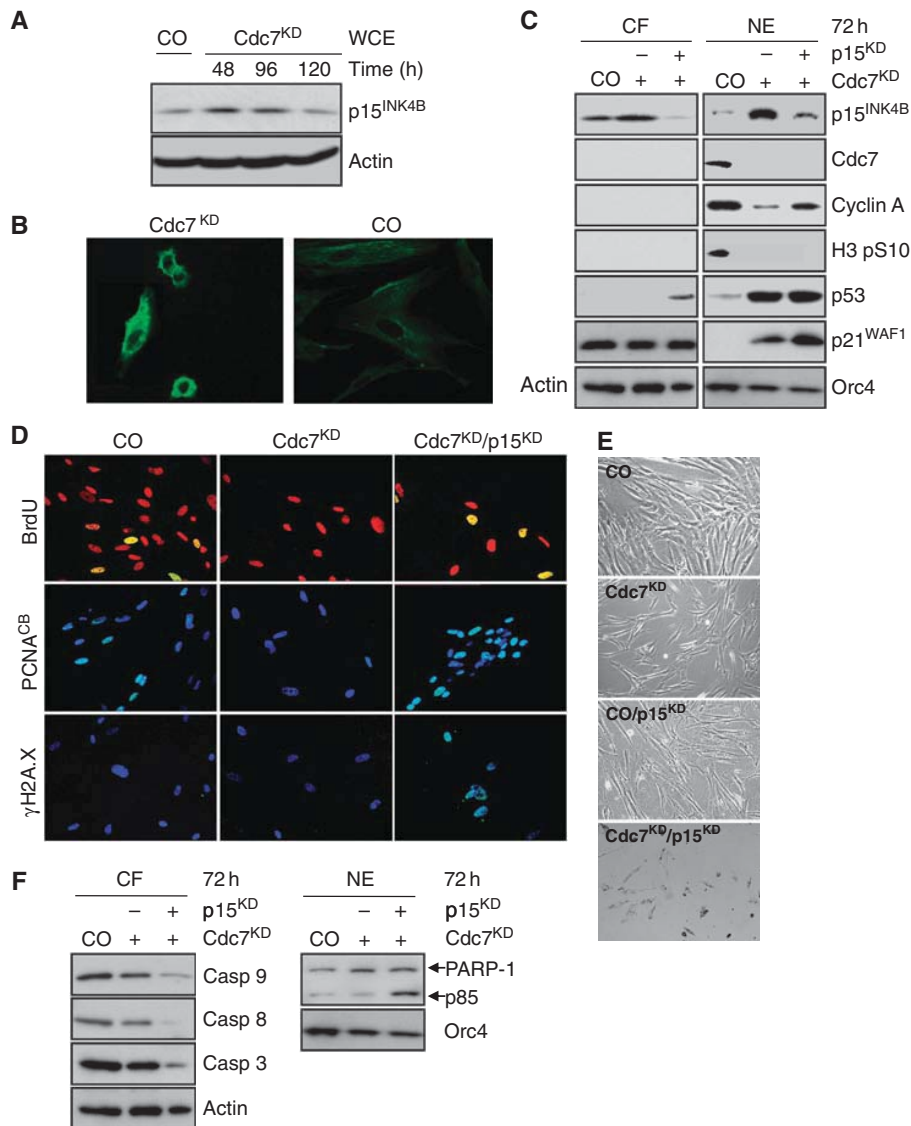


**Figure 5** The Cdc7-depletion-induced cell cycle arrest is p15<sup>INK4B</sup> dependent. (A) Upregulation of p15 levels in Cdc7-depleted IMR90 cells was confirmed by immunoblotting WCE prepared from CO cells and Cdc7-depleted cells 48, 96 and 120 h post-transfection with antibodies against p15 and β-actin (loading control). (B) Cdc7<sup>KD</sup> and CO cells were fixed 96 h post-transfection and p15 detected by indirect immunofluorescence using a fluorescein-labelled secondary antibody. (C) CF and NE prepared from CO, Cdc7<sup>KD</sup> and doubly depleted Cdc7/p15 (Cdc7<sup>KD</sup>/p15<sup>KD</sup>) cells 72 h post-transfection were analysed by immunoblotting with the indicated antibodies (β-actin and Orc4—loading controls). (D) 72 h post-transfection CO, Cdc7<sup>KD</sup> and Cdc7<sup>KD</sup>/p15<sup>KD</sup> cells were pulsed for 2 h with BrdU, fixed and detected with an FITC-conjugated anti-BrdU antibody. Chromatin-bound PCNA and γH2A.X were detected as described in Figure 3 legend. Apoptotic cell death was detected 72 h post-transfection in doubly depleted Cdc7<sup>KD</sup>/p15<sup>KD</sup> cells by (E) phase contrast microscopy and by (F) immunoblot analysis of CF and NE with the indicated antibodies (β-actin and Orc4—loading controls).

**Discussion**

Cells have evolved elaborate checkpoint mechanisms for maintenance of the genome. Checkpoints guard critical cell cycle transitions by preventing future events from happening if the prior event is not completed and error free. Previous studies have shown that inhibition of replication initiation proteins arrests the cell cycle in G1, pointing towards the existence of a checkpoint that prevents premature entry into S phase until a sufficient number of origins are replication competent (Blow and Gillespie, 2008). Here, we have used RNAi against *CDC7* to reveal the activities of the

origin activation checkpoint and to investigate its molecular architecture.

Our results show that Cdc7 depletion arrests cell cycle progression in diploid human fibroblasts. Immunoblotting showed that the DNA polymerase processivity factor PCNA was not associated with chromatin in Cdc7-depleted cells, whereas the proportion of BrdU-incorporating cells was reduced by >90% compared with control cells. Moreover, cyclin A, a marker for entry into S-G2-M phase, became undetectable in arrested cells. Phosphorylation of Chk1 on Ser-345, involved in activation of this checkpoint kinase in response to blocked DNA replication (Zhao and

Piwnicka-Worms, 2001), was also not detectable in Cdc7-depleted cells, arguing against the cell cycle arrest being triggered in early S phase by a signal generated from a few stalled replication forks that escaped the block. Downregulation of the DNA damage checkpoint controls kinases ATM and ATR and the lack of p53 phosphorylation on Ser-15 argues further against early S phase arrest in Cdc7-depleted cells. These results, therefore, suggest that fibroblasts depleted of Cdc7 arrest before entry into S phase. We found p53 and p21 levels to be elevated and Rb hypo-phosphorylated in Cdc7-depleted cells, whereas *in vitro* kinase assays confirmed a loss of CDK activity, which could mediate the G1 arrest.

Conceptually, the process of DNA checkpoint control is viewed as analogous to a signal transduction pathway. In this analogy, if replication initiation is impaired for any reason, a signal is detected by ‘sensor’ proteins and then sent by ‘transducer’ proteins to ‘effector’ proteins, which block the cell cycle until a sufficient number of origins are replication competent. Owing to experimental limitations of transient RNAi gene silencing, in particular the half-life of the CDC7 message and/or protein, our study has been restricted to elucidating the transducer and effector mechanisms of the origin activation checkpoint. Future investigations into how impaired replication initiation is sensed and signalled to transducer proteins, will be critically dependent on the availability of specific small molecule Cdc7 kinase inhibitors, which should allow activation of the checkpoint on a more rapid time scale.

As the FoxO subfamily has been previously implicated in cell cycle arrest (Huang and Tindall, 2007), we reasoned that this family of stress-activated transcription factors might serve as transducer proteins in the origin activation checkpoint. FoxO transcription factors have been shown to rapidly modulate the expression of genes involved in cell cycle transitions (Huang and Tindall, 2007) and themselves are regulated by subcellular localization, with cytoplasmic sequestration preventing transactivation of target genes (Calnan and Brunet, 2008). Our results show that Cdc7-depletion causes nuclear accumulation of FoxO3a. Among the cohort of known FoxO3a gene targets, we found *CDKN2A* (ARF) (Bouchard *et al.*, 2007), *CDKN2B* (p15) (Katayama *et al.*, 2008) and *CDKN1B* (p27) (Chandramohan *et al.*, 2008) to be upregulated both at transcriptional and protein level in Cdc7-depleted cells. We show that FoxO3a downregulation in cells previously arrested by Cdc7 depletion reduces expression of these critical cell cycle regulators to background levels and bypasses the G1 arrest with cells entering an abortive S phase followed by apoptosis. The same phenotype was also established by co-depletion of Cdc7 and p15, indicating that p15 is an effector of the G1 arrest, most likely through inhibiting cyclin D-CDK4/6 activity. Our results, therefore, show that FoxO3a activity is essential for a functioning origin activation checkpoint and highlight the importance of the FoxO3a → p15 axis (Figure 6). Previous work has established that degradation of the *Xenopus* homologue of p27 occurs at replication origins and is coupled with the initiation of DNA synthesis (Furstenthal *et al.*, 2001; You *et al.*, 2002), whereas in human breast epithelial cells, p27 is stabilized after Orc2 depletion and associated with the cyclin E-Cdk2 complex (Machida *et al.*, 2005). Thus, it is possible that FoxO3a-dependent p27 upregulation forms a separate axis of the

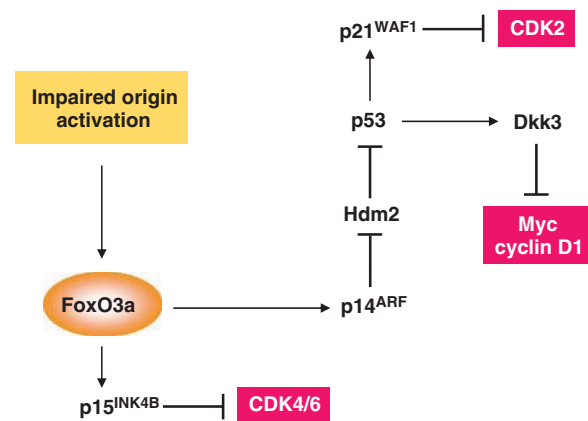


**Figure 6** A proposed model of the origin activation checkpoint.

origin activation checkpoint that results in inhibition of the cyclin E-Cdk2 complex.

We noted elevated levels of p53 and p21 in Cdc7-depleted fibroblasts. As the ATM/ATR checkpoint pathway (Abraham, 2001) does not appear to be active in these cells, FoxO3a-dependent upregulation of ARF provides a plausible explanation for p53 stabilization. By antagonizing the E3 ubiquitin ligase activity of Hdm2, ARF is known to stabilize p53 and increase its transcriptional activity (Pomerantz *et al.*, 1998). One way in which ARF activates nucleoplasmic p53 is by sequestering Hdm2 in the nucleolus (Weber *et al.*, 1999). Given the absence of any detectable Hdm2 either in crude NEs or nucleolar subfractions, however, we speculate that in Cdc7-depleted cells, ARF stabilizes p53 through Hdm2 proteolysis (Zhang *et al.*, 1998) rather than nucleolar sequestration (Figure 6). We show that p21 induction in Cdc7-depleted cells is dependent on p53. The ability of p21 to shut down the activity of E-type and A-type cyclin-CDK complexes ensures that cell cycle progression is blocked in G1. If the cell has managed to escape the checkpoint and advance into S phase with an insufficient number of replication-competent origins, p21 can block progression through S, G2 and M phase by inhibiting A-type and B-type cyclin-CDK complexes and by interfering with PCNA function, thereby halting further advance of replication forks (Sherr and Roberts, 1999). We show that p53 downregulation in fibroblasts previously arrested in G1 by Cdc7 depletion bypasses the cell cycle blockade and results in cells proceeding through S phase to the G2/M boundary before inducing apoptosis. We, therefore, conclude that the FoxO3a → ARF → Hdm2 → p53 → p21 axis is also essential for a functioning origin activation checkpoint (Figure 6).

GEMs revealed a second critical function for p53 in the checkpoint. Among known p53-target genes that were differentially expressed in cells arrested by *CDC7* knock-down is *DKK3*, a negative regulator of the Wnt/β-catenin signalling pathway (Niehrs, 2006). Dkk3 is a glycoprotein that prevents nuclear accumulation of β-catenin, resulting in downregulation of its downstream targets *MYC* and *CCND1* (Lee *et al.*, 2009). As expected, immunoblotting showed an increase in the inducible, faster migrating Dkk3 isoform in Cdc7-depleted cells and revealed strongly diminished nuclear β-catenin levels as well as Myc and cyclin D1 downregulation. Dkk3 upregulation was reversed in cells co-depleted of Cdc7 and

p53, whereas nuclear  $\beta$ -catenin, Myc and cyclin D1 levels were restored upon downregulation of Dkk3 in cells previously arrested by Cdc7 depletion. We speculate that Dkk3-mediated cyclin D1 downregulation halts progression through most of G1, whereas a decrease in transcription of the *MYC* gene prevents Myc-driven gene expression changes that normally drive the cell through G1 (Figure 6). It can be postulated, for example, that a sharp fall in Myc levels leads to downregulation of the cyclin D2 and CDK4 genes and a reduction in Cul1 levels, a protein required for p27 degradation (Eilers and Eisenman, 2008). Reduced Myc levels may also attenuate the expression of E2F1-3 and prevent Myc-Max-mediated repression of p15 and p21 expression (Eilers and Eisenman, 2008). As Myc has been implicated in stabilizing pre-RCs assembled at origins (Dominguez-Sola *et al.*, 2007), Dkk3-mediated downregulation of *MYC* expression might also explain the decrease in chromatin-bound origin licensing factors seen in Cdc7-depleted cells. The ability of Myc to modulate the actions of a number of positive and negative regulators of cell cycle advance provides a firm rationale for the requirement to downregulate this critical driver of cell proliferation if cells sense inhibition of the DNA replication initiation pathway. Importantly, we show that Dkk3 downregulation in Cdc7-depleted-arrested fibroblasts also bypasses the cell cycle blockade, enabling cells to proceed into an abortive S phase followed by apoptosis. These data highlight the critical function of Dkk3 in linking the FoxO3a $\rightarrow$ ARF $\rightarrow$ Hdm2 $\rightarrow$ p53 axis to the Wnt/ $\beta$ -catenin signalling pathway (Figure 6). We conclude that FoxO3a lies at the core of a complex molecular circuitry that resets the regulatory dials of the cell cycle clock in response to blocked-replication initiation and thereby shifts the balance of growth-promoting and growth-inhibiting mechanisms in a way that favours G1 arrest. Pathway specificity tests in fibroblasts arrested by oxidative stress (Chen *et al.*, 2004) or through specific activation of the p53 pathway by low dose actinomycin D (Choong *et al.*, 2009) show that while p15 and p27 upregulation in Cdc7-depleted cells overlap with the common FoxO-induced cell cycle arrest pathway (Huang and Tindall, 2007), inducible ARF and Dkk3 expression are more specific events associated with DNA replication control. Our microarray data indicate that the resulting loss of CDK activity inactivates the Rb-E2F signalling pathway, which in turn overrides the regular E2F-driven G1/S transcriptional programme.

The pathways elucidated in this study in response to impaired origin activation comply with two essential criteria of checkpoint control originally proposed by Hartwell and Weinert (1989). First, checkpoints are considered external control mechanisms that are not required for forward cell cycle progression. Conforming to this defining feature, FoxO3a-mediated activation of the three checkpoint axes does not occur during normal G1 progression when the potential for errors in the DNA replication initiation pathway is minimal. The second is the relief-of-dependence criterion, which stipulates that ‘the existence of a control mechanism is suggested when one finds chemicals, mutants or other conditions that ... permit a late event to occur even when an early, normal prerequisite event is prevented’ (Hartwell and Weinert, 1989). In line with this hallmark of checkpoint control, double depletion of Cdc7 and any of the checkpoint proteins FoxO3a, p15, p53 or Dkk3 abrogates the

checkpoint itself and allows S phase entry. Single knock-downs of these checkpoint components, on the contrary, do not cause strong S phase stimulation on their own.

Several different conditions must be met during G1 phase to ensure origin activation and DNA synthesis. These include origin recognition through ORC binding, origin licensing through the assembly of ORC, Cdc6, Cdt1 and the replicative MCM helicase into pre-RCs, origin activation through CDK and Cdc7-dependent phosphorylation events resulting in origin unwinding and the recruitment of the replisome required for initiation of DNA synthesis. Thus, as noted by Khodjakov and Rieder (2009), there is the possibility of multiple checkpoints, each detecting one of these conditions or, alternatively, that a range of abnormalities may cause a single condition detected by just one checkpoint. A G1 arrest phenotype, for example, has been reported in response to RNAi against *ORC2* (Machida *et al.*, 2005) and inhibition of MCM loading by overexpressing a stable form of geminin (Shreeram *et al.*, 2002) or MCM helicase activity by RNAi against *CDC7* (Montagnoli *et al.*, 2004). Thus, the question arises whether these abnormalities are activating multiple different checkpoints or a single master checkpoint. It is of interest in this context that in our study the cellular effects of *ORC2* knock-down were remarkably similar to those caused by *CDC7* knock-down, suggesting that overlapping checkpoint pathways are governing at least origin licensing and origin firing. The activation of overlapping pathways by *Orc2* and *Cdc7* downregulation also argues against the possibility that the checkpoint described here is triggered by loss of other, less well understood, *Cdc7* functions in, for example, mitotic chromosomal segregation (Takahashi *et al.*, 2008) or DNA damage response (Takeda *et al.*, 1999; Costanzo *et al.*, 2003; Dierov *et al.*, 2004; Tenca *et al.*, 2007; Kim *et al.*, 2008).

In separate studies, we found that RNAi against *CDC7* in primary human breast and bronchial epithelial cells triggers a cell cycle blockade that phenotypically and at the molecular level strongly resembles the G1 arrest described here for diploid human fibroblasts (Rodriguez-Acebes *et al.*, 2010; Kingsbury *et al.*, in preparation). This suggests that the origin activation checkpoint is conserved in somatic cells of different embryological origin. The integrated nature of the underlying molecular circuitry explains how cells arrested by Cdc7 depletion can bypass the cell cycle arrest if the activity of important constituents of any of the three axes identified in this study is inhibited. Cells that bypass the checkpoint are able to support a low level of DNA synthesis and either arrest in S phase or proceed to the G2/M boundary if p53 function is lost. One explanation for FoxO3a-, p15-, p53- and Dkk3-depleted cells with reduced Cdc7 levels being able to synthesize DNA is the initiation of replication forks from isolated origins that escaped checkpoint function. Irrespective of p53 status, entry into S phase with an insufficient number of replication-competent origins is lethal, with cells experiencing replication stress and inducing apoptosis.

Recent studies have established that inhibition of the DNA replication initiation machinery causes cancer-cell-specific killing (Blow and Gillespie, 2008), validating replication initiation as a new target class for cancer cell chemotherapy (Jackson, 2008). Inhibiting an early step in replication initiation upstream of DNA polymerase should result in G1 arrest and, therefore, be non-genotoxic in normal cells with a functioning checkpoint. Given the reappearance of

proliferative activity in fibroblasts several days after RNAi against *CDC7*, we speculate that the G1 arrest enforced in normal cells might also be reversible. The high levels of apoptosis reported for cancer cell lines subjected to inhibition of origin licensing or firing (Shreeram *et al.*, 2002; Feng *et al.*, 2003; Montagnoli *et al.*, 2004) indicate that the origin activation checkpoint is most likely lost or impaired in transformed cells. This is in keeping with the dependency of the underlying molecular circuitry on a number of tumour suppressor proteins (p53, Hdm2, ARF, FoxO3a, Dkk3 and Rb), one or more of which are commonly inactivated during tumourigenesis. Thus, our findings support the concept of emerging pharmacological Cdc7 inhibitors (Montagnoli *et al.*, 2008; Swords *et al.*, 2010) as potentially powerful anti-cancer agents with broad tumour spectrum activity. Knowledge of the complex regulatory network underlying the checkpoint may help predict individual patient response to Cdc7 inhibitors in the future.

## Materials and methods

### Cell culture and cell synchronization

IMR90 (ATCC# CCL-186), a diploid human fibroblast adherent cell strain derived from foetal lung tissue, was obtained from LGC Standards (Middlesex, UK) at population doubling (PD) 12. All culture passages and PDs were recorded and all experiments were performed with IMR90 cells under a PD of 22. WI-38 (ATCC# CCL-75) diploid human fibroblasts were obtained from LGC standards at PD 6. All experiments with WI-38 cells were performed under a PD of 15. IMR90 and WI-38 cells were cultured at 37°C with 5% CO<sub>2</sub> in DMEM (Invitrogen, Paisley, UK) supplemented with 10% defined FCS (Invitrogen), 100 U/ml penicillin and 100 µg/ml streptomycin. For preparation of synchronous cell populations, IMR90 cells were synchronized in early S phase by two sequential 25 h blocks in 2.5 mM thymidine (Sigma, Gillingham, UK) separated by a 12 h interval without thymidine (Krude *et al.*, 1997).

### Cell treatments

IMR90 fibroblasts were oxidatively stressed through H<sub>2</sub>O<sub>2</sub> treatment as described (Chen *et al.*, 2004) with the following minor modifications. Cells were cultured in medium containing 600 µM H<sub>2</sub>O<sub>2</sub> for 2 h. After 24 h, cells were treated again for 2 h with 600 µM H<sub>2</sub>O<sub>2</sub> and collected 4 h after the second treatment. Specific activation of the p53 pathway in IMR90 cells was induced by 24 h low dose (1 nM) actinomycin D treatment as described (Choong *et al.*, 2009).

### Cell population growth assessment and cell cycle analysis

Phase contrast microscopy was performed with an inverted Axiovert 200 M (Carl Zeiss, Welwyn Garden City, UK) and Axiovision software. Flow cytometric cell cycle analyses were performed as described (Eward *et al.*, 2004). The proportion of cells with less than 2C DNA content was calculated as an estimate of the apoptotic cell population.

### Cell sorting

For preparation of G1 phase cell populations, 5 × 10<sup>6</sup> of each asynchronous control cells and Cdc7-depleted cells were collected and fixed for 3 h at -20°C in 80% methanol in PBS with added protease inhibitors (one complete EDTA-free protease inhibitor cocktail tablet (Roche Diagnostics, Burgess Hill, UK) per 25 ml of buffer). Cells were precipitated by centrifugation at 500g for 5 min and resuspended in a mixture containing 50 µg/ml PI, 20 µg/ml RNase A and protease inhibitors. The cells were sorted on a DAKO/Beckman Coulter MoFlo High Speed Sorter (Beckman Coulter Inc., Orange County, CA). The forward scatter signal was used to trigger the detection of cells and the PI signal fluorescence was linearly quantified to rationalize DNA content after excitation at 488 nm in the orange/red channel (613/20 nm bandpass filter). Cells in G1 phase of the cell cycle were sorted through one-way sorting into round-bottomed Falcon tubes containing PBS with protease

inhibitors (Roche Diagnostics). Cells were precipitated at 16000g for 5 min and lysed with modified RIPA buffer (300 mM NaCl).

### Cell fractionation and immunoprecipitation

For western blot analysis, cells were harvested and WCE and subcellular fractions were prepared. For WCE, cells were lysed for 45 min on ice in modified RIPA lysis buffer (50 mM Tris-HCl, 300 mM NaCl, 1% NP40, 0.5% sodium deoxycholate, 0.1% SDS, 1 mM EDTA and protease inhibitors) and sonicated for 10 s. For crude nuclear extraction, cells were lysed in buffer containing 10 mM HEPES pH 7.9, 10 mM KCl, 1.5 mM MgCl<sub>2</sub>, 0.34 M sucrose, 10% glycerol, 0.1% Triton X-100, 1.0 mM DTT and protease inhibitors and gently homogenized. Nuclei were precipitated by centrifuging at 1000 g for 5 min at 4°C and the CF was removed. For preparation of NE, nuclear pellets were washed twice with the same buffer, lysed in modified RIPA buffer for 30 min, sonicated and centrifuged at 13000 g. Nucleoli and CBF were isolated as described (Muramatsu and Onishi, 1978; Kingsbury *et al.*, 2005). *In vitro* kinase assays were performed as described (Jinno *et al.*, 2002) with minor modifications. Briefly, cell lysates were incubated at 4°C for 2 h with cyclin A and cyclin E antibodies. The kinase activity of immunoprecipitated Cdk2 in complex with cyclin A and cyclin E was assayed as described (Jinno *et al.*, 1999). Phosphorylation of truncated Rb (Cdk2 substrate; QED Bioscience, San Diego, CA) was detected with anti-Rb phospho-Thr-821 antibody (Invitrogen).

### Immunoblotting

Protein concentration was determined using the DC Bio-Rad protein assay kit (Bio-Rad Hemel Hempstead, UK); 60 µg of total protein was loaded in each lane and separated by 4–20% SDS-PAGE. Protein was transferred from polyacrylamide gels onto PVDF membranes (Bio-Rad) by semi-dry electroblotting. Blocking, antibody incubations and washing steps were performed as described (Kingsbury *et al.*, 2005). Antibodies used for immunoblotting and immunofluorescence (see below) included caspase 3 from Novus (Littleton, CO); Chk1-pSer-345 (2341) from Cell Signaling Technology (Danvers, MA); caspase 9 (F-7), cyclin D1 (H-295), p16<sup>INK4A</sup> (H-156), c-Myc (N-262), PCNA (F-2), Cdc6 (180.2) and histone H1 (AE-4) from Santa Cruz (Santa Cruz, CA); FoxO3a, caspase 8, β-catenin and phospho-histone H3 (Ser-10) from Millipore (Billerica, MA); cyclin A (6E6) and cyclin E (Ab-4) (HE-172) from Thermo Fisher Scientific (Fremont, CA); p27<sup>KIP1</sup>, Orc4, Mcm2 (BM28), p21<sup>WAF1</sup>, cyclin B1, PARP-1, pRb and Orc2 from BD Biosciences (Oxford, UK); p15<sup>INK4B</sup> (15PO6), Cdt1, Hdm2 and Dkk3 from Abcam (Cambridge, UK); p53 (Ab-6) from Merck (Beeston, UK); Cdc7 from MBL International (Woburn, MA); p14<sup>ARF</sup> (DCS-240) and β-actin from Sigma; p53 phospho-Ser-15, Rb phospho-Ser-807/811, phospho-histone γH2A.X (Ser-139) from New England Biolabs (Hitchin, UK) and Mcm2 phospho-Ser-53, Mcm2 phospho-Ser-27, Mcm2 phospho-Ser-41, Mcm2 phospho-Ser-40/41 and Mcm2 phospho-Ser-108 from Bethyl Laboratories (Montgomery, TX). Affinity-purified rabbit polyclonal anti-geminin antibody G95 was generated as described (Wharton *et al.*, 2004). Affinity-purified rabbit polyclonal antibodies to Mcm10, Cdc45 and Dbf4 were generated by Eurogentec (Seraing, Belgium) following the manufacturer's protocol. The positive control lysate for p53 phospho-Ser-15 was prepared from IMR90 cells treated with 17 µM cisplatin for 24 h (Pabla *et al.*, 2008). Neuroblastoma SK-N-SH cell lysate from Insight Biotechnologies (Wembley, UK) was used as a lysate control for Dkk3 protein. Immunodetection of Dkk3 was blocked by preincubation of Dkk3 antibody with recombinant human Dkk3 (1118-DK-050; R&D Systems Europe, Abingdon, UK) (1:1 w/w).

### N-glycanase digestion

Cytoplasmatic protein fractions (125 µg or 50 µg total protein) were treated with N-glycanase (recombinant from *Chriseobacterium (Flavobacterium) meningosepticum*, expressed in *Escherichia coli*; ProZyme, Hayward, CA) as described (Krupnik *et al.*, 1999).

### Immunofluorescence

For detection of BrdU incorporation, cells pulsed for 2 h with 100 µM BrdU were fixed with 3.7% paraformaldehyde for 5 min and permeabilized with 0.2% Triton X-100 for 5 min. Coverslips were incubated with 2N HCl for 1 h, washed with PBS and incubated for 1 h at 37°C with primary anti-BrdU antibody (Alexis Biochemicals, Exeter, UK), diluted 1/10 vol/vol in 0.1% BSA in PBS containing 50 ng/ml PI and 50 ng/ml RNase A. Fluorescence confocal microscopy of random fields of cells was performed on a Leica TCS SP



confocal microscope (Leica, Milton Keynes, UK). Images of the rhodamine (red) and fluorescein (green) channels were obtained using Leica TCS PowerScan software. At least 400 cells were routinely scored for each treatment and quantitated as percentages of the total number of cells. Indirect immunofluorescence of chromatin-bound PCNA was performed as described (Miura and Sasaki, 1999) with minor modifications. For detection of  $\beta$ -catenin, Myc, cyclin D1, p15<sup>INK4B</sup> and  $\gamma$ -H2A.X, after paraformaldehyde fixation and permeabilization, coverslips were saturated with blocking buffer (5% BSA in PBS) for 1 h at RT, incubated with primary antibody diluted in blocking buffer for 1 h at 37°C and incubated overnight at 4°C. FITC-conjugated anti-mouse antibody from Dako (Glostrup, Denmark) was used at dilution 1/1000. Slides were mounted in Vectashield mounting medium (Vector Laboratories, Peterborough, UK) with 1.5  $\mu$ g/ml DAPI to visualize DNA. Coverslips for p14<sup>ARF</sup> detection were fixed with methanol/acetone (3:2 vol/vol) and stained as described above.

### RNA interference

*CDC7*, *p53* and *CDKN2B* (p15<sup>INK4B</sup>) expression was inhibited with double-stranded RNA oligos for *CDC7* (A- and B- custom, and V—validated siRNAs), *p53* (custom siRNA) and p15<sup>INK4B</sup> (silencer pre-designed and validated siRNAs) synthesized by Ambion (Supplementary Table 1). *DKK3* was specifically inhibited with a cocktail of two ON-TARGET plus siRNAs (J-018352-11 and -12; Dharmacon, Fremont, CA) and *FOXO3A* was inhibited with siGENOME SMART pool (M-003007-02-0005, Dharmacon). Non-targeting siRNA was used as a negative control. Lipofectamine 2000 (Invitrogen) was used in all transfections according to the manufacturer's recommendations. Briefly, cells were seeded at a density to reach 50% confluence on the day of transfection. The transient transfections were performed using 10 nM of *CDC7* siRNA duplex or 10 nM of *ORC2* siRNA duplex. For double knock-downs, cells were first transfected with *CDC7*-siRNA and after 72 h (after replating at low density for CO cells) transfected with either *CDC7* (10 nM) and control (10 nM) oligos, or *CDC7* (10 nM) and *p53* (10 nM) or *FOXO3A* (10 nM) oligos. *DKK3* and p15<sup>INK4B</sup> cotransfections were performed with *CDC7* oligo (10 nM) and a cocktail of two *DKK3* oligos (each 10 nM) or a cocktail of p15<sup>INK4B</sup> oligos 1, 2 and 3 (each 5 nM). In this case, *CDC7* oligo pulsing at 72 h was adjusted with 20 and 15 nM control (CO) oligo, respectively, to reach the same amount of oligos in both samples (single and double knock-down). For *p53*, *Dkk3*, *FoxO3a* and p15 single knock-downs, cells were first transfected with CO oligo and after 72 h replated at low density and transfected with CO, CO and p53-siRNAs (p53<sup>KD</sup>), or CO and *DKK3* (Dkk3<sup>KD</sup>) or *FOXO3A* (FoxO3a<sup>KD</sup>) or *CDKN2B* (p15<sup>KD</sup>) oligos. siRNAs were complexed with transfection reagent in serum-free and antibiotic-free culture medium according to the manufacturer's instructions (Invitrogen). Cells were incubated from

48 to 120 h. All experiments were performed at least three times. The transfection efficiency was determined for fluorescein-conjugated non-specific siRNA-transfected cells (BLOCK-iT Transfection Optimization kit; Invitrogen) using a Leica TCS SP confocal fluorescence microscope. Selective silencing of the corresponding proteins was confirmed by western blotting. For rescue experiments, the full 1725 bp *CDC7* cDNA sequence containing four silent, single base pair mutations in the 21 bp *CDC7*-siRNA (oligo-A) interaction region was inserted into pCMV6-AC expression vector (OriGene) to fully abolish the siRNA effect.

### RNA extraction and qRT-PCR

To evaluate the efficiency of transfection with *CDC7*, *p53*, *DKK3*, p15<sup>INK4B</sup> and *FOXO3A* siRNAs, mRNA transcription levels of *CDC7*, *p53*, p15<sup>INK4B</sup>, *DKK3* isoforms A and B and *FOXO3A* were detected by qRT-PCR. Total RNA was isolated using a PureLink Micro-to-Midi kit (Invitrogen) according to the manufacturer's instructions. Reverse transcription reactions using 40 ng of total RNA in a final reaction volume of 20  $\mu$ l were performed in one step using SuperScript III Platinum SYBR Green One Step qRT-PCR Kit (Invitrogen). Relative quantitation data were obtained using the comparative C<sub>t</sub> method with Realplex software according to the manufacturer's protocol (Eppendorf, Heidelberg, Germany). Glyceraldehyde-3-phosphate dehydrogenase was used to normalize each of the extracts for amplifiable human DNA. Primers (Supplementary Table 3) were provided by Eurofins MWG Operon (Ebersberg, Germany). Cycle conditions are available upon request.

Additional information on cRNA labelling and hybridization for microarray and Microarray data processing and analysis is available in the Supplementary data section.

### Supplementary data

Supplementary data are available at *The EMBO Journal* Online (<http://www.embojournal.org>).

### Acknowledgements

We thank Hye-Kyung Hong and Richard Sainsbury for insightful discussion of the data and Arnold Pizzey and Tomas Adejumo for supporting the flow cytometric analyses with their expertise and advice. This study has been supported by Cancer Research UK scientific programme grant C428/A6263 (KS and GHW) and by an MRC Centre Grant (MWT).

### Conflict of interest

The authors declare that they have no conflict of interest.

### References

- Abraham RT (2001) Cell cycle checkpoint signaling through the ATM and ATR kinases. *Genes Dev* **15**: 2177–2196
- Biamonti G, Paixao S, Montecucco A, Peverali FA, Riva S, Falaschi A (2003) Is DNA sequence sufficient to specify DNA replication origins in metazoan cells? *Chromosome Res* **11**: 403–412
- Blow JJ, Gillespie PJ (2008) Replication licensing and cancer—a fatal entanglement? *Nat Rev Cancer* **8**: 799–806
- Bouchard C, Lee S, Paulus-Hock V, Lodenkemper C, Eilers M, Schmitt CA (2007) FoxO transcription factors suppress Myc-driven lymphomagenesis via direct activation of Arf. *Genes Dev* **21**: 2775–2787
- Brunet A, Bonni A, Zigmond MJ, Lin MZ, Juo P, Hu LS, Anderson MJ, Arden KC, Blenis J, Greenberg ME (1999) Akt promotes cell survival by phosphorylating and inhibiting a Forkhead transcription factor. *Cell* **96**: 857–868
- Calnan DR, Brunet A (2008) The FoxO code. *Oncogene* **27**: 2276–2288
- Chandramohan V, Mineva ND, Burke B, Jeay S, Wu M, Shen J, Yang W, Hann SR, Sonenshein GE (2008) c-Myc represses FOXO3a-mediated transcription of the gene encoding the p27(Kip1) cyclin dependent kinase inhibitor. *J Cell Biochem* **104**: 2091–2106
- Chen JH, Stoeber K, Kingsbury S, Ozanne SE, Williams GH, Hales CN (2004) Loss of proliferative capacity and induction of senescence in oxidatively stressed human fibroblasts. *J Biol Chem* **279**: 49439–49446
- Chi Y, Welcker M, Hizli AA, Posakony JJ, Aebersold R, Clurman BE (2008) Identification of CDK2 substrates in human cell lysates. *Genome Biol* **9**: R149
- Choong ML, Yang H, Lee MA, Lane DP (2009) Specific activation of the p53 pathway by low dose actinomycin D: a new route to p53 based cyclotherapy. *Cell Cycle* **8**: 2810–2818
- Chopra S, Fernandez De MS, Lam EW, Mann DJ (2002) Jab1 co-activation of c-Jun is abrogated by the serine 10-phosphorylated form of p27Kip1. *J Biol Chem* **277**: 32413–32416
- Clevers H (2006) Wnt/beta-catenin signaling in development and disease. *Cell* **127**: 469–480
- Connell-Crowley L, Harper JW, Goodrich DW (1997) Cyclin D1/Cdk4 regulates retinoblastoma protein-mediated cell cycle arrest by site-specific phosphorylation. *Mol Biol Cell* **8**: 287–301
- Costanzo V, Shechter D, Lupardus PJ, Cimprich KA, Gottesman M, Gautier J (2003) An ATR- and Cdc7-dependent DNA damage checkpoint that inhibits initiation of DNA replication. *Mol Cell* **11**: 203–213
- Dierov J, Dierova R, Carroll M (2004) BCR/ABL translocates to the nucleus and disrupts an ATR-dependent intra-S phase checkpoint. *Cancer Cell* **5**: 275–285

- Dominguez-Sola D, Ying CY, Grandori C, Ruggiero L, Chen B, Li M, Galloway DA, Gu W, Gautier J, Ia-Favera R (2007) Non-transcriptional control of DNA replication by c-Myc. *Nature* **448**: 445–451
- Eilers M, Eisenman RN (2008) Myc's broad reach. *Genes Dev* **22**: 2755–2766
- Eward KL, Obermann EC, Shreeram S, Loddo M, Fanshawe T, Williams C, Jung HI, Prevost AT, Blow JJ, Stoeber K, Williams GH (2004) DNA replication licensing in somatic and germ cells. *J Cell Sci* **117**: 5875–5886
- Feng D, Tu Z, Wu W, Liang C (2003) Inhibiting the expression of DNA replication-initiation proteins induces apoptosis in human cancer cells. *Cancer Res* **63**: 7356–7364
- Furthesthal L, Swanson C, Kaiser BK, Eldridge AG, Jackson PK (2001) Triggering ubiquitination of a CDK inhibitor at origins of DNA replication. *Nat Cell Biol* **3**: 715–722
- Hartwell LH, Weinert TA (1989) Checkpoints: controls that ensure the order of cell cycle events. *Science* **246**: 629–634
- Hsieh SY, Hsieh PS, Chiu CT, Chen WY (2004) Dickkopf-3/REIC functions as a suppressor gene of tumor growth. *Oncogene* **23**: 9183–9189
- Huang H, Tindall DJ (2007) Dynamic FoxO transcription factors. *J Cell Sci* **120**: 2479–2487
- Jackson PK (2008) Stopping replication, at the beginning. *Nat Chem Biol* **4**: 331–332
- Jinno S, Hung SC, Yamamoto H, Lin J, Nagata A, Okayama H (1999) Oncogenic stimulation recruits cyclin-dependent kinase in the cell cycle start in rat fibroblast. *Proc Natl Acad Sci USA* **96**: 13197–13202
- Jinno S, Yageta M, Nagata A, Okayama H (2002) Cdc6 requires anchorage for its expression. *Oncogene* **21**: 1777–1784
- Katayama K, Nakamura A, Sugimoto Y, Tsuruo T, Fujita N (2008) FOXO transcription factor-dependent p15(INK4b) and p19(INK4d) expression. *Oncogene* **27**: 1677–1686
- Khodjakov A, Rieder CL (2009) The nature of cell-cycle checkpoints: facts and fallacies. *J Biol* **8**: 88
- Kim JM, Kakusho N, Yamada M, Kanoh Y, Takemoto N, Masai H (2008) Cdc7 kinase mediates Claspin phosphorylation in DNA replication checkpoint. *Oncogene* **27**: 3475–3482
- Kingsbury SR, Loddo M, Fanshawe T, Obermann EC, Prevost AT, Stoeber K, Williams GH (2005) Repression of DNA replication licensing in quiescence is independent of geminin and may define the cell cycle state of progenitor cells. *Exp Cell Res* **309**: 56–67
- Krude T, Jackman M, Pines J, Laskey RA (1997) Cyclin/CDK-dependent initiation of DNA replication in a human cell-free system. *Cell* **88**: 109–119
- Krupnik VE, Sharp JD, Jiang C, Robison K, Chickering TW, Amaravadi L, Brown DE, Guyot D, Mays G, Leiby K, Chang B, Duong T, Goodearl AD, Gearing DP, Sokol SY, McCarthy SA (1999) Functional and structural diversity of the human Dickkopf gene family. *Gene* **238**: 301–313
- Lee EJ, Jo M, Rho SB, Park K, Yoo YN, Park J, Chae M, Zhang W, Lee JH (2009) Dkk3, downregulated in cervical cancer, functions as a negative regulator of beta-catenin. *Int J Cancer* **124**: 287–297
- Machida YJ, Teer JK, Dutta A (2005) Acute reduction of an origin recognition complex (ORC) subunit in human cells reveals a requirement of ORC for Cdk2 activation. *J Biol Chem* **280**: 27624–27630
- Matos J, Lipp JJ, Bogdanova A, Guillot S, Okaz E, Junqueira M, Shevchenko A, Zachariae W (2008) Dbf4-dependent CDC7 kinase links DNA replication to the segregation of homologous chromosomes in meiosis I. *Cell* **135**: 662–678
- Matsuzawa SI, Reed JC (2001) Siah-1, SIP, and Ebi collaborate in a novel pathway for beta-catenin degradation linked to p53 responses. *Mol Cell* **7**: 915–926
- Mechali M (2001) DNA replication origins: from sequence specificity to epigenetics. *Nat Rev Genet* **2**: 640–645
- Miller CT, Gabrielse C, Chen YC, Weinreich M (2009) Cdc7p-Dbf4p regulates mitotic exit by inhibiting Polo kinase. *PLoS Genet* **5**: e1000498
- Miura M, Sasaki T (1999) Detection of chromatin-bound PCNA in cultured cells following exposure to DNA-damaging agents. *Methods Mol Biol* **113**: 577–582
- Montagnoli A, Tenca P, Sola F, Carpani D, Brotherton D, Albanese C, Santocanale C (2004) Cdc7 inhibition reveals a p53-dependent replication checkpoint that is defective in cancer cells. *Cancer Res* **64**: 7110–7116
- Montagnoli A, Valsasina B, Brotherton D, Troiani S, Rainoldi S, Tenca P, Molinari A, Santocanale C (2006) Identification of Mcm2 phosphorylation sites by S-phase-regulating kinases. *J Biol Chem* **281**: 10281–10290
- Montagnoli A, Valsasina B, Croci V, Menichincheri M, Rainoldi S, Marchesi V, Tibolla M, Tenca P, Brotherton D, Albanese C, Patton V, Alzani R, Ciavolella A, Sola F, Molinari A, Volpi D, Avanzi N, Fiorentini F, Cattoni M, Healy S *et al* (2008) A Cdc7 kinase inhibitor restricts initiation of DNA replication and has antitumor activity. *Nat Chem Biol* **4**: 357–365
- Muramatsu M, Onishi T (1978) Isolation and purification of nucleoli and nucleolar chromatin from mammalian cells. *Methods Cell Biol* **17**: 141–161
- Niehrs C (2006) Function and biological roles of the Dickkopf family of Wnt modulators. *Oncogene* **25**: 7469–7481
- Pabla N, Huang S, Mi QS, Daniel R, Dong Z (2008) ATR-Chk2 signaling in p53 activation and DNA damage response during cisplatin-induced apoptosis. *J Biol Chem* **283**: 6572–6583
- Pomerantz J, Schreiber-Agus N, Liegeois NJ, Silverman A, Alland L, Chin L, Potes J, Chen K, Orlow I, Lee HW, Cordon-Cardo C, DePinho RA (1998) The Ink4a tumor suppressor gene product, p19Arf, interacts with MDM2 and neutralizes MDM2's inhibition of p53. *Cell* **92**: 713–723
- Rodier G, Montagnoli A, Di ML, Coulombe P, Draetta GF, Pagano M, Meloche S (2001) p27 cytoplasmic localization is regulated by phosphorylation on Ser10 and is not a prerequisite for its proteolysis. *EMBO J* **20**: 6672–6682
- Rodriguez-Acebes S, Proctor I, Loddo M, Wollenschlaeger A, Falzon M, Prevost AT, Sainsbury R, Williams GH, Stoeber K (2010) Targeting DNA replication before it starts: Cdc7 as a therapeutic target in p53-mutant breast cancers. *Am J Pathol* (in press)
- Sclafani RA, Holzen TM (2007) Cell cycle regulation of DNA replication. *Annu Rev Genet* **41**: 237–280
- Sherr CJ, Roberts JM (1999) CDK inhibitors: positive and negative regulators of G1-phase progression. *Genes Dev* **13**: 1501–1512
- Shreeram S, Sparks A, Lane DP, Blow JJ (2002) Cell type-specific responses of human cells to inhibition of replication licensing. *Oncogene* **21**: 6624–6632
- Swords R, Mahalingam D, O'Dwyer M, Santocanale C, Kelly K, Carew J, Giles F (2010) Cdc7 kinase—a new target for drug development. *Eur J Cancer* **46**: 33–40
- Takahashi TS, Basu A, Bermudez V, Hurwitz J, Walter JC (2008) Cdc7-Drf1 kinase links chromosome cohesion to the initiation of DNA replication in *Xenopus* egg extracts. *Genes Dev* **22**: 1894–1905
- Takeda T, Ogino K, Matsui E, Cho MK, Kumagai H, Miyake T, Arai K, Masai H (1999) A fission yeast gene, him1(+)/dip1(+), encoding a regulatory subunit for Hsk1 kinase, plays essential roles in S-phase initiation as well as in S-phase checkpoint control and recovery from DNA damage. *Mol Cell Biol* **19**: 5535–5547
- Tenca P, Brotherton D, Montagnoli A, Rainoldi S, Albanese C, Santocanale C (2007) Cdc7 is an active kinase in human cancer cells undergoing replication stress. *J Biol Chem* **282**: 208–215
- Weber JD, Taylor LJ, Roussel MF, Sherr CJ, Bar-Sagi D (1999) Nucleolar Arf sequesters Mdm2 and activates p53. *Nat Cell Biol* **1**: 20–26
- Wei CL, Wu Q, Vega VB, Chiu KP, Ng P, Zhang T, Shahab A, Yong HC, Fu Y, Weng Z, Liu J, Zhao XD, Chew JL, Lee YL, Kuznetsov VA, Sung WK, Miller LD, Lim B, Liu ET, Yu Q *et al* (2006) A global map of p53 transcription-factor binding sites in the human genome. *Cell* **124**: 207–219
- Wharton SB, Hibberd S, Eward KL, Crimmins D, Jellinek DA, Levy D, Stoeber K, Williams GH (2004) DNA replication licensing and cell cycle kinetics of oligodendroglial tumours. *Br J Cancer* **91**: 262–269
- You Z, Harvey K, Kong L, Newport J (2002) Xic1 degradation in *Xenopus* egg extracts is coupled to initiation of DNA replication. *Genes Dev* **16**: 1182–1194
- Zhang Y, Xiong Y, Yarbrough WG (1998) ARF promotes MDM2 degradation and stabilizes p53: ARF-INK4a locus deletion impairs both the Rb and p53 tumor suppression pathways. *Cell* **92**: 725–734
- Zhao H, Piwnicka-Worms H (2001) ATR-mediated checkpoint pathways regulate phosphorylation and activation of human Chk1. *Mol Cell Biol* **21**: 4129–4139





## Chapter 7

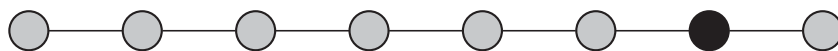
# Targeting DNA replication before it starts: Cdc7 as a therapeutic target in p53-mutant breast cancers

S Rodriguez-Acebes, I Proctor, M Loddo, A Wollenschlaeger, M Rashid, M Falzon, AT Prevost, R Sainsbury, K Stoeber, GH Williams

American Journal of Pathology 2010 177 (4): 2034-2045.

Supplementary material related to this article is available online at:

<http://www.journals.elsevierhealth.com/periodicals/ajpa/article/S0002-9440%2810%2960253-2/add0ns>



# Targeting DNA Replication before it Starts

## *Cdc7 as a Therapeutic Target in p53-Mutant Breast Cancers*

Sara Rodriguez-Acebes,\* Ian Proctor,<sup>†</sup>  
Marco Loddo,\* Alex Wollenschlaeger,\*  
Mohammed Rashid,<sup>†</sup> Mary Falzon,<sup>†</sup>  
A. Toby Prevost,<sup>†‡</sup> Richard Sainsbury,<sup>§</sup>  
Kai Stoeber,\*<sup>†</sup> and Gareth H. Williams\*<sup>†</sup>

From the Wolfson Institute for Biomedical Research,\* the Departments of Pathology and UCL Cancer Institute,<sup>†</sup> and Surgery,<sup>§</sup> University College London, London; and the Department of Primary Care and Public Health Sciences,<sup>‡</sup> Guy's Campus, King's College London, London, United Kingdom

**Treatment options for triple-receptor negative (ER-/PR-/Her2-) and Her2-overexpressing (ER-/PR-/Her2+) breast cancers with acquired or *de novo* resistance are limited, and metastatic disease remains incurable. Targeting of growth signaling networks is often constrained by pathway redundancy or growth-independent cancer cell cycles. The cell-cycle protein Cdc7 regulates S phase by promoting DNA replication. This essential kinase acts as a convergence point for upstream growth signaling pathways and is therefore an attractive therapeutic target. We show that increased Cdc7 expression during mammary tumorigenesis is linked to Her2-overexpressing and triple-negative subtypes, accelerated cell cycle progression ( $P < 0.001$ ), arrested tumor differentiation ( $P < 0.001$ ), genomic instability ( $P = 0.019$ ), increasing NPI score ( $P < 0.001$ ), and reduced disease-free survival (HR = 1.98 [95% CI: 1.27–3.10];  $P = 0.003$ ), thus implicating its deregulation in the development of aggressive disease. Targeting Cdc7 with RNAi, we demonstrate that p53-mutant Her2-overexpressing and triple-negative breast cancer cell lines undergo an abortive S phase and apoptotic cell death due to loss of a p53-dependent Cdc7-inhibition checkpoint. In contrast, untransformed breast epithelial cells arrest in G1, remain viable, and are able to resume cell proliferation on recovery of Cdc7 kinase activity. Thus, Cdc7 appears to represent a potent and highly specific anticancer target in Her2-overexpressing and triple-negative breast cancers. Emerging Cdc7 kinase inhibitors may therefore significantly broaden the therapeutic armamentarium for treatment of the**

**aggressive p53-mutant breast cancer subtypes identified in this study.** (*Am J Pathol* 2010, 177:2034–2045; DOI: 10.2353/ajpath.2010.100421)

Breast cancer is the most frequently diagnosed malignancy in women in the Western world and accounts for around 16% of all cancer death.<sup>1</sup> Despite increasing incidence, these mortality figures are decreasing as a result of widespread screening programs and systemic use of adjuvant hormonal therapy and chemotherapy.<sup>2,3</sup> Moreover, targeted therapies for breast cancer are evolving rapidly and are broadening available therapeutic options.<sup>4,5</sup> Targeting of Her2/neu with trastuzumab has resulted in remarkable reductions in relapse when combined with chemotherapy in Her2-positive breast cancers.<sup>6</sup> However, the majority of patients are Her2-negative, and acquired and *de novo* resistance further limits this type of therapeutic intervention. This has led to the targeting of additional components of growth and survival signaling pathways including ras, raf, Mek, PI3K, and mTOR.<sup>7</sup> It is not yet clear how maximal blockade of vertical signal transduction pathways with a combination of receptor and downstream agents will be tolerated. This approach is further compromised by pathway redundancy and cancer cell cycles becoming independent of upstream growth signaling pathways, so-called autonomous cancer cell cycles.<sup>8</sup> In particular, therapeutic options for treatment of basal-like cancers are severely constrained by their estrogen (ER), progesterone (PR), and Her2 triple-receptor negative status. New molecularly targeted therapies are therefore urgently required for aggressive breast cancers if further decline in mortality is to be achieved.

Supported by Cancer Research UK Scientific Program grant C428/A6263 (to K.S. and G.H.W.).

S.R.-A. and I.P. contributed equally to this study.

Accepted for publication June 10, 2010.

Supplemental material for this article can be found on <http://ajp.amjpathol.org>.

Address reprint requests to Dr. Kai Stoeber, Ph.D., Department of Pathology, Rockefeller Building, 21 University Street, London, WC1E 6JJ, UK. E-mail: k.stoeber@ucl.ac.uk.

An alternative approach to the vertical targeting of signal transduction pathways is to direct therapeutic interventions downstream at the DNA replication initiation machinery.<sup>8</sup> Cdc7 kinase is a core component of this machinery and is therefore a potentially attractive target for cancer therapy.<sup>9</sup> Cdc7 kinase phosphorylates and activates the Mcm2-7 replicative helicase, an essential step for the initiation of DNA synthesis at chromosomal replication origins.<sup>10–12</sup> Cancer cells have been shown to establish only limited numbers of replication forks under Cdc7 rate-limiting conditions, causing fork stalling/collapse during an abortive S phase that is followed by apoptotic cell death.<sup>13,14</sup> Untransformed human fibroblasts, on the contrary, appear to avoid lethal S phase progression in the presence of low Cdc7 levels by eliciting a p53-dependent Cdc7-inhibition checkpoint that arrests cells at the G1/S boundary.<sup>13</sup> However, it has not yet been established whether this checkpoint is active in cell types of epithelial lineage, such as mammary epithelial cells. Furthermore, it is currently unclear whether the cell cycle arrest after Cdc7 inhibition is reversible. This is an essential prerequisite in the therapeutic context, as an irreversible cytostatic arrest would cause severe toxicity effects in self-renewing tissues with high turnover (eg, skin, gut mucosa and bone marrow).

The Mcm2-7 replication initiation factors (MCM) have emerged as diagnostic and prognostic biomarkers for cancer.<sup>8</sup> More recently, we have reported that combined analysis of MCM expression and biomarkers of S-G2-M cell cycle phase progression (eg, geminin, Plk-1, Aurora A, and histone H3) allows *in vivo* determination of tumor cell cycle kinetics.<sup>8</sup> This has led to the identification of three discrete tumor cell cycle phenotypes in breast cancer: (I) well-differentiated tumors composed predominantly of MCM-negative cells, indicative of an out-of-cycle state; (II) tumors composed of cells with high MCM but low geminin, Plk-1, Aurora A, and histone H3 phosphorylated on Ser-10 (H3S10ph) levels, indicative of a G1-delayed/arrested state; and (III) tumors showing high MCM and S-G2-M marker expression, indicative of accelerated cell cycle progression (Figure 1).<sup>8,15</sup> The accelerated cell cycle phenotype had a higher risk of relapse when compared with out-of-cycle and G1-delayed/arrested phenotypes (hazard ratio [HR] = 3.90) and was tightly associated with the Her2-overexpressing and triple-receptor negative subtypes.<sup>15</sup> Because Cdc7 activity is rate-limiting for entry into S phase, the important question arises regarding whether overexpression of this essential kinase might be linked to breast cancers displaying the accelerated cell cycle phenotype (phenotype III) and thereby present an attractive target in Her2-overexpressing and triple-receptor negative cancers. Moreover, a high proportion (40–80%) of these aggressive tumor subtypes harbor p53 mutations,<sup>16–19</sup> suggesting that a large proportion of these breast cancers are likely to respond to Cdc7 inhibitors due to an impaired Cdc7-inhibition checkpoint.

Here we report the first detailed investigation of Cdc7 expression dynamics in breast cancer and investigate Cdc7 as a novel therapeutic target in p53<sup>mut</sup> Her2-overexpressing and triple-receptor negative tumors. Importantly,

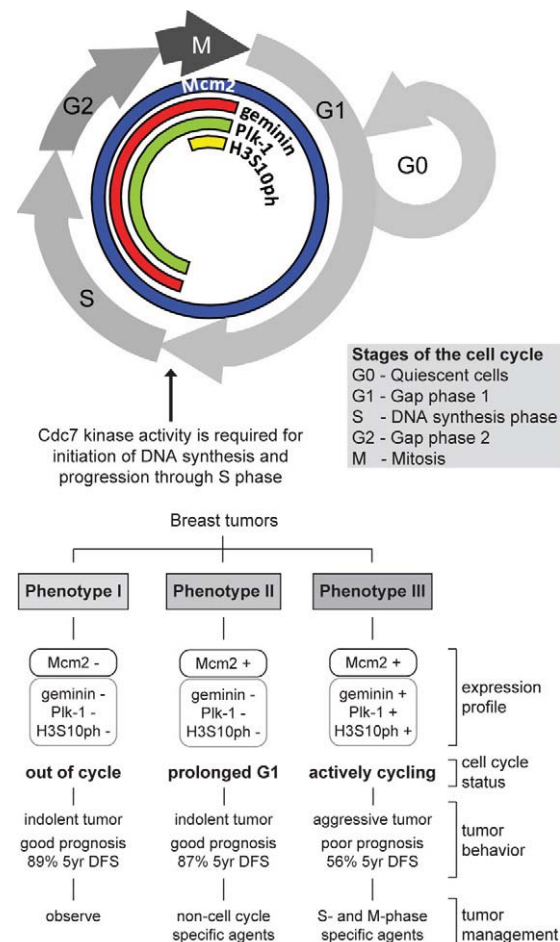


**Figure 1.** Phase-specific distribution of cell-cycle biomarkers in proliferating cells and out-of-cycle states. Three distinct cell-cycle phenotypes (I, II, and III) are characterized by the differential expression of cell-cycle biomarkers Mcm2, geminin, Plk-1, and histone H3 phosphorylated on Ser-10 (H3S10ph). Prognosis and treatment response can be predicted from the distinct immunoproteomic profile displayed by a tumor.<sup>15</sup> DFS indicates disease-free survival.

we also tested in untransformed breast epithelial cells whether the Cdc7-inhibition checkpoint is reversible, a prerequisite for targeting Cdc7 in cancer therapy.

## Materials and Methods

### Study Cohort

Patients diagnosed with invasive breast cancer between 1999 and 2004 were identified retrospectively at University College London Hospital (London, UK). Clinical characteristics of the patient cohort are presented in Supplemental Table 1 (at <http://ajp.amjpathol.org>). Histological specimens were assessed for histological subtype and tumor grade based on Royal College of Pathologists guidelines and established histological<sup>20</sup> and clinical criteria.<sup>21</sup> Archival patient breast tissue samples were retrieved from the archives of the UCLH Department of Pathology and included cases spanning histological grades 1–3. The 171 breast cancers were subdivided according to their ER, PR, and Her2 receptor status into

three distinct groups: ER+/PR+/Her2± ( $n = 135$ ), ER-/PR-/Her2+ ( $n = 8$ ), and ER-/PR-/Her2- ( $n = 28$ ). These subgroups, commonly termed “luminal,” “Her2,” and “triple-negative” cancers, respectively, approximate to subtypes previously defined by gene expression profiling.<sup>16</sup> Breast cancers were characterized according to cell cycle phenotype as described.<sup>15</sup> For each patient the Nottingham Prognostic Index (NPI) was calculated as described.<sup>21</sup> Randomly selected cases of clinically and histologically normal breast tissue from 21 premenopausal women who had undergone reduction mammoplasty were included in the study. Local research ethics approval for the study was obtained from the Joint UCL/UCLH Committees on the Ethics of Human Research.

### Antibodies

Rabbit polyclonal antibody (PAb) against human geminin was generated as described.<sup>22</sup> Antibodies were purchased from the following suppliers: Mcm2 (BM28, clone 46), p21 (SX118), and Rb (G3-245) monoclonal antibodies (MAb) from BD Biosciences (Oxford, UK); Mcm2 phosphorylated on Ser-53 (Mcm2S53ph) PAb from Bethyl Laboratories (Montgomery, TX); p53 (Ab-6 DO-1) and poly ADP ribose polymerase (PARP-1) (Ab-2 C-2-10) MAbs from Calbiochem Nottingham, UK; histone  $\gamma$ H2A.X and Rb phosphorylated on Ser-807/811 (pRbS807/811ph) PAbs from Cell Signaling (Danvers, MA); ER (1D5), Ki-67 (MIB-1) and PR (PgR 636) MAbs from Dako (Glostrup, Denmark); Cdc7 MAb from MBL International (Woburn, MA); caspase 8 (1-1-37) MAb, histone H3 phosphorylated on Ser-10 (H3S10ph) PAb and Plk-1 (35-206) MAb from Millipore (Watford, UK); caspase 3 (CPP32 4-1-18) MAb from Novus Biologicals (Cambridge, UK); caspase 9 (F7) MAb, cyclin A (C-19) PAb, cyclin B (GNS1) MAb, and cyclin E (C-19) PAb from Santa Cruz Biotechnology (Santa Cruz, CA); and  $\beta$ -actin MAb from Sigma (Dorset, UK).

### Immunoexpression Profiling

Paraffin wax-embedded tissue obtained at initial diagnosis was available for all patients. Tissue blocks were chosen that contained representative tumor sample. Immunoexpression profiling was performed as described.<sup>15</sup> Primary antibodies were applied at the following dilutions: Cdc7 (1:100), ER (1:200), and PR (1:200). Her2 immunostaining was performed using a HercepTest kit (Dako). Incubation without primary antibody was used as a negative control, and colonic epithelium was used as a positive control. Labeling indices (LI) of the markers in each tumor were determined as described.<sup>15,23–25</sup> To evaluate ER and PR expression, the quick (Allred) scoring system was used and positivity was defined as a score  $>2$ .<sup>26</sup> Her2 expression was assessed using the manufacturer's scoring system.

### DNA Image Analysis

For each case, one 40- $\mu$ m section of paraffin wax-embedded tissue obtained from the same block as that

assessed by immunohistochemistry was used to prepare nuclei as described.<sup>27</sup> Tumor DNA ploidy status was determined using the Fairfield DNA Ploidy System (Fairfield Imaging, Nottingham, UK) as described.<sup>15</sup> For statistical analysis, tetraploid and polyploid tumors were grouped with aneuploid tumors.

### Cell Culture, Population Growth Assessment, and Cell Cycle Analysis

BT549 cells (ATCC HTB-122, LGC Standards, Middlesex, UK) and T47D cells (ATCC HTB-133) were cultured in RPMI 1640 medium (Invitrogen, Paisley, UK) supplemented with 10% fetal bovine serum (FBS, Invitrogen) and 10  $\mu$ g/ml insulin (Sigma). MDAMB157 (ATCC HTB-24) cells were cultured in DMEM (Invitrogen) plus 15% FBS and 10  $\mu$ g/ml insulin. MDAMB453 and MDAMB231 (ATCC HTB-131 and HTB-26) were cultured in DMEM plus 10% FBS. MCF7 cells (ATCC HTB-22) were grown in MEM (Invitrogen) plus 10% FBS and 10  $\mu$ g/ml insulin. MCF10A cells (ATCC CRL-10317) were cultured in DMEM/F12 medium (Invitrogen) supplemented with 5% horse serum (Invitrogen), 20 ng/ml human EGF (Prepro-Tech, Rocky Hill, NJ), 0.5  $\mu$ g/ml hydrocortisone, 100 ng/ml cholera toxin, and 10  $\mu$ g/ml insulin (Sigma). Human Mammary Epithelial Cells (HMEpC) were obtained from ECACC (830-05, Health Protection Agency Culture Collections, Salisbury, UK) and cultured at population doublings 10–20 in Mammary Epithelial Cell Growth Medium KIT (PromoCell, Heidelberg, Germany). All cells were cultured at 37°C with 5% CO<sub>2</sub>. Cell proliferation assessment and flow cytometric cell cycle analysis were performed as described.<sup>28,29</sup>

### CldU and IdU Incorporation Assay

Double-labeling experiments with 5-chloro-2'-deoxyuridine (CldU) and 5-iodo-2'-deoxyuridine (IdU) (Sigma) were performed as described.<sup>30</sup> Primary antibodies used were mouse anti-5-bromo-2'-deoxyuridine (BrdU) for IdU (B44, BD Biosciences) and rat anti-BrdU for CldU (BU1/75, Abcam, Cambridge, UK). DNA was visualized with DAPI. Confocal fluorescence microscopy of random fields of nuclei was performed as below and images of the DAPI channel (blue), Alexa Fluor 488 channel (green, CldU), and Alexa Fluor 594 channel (red, IdU) were obtained. Three hundred to 500 DAPI-stained nuclei (blue) were routinely counted for each treatment, and the percentage of labeled nuclei was quantified. Images of individual nuclei were acquired at  $\times 1000$  magnification.

### RNA Interference

Small interfering RNA (siRNA) experiments in transformed cell lines were performed as described<sup>29</sup> using a specific RNA duplex targeting Cdc7 mRNA (Thermo Scientific, Chicago, IL): sense 5'-GCT CAG CAG GAA AGG TGT TTT-3' and antisense 5'-AAC ACC TTT CCT GCT GAG CTT-3'. Nontargeting siRNA (Invitrogen) was used as negative con-



trol for all transformed cells. All transfections were performed with Lipofectamine 2000 (Invitrogen) according to the manufacturer's directions, and 75 nmol/L (BT549), 100 nmol/L (MDAMB157 and MDAMB453), or 10 nmol/L (HMEpC) of CDC7 siRNA was used to achieve efficient knockdown. For double-transfection with CDC7 and p53 siRNAs (p53 specific duplex, sense 5'-GGA AGA CUC CAG UGG UAA UUU-3' and antisense 5'- AUU ACC ACU GGA GUC UUC CUU-3' and ON-TARGETplus SMARTpool TP53 L-003329-00 [Thermo Scientific]), HMEpC and MCF10A cells were first transfected with 10 nmol/L CDC7 or control (Luciferase siRNA, Ambion, Austin, TX) siRNA. After 24 hours medium was removed and cells were retransfected with control (20 nmol/L), CDC7 (10 nmol/L) plus control (10 nmol/L), or CDC7 (10 nmol/L) plus p53 (9 nmol/L duplex plus 1 nmol/L SMARTpool) siRNA mixtures. Cells were harvested at the indicated time points after the second transfection. Efficient knockdown was assessed by qRT-PCR and/or Western blot.

### Real-Time PCR

Total RNA was isolated from cells with the PureLink Microto-Midi Total RNA Purification System (Invitrogen) according to the manufacturer's instructions. Total RNA (40 ng) was reverse transcribed, and real-time PCR was performed using a SuperScript III Platinum SYBR Green OneStep qRT-PCR kit (Invitrogen) following the manufacturer's instructions. Reactions were carried out in an Eppendorf Mastercycler ep Realplex Real-Time PCR System (Eppendorf, Cambridge, UK), and results were analyzed with Realplex v1.5 software (Eppendorf). Primer sequences were: CDC7 forward 5'-AACTTGCAGGTGTTAAAAAAG-3' and reverse 5'-TGAAAGTGCCTTCTCCAAT-3'; GAPDH (invariant control) forward 5'-TCAACTACATGGTTTACATGTTC-3' and reverse 5'-GATCTCGCTCCTGGAAGAT-3'.

### BrdU Cell Proliferation Assay

Cells were seeded on glass coverslips and subjected to RNA interference as described above. Before harvest, cells were pulsed with 10  $\mu$ mol/L BrdU (Sigma) for 1 hour at 37°C. Cells were fixed with 1% paraformaldehyde and permeabilized with PBS/0.2% Triton X-100. DNA was denatured with 2 N HCl for 1 hour and cells were incubated with anti-BrdU-FITC antibody (Alexis Biochemicals, Exeter, UK), 50 ng/ml propidium iodide (PI), and 50 ng/ml RNase A (both from Sigma). Each coverslip received a final wash with PBS before being mounted in Vectashield (Vector Laboratories, Peterborough, UK) mounting medium. Fluorescence confocal microscopy of random fields of nuclei was performed on a Leica TCS SP confocal microscope (Leica, Buckinghamshire, UK). Images were collected, and pictures of the PI channel (red) and FITC channel (green) were obtained using Leica TCS PowerScan software (Leica). The original magnification was  $\times 200$ . Three hundred to 500 PI-stained nuclei (red) were routinely counted for each treatment, and the percentage of nuclei incorporating BrdU (green) was quantified.

### Western Blot Analysis

Whole cell extracts (WCE) were prepared by cell lysis in modified RIPA buffer (50 mmol/L Tris-Cl pH 7.4, 300 mmol/L NaCl, 0.1% NP40, 1% Triton X-100, 0.5% sodium deoxycholate, 0.1% SDS, 5 mmol/L EDTA, 1 mmol/L EGTA, 100 mmol/L sodium fluoride and 1 mmol/L sodium orthovanadate) followed by sonication for 10 seconds. Fifty micrograms of protein was loaded in each lane, separated by 4–20% SDS-PAGE, and transferred by semidry electroblotting onto Hybond C Extra nitrocellulose membranes (GE Healthcare, Buckinghamshire, UK). Blocking, antibody incubations, and washing steps were performed as described.<sup>31</sup>

### TUNEL Assay

Cells were seeded on glass coverslips and subjected to RNA interference as described above. After 96 hours cells were fixed in 1% paraformaldehyde. The TUNEL assay was performed using an ApopTag Fluorescein Direct In Situ Apoptosis Detection kit (Millipore) according to the manufacturer's instructions. Coverslips were washed in PBS before being mounted in Vectashield with 1.5  $\mu$ g/ml DAPI. Confocal fluorescence microscopy of random fields of nuclei was performed as described above, and images of the DAPI channel (blue) and FITC channel (green) were obtained. Three hundred to 500 DAPI-stained nuclei (blue) were routinely counted for each treatment, and the percentage of TUNEL-positive nuclei (green) was quantified.

### Statistical Analysis

Labeling indices were summarized using median and interquartile range. Relationships between Cdc7 expression and tumor grade, lymph node status, tumor subtype, NPI, DNA ploidy status, and cell cycle phenotype were assessed using a combination of nonparametric Jonckheere-Terpstra, Mann-Whitney, and Kruskal Wallis analysis of variance tests as appropriate (Supplemental Table 2 at <http://ajp.amjpathol.org>). Analysis of disease-free and overall survival was performed using Kaplan-Meier plots (using high and low categories of Cdc7 as above and below the median value, respectively) and Cox regression (treating Cdc7 expression level as a continuous variable). Hazard ratios (with 95% confidence intervals [CI]) for Cdc7 and cell cycle phenotype were estimated separately in univariate analysis and then combined in multivariate analysis. Patients with incomplete data were excluded from multivariate analysis. All tests were two-sided and used a significance level of 0.05. Analysis was carried out using SPSS 12.0 for Windows (SPSS, Chicago, IL).

## Results

### Deregulated Cdc7 Expression Is Linked to Mammary Epithelial Tumorigenesis

Cdc7 protein levels are tightly down-regulated in quiescent and differentiated human cells.<sup>29</sup> Cdc7 dereg-



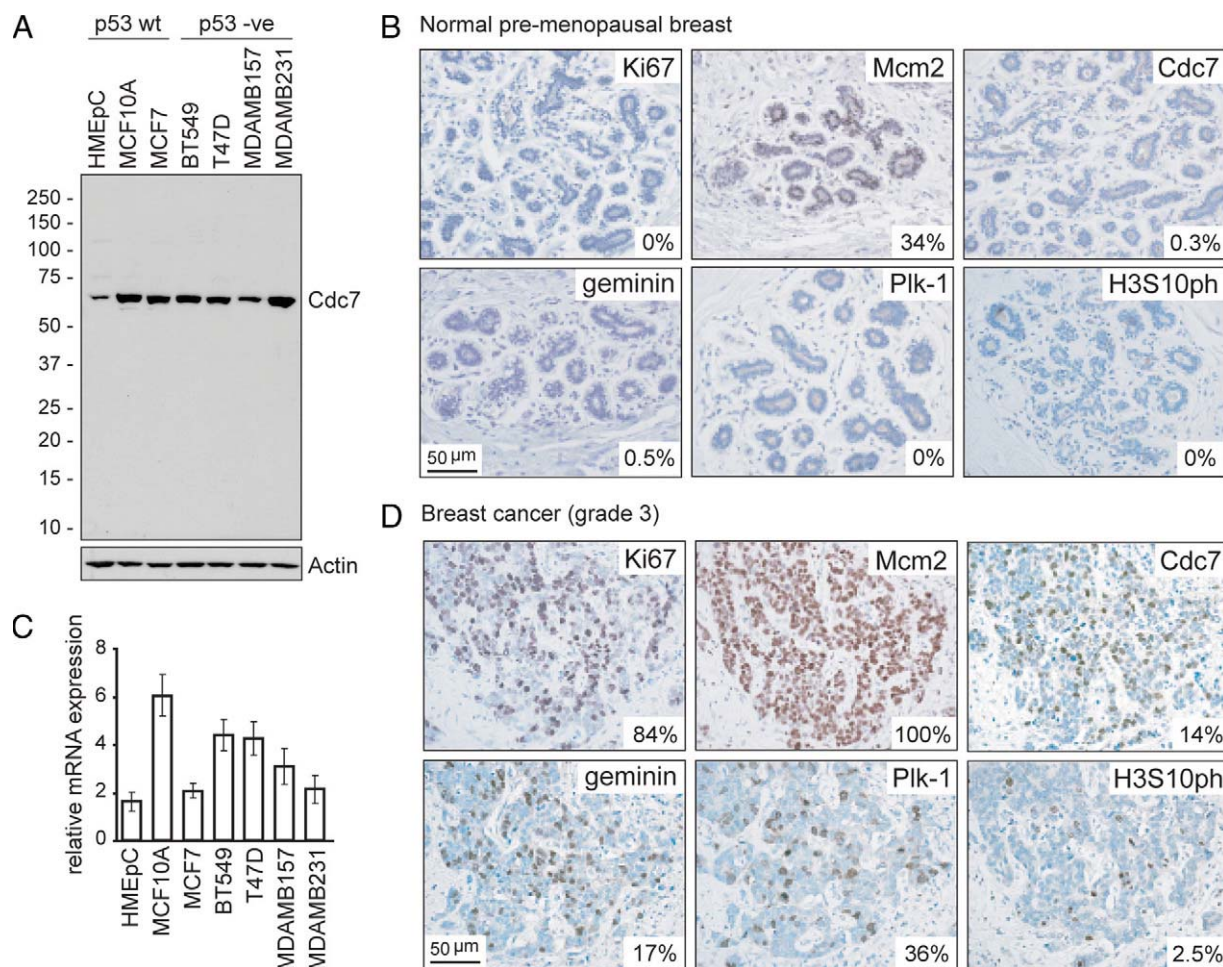


**Figure 2.** Cdc7 expression in breast epithelial cell lines and tissue. **A:** Immunoblot analysis of whole cell extracts (WCE) prepared from asynchronously proliferating cultures of normal (HMEpC), hyperproliferating (MCF10A), and malignantly transformed (MCF7, BT549, T47D, MDAMB157, and MDAMB231) breast epithelial cells probed with antibodies against Cdc7 and actin (loading control). **C:** CDC7 mRNA levels relative to GAPDH (invariant control) for each cell line as determined by qRT-PCR. **B and D:** Photomicrographs of tissue sections of representative normal premenopausal breast (**B**) and high-grade (grade 3) breast cancer (**D**) immunohistochemically stained with antibodies to the indicated proteins (original magnification,  $\times 400$ ). The median labeling index (LI) is shown for each marker. Median values and interquartile ranges for the cohort were as follows: Ki-67 40% (25%–69%); Mcm2 93% (70%–100%); Cdc7 14% (9%–22%); geminin 17% (11%–25%); Plk-1 14% (9%–20%); and H3S10ph 3% (1%–4%).

ulation leading to elevated levels of this essential kinase has been linked to acquisition of the malignant, hyperproliferative phenotype *in vitro* and *in vivo*.<sup>9</sup> Whether elevated Cdc7 levels are also associated with mammary epithelial tumorigenesis is not known. To address this question, we compared Cdc7 expression at RNA and protein level in asynchronously proliferating normal (HMEpC), hyperproliferating untransformed (MCF10A), and a panel of malignantly transformed (MCF7, BT549, T47D, MDAMB157, and MDAMB231) breast epithelial cell lines. Compared to primary cells, Cdc7 protein levels were between four- and 10-fold higher in hyperproliferating and the malignantly transformed cell lines as determined by Image J densitometry analysis (Figure 2A). Cdc7 mRNA levels were also raised in hyperproliferating and transformed cells, but to a lesser degree (Figure 2C). Next, we sought to investigate whether elevated Cdc7 levels are also associated with malignant transformation in breast epithelial cells *in vivo*. Epithelial cells of the terminal duct lobular unit appear to reside in a G1 arrested, “li-

censed” (primed) state, indicated by high MCM protein expression (median: 33.5%) and the absence of S-G2-M markers (<1%) (Figures 1 and 2B). Consistent with the finding that mammary epithelial cells withhold from progression through S-G2-M phase, Cdc7 expression was very low (median: 0.3%) (Figure 2B). In striking contrast, progression to the fully developed malignant phenotype (poorly differentiated, aggressive high-grade [grade 3] tumors) is associated with up-regulation of Cdc7 levels (median values: 0.3% versus 13.9%,  $P < 0.001$ ) (Figure 2, B and D). This is coupled with cell cycle progression as indicated by a significant increase in the proportion of cells expressing the S-G2-M markers geminin (median values: 0.5% versus 17.2%,  $P < 0.001$ ), Plk-1 (median values: 0% versus 36%,  $P < 0.001$ ), Aurora A (median values: 0% versus 11.4%,  $P < 0.001$ ) and H3S10ph (median values: 0% versus 2.5%,  $P < 0.001$ ) (Figure 2, B and D and data not shown). Taken together, these findings are in keeping with the rate-limiting effects of Cdc7 on cell proliferation.

### Increased Cdc7 Expression Is Associated with Arrested Tumor Differentiation and Genomic Instability

Next we examined the relationship between Cdc7 expression and pathological features associated with malignant behavior and clinical outcome in a cohort of 171 breast cancer cases (Supplemental Table 2 at <http://ajp.amjpathol.org>). Cdc7 expression showed a strong positive correlation with tumor grade ( $P < 0.001$ ), increasing markedly with the degree of arrested differentiation (Supplemental Fig. S1A at <http://ajp.amjpathol.org>). Increased Cdc7 expression was also associated with acquisition of genomic instability as defined by DNA ploidy status ( $P = 0.019$ ; Supplemental Fig. S1B at <http://ajp.amjpathol.org>). In contrast, no significant association was found between Cdc7 expression and nodal metastases ( $P = 0.54$ ; Supplemental Fig. S1C at <http://ajp.amjpathol.org>). Increased Cdc7 expression was also found to positively correlate with increasing NPI score ( $P < 0.001$ ) (Supplemental Fig. S2 at <http://ajp.amjpathol.org>).

### Increased Cdc7 Expression Is Associated with Accelerated Cell Cycle Progression, Breast Cancer Subtype and Reduced Disease-Free Survival

We have previously identified three distinct cell cycle phenotypes in this patient cohort of 171 breast cancers: (I) an “out-of-cycle” state ( $n = 30$ ); (II) a G1 arrested/delayed state ( $n = 41$ ); and (III) accelerated S-G2-M phase progression ( $n = 100$ ) (Figure 1).<sup>15</sup> The accelerated cell cycle progression phenotype has a fourfold higher risk of relapse when compared with the out-of-cycle and G1-delayed/arrested phenotypes (HR = 3.90 [95% CI: 1.81–8.4],  $P < 0.001$ ).<sup>15</sup> Extending our reported findings, we noted that Cdc7 expression was significantly increased in phenotype III tumors compared to phenotype I and II tumors (median values: 12.3% versus 1.0% and 4.1% respectively,  $P < 0.001$ ) (Figure 3A). The link between high Cdc7 expression levels and accelerated cell cycle progression is further reflected in the strong positive correlation between Cdc7 and the S-G2-M phase progression markers geminin (Spearman correlation coefficient = 0.8 [0.74–0.85],  $P < 0.001$ ), Plk-1 (0.74 [0.66–0.8],  $P < 0.001$ ), Aurora A (0.59 [0.48–0.68],  $P < 0.001$ ), and H3S10ph (0.63 [0.53–0.71],  $P < 0.001$ ).

Cdc7 expression was also significantly associated with breast cancer subtype. In contrast to “luminal” tumors (ER+/PR+/Her2+/-), Cdc7 expression in “Her2” (ER-/PR-/Her2+) and “triple-negative” (ER-/PR-/Her2-) tumors was significantly elevated (median values: 5.2% versus 19.6% and 20.6% respectively,  $P < 0.001$ ) (Supplemental Fig. S1D at <http://ajp.amjpathol.org>). Correspondingly, the majority of Her2 (91%) and triple-negative tumors (96%) were associated with the actively cycling phenotype III (Figure 3B). Taken together, these results establish a strong link between Cdc7 expression and accelerated cell cycle progression in breast cancer

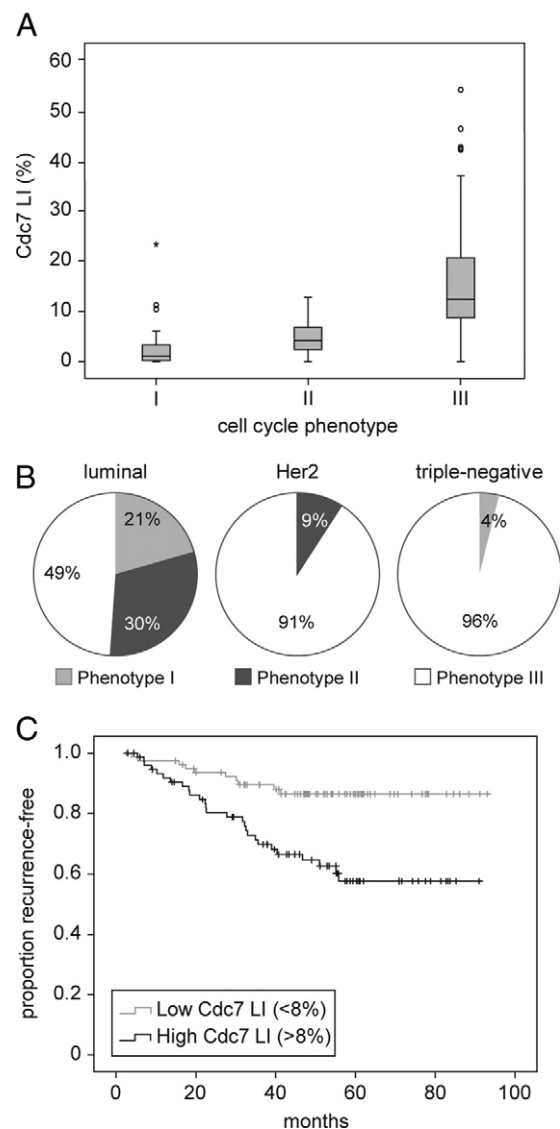


**Figure 3.** Relationship between Cdc7 expression, cell cycle phenotype, breast cancer subtype, and disease-free survival. **A:** The median (solid black line), interquartile range (boxed), and range (enclosed by lines) of Cdc7 expression across the breast cancer series are shown according to cell cycle phenotype (see text and Figure 1). Outlying cases are shown by isolated points. **B:** Relationship between cell-cycle phenotype and breast cancer subtypes. The panels show the proportion of each breast cancer subtype that display cell-cycle phenotypes I, II, and III. **C:** Kaplan–Meier curves showing an association between Cdc7 and disease-free survival (months from diagnosis to death, recurrence, or last follow-up) across the whole breast cancer series.

and show that increased Cdc7 expression is strongly associated with both Her2-overexpressing and triple-receptor negative breast cancer subtypes.

We have reported that the accelerated cell cycle phenotype (III) has a poor prognosis when compared with the out-of-cycle (I) and G1 delayed/arrested (II) phenotypes (HR = 3.90) and is an independent predictor of survival when compared with NPI in multivariate analysis (HR = 2.71).<sup>15</sup> In keeping with this finding, in the same patient cohort Cdc7 is a predictor of disease-free survival in both univariate and multivariate (NPI-adjusted) analyses (HR = 1.98 [1.27–3.10],  $P = 0.003$  and HR = 1.80 [1.43–2.28],  $P = 0.025$  [per 20% increase in Cdc7 levels] respectively) (Fig-

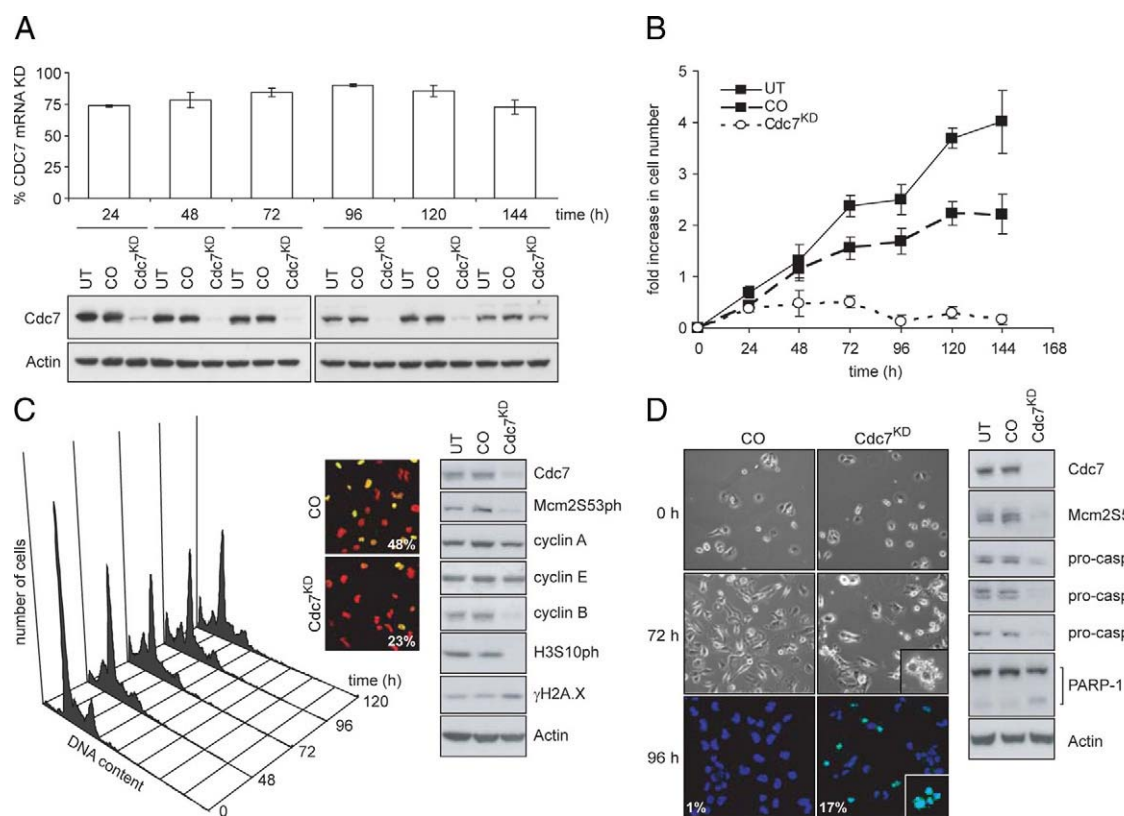


**Figure 4.** Cdc7 depletion causes apoptosis in BT549 (triple-receptor negative) breast cancer cells. **A:** Time course of CDC7 mRNA knockdown (KD) in BT549 cells relative to cells transfected with control-siRNA (CO) (**upper panel**). Immunoblot analysis of untreated (UT), control-siRNA-, and CDC7-siRNA-transfected BT549 whole cell extracts (WCE) probed with the indicated antibodies (**lower panel**). **B:** At the indicated time points, cell number was measured in UT, CO, and Cdc7-depleted (Cdc7<sup>KD</sup>) cell populations. The graph shows fold-increase in cell numbers calculated for each time point relative to the number of cells seeded. **C:** DNA content of Cdc7<sup>KD</sup> cells at the indicated times (**left panel**). At 72 hours posttransfection, BrdU incorporation was assayed. DNA was stained with propidium iodide (PI). Merged images of the BrdU-FITC (green) and PI (red) channels show the percentage of BrdU-positive cells (**center panel**). WCE from UT, CO, and Cdc7<sup>KD</sup> cells immunoblotted with the indicated antibodies (**right panel**). **D:** Cell death and fragmented apoptotic nuclei (**inset**) were analyzed by phase-contrast microscopy and positive TUNEL staining in Cdc7<sup>KD</sup> and CO cells (**left panel**). DAPI was used to stain DNA. Apoptotic cell death was confirmed in Cdc7<sup>KD</sup> cells by WCE immunoblotting with the indicated antibodies (**right panel**).

ure 3C). These data further implicate Cdc7 deregulation in the development of aggressive disease.

### Loss of Cdc7 Function Causes Apoptosis in Her2-Overexpressing and Triple-Receptor Negative Breast Cancer Cells

The majority of Her2-overexpressing and triple-receptor negative breast tumors harbor p53 mutations.<sup>16,18</sup> Because loss of functional p53 appears to impair the Cdc7-inhibition checkpoint,<sup>13</sup> Cdc7 kinase might be a new therapeutic target in these aggressive tumor subtypes. To test this hypothesis, we have used RNAi against CDC7 in three breast cancer cell lines (BT549, MDAMB157, and MDAMB45) with molecular characteristics approximating to Her2-overexpressing and triple-negative tumors.<sup>32,33</sup> BT549 cells (ER<sup>-</sup>/PR<sup>-</sup>/Her2 nonamplified, p53<sup>mut</sup>) were transfected with previously characterized CDC7-siRNA.<sup>13</sup> Relative to nontargeting control-siRNA (CO), transfection with CDC7-siRNA (Cdc7<sup>KD</sup>) reduced CDC7 mRNA levels by >90% at 96 hours posttransfection (Figure 4A). Correspondingly, in WCE Cdc7 protein was undetectable by Western blotting from 48 hours to 96 hours posttransfection, with levels increasing again from 120 hours onwards when

the RNAi effect had been washed out (Figure 4A). Consistent with efficient Cdc7 depletion at 72 hours posttransfection, Mcm2 phosphorylation at Ser-53, a known phosphosite for Cdc7,<sup>34</sup> was abolished (Figure 4, C and D). In addition, CDC7 down-regulation caused a cessation of cell proliferation. Cdc7-depleted cells showed an increase in cell numbers of just 0.2-fold at 144 hours, compared with increases of 4.0-fold for untreated (UT) cells and 2.2 fold for control-transfected (CO) cells (Figure 4B). BT549 cells depleted of Cdc7 appeared to enter an abortive S phase as demonstrated by a decrease in both the percentage of BrdU-incorporating cells (23% compared to 48% in CO cells) and the intensity of fluorescence, which directly correlates with the amount of BrdU incorporation (Figure 4C). Cdc7-depleted cells exhibited an increase in  $\gamma$ H2A.X levels, indicative of DNA double strand breaks (Figure 4C) and, further supporting the notion of an abortive S phase, did not progress to G2/M phase as demonstrated by the lack of cyclin B and histone H3 Ser-10 phosphorylation (Figure 4C).<sup>35</sup> Flow cytometry confirmed a progressive decline in the G2/M population in Cdc7-depleted cells and revealed a concomitant increase in the number of cells with less than 2C DNA content (Figure 4C). The detection of a sub-G1 population of cells, as well as morphological changes such



as cell shrinkage and nuclear blebbing and abundant TUNEL staining (Figure 4D) compared to controls suggests that failure to elicit the Cdc7-inhibition checkpoint leads to apoptotic cell death in p53<sup>mut</sup> BT549 cells. As expected, activation of the apoptotic pathway in Cdc7-depleted BT549 cells 96 hours posttransfection was confirmed by a marked decrease in pro-caspase 3, 8, and 9 levels and detection of the apoptotic cleavage product of poly ADP ribose polymerase (PARP-1) (Figure 4D). MDAMB157 (ER-/PR-/Her2 nonamplified, p53<sup>mut</sup>) and MDAMB453 (ER-/PR-/Her2 amplified, p53<sup>mut</sup>) cells responded to CDC7 depletion in a similar manner to BT549 cells by entering an abortive S phase followed by induction of apoptosis in a significant proportion of cells (Supplemental Figs. S3 and S4 at <http://ajp.amjpathol.org>). The *in vitro* cell line data suggest that loss of p53 function may either contribute to or be sufficient for abrogation of the Cdc7-inhibition checkpoint in mammary epithelium.

### Loss of Functional p53 Disables the Cdc7-Inhibition Checkpoint in Untransformed Breast Epithelial Cells

To further investigate the link between p53 function and the Cdc7-inhibition checkpoint response, we first asked whether the checkpoint is active in untransformed mammary epithelial cells. To address this question, HMEpC and immortalized nontumorigenic MCF10A cells (p53<sup>wild</sup>) were first transfected with CDC7-siRNA. Relative to control-siRNA (CO) at 72 hours posttransfection, CDC7-siRNA (Cdc7<sup>KD</sup>) reduced CDC7 mRNA levels in HMEpC and MCF10A cells by 90% and 95%, respectively (data not shown). At this time point, Cdc7 protein levels were undetectable in WCE prepared from MCF10A cells and were found to be markedly reduced in HMEpC cells (Figure 5A and Supplemental Fig. S5A at <http://ajp.amjpathol.org>). In both lines, Cdc7 levels eventually recovered to a detectable level after washing out of the RNAi effect (at 96 hours in MCF10A cells and 144 hours in HMEpC, reflecting the shorter population doubling time of the immortalized line). CDC7 down-regulation prevented an increase in cell numbers up to 96 hours posttransfection in both cell lines (Figure 5B and Supplemental Fig. S5B at <http://ajp.amjpathol.org>). Cell proliferation resumed on recovery of Cdc7 levels at later time points, indicating that untransformed mammary epithelial cells retain the ability to re-enter the cell division cycle after Cdc7 levels are restored. Flow cytometry revealed that the majority of Cdc7-depleted HMEpC and MCF10A cells accumulated with G1 DNA content consistent with either a G1 or early S-phase arrest, while only a small fraction showed G2/M content (Figure 5C and Supplemental Fig. S5C at <http://ajp.amjpathol.org>). In keeping with the cell cycle profiles, the percentage of cells incorporating BrdU fell from 26% and 34% in control-transfected cells to 6% and 9% in Cdc7-depleted HMEpC and MCF10A cells (Figure 5C; and Supplemental Fig. S5D at <http://ajp.amjpathol.org>), indicating that the majority of cells had failed to synthesize DNA. Western blotting of WCE prepared from Cdc7-depleted HMEpC and MCF10A cells 72

hours posttransfection showed a marked increase in cyclin E levels, while levels of the S phase cyclin A and the mitotic cyclin B were reduced below the detection limit (Figure 5C and Supplemental Fig. S5E at <http://ajp.amjpathol.org>). Both Cdc7-depleted cell lines also showed loss of Rb phosphorylation at Ser-807/811, thought to be either Cdk4 or Cdk2 phosphorylation sites,<sup>36,37</sup> p53 stabilization and induction of p21 expression (Figure 5C and Supplemental Fig. S5E at <http://ajp.amjpathol.org>). Only a minute fraction of Cdc7-depleted HMEpC and MCF10A cells with less than 2C (sub G1) DNA content was detected by flow cytometry (Figure 5C and Supplemental Fig. S5C at <http://ajp.amjpathol.org>). Moreover, compared to control-transfected cells, neither an increase in cells with morphological features of apoptosis and positive TUNEL staining of nuclei (Figure 5D and Supplemental Fig. S5F at <http://ajp.amjpathol.org>) nor cleavage of pro-caspases 3 and 9 was observed in either cell line (Figure 5D and Supplemental Fig. S5E at <http://ajp.amjpathol.org>), indicating that arrested cells did not activate the cell death effector machinery. Taken together, the cell cycle phase distribution and cyclin profiles, low CDK activity evident from hypophosphorylated pRb, and the loss of BrdU incorporation support the notion that, in line with other untransformed cell types, breast epithelial cells operate a Cdc7-inhibition checkpoint that arrests the cell cycle at the G1-S boundary in response to low Cdc7 levels.

To test the supposition that loss of p53 function is sufficient to abrogate the Cdc7-inhibition checkpoint in mammary epithelial cells, we used RNAi to down-regulate p53 in HMEpC cells arrested by Cdc7 depletion. Western blot analysis of WCE prepared from cotransfected cells 72 hours posttransfection shows down-regulation of p53 to below baseline levels found in control cells, which in turn resulted in p21 down-regulation (Figure 5, A and C). Flow cytometry analysis of doubly depleted Cdc7/p53 cells shows an increase in the number of cells with S phase and G2/M DNA content 72 hours posttransfection. The number of cells with less than 2C DNA content progressively increased between 72 and 144 hours, coinciding with a sharp decline in the G2/M population (Figure 5C). Notably, in doubly depleted Cdc7/p53 cells Rb phosphorylation at Ser-807/811 increased, indicating recovery of CDK activity which is in keeping with low p21 levels (Figure 5C). The notion that cells lacking p53 function fail to maintain the Cdc7-inhibition checkpoint arrest, instead accumulating DNA double strand breaks ( $\gamma$ H2AX immunostaining; Figure 5D) while progressing through S phase (increase in the percentage of cells incorporating BrdU; Figure 5C) to the G2/M boundary, is further supported by the increase in cyclin A and cyclin B levels (Figure 5C). The decline in the G2/M population in doubly depleted Cdc7/p53 cells and concomitant increase in the number of cells with less than 2C DNA content (Figure 5C) suggests that failure to maintain the Cdc7-inhibition checkpoint leads to apoptotic cell death. As expected, induction of apoptosis in Cdc7/p53 doubly depleted cells was confirmed by the appearance of cells with morphological features of apoptosis, positive TUNEL staining of nuclei and procaspase

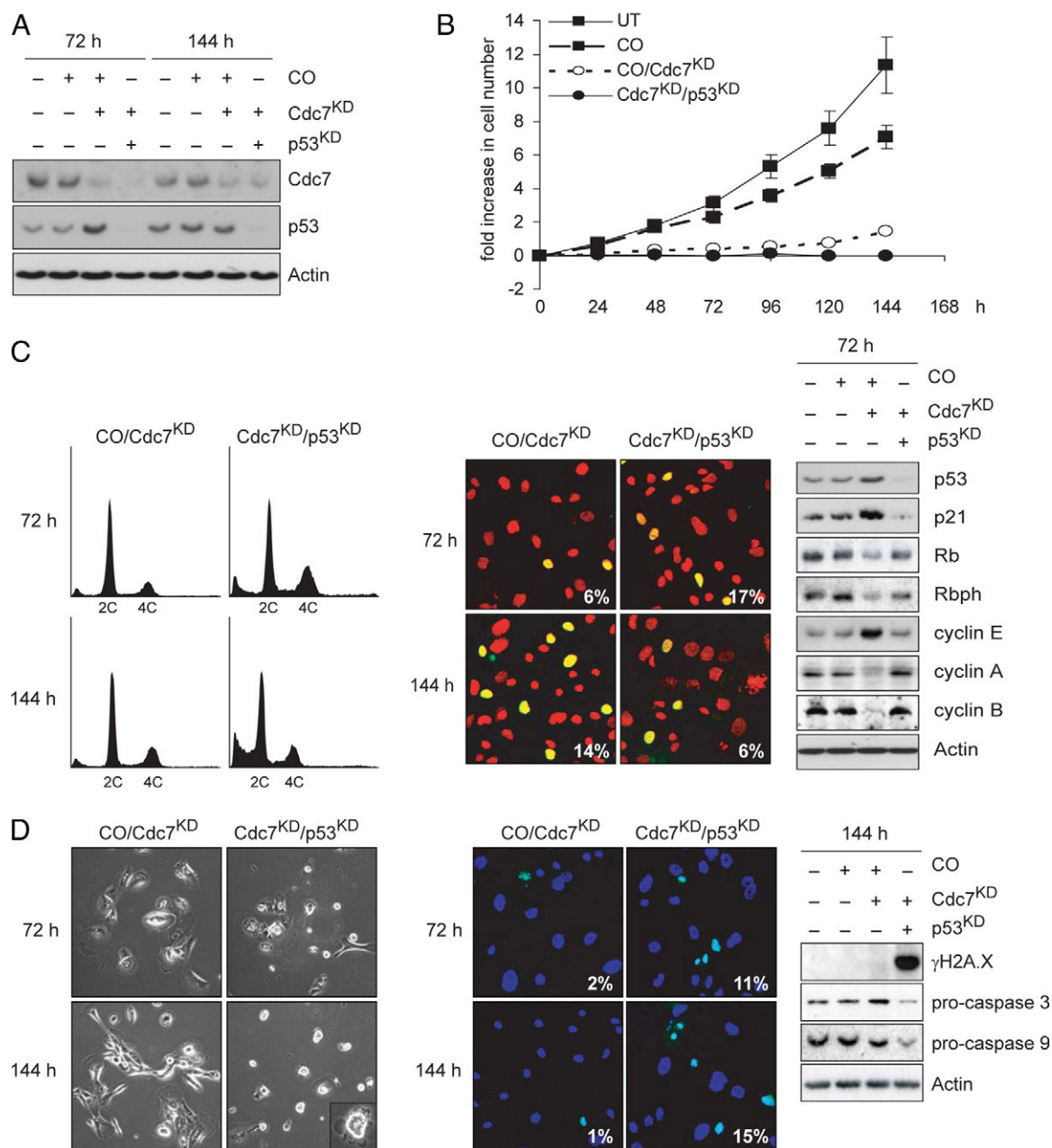


**Figure 5.** Cell cycle arrest in HMEpC cells following Cdc7 depletion is p53-dependent. **A:** Immunoblot analysis of WCE prepared from untreated (UT) HMEpC cells and cells transfected with control (CO), CDC7- plus CO- (CO/Cdc7<sup>KD</sup>), or CDC7- plus p53- (Cdc7<sup>KD</sup>/p53<sup>KD</sup>) siRNA probed with antibodies against Cdc7, p53, and actin (loading control). **B:** At the indicated time points, cell number was measured in UT, CO, CO/Cdc7<sup>KD</sup>, and Cdc7<sup>KD</sup>/p53<sup>KD</sup> cell populations. **C:** Cell cycle progression analysis of CO/Cdc7<sup>KD</sup> and Cdc7<sup>KD</sup>/p53<sup>KD</sup> HMEpC cells at the indicated time points, determined by DNA content (**left panel**), percentage of CO/Cdc7<sup>KD</sup>, and Cdc7<sup>KD</sup>/p53<sup>KD</sup> HMEpC cells incorporating BrdU (**center panel**), and WCE immunoblotting with the indicated antibodies (**right panel**). **D:** Apoptotic cell death was detected in Cdc7<sup>KD</sup>/p53<sup>KD</sup> HMEpC cells but not in CO or CO/Cdc7<sup>KD</sup> cells by phase-contrast microscopy (**left panel**), TUNEL staining (**center panel**), and immunoblotting for procaspase cleavage (**right panel**).

cleavage (Figure 5D). Thus loss of p53 function in early breast multistep tumorigenesis appears to be sufficient to override the Cdc7-inhibition checkpoint.

*The Cdc7-Inhibition Checkpoint-Mediated Cell Cycle Arrest Is Fully Reversible in Breast Epithelial Cells*

The RNAi data discussed above show that in untransfected breast epithelial cells, the Cdc7-inhibition check-

point blocks S phase progression without affecting cell viability. Notably, Cdc7 levels and proliferative capacity were restored between 96 and 144 hours posttransfection (Figure 6, A and B), most likely due to a wash out of the RNAi effect at later time points. An alternative explanation for the recovery of cell proliferation several days posttransfection would be the emergence of a population of proliferating cells that originated from a small fraction of nontransfected cells. To directly test whether arrested cells are able to initiate DNA synthesis after recovery of Cdc7 levels, we performed double-labeling of HMEpC

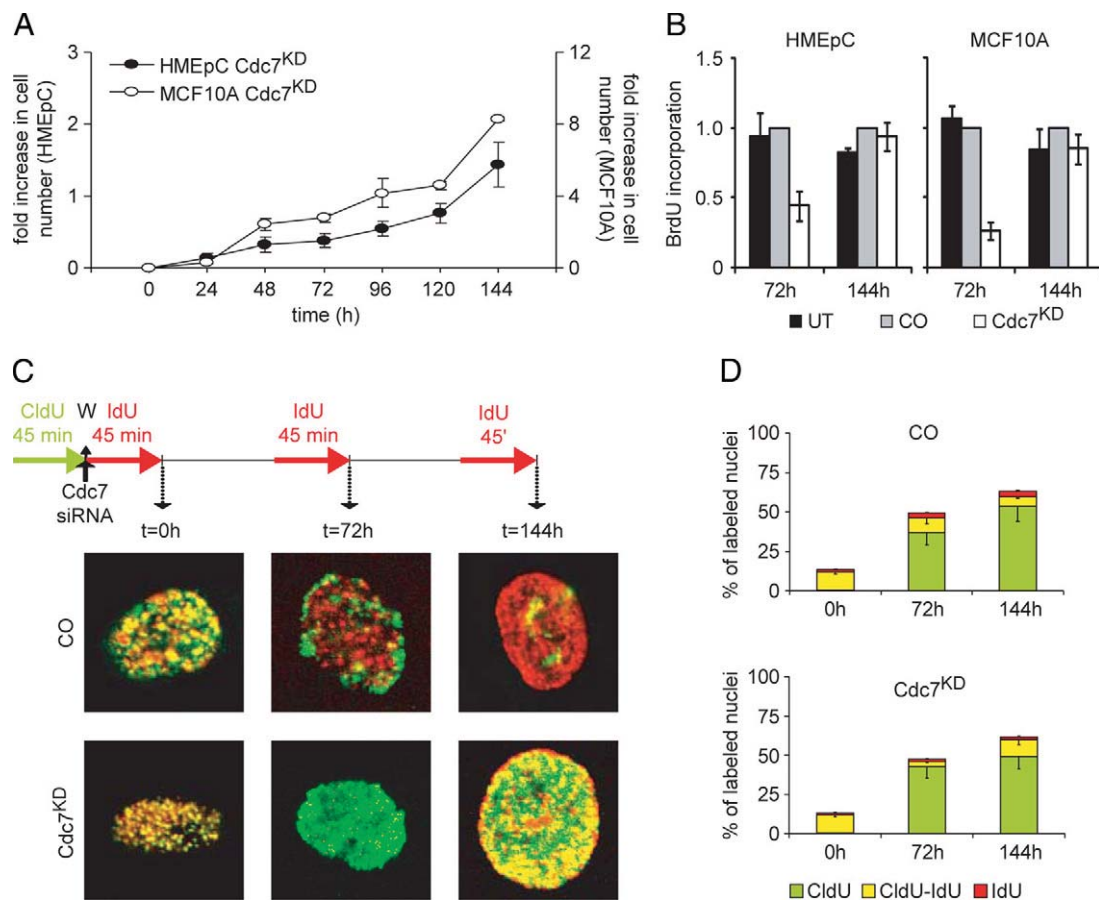


**Figure 6.** Cell cycle arrest in HMEpC cells after Cdc7 depletion is reversible. **A:** At the indicated time points, cell number was measured in Cdc7-depleted ( $Cdc7^{KD}$ ) HMEpC and MCF10A cell populations. **B:** BrdU incorporation in untreated (UT), control (CO), and CDC7-siRNA transfected HMEpC and MCF10A cells at the indicated time points (relative to CO). **C:** Cells transfected with CO- or CDC7- ( $Cdc7^{KD}$ ) siRNA were double-labeled with chlorodeoxyuridine (CldU) and iododeoxyuridine (IdU) as shown (W, washing step). Representative images of individual nuclei for each treatment are shown at high magnification. **D:** Percentage of nuclei labeled with halogenated nucleotides.

cells with CldU and IdU<sup>30</sup> pre- and posttransfection with CDC7-siRNA according to the protocol shown in Figure 6C. Cells were transfected with control- or CDC7-siRNA 45 minutes after the addition of CldU. Directly after the transfection ( $t_0$ ) and 71¼ hours ( $t_{72}$ ) and 143¼hours ( $t_{144}$ ) posttransfection, siRNA was washed out, and IdU was added to the medium for the next 45 minutes. Cells were then fixed and studied by confocal fluorescence microscopy with antibodies to CldU (green channel) and IdU (red channel). Representative cells are shown in Figure 6C, revealing different patterns of incorporation of the halogenated nucleotides into DNA. Control-transfected cells that were exponentially proliferating over the course of the experiment continued DNA synthesis at  $t_0$  which resulted in replication foci that were labeled green, red, or yellow (green + red) in merged images of the two channels. At  $t_{72}$  and  $t_{144}$ , control-transfected cells continued to synthesize DNA as indicated by IdU-incorporation (red pixels), while green pixel intensity per nucleus progressively decreased due to the distribution of incorporated CldU among daughter cells (Figure 6, C and D). In Cdc7-depleted cells only a minute population of 5% were incorporating IdU at  $t_{72}$ , whereas the amount of incorporated CldU (green pixel intensity per nucleus) was unaffected, consistent with cell cycle arrest. Importantly, in

line with the observed recovery of Cdc7 levels, at  $t_{144}$  cells were able to overcome the cell cycle arrest and initiated DNA synthesis as demonstrated by a 3.5-fold increase in the percentage of cells with double-labeled (yellow) nuclei (Figure 6, C and D). Thus primary breast epithelial cells respond to loss of Cdc7 function with a checkpoint-induced cell cycle arrest that is fully reversible when Cdc7 levels are restored.

## Discussion

The systemic treatment for patients with Her2-negative disease is still limited to endocrine and cytotoxic therapies,<sup>2</sup> and increasing use of taxanes and anthracyclines in early stage disease has reduced available therapeutic options after relapse. The vertical targeting of growth signaling pathways, for example with ras and mTOR antagonists, has shown efficacy in advanced breast cancer, but response rates are restricted to around 10% of patients.<sup>38,39</sup> Signaling pathway redundancy and establishment of autonomous cancer cell cycles potentially limits the efficacy of this approach. Novel therapeutic interventions are therefore urgently required for the treat-



ment of aggressive Her2-overexpressing and triple-negative breast cancers.

Here we have identified Cdc7 kinase as a potential therapeutic target in the treatment of Her2-overexpressing and triple-receptor negative breast cancers. Cdc7 lies at the convergence point of upstream growth signaling pathways and may therefore circumvent problems associated with pathway redundancy.<sup>8</sup> Moreover, Cdc7 activity is essential for S phase progression and therefore remains a potent target in cancer cell cycles that have become growth independent. Importantly, dysregulation of Cdc7 in breast cancer appears to be associated with the development of an aggressive malignant phenotype. Cdc7 overexpression was observed in immortalized and malignant cell lines when compared with primary mammary epithelial cells. Notably, increased Cdc7 expression was found to be linked to arrested tumor differentiation, genomic instability, reduced disease-free survival, an accelerated cell cycle phenotype, and Her2 (ER-/PR-/Her2+) and triple-receptor negative (ER-/PR-/Her2-) subtypes, implicating Cdc7 deregulation in the development of aggressive disease and thus providing further target validation for Cdc7 in breast cancer. RNAi targeting of Cdc7 resulted in potent cancer-cell-specific killing in p53<sup>mut</sup> triple-negative and Her2-overexpressing breast cancer cell lines. Primary mammary (HMEpC) and immortalized nontumorigenic (MCF10A) cell lines, on the contrary, avoided lethal S phase entry by activating a p53-dependent Cdc7-inhibition checkpoint resulting in cell cycle arrest at the G1-S boundary. Notably, RNAi targeting of p53 in HMEpC cells arrested by Cdc7 depletion resulted in abrogation of the Cdc7-inhibition checkpoint, which was followed by lethal S-G2-M phase progression, thus recapitulating the response observed in triple-negative and Her2-overexpressing p53<sup>mut</sup> cancer cell lines. Importantly, loss of p53 function is an early event in mammary multistep tumorigenesis, occurring at the preinvasive stage, with up to 60% of high-grade ductal carcinoma *in situ* lesions harboring p53 mutations.<sup>40–43</sup> Moreover, triple-receptor negative and Her2-overexpressing breast cancer subtypes have a high proportion, 40–80%, of p53 mutations, in keeping with the fact that these aggressive tumors are thought to arise from high-grade ductal carcinoma *in situ* lesions.<sup>16–19,43</sup> These observations indicate that loss of the Cdc7-inhibition checkpoint is likely to occur at an early stage in mammary multistep tumorigenesis and that pharmacological Cdc7 inhibitors currently in development<sup>9</sup> may thus have clinical utility not only in the treatment of aggressive Her2-overexpressing and triple-receptor negative tumor types but also in the treatment of ductal carcinoma *in situ* lesions. In addition, a proportion of luminal type tumors harbor p53 mutations (9 to 13%) display the aggressive cell cycle phenotype (III) and may therefore respond to Cdc7 inhibitors.

The double-labeling synthetic nucleoside incorporation experiments clearly demonstrate that the cell cycle arrest after activation of the Cdc7-inhibition checkpoint in primary somatic cells is reversible on recovery of Cdc7 kinase activity, and secondly, that cells remain fully viable while arrested at the G1-S boundary. This suggests that

Cdc7 inhibitors may have limited toxicity in self-renewing tissues with high turnover (eg, gut or the hemopoietic system), thus widening the potential therapeutic window. Interestingly, most systemic chemotherapeutic regimes for breast cancer, whether in the adjuvant setting or for the treatment of metastatic disease, involve combinations of S phase agents that target DNA synthesis (eg, anthracyclines and antimetabolites) and M phase agents with antimitotic activity (eg, taxanes, vinca alkaloids and epothilones).<sup>2</sup> The Achilles heel of these chemotherapeutic regimens is that S- and M-phase agents also affect normal cycling cells, resulting in marrow suppression (neutropenia), hair loss, and gut toxicity. Activation of the Cdc7-inhibition checkpoint in normal cycling cells using Cdc7 inhibitors before systemic chemotherapy with S- and/or M-phase agents may therefore provide a method of shielding normal cells from chemotherapeutic agents. In support of this concept, we have observed that primary somatic cells arrested by the Cdc7-inhibition checkpoint are completely shielded from anti-mitotic cyclotherapy (S. R. Kingsbury, A. Wollenschlaeger, R. Sainsbury, K. Stoeber, G. H. Williams, manuscript submitted for publication).

In summary, our findings show that Cdc7 kinase is a potent and highly specific anti-cancer target in Her2-overexpressing and triple-receptor negative breast cancers. Pharmacological Cdc7 kinase inhibitors emerging from drug development programs worldwide are therefore likely to significantly broaden the therapeutic armamentarium available for treatment of aggressive p53<sup>mut</sup> breast cancers, both in the adjuvant and metastatic setting. Analysis of cell cycle phenotype, Cdc7 expression levels, and p53 status may allow prediction of therapeutic response to such inhibitors. Forthcoming clinical trials with Cdc7 inhibitors will provide an opportunity for this novel treatment paradigm to be tested.

### Acknowledgments

We thank Joanna Franks and Caroline Richardson for assistance in retrieving archival tissue and recording clinicopathological parameters.

### References

1. Feuer EJ, Wun LM, Boring CC, Flanders WD, Timmel MJ, Tong T: The lifetime risk of developing breast cancer. *J Natl Cancer Inst* 1993, 85:892–897
2. Miles DW: Recent advances in systemic therapy. When HER2 is not the target: advances in the treatment of HER2-negative metastatic breast cancer. *Breast Cancer Res* 2009, 11:208
3. La Vecchia C, Bosetti C, Lucchini F, Bertuccio P, Negri E, Boyle P, Levi F: Cancer mortality in Europe, 2000–2004, and an overview of trends since 1975. *Ann Oncol* 2010, 21:1323–1360
4. Petrelli F, Cabiddu M, Cazzaniga ME, Cremonesi M, Barni S: Targeted therapies for the treatment of breast cancer in the post-trastuzumab era. *Oncologist* 2008, 13:373–381
5. Di Cosimo S, Baselga J: Targeted therapies in breast cancer: where are we now? *Eur J Cancer* 2008, 44:2781–2790
6. Hortobagyi GN: Trastuzumab in the treatment of breast cancer. *N Engl J Med* 2005, 353:1734–1736
7. Johnston SR: Targeting downstream effectors of epidermal growth factor receptor/HER2 in breast cancer with either farnesyltransferase

- inhibitors or mTOR antagonists. *Int J Gynecol Cancer* 2006, 16(Suppl 2):543–548
8. Williams GH, Stoeber K: Cell cycle markers in clinical oncology. *Curr Opin Cell Biol* 2007, 19:672–679
  9. Swords R, Mahalingam D, O'Dwyer M, Santocanale C, Kelly K, Carew J, Giles F: Cdc7 kinase - a new target for drug development. *Eur J Cancer* 2010, 46:33–40
  10. Machida YJ, Hamlin JL, Dutta A: Right place, right time, and only once: replication initiation in metazoans. *Cell* 2005, 123:13–24
  11. Remus D, Diffley JF: Eukaryotic DNA replication control: lock and load, then fire. *Curr Opin Cell Biol* 2009, 21:771–777
  12. Masai H, You Z, Arai K: Control of DNA replication: regulation and activation of eukaryotic replicative helicase. *MCM IUBMB Life* 2005, 57:323–335
  13. Montagnoli A, Tenca P, Sola F, Carpani D, Brotherton D, Albanese C, Santocanale C: Cdc7 inhibition reveals a p53-dependent replication checkpoint that is defective in cancer cells. *Cancer Res* 2004, 64:7110–7116
  14. Blow JJ, Gillespie PJ: Replication licensing and cancer—a fatal entanglement? *Nat Rev Cancer* 2008, 8:799–806
  15. Loddo M, Kingsbury SR, Rashid M, Proctor I, Holt C, Young J, El-Sheikh S, Falzon M, Eward KL, Prevost T, Sainsbury R, Stoeber K, Williams GH: Cell-cycle-phase progression analysis identifies unique phenotypes of major prognostic and predictive significance in breast cancer. *Br J Cancer* 2009, 100:959–970
  16. Sorlie T, Perou CM, Tibshirani R, Aas T, Geisler S, Johnsen H, Hastie T, Eisen MB, van de Rijn M, Jeffrey SS, Thorsen T, Quist H, Matese JC, Brown PO, Botstein D, Eystein LP, Borresen-Dale AL: Gene expression patterns of breast carcinomas distinguish tumor subclasses with clinical implications. *Proc Natl Acad Sci USA* 2001, 98:10869–10874
  17. Calza S, Hall P, Auer G, Bjohle J, Klaar S, Kronenwett U, Liu ET, Miller L, Ploner A, Smeds J, Bergh J, Pawitan Y: Intrinsic molecular signature of breast cancer in a population-based cohort of 412 patients. *Breast Cancer Res* 2006, 8:R34
  18. Tan DS, Marchio C, Jones RL, Savage K, Smith IE, Dowsett M, Reis-Filho JS: Triple negative breast cancer: molecular profiling and prognostic impact in adjuvant anthracycline-treated patients. *Breast Cancer Res Treat* 2008, 111:27–44
  19. Carey LA, Perou CM, Livasy CA, Dressler LG, Cowan D, Conway K, Karaca G, Troester MA, Tse CK, Edmiston S, Deming SL, Geradts J, Cheang MC, Nielsen TO, Moorman PG, Earp HS, Millikan RC: Race, breast cancer subtypes, and survival in the Carolina Breast Cancer Study. *JAMA* 2006, 295:2492–2502
  20. Bloom HJ, Richardson WW: Histological grading and prognosis in breast cancer; a study of 1409 cases of which 359 have been followed for 15 years. *Br J Cancer* 1957, 11:359–377
  21. Rampaul RS, Pinder SE, Elston CW, Ellis IO: Prognostic and predictive factors in primary breast cancer and their role in patient management: the Nottingham Breast Team. *Eur J Surg Oncol* 2001, 27:229–238
  22. Wharton SB, Hibberd S, Eward KL, Crimmins D, Jellinek DA, Levy D, Stoeber K, Williams GH: DNA replication licensing and cell cycle kinetics of oligodendroglial tumours. *Br J Cancer* 2004, 91:262–269
  23. Dudderidge TJ, Stoeber K, Loddo M, Atkinson G, Fanshawe T, Griffiths DF, Williams GH: Mcm2, Geminin, and Ki67 define proliferative state and are prognostic markers in renal cell carcinoma. *Clin Cancer Res* 2005, 11:2510–2517
  24. Kulkarni AA, Loddo M, Leo E, Rashid M, Eward KL, Fanshawe TR, Butcher J, Frost A, Ledermann JA, Williams GH, Stoeber K: DNA replication licensing factors and aurora kinases are linked to aneuploidy and clinical outcome in epithelial ovarian carcinoma. *Clin Cancer Res* 2007, 13:6153–6161
  25. Shetty A, Loddo M, Fanshawe T, Prevost AT, Sainsbury R, Williams GH, Stoeber K: DNA replication licensing and cell cycle kinetics of normal and neoplastic breast. *Br J Cancer* 2005, 93:1295–1300
  26. Harvey JM, Clark GM, Osborne CK, Allred DC: Estrogen receptor status by immunohistochemistry is superior to the ligand-binding assay for predicting response to adjuvant endocrine therapy in breast cancer. *J Clin Oncol* 1999, 17:1474–1481
  27. Haroske G, Giroud F, Reith A, Bocking A: 1997 ESACP consensus report on diagnostic DNA image cytometry. Part I: basic considerations and recommendations for preparation, measurement and interpretation European Society for Analytical Cellular Pathology. *Anal Cell Pathol* 1998, 17:189–200
  28. Eward KL, Obermann EC, Shreeram S, Loddo M, Fanshawe T, Williams C, Jung HI, Prevost AT, Blow JJ, Stoeber K, Williams GH: DNA replication licensing in somatic and germ cells. *J Cell Sci* 2004, 117:5875–5886
  29. Kulkarni AA, Kingsbury SR, Tudzarova S, Hong HK, Loddo M, Rashid M, Rodriguez-Acebes S, Prevost AT, Ledermann JA, Stoeber K, Williams GH: Cdc7 kinase is a predictor of survival and a novel therapeutic target in epithelial ovarian carcinoma. *Clin Cancer Res* 2009, 15:2417–2425
  30. Seiler JA, Conti C, Syed A, Aladjem MI, Pommier Y: The intra-S-phase checkpoint affects both DNA replication initiation and elongation: single-cell and -DNA fiber analyses. *Mol Cell Biol* 2007, 27:5806–5818
  31. Kingsbury SR, Loddo M, Fanshawe T, Obermann EC, Prevost AT, Stoeber K, Williams GH: Repression of DNA replication licensing in quiescence is independent of geminin and may define the cell cycle state of progenitor cells. *Exp Cell Res* 2005, 309:56–67
  32. Neve RM, Chin K, Fridlyand J, Yeh J, Baehner FL, Fevr T, Clark L, Bayani N, Coppe JP, Tong F, Speed T, Spellman PT, DeVries S, Lapuk A, Wang NJ, Kuo WL, Stilwell JL, Pinkel D, Albertson DG, Waldman FM, McCormick F, Dickson RB, Johnson MD, Lippman M, Ethier S, Gazdar A, Gray JW: A collection of breast cancer cell lines for the study of functionally distinct cancer subtypes. *Cancer Cell* 2006, 10:515–527
  33. Mackay A, Tamber N, Fenwick K, Iravani M, Grigoriadis A, Dexter T, Lord CJ, Reis-Filho JS, Ashworth A: A high-resolution integrated analysis of genetic and expression profiles of breast cancer cell lines. *Breast Cancer Res Treat* 2009, 118:481–498
  34. Montagnoli A, Valsasina B, Brotherton D, Troiani S, Rainoldi S, Tenca P, Molinari A, Santocanale C: Identification of Mcm2 phosphorylation sites by S-phase-regulating kinases. *J Biol Chem* 2006, 281:10281–10290
  35. Crosio C, Fimia GM, Loury R, Kimura M, Okano Y, Zhou H, Sen S, Allis CD, Sassone-Corsi P: Mitotic phosphorylation of histone H3: spatio-temporal regulation by mammalian Aurora kinases. *Mol Cell Biol* 2002, 22:874–885
  36. Connell-Crowley L, Harper JW, Goodrich DW: Cyclin D1/Cdk4 regulates retinoblastoma protein-mediated cell cycle arrest by site-specific phosphorylation. *Mol Biol Cell* 1997, 8:287–301
  37. Chi Y, Welcker M, Hizli AA, Posakony JJ, Aebersold R, Clurman BE: Identification of CDK2 substrates in human cell lysates. *Genome Biol* 2008, 9:R149
  38. Johnston SR, Hickish T, Ellis P, Houston S, Kelland L, Dowsett M, Salter J, Michiels B, Perez-Ruixo JJ, Palmer P, Howes A: Phase II study of the efficacy and tolerability of two dosing regimens of the farnesyl transferase inhibitor. R115777, in advanced breast cancer *J Clin Oncol* 2003, 21:2492–2499
  39. Chan S, Scheulen ME, Johnston S, Mross K, Cardoso F, Dittrich C, Eiermann W, Hess D, Morant R, Semiglazov V, Borner M, Salzberg M, Ostapenko V, Illiger HJ, Behringer D, Bardy-Bouxin N, Boni J, Kong S, Cincotta M, Moore L: Phase II study of temsirolimus (CCI-779), a novel inhibitor of mTOR, in heavily pretreated patients with locally advanced or metastatic breast cancer. *J Clin Oncol* 2005, 23:5314–5322
  40. Arpino G, Laucirica R, Elledge RM: Premalignant and in situ breast disease: biology and clinical implications. *Ann Intern Med* 2005, 143:446–457
  41. Nofech-Mozes S, Spayne J, Rakovitch E, Hanna W: Prognostic and predictive molecular markers in DCIS: a review. *Adv Anat Pathol* 2005, 12:256–264
  42. Meijnen P, Peterse JL, Antonini N, Rutgers EJ, van de Vijver MJ: Immunohistochemical categorisation of ductal carcinoma in situ of the breast. *Br J Cancer* 2008, 98:137–142
  43. Wiechmann L, Kuerer HM: The molecular journey from ductal carcinoma in situ to invasive breast cancer. *Cancer* 2008, 112:2130–2142



# Chapter 8

## Discussion

Despite decades of research, cancer remains a leading cause of death worldwide. The National Cancer Institute predicted that there would be 1,529,560 new cancer diagnoses and 569,490 cancer-related deaths in the US in 2010 (1). Early, accurate detection of malignancy would allow better treatment decisions and there is consequently an urgent need for new cancer biomarkers. Research output related to biomarker development continues to rise, although with rare exceptions, few new biomarkers have received regulatory approval for clinical use, leading to what some have dubbed the biomarker paradox (2).

The recent introduction of large-scale omics technologies has led to a surge of interest in biomarkers based on systems biology approaches (3). The coupling of new tools such as second-generation sequencing and proteomics to a more detailed understanding of cancer biology derived through basic research presents an approach that holds great promise for cancer diagnosis and individual-specific treatment, but there are still important obstacles to overcome, not least the excessive costs and technical limitations associated with these approaches (4).

Many current hypothesis-driven approaches to biomarker development target the complex networks of partially redundant signalling pathways that drive growth in normal cells and are deregulated in cancer (5-8). An important limitation to this approach is tumour heterogeneity. Three studies in 2008 using whole genome analysis on patients with pancreatic cancer and glioblastoma multiforme found that patients with pancreatic cancer carried on average 63 genetic lesions and those with glioblastoma multiforme had on average 47 alterations (9-11). The studies also found extensive mutation spectrum heterogeneity between patients. Considered together, these studies demonstrate the complexity inherent in cancer and highlight the obstacles that have so far prevented widespread clinical adoption of omics technology for diagnosis and therapeutic decisions. A second approach for biomarker development is to target the DNA replication initiation machinery, which acts downstream of these complex events (12, 13).

## Replication initiation proteins as diagnostic and prognostic cancer biomarkers

The six minichromosome maintenance proteins comprise the heterohexameric Mcm2-7 replicative helicase (14, 15). MCMs are downregulated in out-of-cycle states and are associated with differentiation arrest and aberrant growth, typical of dysplastic and neoplastic growth (12, 16, 17). MCMs are therefore potentially useful for detecting malignancy (Chapter 1). In this thesis I show that the replication initiation protein Mcm5 is a sensitive and specific diagnostic biomarker in bladder, prostate and pancreaticobiliary tract cancers.

Previous proof-of-concept studies demonstrated the potential of Mcm5 to diagnose bladder cancer, however most of these studies were based on small patient cohorts (16, 18). In Chapter 2, I present data from the first large-scale blinded multicentre study of Mcm5 as a biomarker for bladder cancer detection (Wollenschlaeger et al, manuscript in preparation). In a study of 1677 patients, the immunofluorometric Mcm5 test was able to detect bladder cancer in urine sediments with high sensitivity and specificity. The Mcm5 test had an area under the receiver operating characteristic curve (AUC) of 0.72 and, at the cut-point where specificity was equal to that of cytology, Mcm5 had significantly higher sensitivity for bladder cancer detection. The Mcm5 test showed performance similar to the US Food and Drug Administration approved urinary marker NMP22. In addition, combined detection of Mcm5 and NMP22 improved performance relative to either test alone, allowing detection of nearly all life-threatening cancers (muscle invasive and grade 3 tumours, including carcinoma in situ). A common shortcoming of current urinary bladder cancer markers is false positives due to benign conditions such as urinary tract infection and benign prostatic hyperplasia (19, 20). The results presented in Chapter 2 demonstrate that Mcm5 is not elevated by urinary tract infection, in contrast to NMP22 and consistent with indications from earlier studies (18). Mcm5 therefore appears to be a sensitive and specific biomarker for bladder cancer.

An important consideration in biomarker development is cost, particularly for non-muscle invasive bladder cancer, which has a high rate of recurrence that demands lifelong surveillance, making it among the most expensive cancers to treat (21-23). Currently surveillance relies on a combination of cystoscopy and cytology, which is demanding and has high patient morbidity (21, 24). Testing for Mcm5 is non-invasive and relies on antibody-based detection of the analyte in urine sediments, therefore making it potentially simple and cost-effective. Further improvement of Mcm5 as a diagnostic biomarker could include development of a standalone test that analyses urine directly to provide a rapid result in the examination room. Such a test, developed with an appropriate Mcm5 cut-point, has potential value in the screening setting but it would need to be extensively validated to ensure the population to be screened is correctly identified (21).

At present there are few screening programs in place, with those for breast, cervical, colon and prostate cancers being the best studied. In cervical cancer, the Papanicolaou stain cytological test is commonly used for screening, however the test is hindered by low sensitivity. One alternative to traditional screening is testing directly for human papilloma virus, a causal agent of cervical cancer (25). A second alternative is to increase the performance of the traditional screening test. ProEx C (Becton Dickinson/TriPath Imaging) is an immunoenhanced modification of the routine Papanicolaou test that includes immunodetection of Mcm5. The additional information provided by Mcm5 detection has previously been shown to improve the sensitivity of the Papanicolaou smear test without decreasing its specificity, demonstrating the potential of MCMs in the screening setting (12, 26).

Prostate cancer offers a compelling example of the need for constant evaluation of screening protocols, as there is growing awareness that patients are being overdiagnosed by current methods (27). The multinational European Randomized Study of Screening for Prostate Cancer study found that to prevent one death from prostate cancer, 1410 men would need to be screened and a further 48 cases would need to be treated (28). Similar results are emerging in preliminary reports from the Prostate, Lung, Colorectal, and Ovarian (PLCO) Cancer Screening Trial (29). These studies highlight the need for new biomarkers for prostate cancer.

A previous study observed that patients with prostate cancer were identified by the immunofluorometric Mcm5 urine test (18). The results presented in Chapter 3 demonstrate that Mcm5 has great potential as a diagnostic biomarker for this malignancy. In a study of 88 patients with confirmed prostate cancer and two control groups negative for malignancy, the Mcm5 test had peak sensitivity of 82% and specificity of 93% in a strictly normal control group of men with a benign final diagnosis and low PSA value, compared with 73% in an expanded control group chosen irrespective of their PSA reading (30). One possibility for the reduced specificity seen in the larger control group is the presence of occult tumours that were invisible to the diagnostic protocol employed, a suggestion supported by the rate of occult cancers seen in previous studies (31).

An important result from Chapter 3 is that the Mcm5 test did not give a higher signal in patients with benign prostatic hyperplasia. Among the major concerns about PSA is that it is organ specific rather than cancer specific and so is elevated in benign conditions. Studies have also shown that prostate cancer is common in patients with low PSA values, a finding supported by our study (30, 32). PSA values have been shown to rise naturally as men grow older. Attempts to account for this by measuring so-called PSA velocity and defining age-specific cut-offs have not had a major impact on the performance of PSA. To examine whether Mcm5 test sensitivity could be further improved, patients in our study underwent prostate massage prior to voiding to stimulate prostatic secretions. The sensitivity of the Mcm5 test was significantly higher following prostate massage in prostate cancer patients but not in normal controls, suggesting that this simple procedure may serve to further improve the performance of the Mcm5 test.



Together these findings suggest that Mcm5 is a sensitive marker for prostate cancer detection and warrant follow-up studies to confirm the results in a larger patient cohort.

Further evidence for the efficacy of Mcm5 as a cancer biomarker is presented in Chapter 4, in a study into use of Mcm5 detection for diagnosis of pancreaticobiliary tract cancer. This malignancy has a low 5-year survival rate, principally due to the advanced stage of the disease at primary detection and there are as yet no regulator approved diagnostic biomarkers. The study presented here demonstrates that MCMs are dysregulated in pancreaticobiliary tract cancer and that detection of Mcm5 is an accurate test for this malignancy (33). Immunofluorometric detection of Mcm5 in cells obtained from bile samples had significantly higher sensitivity compared with routine brush cytology (66 vs 20%) and had comparable positive predictive value (97 vs 100%). Preliminary findings suggest that test performance may be further improved by analysing cells obtained from biliary brushings (unpublished data). Previous studies suggested that bile samples were an inappropriate biofluid for cytologic analysis, principally due to reduced cellularity (34). The study presented here shows that bile, which is readily obtained during endoscopic retrograde cholangiopancreatography, is a viable medium for biomarker detection. Similar to bladder and prostate cancer, in pancreaticobiliary tract cancer the Mcm5 test was not affected by benign conditions including gallstones and chronic inflammation (33). These exciting findings suggest that Mcm5 is potentially a useful biomarker for pancreaticobiliary tract cancer diagnosis and require verification in an expanded study.

In addition to diagnostic utility, replication initiation proteins can potentially provide important prognostic information. The results presented in Chapter 5 show that replication initiation proteins together with markers of cell cycle progression and proliferation are potential prognostic markers in penile squamous cell carcinoma. Aggressive PeSCC is associated with poor prognosis and there are currently few prognostic markers. In a study of 141 men with PeSCC, Mcm2, geminin and the proliferation marker Ki67 were tightly associated with tumour differentiation and DNA ploidy status and identified men with a high risk of disease progression (35). Labelling indices for Mcm2 and Ki67 and Ki67-geminin score (reflective of an increase in the proportion of cells in G1; see Chapter 1) and DNA ploidy were significantly associated with overall survival on univariate analysis. In addition, a multivariate model comprising the conventional prognostic indicators age, lymph node status and tumour multifocality together with DNA ploidy status was able to stratify patients in low, middle and high risk groups. This study suggests that DNA replication initiation proteins are useful as prognostic markers in PeSCC.

A previous study demonstrated that the replication initiation proteins Mcm2 and geminin, the mitotic kinases Aurora A and Plk1, and the Aurora A substrate histone H3 phosphorylated on serine 10 together define a novel cell cycle progression readout. Applied to breast cancer, this cell cycle progression algorithm uniquely identified three cell cycle phenotypes: (1) a G0 out-of-cycle phenotype characterized by downregulation of Mcm2; (2) a G1 delayed/arrested phenotype

positive for Mcm2; and (3) an accelerated cell cycle progression phenotype in which all four makers were present (36). The accelerated cell cycle progression phenotype was associated with the aggressive human epidermal growth factor receptor 2 (HER2)-overexpressing and triple negative (oestrogen receptor negative, progesterone receptor negative, HER2 negative) breast cancer subtypes and identified tumours with a significantly higher risk of relapse when compared with the G0 out-of-cycle and G1 delayed/arrested phenotypes. Taken together, these studies suggest that replication initiation proteins in combination with specific markers of cell cycle progression and mitotic regulation hold potential to provide clinically important prognostic information that is able to guide further treatment selection.

## Characterization of the origin activation checkpoint

Replication initiation is a crucial event in the cell cycle that is under tight control. Previous studies showed that downregulation of the replication initiation protein Orc2 or expression of a nondegradable form of geminin leads to a block of cell cycle progression at the G1-S boundary with low CDK activity (37, 38). MCM proteins are key targets of the Dbf4-dependent kinase Cdc7 (39). Recent work by Montagnoli and colleagues showed that depletion of Cdc7 through RNA inhibition leads to a p53-dependent cell cycle arrest in normal cells, while cancer cells proceed into an abnormal S phase and subsequently induce apoptosis (40). These and other studies suggest that, faced with perturbed replication initiation, normal cells engage a putative origin activation checkpoint and prevent entry into S phase and that this checkpoint appears to be frequently lost in cancer cells (41). Consequently, Cdc7 has been identified as an important new target for directed therapeutic intervention (42-44). In the last five years, Cdc7 has drawn the attention of major pharmaceutical companies and spurred the development of new small molecule inhibitors (42, 43, 45-47).

Clinical utilization of the putative origin activation checkpoint for cancer cell specific killing demands a better understanding of the molecular response following Cdc7 inhibition in normal cells. In the study presented in Chapter 6, the response to Cdc7 depletion was examined in IMR90 human diploid fibroblasts. Normal human diploid fibroblasts were previously shown to engage a p53-dependent cell cycle arrest at the G1-S boundary following Cdc7 depletion (40). In the study presented here, evidence from gene expression microarray analysis demonstrates that the cell cycle block induced by Cdc7 downregulation is mediated by FoxO3a (48). FoxO3a is a transcription factor implicated in tumour suppression, longevity, cell cycle arrest other cellular functions (49, 50). It is controlled through numerous post-translational modifications, including phosphorylation, ubiquitination and acetylation, which alter its subcellular localization, DNA binding affinity and transcriptional activity. It is thought that these modifications comprise a code that is recognized by specific partners to guide individual modes of action (51).

The results presented in Chapter 6 suggest a model for the origin activation checkpoint in which FoxO3a mediates a checkpoint response following Cdc7 depletion in normal cells by modulating the activity of three checkpoint axes: p14<sup>ARF</sup>-Hdm2-p53-p21, p15<sup>INK4B</sup>-cyclin D-CDK4/6 and p53-Dkk3- $\beta$ -catenin (48). In addition, FoxO3a interacts with p27 (unpublished data). These data demonstrate that the origin activation checkpoint is dependent on numerous proto-oncogenic and tumour suppressor proteins that are commonly dysregulated in cancer. In normal cells, the three checkpoint axes are non-redundant, as demonstrated by the ability of normal cells co-depletion of Cdc7 and either FoxO3a, p15, p53 or Dkk3 to bypass the origin activation checkpoint, leading to an abortive S phase and apoptotic cell death. The results show that the origin activation checkpoint is distinct from the response to oxidative stress or direct upregulation of p53 (52, 53). The origin activation checkpoint depends on p53 activity to activate Dkk3 (Dickkopf 3), an antagonist of the Wnt/ $\beta$ -catenin pathway that prevents nuclear accumulation of  $\beta$ -catenin, which in turn downregulates Myc and cyclin D1 expression (54). Consistent with the involvement of Cdc7 in the origin activation checkpoint, this study shows that Orc 2 depletion produces a response similar to that observed following Cdc7 depletion (37, 48).

An open question is the temporal location of the arrest following Cdc7 depletion. Previous studies suggested the arrest was activated in either late G1 or early S. The study presented here provides further evidence that the checkpoint is engaged in G1 by demonstrating that cells arrest with low CDK activity and in the absence of chromatin-bound PCNA and BrdU incorporation (48). An important future study will be to provide more direct evidence for the replication status of normal cells arrested by Cdc7 depletion, possibly using DNA combing. This technique involves stretching chromatin fibres of up to 2 Mbp across glass slides, which are then analysed microscopically using fluorescent probes to identify replication fork status (55). DNA combing should allow direct confirmation of the temporal characteristics of the origin activation checkpoint.

## Clinical utility of the origin activation checkpoint

The differential effect of Cdc7 inhibition on normal and cancer cell lines makes Cdc7 an attractive therapeutic target and has prompted a concerted effort to develop targeted small molecule inhibitors of Cdc7 (42, 43). The study presented in Chapter 7 presents data from a detailed study of breast cancer cell lines and tissue samples with different tumour suppressor and proto-oncogene mutation spectra to examine Cdc7 as an anticancer target (56). Immunostaining of Cdc7 in 171 breast cancer cases demonstrated that Cdc7 was overexpressed in HER2-overexpressing and triple negative breast cancers. These aggressive breast cancer subtypes are linked with poor survival and correlate with the accelerated cell cycle phenotype (discussed above) (36). Cdc7 upregulation was linked to accelerated cell cycle progression, ar-

rested tumour differentiation, genomic instability, an increasing Nottingham Prognostic Index and reduced disease-free survival. This evidence suggests that Cdc7 deregulation is associated with aggressive breast cancer, consistent with earlier observations in epithelial ovarian carcinoma (57).

These findings suggest that the cell cycle progression phenotype is able to identify tumours where the majority of cells are actively cycling and so are likely to respond to Cdc7-targeted therapies. In addition, the cell cycle progression algorithm may be useful more generally to identify patients with tumours that are likely to be more responsive to cell cycle phase specific chemotherapeutic agents. Not only could this important predictive information drive the development of new targeted agents but, by identifying potentially more responsive subgroups, it could also allow the re-evaluation of agents that have previously demonstrated poor performance in studies where no allowance was made for cell cycle progression phenotype heterogeneity.

These findings were extended by studying the effect of Cdc7 downregulation by siRNA in p53-mutant HER2-overexpressing and triple negative breast cancer cell lines, which have high levels of Cdc7 (56). In these model systems, downregulation of Cdc7 was followed by an abortive S phase and apoptotic cell death, presumably due to loss of the origin activation checkpoint (48). Consistent with previous studies in normal human fibroblasts, the p53-wildtype human mammary epithelial cell line (HMEpC) underwent a cell cycle arrest following Cdc7 depletion, while concomitant depletion of Cdc7 and p53 induced apoptotic cell death (40, 48). A crucial finding in this study is the demonstration that untransformed breast epithelial HMEpC cells arrested by Cdc7 depletion resume passage through the cell cycle several days post-transfection with siRNA against Cdc7. Confirmation that the arrest induced by engagement of the origin activation checkpoint is reversible answers a major open question surrounding clinical use of Cdc7 inhibitors and provides important information that is vital to the use of pharmacological small molecular inhibitors that target Cdc7 for inhibition.

Cell cycle checkpoints are present in normal cells but are frequently lost or dysregulated in cancer. Previously, Pardee and colleagues suggested that an effective cancer treatment approach would be to exploit this difference, using drugs to selectively block normal cells while allowing cancer cells to proceed through the cell cycle, making them vulnerable to cell cycle phase specific chemotherapeutic agents (58). Such a cyclotherapy approach depends on a mechanism to induce a reversible G1 arrest in normal cells. The studies presented in Chapters 6 and 7 suggest an attractive strategy for combination therapy with Cdc7 small molecular inhibitors and cell cycle phase specific chemotherapeutic agents. In this strategy, a Cdc7 inhibitor has the dual effect of arresting normal cells with intact p53 by engaging the origin activation checkpoint while p53-defective cancer cells that have lost the checkpoint proceed into an abnormal S phase leading to apoptosis. Additional cancer cell specific killing can then be initiated by M-phase targeted chemotherapeutic agents. Since cells in normal self-renewing tissues undergo arrest following engagement of the origin activation checkpoint, normal cells should not be affected

by chemotherapy, thereby minimizing the serious side effects due to toxicity of cell cycle phase specific chemotherapeutic agents in normal self-renewing tissues. Stopping treatment with the chemotherapeutic agent and Cdc7 inhibitor would then allow normal cells to resume passage through the cell cycle. Cdc7 inhibitors therefore induce a shielding effect in normal cells, protecting them from the harm induced by targeted therapies.

Taken together, the studies presented here demonstrate that disruption of the origin activation checkpoint in cancer cells allows for cancer cell specific killing, while normal cells undergo a cell cycle arrest in G1, and also how this may be used in the context of breast cancer to cause cancer cell specific killing. An important extension of this work would be to more clearly demonstrate the ability of the origin activation checkpoint to shield normal cells from the deleterious effects of cell cycle targeted chemotherapeutic agents. The nature of the checkpoint suggests that treatment with both Cdc7 inhibitors and chemotherapeutic agents will lead to additive or even synergistic cancer cell specific killing, while leaving normal cells relatively unscathed. Further studies are required to confirm this exciting possibility.

Considered as a whole, the studies reported in this thesis support the model that the replication initiation proteins are useful as biomarkers for the detection of cancer and that are able to provide additional prognostic information and predict the response to therapeutic intervention. In addition, characterization of the origin activation checkpoint and its deregulation in breast cancer demonstrate that the replication initiation machinery is an important target for anticancer therapies.

## References

1. Altekruse SF, Kosary CL, Krapcho M, et al. SEER Cancer Statistics Review, 1975-2007, National Cancer Institute. Bethesda, MD, [seer.cancer.gov/csr/1975\\_2007](http://seer.cancer.gov/csr/1975_2007)
2. Ludwig JA, Weinstein JN. Biomarkers in cancer staging, prognosis and treatment selection. *Nat Rev Cancer* 2005;5:845-56.
3. Sawyers CL. The cancer biomarker problem. *Nature* 2008;452:548-52.
4. Stratton MR, Campbell PJ, Futreal PA. The cancer genome. *Nature* 2009;458:719-24.
5. Chin L, Gray JW. Translating insights from the cancer genome into clinical practice. *Nature* 2008;452:553-63.
6. Van't Veer LJ, Bernards R. Enabling personalized cancer medicine through analysis of gene-expression patterns. *Nature* 2008;452:564-70.
7. Hanash SM, Pitteri SJ, Faca VM. Mining the plasma proteome for cancer biomarkers. *Nature* 2008;452:571-9.
8. Swami M. Proteomics: A discovery strategy for novel cancer biomarkers. *Nat Rev Cancer* 2010;10:597.

9. Parsons DW, Jones S, Zhang X, et al. An integrated genomic analysis of human glioblastoma multiforme. *Science* 2008;321:1807-12.
10. Jones S, Zhang X, Parsons DW, et al. Core signaling pathways in human pancreatic cancers revealed by global genomic analyses. *Science* 2008;321:1801-6.
11. Comprehensive genomic characterization defines human glioblastoma genes and core pathways. *Nature* 2008;455:1061-8.
12. Williams GH, Stoeber K. Cell cycle markers in clinical oncology. *Curr Opin Cell Biol* 2007;19:672-9.
13. Gonzalez MA, Tachibana KE, Laskey RA, Coleman N. Control of DNA replication and its potential clinical exploitation. *Nat Rev Cancer* 2005;5:135-41.
14. Kearsley SE, Labib K. MCM proteins: evolution, properties, and role in DNA replication. *Biochim Biophys Acta* 1998;1398:113-36.
15. Ritzi M, Knippers R. Initiation of genome replication: assembly and disassembly of replication-competent chromatin. *Gene* 2000;245:13-20.
16. Stoeber K, Halsall I, Freeman A, et al. Immunoassay for urothelial cancers that detects DNA replication protein Mcm5 in urine. *Lancet* 1999;354:1524-5.
17. Freeman A, Morris LS, Mills AD, et al. Minichromosome maintenance proteins as biological markers of dysplasia and malignancy. *Clin Cancer Res* 1999;5:2121-32.
18. Stoeber K, Swinn R, Prevost AT, et al. Diagnosis of genito-urinary tract cancer by detection of minichromosome maintenance 5 protein in urine sediments. *J Natl Cancer Inst* 2002;94:1071-9.
19. Mitra AP, Cote RJ. Molecular pathogenesis and diagnostics of bladder cancer. *Annu Rev Pathol* 2009;4:251-85.
20. Mowatt G, Zhu S, Kilonzo M, et al. Systematic review of the clinical effectiveness and cost-effectiveness of photodynamic diagnosis and urine biomarkers (FISH, ImmunoCyt, NMP22) and cytology for the detection and follow-up of bladder cancer. *Health Technol Assess* 2010;14:1-iv.
21. Lotan Y. Commentary on prostate and urothelial carcinoma in cystoprostatectomy specimens. *J Urol* 2008;179:S33-S34.
22. Hemani ML, Bennett CL. The excessive cost of early stage bladder cancer care: are providers really to blame? *Cancer* 2010;116:3530-2.
23. Botteman MF, Pashos CL, Redaelli A, Laskin B, Hauser R. The health economics of bladder cancer: a comprehensive review of the published literature. *Pharmacoeconomics* 2003;21:1315-30.
24. Babjuk M, Oosterlinck W, Sylvester R, Kaasinen E, Bohle A, Palou-Redorta J. EAU guidelines on non-muscle-invasive urothelial carcinoma of the bladder. *Eur Urol* 2008;54:303-14.
25. Mayrand MH, Duarte-Franco E, Rodrigues I, et al. Human papillomavirus DNA versus Papanicolaou screening tests for cervical cancer. *N Engl J Med* 2007;357:1579-88.
26. Williams GH, Romanowski P, Morris L, et al. Improved cervical smear assessment using antibodies against proteins that regulate DNA replication. *Proc Natl Acad Sci U S A*



1998;95:14932-7.

27. Welch HG, Black WC. Overdiagnosis in cancer. *J Natl Cancer Inst* 2010;102:605-13.
28. Schroder FH, Hugosson J, Roobol MJ, et al. Screening and prostate-cancer mortality in a randomized European study. *N Engl J Med* 2009;360:1320-8.
29. Andriole GL, Crawford ED, Grubb RL, III, et al. Mortality results from a randomized prostate-cancer screening trial. *N Engl J Med* 2009;360:1310-9.
30. Dudderidge TJ, Kelly JD, Wollenschlaeger A, et al. Diagnosis of prostate cancer by detection of minichromosome maintenance 5 protein in urine sediments. *Br J Cancer* 2010;103:701-7.
31. Thompson IM, Goodman PJ, Tangen CM, et al. The influence of finasteride on the development of prostate cancer. *N Engl J Med* 2003;349:215-24.
32. Thompson IM, Pauler DK, Goodman PJ, et al. Prevalence of prostate cancer among men with a prostate-specific antigen level  $\geq$  4.0 ng per milliliter. *N Engl J Med* 2004;350:2239-46.
33. Ayaru L, Stoeber K, Webster GJ, et al. Diagnosis of pancreaticobiliary malignancy by detection of minichromosome maintenance protein 5 in bile aspirates. *Br J Cancer* 2008;98:1548-54.
34. de BM, Sherman S, Fogel EL, et al. Tissue sampling at ERCP in suspected malignant biliary strictures (Part 1). *Gastrointest Endosc* 2002;56:552-61.
35. Kayes OJ, Loddo M, Patel N, et al. DNA replication licensing factors and aneuploidy are linked to tumor cell cycle state and clinical outcome in penile carcinoma. *Clin Cancer Res* 2009;15:7335-44.
36. Loddo M, Kingsbury SR, Rashid M, et al. Cell-cycle-phase progression analysis identifies unique phenotypes of major prognostic and predictive significance in breast cancer. *Br J Cancer* 2009;100:959-70.
37. Machida YJ, Teer JK, Dutta A. Acute reduction of an origin recognition complex (ORC) subunit in human cells reveals a requirement of ORC for Cdk2 activation. *J Biol Chem* 2005;280:27624-30.
38. Shreeram S, Sparks A, Lane DP, Blow JJ. Cell type-specific responses of human cells to inhibition of replication licensing. *Oncogene* 2002;21:6624-32.
39. Labib K. How do Cdc7 and cyclin-dependent kinases trigger the initiation of chromosome replication in eukaryotic cells? *Genes Dev* 2010;24:1208-19.
40. Montagnoli A, Tenca P, Sola F, et al. Cdc7 inhibition reveals a p53-dependent replication checkpoint that is defective in cancer cells. *Cancer Res* 2004;64:7110-6.
41. Blow JJ, Gillespie PJ. Replication licensing and cancer—a fatal entanglement? *Nat Rev Cancer* 2008;8:799-806.
42. Swords R, Mahalingam D, O'Dwyer M, et al. Cdc7 kinase - a new target for drug development. *Eur J Cancer* 2010;46:33-40.
43. Montagnoli A, Moll J, Colotta F. Targeting cell division cycle 7 kinase: a new approach for cancer therapy. *Clin Cancer Res* 2010;16:4503-8.
44. Jackson PK. Stopping replication, at the beginning. *Nat Chem Biol* 2008;4:331-2.

45. Ermoli A, Bargiotti A, Brasca MG, et al. Cell division cycle 7 kinase inhibitors: 1H-pyrrolo[2,3-b]pyridines, synthesis and structure-activity relationships. *J Med Chem* 2009;52:4380-90.
46. Vanotti E, Amici R, Bargiotti A, et al. Cdc7 kinase inhibitors: pyrrolopyridinones as potential antitumor agents. 1. Synthesis and structure-activity relationships. *J Med Chem* 2008;51:487-501.
47. Montagnoli A, Valsasina B, Croci V, et al. A Cdc7 kinase inhibitor restricts initiation of DNA replication and has antitumor activity. *Nat Chem Biol* 2008;4:357-65.
48. Tudzarova S, Trotter MW, Wollenschlaeger A, et al. Molecular architecture of the DNA replication origin activation checkpoint. *EMBO J* 2010;29:3381-94.
49. Burgering BM. A brief introduction to FOXology. *Oncogene* 2008;27:2258-62.
50. Huang H, Tindall DJ. Dynamic FoxO transcription factors. *J Cell Sci* 2007;120:2479-87.
51. Calnan DR, Brunet A. The FoxO code. *Oncogene* 2008;27:2276-88.
52. Chen JH, Stoeber K, Kingsbury S, Ozanne SE, Williams GH, Hales CN. Loss of proliferative capacity and induction of senescence in oxidatively stressed human fibroblasts. *J Biol Chem* 2004;279:49439-46.
53. Choong ML, Yang H, Lee MA, Lane DP. Specific activation of the p53 pathway by low dose actinomycin D: a new route to p53 based cyclotherapy. *Cell Cycle* 2009;8:2810-8.
54. Lee EJ, Jo M, Rho SB, et al. Dkk3, downregulated in cervical cancer, functions as a negative regulator of beta-catenin. *Int J Cancer* 2009;124:287-97.
55. Bensimon A, Simon A, Chiffaudel A, Croquette V, Heslot F, Bensimon D. Alignment and sensitive detection of DNA by a moving interface. *Science* 1994;265:2096-8.
56. Rodriguez-Acebes S, Proctor I, Loddo M, et al. Targeting DNA replication before it starts: Cdc7 as a therapeutic target in p53-mutant breast cancers. *Am J Pathol* 2010;177:2034-45.
57. Kulkarni AA, Kingsbury SR, Tudzarova S, et al. Cdc7 kinase is a predictor of survival and a novel therapeutic target in epithelial ovarian carcinoma. *Clin Cancer Res* 2009;15:2417-25.
58. Pardee AB, James LJ. Selective killing of transformed baby hamster kidney (BHK) cells. *Proc Natl Acad Sci U S A* 1975;72:4994-8.



# Summary

Cancer is a leading cause of death worldwide. Early, accurate detection of malignancy would allow better treatment decisions and there is consequently an urgent need for new cancer biomarkers. Research output related to biomarker development continues to rise, however few new biomarkers have received regulatory approval for clinical use. The introduction of high-throughput omics technologies has led to a surge of interest in biomarkers based on systems biology approaches. Coupling these new tools to a more detailed understanding of cancer biology presents an approach that holds great promise for cancer diagnosis and individual-specific treatment, but there remain important technical and economic obstacles associated with this approach.

An alternative approach for biomarker development is to target the DNA replication initiation machinery, which acts downstream of complex and overlapping upstream signalling events. The six minichromosome maintenance proteins (MCMs) comprise the Mcm2-7 replicative helicase, which sits at the core of the pre-replication complex. MCMs are downregulated in out-of-cycle states and are associated with differentiation arrest and aberrant growth, typical of dysplastic growth and neoplasia. MCMs are therefore potentially useful for detecting malignancy.

Previous proof-of-concept studies suggested that Mcm5 has the potential to diagnose bladder cancer, however most of these studies were based on small patient cohorts. Chapter 2 presents data from the first large-scale blinded multicentre study of Mcm5 as a biomarker for bladder cancer detection. In a study of 1677 patients, an immunofluorometric Mcm5 test was able to detect bladder cancer in urine sediments with high sensitivity and specificity. At the cut-point where specificity was equal to that of cytology, Mcm5 had significantly higher sensitivity for bladder cancer detection. Combined detection of Mcm5 and the US FDA-approved NMP22 urinary marker improved performance relative to either test alone, allowing detection of nearly all life-threatening cancers. In addition, Mcm5 was not susceptible to false positives due to benign conditions such as urinary tract infection and benign prostatic hyperplasia, a common shortcoming of urinary bladder cancer markers. Mcm5 therefore appears to be a sensitive and specific biomarker for bladder cancer.

A previous study observed that patients with prostate cancer were also identified by the Mcm5 urine test. The results presented in Chapter 3 demonstrate that Mcm5 has great potential as

a diagnostic biomarker for this malignancy. In a study of 88 patients with confirmed prostate cancer and two control groups negative for malignancy, the Mcm5 test had peak sensitivity of 82% and specificity of 93%. Importantly, the Mcm5 test did not give a higher signal in patients with benign prostatic hyperplasia. The sensitivity of the Mcm5 test was significantly higher following prostate massage in prostate cancer patients but not in normal controls, suggesting that this simple procedure may serve to further improve the performance of the Mcm5 test. Together these findings suggest that Mcm5 is a sensitive marker for prostate cancer detection and warrant follow-up studies to confirm the results in a larger patient cohort.

Further evidence for the efficacy of Mcm5 as a cancer biomarker is presented in Chapter 4, in a study into use of Mcm5 detection for diagnosis of pancreaticobiliary tract cancer. This malignancy has a low 5-year survival rate due to the advanced stage of the disease at primary detection and there are as yet no regulator approved diagnostic biomarkers. The study presented here demonstrates that MCMs are dysregulated in pancreaticobiliary tract cancer and that detection of Mcm5 is an accurate test for this malignancy. Immunofluorometric detection of Mcm5 in cells obtained from bile samples had significantly higher sensitivity compared with routine brush cytology (66 vs 20%). Similar to bladder and prostate cancer, in pancreaticobiliary tract cancer the Mcm5 test was not affected by benign conditions including gallstones and chronic inflammation. These exciting findings suggest that Mcm5 is potentially a useful biomarker for pancreaticobiliary tract cancer diagnosis.

In addition to providing diagnostic utility, replication initiation proteins can potentially provide important prognostic information. The results presented in Chapter 5 show that replication initiation proteins together with markers of cell cycle progression and proliferation are potential prognostic markers in penile squamous cell carcinoma. Aggressive PeSCC is associated with poor prognosis and there are currently few prognostic markers. In a study of 141 men with PeSCC, Mcm2, geminin and the proliferation marker Ki67 were tightly associated with tumour differentiation and DNA ploidy status and identified men with a high risk of disease progression. Labelling indices for Mcm2, Ki67, Ki67-geminin score and DNA ploidy were significantly associated with overall survival on univariate analysis. In addition, a multivariate model comprising conventional prognostic indicators age, lymph node status and tumour multifocality together with DNA ploidy status was able to stratify patients in low, middle and high risk groups. This study suggests that DNA replication initiation proteins are useful as prognostic markers in PeSCC.

A crucial event in DNA replication initiation is the assembly of DNA replication forks through phosphorylation of MCM proteins by the cell cycle kinase Cdc7. Depletion of Cdc7 leads to p53-dependent cell cycle arrest in normal cells, while cancer cells proceed into an abnormal S phase and apoptosis. Faced with perturbed replication initiation, normal cells engage a putative origin activation checkpoint and prevent S phase entry. This checkpoint appears to be frequently lost in cancer cells. In the study presented in Chapter 6, the response to

Cdc7 depletion was examined in IMR90 human diploid fibroblasts. Normal human diploid fibroblasts were previously shown to engage a p53-dependent cell cycle arrest at the G1-S boundary following Cdc7 depletion. The present study demonstrates that the cell cycle block induced by Cdc7 downregulation is mediated by FoxO3a, a transcription factor implicated in tumour suppression, longevity, cell cycle arrest and other cellular functions. The results suggest a model for the origin activation checkpoint in which FoxO3a mediates a checkpoint response following Cdc7 depletion in normal cells by modulating the activity of three non-redundant checkpoint axes: p14<sup>ARF</sup>-Hdm2-p53-p21, p15<sup>INK4B</sup>-cyclin D-CDK4/6 and p53-Dkk3- $\beta$ -catenin. The origin activation checkpoint is distinct from the response to oxidative stress or direct upregulation of p53 and is dependent on several proto-oncogenic and tumour suppressor proteins commonly dysregulated in cancer.

The differential effect of Cdc7 inhibition on normal and cancer cell lines makes Cdc7 an attractive therapeutic target and has prompted a concerted effort to develop targeted small molecule inhibitors of Cdc7. The study presented in Chapter 7 presents data from a detailed study of breast cancer cell lines and tissue samples with different mutation spectra to examine Cdc7 as an anticancer target. Immunostaining of Cdc7 in 171 breast cancer cases demonstrated that Cdc7 was overexpressed in HER2-overexpressing and triple negative breast cancers. These aggressive breast cancer subtypes are linked with poor survival and correlate with an accelerated cell cycle phenotype. Cdc7 upregulation was linked to accelerated cell cycle progression, arrested tumour differentiation, genomic instability and reduced disease-free survival, suggesting that Cdc7 deregulation is associated with aggressive breast cancer.

These findings were extended by studying the effect of Cdc7 downregulation by siRNA in p53-mutant HER2-overexpressing and triple negative breast cancer cell lines, which have high levels of Cdc7. In these model systems, Cdc7 downregulation was followed by an abortive S phase and apoptotic cell death. Consistent with the results in Chapter 6, the p53-wildtype human mammary epithelial cell line (HMEpC) underwent a cell cycle arrest following Cdc7 depletion, while concomitant depletion of Cdc7 and p53 induced apoptotic cell death. A crucial finding here is the demonstration that untransformed HMEpC cells arrested by Cdc7 depletion resume passage through the cell cycle several days post-transfection with siRNA against Cdc7. Confirmation that the arrest induced by engagement of the origin activation checkpoint is reversible answers a major open question surrounding clinical use of Cdc7 small molecule inhibitors currently in development.

Considered together, the studies presented in this thesis support the model that replication initiation proteins are useful as biomarkers for the detection of cancer, are able to provide additional prognostic information and can predict the response to therapeutic intervention. In addition, characterization of the origin activation checkpoint and its deregulation in breast and other cancers demonstrate that the replication initiation machinery is also an important target for anticancer therapies.





# Nederlandse Samenvatting

Kanker is een van de meest voorkomende dodelijke ziektes. Door vroege detectie van kanker kunnen betere behandelingstrajecten worden toegepast en is het dus zaak om nieuwe biomarkers voor kanker te ontwikkelen. De koppeling van de nieuwe “omics” methodes met een meer gedetailleerd begrip van het proces dat tot kanker leidt, geeft nieuwe mogelijkheden om betere diagnoses en patient specifieke behandelingen te ontwikkelen.

De machinerie die de initiatie van DNA replicatie regelt is een mogelijk aangrijpingspunt voor de ontwikkeling van biomarkers en in het bijzonder zijn de zes minichromosoom eiwitten (MCMs), die de MCM2-7 replicatie helicases omvatten en de kern van het pre-replicatie complex vormen. MCMs worden negatief rereguleerd in niet delende cellen en zijn geassocieerd met abnormale groei en remming van differentiatie die typisch zijn voor dysplastische groei en neoplasie. MCMs kunnen daarom potentieel nuttig zijn om maligniteit te detecteren.

Eerdere “proof of concept” studies hebben laten zien dat Mcm5 potentieel blaaskanker kan detecteren, maar deze studies zijn gedaan met vrij kleine groepen patiënten. Hoofdstuk 2 beschrijft de bevindingen van de eerste geblindeerde multicentra studie van Mcm5 als biomarker voor het opsporen van blaaskanker. Deze studie met 1667 patiënten laat zien dat een immunofluorimetrische test van Mcm5 met hoge gevoeligheid en specificiteit blaaskanker kan bepalen. Op het zelfde specificiteitsniveau als een cytologische bepaling was Mcm5 detectie veel gevoeliger. Een bepaling met een combinatie van Mcm5 met de FDA goedgekeurde marker NMP22 verbeterde de test in vergelijking met ieder van de markers alleen en deze combinatie kon bijna alle levensbedreigende tumoren detecteren. Bovendien had Mcm5 geen last van het detecteren van vals positieven, zoals infectie van de urinewegen en goedaardige prostaat hyperplasie, iets waar de huidige markers voor blaaskanker last van hebben.

Een eerdere studie heeft laten zien dat ook prostaatkanker met Mcm5 gedetecteerd kan worden. The resultaten in Hoofdstuk 3 laten zien dat Mcm5 potentieel inderdaad een zeer goede biomarker voor prostaatkanker is. In een studie van 88 patiënten met prostaatkanker en twee negatieve controlegroepen heeft de Mcm5 test een gevoeligheid van 82% en een specificiteit van 93%. Belangrijk is hierbij dat de test geen verhoogd signaal geeft in patiënten met een goedaardige prostaat hyperplasie. De gevoeligheid van de Mcm5 test was aanzienlijk beter na prostaat massage in the prostaat kanker patiënten, maar niet in de controle groep. Dit

suggereert dat deze eenvoudige procedure de Mcm5 test verder verbetert.

Meer bewijs voor doeltreffendheid van de Mcm5 test als biomarker voor kanker wordt geleverd in Hoofdstuk 4 door een studie naar de diagnose van kanker van de alvleesklier, een maligniteit met een lage 5 jaar overlevingskans omdat de ziekte pas in een laat stadium ontdekt wordt. De studie laat zien dat MCMs ontregeld zijn in dit type tumor en dat Mcm5 detectie een accurate test is voor deze maligniteit. Immunofluorimetrische detectie van Mcm5 in cellen verkregen uit de gal hadden aanzienlijk hogere gevoeligheid in vergelijking met cytologie (66% versus 20%). Ook hier was de test niet gevoelig voor goedaardige afwijkingen zoals galstenen en chronische ontsteking. Deze interessante vindingen suggereren dat Mcm5 potentieel een goede biomarker is voor de diagnose van kanker van de alvleesklier.

De resultaten in Hoofdstuk 5 laten zien dat de initiatie van replicatie eiwitten samen met markers van de celcyclus ook als prognostische marker kunnen worden gebruikt voor de detectie van huidcel carcinoom van de penis (PeSCC). PeSCC is geassocieerd met een slechte prognose en er zijn nu weinig prognostische markers. In een studie van 141 mannen met PeSCC waren Mcm2, geminin en de proliferatie marker Ki67 nauw geassocieerd met differentiatie van de tumor en DNA ploïdie en identificeerde mannen met een hoge kans op progressie van de ziekte. Deze studie suggereert dat initiatie van replicatie eiwitten nuttiger prognostische markers zijn voor PeSCC.

Een cruciale stap in de initiatie van DNA replicatie is het vormen van DNA replicatievorken. Deze vorken kunnen ontstaan doordat MCM eiwitten worden gefosforyleerd door de celcyclus kinase Cdc7. Afwezigheid van Cdc7 leidt tot p53-afhankelijke celcyclus blokkade in normale cellen. Kankercellen daarentegen stoppen niet, maar gaan door in een abnormale S-fase en apoptose. Normale cellen activeren bij een verstoorde DNA replicatie initiatie een celcyclus controlepunt, zodat de cel niet in S-fase gaat. Dit celcyclus controlepunt lijkt in kankercellen vaak te zijn verdwenen. De studie beschreven in Hoofdstuk 6, “de reactie op de vermindering van de checkpoint kinase Cdc7” is uitgevoerd in IMR90 menselijke diploïde fibroblasten. Het is aangetoond dat normale fibroblasten een p53 afhankelijke stop van de celcyclus ondergaan bij de overgang van G1 naar S als Cdc7 verminderd wordt. Deze studie laat zien dat deze stop gemedieerd wordt door FoxO3a, een transcriptie factor die gempliceerd is in tumor suppressie, levensduur, celcyclus arrest en andere cellulaire processen. Het resultaat suggereert een model voor de activatie van een checkpoint waarin FoxO3a een checkpoint respons medieert na de depletie van Cdc7 in normale cellen door middel van de activatie van drie niet redundante checkpoint processen: p14<sup>ARF</sup>-Hdm2-p53-p21, p15<sup>INK4B</sup>-cyclin D-CDK4/6 en p53-Dkk3- $\beta$ -catenin. De checkpoint van de origine activering verschilt van de oxidatieve stress respons of directe verhoging van p53 en is afhankelijk van een aantal tumor bevorderende en tumor remmende eiwitten die dikwijls gedereguleerd zijn in kanker.

Het verschil in effect van de remming van Cdc7 op normale of kanker cellijnen maakt het dat

Cdc7 een aantrekkelijk therapeutische target is en dit heeft geleid tot een gezamenlijke inspanning om remmers van Cdc7 te vinden. Hoofdstuk 7 beschrijft de data van een uitgebreide studie van borstkanker cellijnen en weefsel met verschillende mutaties om Cdc7 als een antikanker target te testen. Immunokleuring van Cdc7 in 171 borstkanker gevallen liet zien dat Cdc7 tot verhoogde expressie kwam in HER2 overexpressie en drievoudig negatieve borsttumoren. Deze agressieve borstkanker subtypes zijn typerend voor slechte overlevingskansen en correleren met een versnelde celcyclus.

Remming van Cdc7 in p53-mutante borsttumoren met een te hoge HER2 expressie, had een afgebroken S fase en apoptose tot gevolg. In overeenstemming met Hoofdstuk 6 onderging de p53 wildtype borst epitheel cellijn HMEpC een stop van de celcyclus na verlaging van Cdc7, terwijl een gelijktijdige verwijdering van Cdc7 en p53 tot apoptose leidde. Een cruciale vondst hierbij is dat de niet getransformeerde HMEpC cellen waarvan de celcyclus door een vermindering van Cdc7 enige dagen later weer voortgezet wordt. Bevestiging dat de blokkade van de celcyclus die geïnduceerd is door het aanzetten van het checkpoint voor origine activatie reversibel is, beantwoordt een belangrijke open vraag rond de klinische toepassing van Cdc7 remmers die nu ontwikkeld worden.

De in dit proefschrift gepresenteerde resultaten onderschrijven het idee dat eiwitten betrokken bij de initiatie van replicatie nuttig zijn als biomarkers voor de diagnostiek van kanker, dat zij bovendien prognostische informatie verschaffen en de respons op therapie kunnen voorspellen. De karakterisatie van het checkpoint van de activatie van de replicatie origine en de ontregeling daarvan in borst en andere tumoren laat zien dat de replicatie machinerie mogelijk ook een belangrijk aangrijpingspunt is voor de ontwikkeling van antikanker therapieën.



# Acknowledgements

That I have made it this far is thanks to the many people who have been invaluable to me in my scientific career. The work described here was done entirely in the lab of Kai Stoeber and Gareth Williams at the Wolfson Institute for Biomedical Research and at the Department of Pathology, at University College London. Kai and Gareth taught me how to do science, but they also showed me, for better or worse, what it's like to actually be a scientist, and for that I can never repay them.

I would like to thank everyone in Rotterdam who helped me get here. Frank Grosveld gave me a second chance, something that is all too rare in this world. I want to thank the members of my inner committee, Sjaak Philipsen, Dies Meijer and Guido Jenster, who read my thesis on short notice and helped to make it better. In particular, I'd like to thank Marike van Geest. Without her tireless efforts and patience, as I bugged her for the umpteenth time about the smallest of things, getting here would have been much harder than it was.

During my PhD time and before, I've had the privilege of working with a lot of people, in labs in London, Rotterdam and Montreal. I would not be able to do justice to all of you by naming you here, but I want you to know that I have appreciated and enjoyed every minute of it. I would like to single out Eric Milot and Stefania Bottardi in Montreal. I learnt a lot from you, probably more than you realize. Thank you for all that you did for me.

Coming to Europe to do my PhD was an easy decision but it did mean leaving behind my family in South Africa. Strangely, the enormous distance between us brought us closer together, in some ways, and I always felt like they were there with me at every step.

Lastly, I want to thank my wife, Nada Stankova. Thank you, Nada, for always believing in me, and for making every day feel like an adventure.

Alex Wollenschlaeger  
London, 1 June 2011



## Alex Wollenschlaeger

---

### CONTACT INFORMATION

Wolfson Institute for Biomedical Research  
University College London  
London, UK

Voice: +44 7679 0802  
E-mail: rmgzawo@ucl.ac.uk

### EDUCATION

#### **Erasmus University Rotterdam**, Rotterdam, Netherlands

Ph.D. Candidate, Cancer Biology, June 2011

- Thesis: "The DNA replication initiation machinery as a target for cancer diagnosis and therapy"
- Promoter: Prof. Frank G. Grosveld
- Co-promoter: Dr Kai Stoeber

#### **University College London**, London, UK

M.Sc., Economics, November 2009

- Dissertation: "Advertising and Video Games: An Empirical Analysis"
- Supervisor: Prof. Steffen Huck

#### **University of the Orange Free State**, Bloemfontein, South Africa

M.Med.Sc., Haematology and Cell Biology, September 1999

- Dissertation: "Co-expression and functional assay of human Rb and E2F1 proteins in yeast"
- Supervisor: Prof. G.H.J Pretorius

B.Sc.(Honours), Biochemistry, December 1997

B.Sc., Biochemistry, December 1996

### AWARDS

University of the Orange Free State Student Representative Council Award for Second Highest B.Sc. (Honours) Student Achievement in the Faculty of Natural Sciences, 1998

AECI Award for Best B.Sc. (Honours) Student in Biochemistry, University of the Orange Free State, 1998

Boehringer-Mannheim Award for Best Third Year Student in Biochemistry, University of the Orange Free State, 1997

### PROFESSIONAL EXPERIENCE

#### **University College London**, London, UK

Clinical Trials Co-ordinator  
Research Technician

April 2008 - Present  
December 2003 - March 2008

#### **Erasmus University Rotterdam**, Rotterdam, Netherlands

Assistant in Training

September 1999 - September 2003

#### **University of Montreal**, Montreal, Canada

Assistant in Training

September 1999 - September 2003

PUBLICATIONS

Tudzarova S, Trotter MW, Wollenschlaeger A, Mulvey C, Godovac-Zimmermann J, Williams GH, Stoeber K. Molecular architecture of the DNA replication origin activation checkpoint. *EMBO J.* 2010 Oct 6;29(19):3381-94.

Rodriguez-Acebes S, Proctor I, Loddo M, Wollenschlaeger A, Rashid M, Falzon M, Prevost AT, Sainsbury R, Stoeber K, Williams GH. Targeting DNA replication before it starts: Cdc7 as a therapeutic target in p53-mutant breast cancers. *Am J Pathol.* 2010 Oct;177(4):2034-45.

Dudderidge TJ, Kelly JD, Wollenschlaeger A, Okoturo O, Prevost T, Robson W, Leung HY, Williams GH, Stoeber K. Diagnosis of prostate cancer by detection of minichromosome maintenance 5 protein in urine sediments. *Br J Cancer.* 2010 Aug 24;103(5):701-7.

Kayes OJ, Loddo M, Patel N, Patel P, Minhas S, Ambler G, Freeman A, Wollenschlaeger A, Ralph DJ, Stoeber K, Williams GH. DNA replication licensing factors and aneuploidy are linked to tumor cell cycle state and clinical outcome in penile carcinoma. *Clin Cancer Res.* 2009 Dec 1;15(23):7335-44.

Ross J, Bottardi S, Bourgoin V, Wollenschlaeger A, Drobetsky E, Trudel M, Milot E. Differential requirement of a distal regulatory region for pre-initiation complex formation at globin gene promoters. *Nucleic Acids Res.* 2009 Sep;37 (16):5295-308.

Ayaru L, Stoeber K, Webster GJ, Hatfield AR, Wollenschlaeger A, Okoturo O, Rashid M, Williams G, Pereira SP. Diagnosis of pancreaticobiliary malignancy by detection of minichromosome maintenance protein 5 in bile aspirates. *Br J Cancer.* 2008 May 6;98(9):1548-54.

McMorrow T, van den Wijngaard A, Wollenschlaeger A, van de Corput M, Monkhorst K, Trimborn T, Fraser P, van Lohuizen M, Jenuwein T, Djabali M, Philipsen S, Grosveld F, Milot E. Activation of the beta globin locus by transcription factors and chromatin modifiers. *EMBO J.* 2000 Sep 15;19(18):4986-96.

PAPERS IN PREPARATION

Wollenschlaeger A, Kelly JD, Dudderidge TJ, Okoturo O, Burling K, Tulloch F, Halsall I, Prevost T, Prevost AT, Vasconcelos JC, Robson W, Leung HY, Vasdev N, Pickard RS, Williams GH, Stoeber K. Diagnosis of bladder cancer by combined detection of minichromosome maintenance 5 protein and nuclear matrix protein 22.

TEACHING EXPERIENCE

**University College London**, London, UK

Teaching Assistant

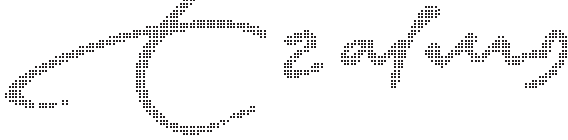
M.Sc. Drug Development, assistant to Dr Kai Stoeber, March 2011

M.Sc. Cancer, assistant to Dr Kai Stoeber, October 2010

**University of the Orange Free State**, Bloemfontein, South Africa

Teaching Assistant

B.Sc. Biochemistry, assistant to Prof Derek Litthauer, January 1997 to November 1997



## PhD Portfolio

### Summary of PhD training and teaching

Name PhD student: Alex Wollenschlaeger Erasmus MC Department: Cell Biology Research School: MGC	PhD period: December 2003 – March 2011 Promotor(s): Prof. Frank G. Grosveld Co-promoter/Supervisor: Dr Kai Stoeber	
<b>1. PhD training</b>		
	<b>Year</b>	<b>Workload (Hours/ECTS)</b>
<b>General courses</b>		
- Laboratory animal science (Article A9)	2000	
- Statistics using SPSS	2004	
- Methodology (Fairfield Imaging aneuploidy analysis)	2004	
- Methodology (confocal microscopy)	2004	
- Science communication	2006	
- Programming in Matlab	2011	
<b>(Inter)national conferences</b>		
- Annual Wolfson Institute for Biomedical Research Symposium	2005-2009	
- UCL Cancer Institute Research Symposium	2009	
<b>Seminars and workshops</b>		
- UCL Cancer Institute seminar series	2008-2011	
<b>2. Teaching</b>		
	<b>Year</b>	<b>Workload (Hours/ECTS)</b>
<b>Lecturing</b>		
- MSc Drug Development (UCL) practical sessions	2011	
<b>Supervising practicals and excursions, Tutoring</b>		
- MSc Cancer (UCL) student supervision	2010	
- MSc Drug Development (UCL) student supervision	2011	
<b>Other</b>		
- BSc student project supervision	2011	